

WORLD METEOROLOGICAL ORGANIZATION

GLOBAL ATMOSPHERE WATCH

WORLD DATA CENTRE FOR GREENHOUSE GASES



**GLOBAL
ATMOSPHERE
WATCH**

WMO WDCGG DATA SUMMARY

WDCGG No. 39

GAW DATA

Volume IV-Greenhouse Gases and Other Atmospheric Gases

**PUBLISHED BY
JAPAN METEOROLOGICAL AGENCY
IN CO-OPERATION WITH
WORLD METEOROLOGICAL ORGANIZATION**

MARCH 2015



Acknowledgements

This issue of *Data Summary* reports the latest status of greenhouse and some reactive gases in the global atmosphere. This *Data Summary* has been prepared by the World Data Centre for Greenhouse Gases (WDCGG), established under the Global Atmosphere Watch (GAW) Programme of the World Meteorological Organization (WMO) and operated by the Japan Meteorological Agency (JMA). This *Data Summary* is based on the data submitted by many contributors worldwide (Appendix: LIST OF CONTRIBUTORS). These contributors include both organizations and individuals involved in observations and research of greenhouse and some reactive gases at stations and laboratories operating within the framework of GAW and some other monitoring and research programmes. The WDCGG thanks all of these organizations and individuals, including those from the global air sampling network of the National Oceanic and Atmospheric Administration (NOAA), for their efforts in maintaining the observation programme and continuous provision of observational data. Not all of the contributors may be explicitly acknowledged in this publication, owing to lack of space, but all the organizations and individuals that have submitted data to the WDCGG are nevertheless here acknowledged as invaluable contributors to this latest issue of *Data Summary*.

CONTENTS

| | Page |
|--|------|
| SUMMARY ----- | 1 |
| 1. INTRODUCTION ----- | 5 |
| 2. ANALYSIS ----- | 7 |
| 3. CARBON DIOXIDE ----- | 9 |
| 4. METHANE ----- | 17 |
| 5. NITROUS OXIDE ----- | 23 |
| 6. HALOCARBONS AND OTHER HALOGENATED SPECIES ----- | 29 |
| 7. SURFACE OZONE ----- | 35 |
| 8. CARBON MONOXIDE ----- | 39 |
| 9. NITROGEN MONOXIDE AND NITROGEN DIOXIDE ----- | 45 |
| 10. SULPHUR DIOXIDE ----- | 49 |
| 11. VOLATILE ORGANIC COMPOUNDS ----- | 53 |
| REFERENCES ----- | 59 |
| APPENDICES ----- | 63 |
| CALIBRATION AND STANDARD SCALES ----- | 64 |
| LIST OF ABBREVIATIONS IN THE CALIBRATION AND STANDARD SCALES ----- | 75 |
| LIST OF OBSERVATIONAL STATIONS ----- | 77 |
| LIST OF UCI SAMPLING SITES ----- | 90 |
| LIST OF CONTRIBUTORS ----- | 92 |
| GLOSSARY ----- | 121 |
| LIST OF WMO/WDCGG PUBLICATIONS ----- | 123 |

SUMMARY

This *Data Summary* reports the results of basic analyses of greenhouse and some reactive gas data submitted to the WMO World Data Centre for Greenhouse Gases (WDCGG) by contributing organizations and individuals. This issue covers observations from 1968 through 2013, based on data reported to the WDCGG by November 2014, except for the greenhouse gas species CO₂, CH₄, N₂O, SF₆ and halocarbons, for which the submission period ended in July 2014. The *Data Summary* includes analyses of global, hemispheric and latitudinal monthly mean mole fractions of greenhouse and some reactive gases calculated using data from observations at marine and continental surface-based stations, and provides current information on the state of mole fractions of these gases.

Although monthly mean mole fractions were mainly used for the analyses, the WDCGG greatly appreciates those stations that submit daily, hourly and occasional mean mole fractions, which are important for analysis of variations on shorter time scales. All data submitted to the WDCGG are available on its website, <http://ds.data.jma.go.jp/gmd/wdogg/>. In this *Data Summary*, data are reported as dry air mole fractions defined as the number of molecules of a target gas species divided by the number of all molecules in the air including the target itself, but excluding water vapor. Mole fractions are expressed as parts per million (ppm), parts per billion (ppb), and parts per trillion (ppt), which correspond to the SI units of $\mu\text{mol/mol}$, nmol/mol and pmol/mol , respectively.

Variations in the mole fractions of some gases are presented as combinations of seasonal cycles and deseasonalized long-term trends. Growth rates are presented as time derivatives of the long-term trends. Global average mole fractions are presented with accompanying uncertainty. The analytical results are summarized below for each greenhouse and reactive gas.

Carbon Dioxide (CO₂)

The level of carbon dioxide (CO₂), which contributes the most to increases in anthropogenic induced radiative forcing, has been increasing since the beginning of the industrial era. The global average mole fraction of CO₂ reached a new high of 396.0 ± 0.1 ppm in 2013, which constitutes 142% of the pre-industrial level (in 1750). The annual average increase of 2.9 ppm from 2012 to 2013 was the largest year to year change in the period 1984 to 2013, and much greater than the average growth rate for the 1990s (about 1.5 ppm/year) and that for the past decade (about 2.1 ppm/year).

The global growth rate of CO₂ has a significant

interannual variability driven by natural processes. Interannual changes higher than 2 ppm/year in 1987/1988, 1997/1998, 2002/2003 and 2009/2010 resulted from warmer conditions caused by El Niño-Southern Oscillation (ENSO) events. The anomalously strong El Niño event in 1997/1998 resulted in greater annual increases in CO₂ worldwide in 1998 than during any other one-year period. The high growth rate in 2006 may have been related to the global high temperature during the same year. The high growth rate in 2012/2013 may be the result of small changes in fluxes between the atmosphere and terrestrial biosphere (WMO, 2014). The exceptionally low growth rate in 1992, including negative values in northern high latitudes, may have been due to low global temperatures following the eruption of Mount Pinatubo in 1991. Variations in CO₂ mole fraction can be seen both on seasonal and long-term scales. The seasonal amplitudes are large in northern high and mid-latitudes and small in the Southern Hemisphere. In southern low latitudes, there is no clear annual cycle, but a semiannual cycle can be determined.

Methane (CH₄)

Methane (CH₄) is the second most significant greenhouse gas which is largely influenced by anthropogenic activity and whose level has been increasing since the beginning of the industrial era. The annual average mole fraction was 1824 ± 2 ppb in 2013, an increase of 6 ppb since 2012. The mole fraction is now 253% of that in the pre-industrial period. This is the seventh year of marked methane increases since levelling-off at the beginning of this century.

The latitudinal gradient of CH₄ mole fraction is large from the northern mid-latitudes to the tropics, suggesting that the major sources of CH₄ are located in the Northern Hemisphere.

CH₄ growth rates decreased significantly in some years, including 1992, when negative values were recorded in northern high and mid-latitudes. However, both hemispheres experienced high growth rates in 1998, caused by the higher than average global mean temperature. The global growth rates were generally low from 1999 to 2006, except during the El Niño event of 2002/2003. The global growth rate averaged over the period 1984-1990 was 11.7 ppb/year, but decreased markedly in the 1990s. The mean annual absolute increase during the last 10 years was 3.8 ppb/year, but in the last seven years through 2013, the global mole fraction increased by 5.6 ppb/year.

CH₄ mole fractions vary seasonally, being relatively high in winter and low in summer. Unlike CO₂, the seasonal amplitudes of CH₄ are large, not only in the

Northern Hemisphere but also in southern high and mid-latitudes which are associated with methane sinks. In southern low latitudes, a distinct secondary maximum in boreal winter overlies the annual cycle.

Nitrous Oxide (N₂O)

Nitrous oxide (N₂O) is an important greenhouse gas whose level is increasing globally. N₂O data submitted to the WDCGG show that mole fractions are increasing in both hemispheres. The global mean mole fraction reached a new high of 325.9±0.1 ppb in 2013, which is 0.8 ppb higher than that in the previous year. This mole fraction corresponds to 121% of that in the pre-industrial period. The mean annual absolute increase during the last 10 years was 0.82 ppb/year and the inter-hemispheric gradient in N₂O is 1.0 ppb (averaged over the years 1980 to 2013), indicating that the majority of N₂O sources are situated in the Northern Hemisphere.

Halocarbons and Other Halogenated Species

Halocarbons, most of which are anthropogenic and generated since the 20th century, are potent greenhouse gases, with some also acting as ozone-depleting compounds. Levels of some halocarbons (e.g. CFCs) increased in the 1970s and 1980s, but this increase has almost ceased by now, due to the production and consumption control of halocarbons under the Montreal Protocol on Substances that Deplete the Ozone Layer and its subsequent Adjustments and Amendments. However, some substances targeted by the Kyoto Protocol but not regulated by the Montreal Protocol, such as HFCs and SF₆, are increasing.

The mole fraction of CFC-11 peaked around 1992 and then started decreasing. The mole fraction of CFC-12 increased until around 2005 and then started decreasing gradually. The mole fraction of CFC-113 stopped increasing in the 1990s, followed by a slight decrease over about twenty years. The mole fractions of HCFCs, used mainly as substitutes for CFCs, have increased significantly during the last decade. The growth of HCFC-141b decelerated around 2005, but has accelerated over the last few years. The mole fraction of Halon-1211 has decreased since 2005, whereas the mole fraction of Halon-1301 is increasing. The mole fraction of CCl₄ was maximal around 1991 and has since decreased slowly. The mole fraction of CH₃CCl₃ peaked around 1992 and decreased thereafter. The mole fractions of HFC-134a, HFC-152a and SF₆ are increasing, but the growth of HFC-152a decelerated in the second half of the decade.

Surface Ozone (O₃)

Ozone (O₃) plays important roles in the atmospheric environment through radiative and chemical processes. It absorbs solar UV radiation in the stratosphere, influencing the vertical temperature profile as well as

terrestrial IR radiation, and contributing to the greenhouse effect as a greenhouse gas. Ozone is also involved in the chemical transformations of the primary air pollutants, as its mole fraction in the boundary layer serves as an indicator of air quality.

The mole fraction of O₃ near the surface, so-called surface ozone, reflects various processes. While some of the O₃ in the troposphere comes from the stratosphere, the rest is chemically produced in the troposphere through oxidation of CO or hydrocarbons in the presence of NO_x.

The mole fraction of surface ozone is measured at many locations in various environments. Continuous ozone observations are reported mostly as wet mole fraction. Due to uneven geographic distribution of surface ozone, it is difficult to identify its global long-term trend (WMO, 2011b).

Carbon Monoxide (CO)

Carbon monoxide (CO) is not a greenhouse gas itself but influences the mole fractions of greenhouse gases by affecting hydroxyl radicals (OH). Beginning in 1950, the CO mole fraction increased at a rate of 1% per year but started to decrease in the late 1980s (WMO, 1999). In 2013, the global mean mole fraction of CO was about 90±2 ppb. The mole fraction is high in the Northern Hemisphere and low in the Southern Hemisphere, suggesting substantial anthropogenic emissions in the Northern Hemisphere.

There is a large interannual variability of CO growth rates. The growth rate increases are usually attributed to biomass burning emissions during El Niño conditions.

The monthly mean mole fractions show seasonal variations, with large amplitudes in the Northern Hemisphere and small amplitudes in the Southern Hemisphere with opposite phase.

Nitrogen Monoxide (NO) and Nitrogen Dioxide (NO₂)

Nitrogen oxides (NO_x, i.e., NO and NO₂) are not greenhouse gases, but they are involved in the photochemical production of ozone in the troposphere. In the presence of NO_x, CO and hydrocarbons are oxidized to produce ozone (O₃), which affects the Earth's radiative balance as a greenhouse gas and the oxidization capacity of the atmosphere by reproducing OH.

Most of the stations that have so far reported NO_x data to the WDCGG are located in Europe. NO_x has a large temporal and spatial variability, and it is difficult to identify its long-term global trend based on a spatially limited dataset.

Sulphur Dioxide (SO₂)

Sulphur dioxide (SO₂) is not a greenhouse gas but a precursor of atmospheric sulphate aerosols. Sulphate

aerosols are produced by SO₂ oxidation through photochemical gas-to-particle conversion. SO₂ has also been a major source of acid rain and deposition throughout the industrial era.

Most of the stations reporting SO₂ data to the WDCGG are located in Europe, and it is difficult to identify its long-term global trend based on a spatially limited dataset.

Volatile Organic Compounds (VOCs)

Volatile organic compounds (VOCs) are organic chemicals that easily evaporate or sublime at ordinary atmospheric temperatures (vapor pressure \geq 0.01 kPa at 20°C). Many are in the form of non-methane hydrocarbons (NMHCs) of different complexity including aliphatics and aromatics which dominate anthropogenic emissions, and unsaturated molecules including terpenes which dominate natural emissions. They also exist as oxygenated hydrocarbons such as acetone and methanol, and sulphur-containing molecules such as dimethyl sulphide.

Although they are not important greenhouse gases in themselves, they are of interest to Global Atmosphere Watch (GAW) because of their environmental impacts, including ozone production and precursors to aerosols. Their main interest to GAW is as tracers of processes which either produce or destroy other major species in the atmosphere measured by GAW. An example is given in chapter 11 of how ethane measurements increase understanding of the behavior of methane.

In its role as the World Data Centre for reactive gases and GHGs, as of November 2014, WDCGG records 53 individual species of VOCs from which a subset, widespread throughout the global atmosphere has been selected as a focus for the GAW VOC Programme. Temporal coverage of VOC measurements has grown extensively over the last decade, since a global flask network came into operation in 2005, supplementing the longer series of measurements made at a few continental sites.

In this 39th edition of the WDCGG *Data Summary*, global analyses are performed for ethane and propane with their relatively long lifetime and wide measurement network. The data coverage in the analyses was remarkably expanded from the last issue with including the European Monitoring and Evaluation Programme (EMEP) non-GAW data and the massive dataset newly submitted from the Department of Chemistry, University of California, Irvine (UCI).

Ethane mole fractions are relatively high in winter and low in summer. The seasonal amplitudes are large in northern high and mid-latitudes but very small in the southern latitudes. Observed seasonal

differences are connected with photochemical processes, whereas hemispheric differences indicate the majority of ethane sources in northern latitudes. The propane distribution shows features similar to those of ethane albeit with greater seasonality and more pronounced latitudinal gradients in the Northern Hemisphere during winter. This greater seasonality is mainly because of its higher reactivity. Also, due to its shorter atmospheric lifetime compared to ethane, the Northern Hemisphere seasonal cycle of propane shows a maximum close to mid-winter.

1. INTRODUCTION

Human activities have had major impacts on the global environment. Since the beginning of the industrial era, mankind has increasingly made use of land, water, minerals and other natural resources, and continuous growth of the world human population and economies may further increase our impact on the environment. As the climate, biogeochemical processes and natural ecosystems are closely interlinked, changes in any one of these may affect the others and be detrimental to humans and other organisms. Emissions of anthropogenic gaseous species and particulate matter alter the energy balance of the atmosphere, which in turn has implications for the multiple interactions within the complex Earth's system. These interactions are not fully understood, partly due to the lack of high quality observations.

The World Meteorological Organization (WMO) established the Global Atmosphere Watch (GAW) Programme in 1989 to promote systematic and reliable observations of the global environment, including but not limited to greenhouse gases (*e.g.*, CO₂, CH₄, CFCs, and N₂O) and some reactive gases (*e.g.*, O₃, CO, VOCs, NO_x, and SO₂) in the atmosphere. In October 1990, WMO designated the Japan Meteorological Agency (JMA) in Tokyo to serve as the World Data Centre for Greenhouse Gases (WDCGG). The WDCGG is responsible for collecting, archiving and providing data on greenhouse and reactive gases in the atmosphere and oceans from a number of observational sites throughout the world that participate in GAW and other scientific monitoring programmes (Appendix: LIST OF OBSERVATIONAL STATIONS). In August 2002, the WDCGG took over the role of the World Data Centre for Surface Ozone from the Norwegian Institute for Air Research (NILU).

With regard to the issue of climate change the Kyoto Protocol to the United Nations Framework Convention on Climate Change came into force in February 2005. In March 2006, WMO commenced annual publication of the WMO Greenhouse Gas Bulletin, which summarizes the state of greenhouse gases in the atmosphere. The tenth issue of the Bulletin was published in November 2014. The WDCGG contributes to the production of the Bulletin through timely and adequate collection and analysis of data in cooperation with the contributors of the data.

Since its establishment, the WDCGG has provided its users with data and other information through its regular publications, including the *Data Summary* and *DVD* (Appendix: LIST OF WMO WDCGG PUBLICATIONS). In accordance with the GAW Strategic Plan: (2008–2015) and its Addendum, all data and information have been made available on the WDCGG web site, improving the accessibility of data, information and products (WMO, 2007a; WMO, 2011a). The WDCGG published the Data Submission and Dissemination Guide in 2007 (WMO, 2007b), which,

with its revision in 2009 (WMO, 2009b), is designed to facilitate submission of observational data and provide access to archived data in the WDCGG. Clear guidelines for data submission are included in the measurement guidelines published by GAW for the variables, which are under the responsibility of WDCGG.

The GAW Strategic Plan requests that World Data Centres assist data users by providing the data and analysis related to atmospheric observations. To this end, the WDCGG provides global and integrated diagnostics on the state of greenhouse and some reactive gases as analytical information in the *Data Summary*. The WDCGG global analysis method has been described in a GAW technical report (WMO, 2009a). The content of the *Data Summary* is revised and improved based on comments from data contributors and scientists. We hope the diagnostic information presented here will promote the use of data on greenhouse and reactive gases and will enhance appreciation of the value of the GAW Programme.

All users are required to accept the following statement endorsed by the Commission for Atmospheric Sciences (CAS) at its thirteenth session: “For scientific purposes, access to these data is unlimited and provided without charge. By their use you accept that an offer of co-authorship will be made through personal contact with the data providers or owners whenever substantial use is made of their data. In all cases, an acknowledgement must be made to the data providers or owners and to the data centre when these data are used within a publication.” The WDCGG requests data users to make appropriate acknowledgements. The principal investigators and other contacts can be obtained from the WDCGG website, as well as from the GAW Station Information System (GAWSIS) website, <http://gaw.empa.ch/gawsis/>. Information on these websites is updated in cooperation with the data contributors and the WMO Secretariat.

Finally, the WDCGG would like to thank all data contributors worldwide, including those involved in on-site measurements, for their efforts in maintaining the observational programmes and for continuous data provision.

Mailing address:

WMO World Data Centre for Greenhouse Gases (WDCGG)

c/o Japan Meteorological Agency

1-3-4, Otemachi, Chiyoda-ku, Tokyo 100-8122, Japan

E-mail: wdcgg@met.kishou.go.jp

Telephone: +81-3-3287-3439

Facsimile: +81-3-3211-4640

Web Site: <http://ds.data.jma.go.jp/gmd/wdcgg/>

2. ANALYSIS

The WDCGG gathers, archives and provides observational data on the mole fractions of greenhouse and some reactive gases, and publishes diagnostic information on these gases based on the reported data.

The long-term trends and seasonal variations in the mole fractions of CO₂, CH₄, N₂O and CO are calculated for the whole globe (global means) and for latitudinal belts (zonal means). Global long-term trends in the surface O₃, are not analyzed due to its substantial spatial gradients, and its uneven geographic distribution which is poorly covered by observational sites. Zonal mean time series for selected VOCs (ethane and propane) are also calculated. For halocarbons, NO_x and SO₂, only monthly mean mole fractions over time are presented without global, hemispheric or zonal averaging, due to insufficient number of reporting sites for each compound.

Mole fractions are expressed as parts per million (ppm), parts per billion (ppb), and parts per trillion (ppt), which correspond to the SI units of $\mu\text{mol/mol}$, nmol/mol and pmol/mol , respectively.

The method of analysis for CO₂, CH₄, N₂O and CO is summarized below. The details of the global analysis method are provided in the *Technical Report of Global Analysis Method for Major Greenhouse Gases by the World Data Centre for Greenhouse Gases*, published as a GAW technical report (WMO, 2009a). Additional uncertainty can be expected in the result of CO global analysis due to diversity of scales. When assessing long-term trends for CO₂, CH₄ and N₂O, the growth rates at both ends of the period were assumed to be simple linear extensions of the adjacent year, thus avoiding end effects. For simplicity, the rates for the rest of the period were approximated using linear functions.

(1) Site selection

For CO₂, CH₄ and N₂O, the diagnostic analyses, including global, hemispheric and zonal means, were based on data from sites that have adopted a standard scale traceable to the Primary Standard designated by WMO. These analyses also utilize data on other standard scales that are convertible to the WMO scale through a proven equation. Letters informing data submitters of the most recent WMO scales are sent out regularly by the WDCGG as well as discussed at the regular expert meetings (WMO, 2014a).

Selection of observational sites is also based on whether they provide data representing a reasonably large geographical area, considering the fact that some sites may be susceptible to local sources and sinks. Sites are selected objectively using data submitted to the WDCGG. For CO₂, CH₄ and CO, only those sites that provide annual mean mole fractions falling within

a range of $\pm 3\sigma$ from a curve fitted to the LOESS model curve (Cleveland and Devlin, 1988) have been selected, with outliers rejected in an iterative manner. This procedure does not affect the datasets residing in the WDCGG, and these data may be useful for purposes other than global analysis, such as identification of sources and sinks.

The sites selected according to the above criteria are marked with asterisks in Plate 3.1 for CO₂, Plate 4.1 for CH₄, Plate 5.1 for N₂O and Plate 8.1 for CO, which represent 124 (65%), 121 (74%), 33 (39%) and 113 (78%) of the submitted datasets respectively (detailed in 'LIST OF OBSERVATIONAL STATIONS' in this issue).

(2) Analysis of long-term trends

The mole fractions of greenhouse and reactive gases over time, measured under unpolluted conditions, exhibit variations on different time scales. The two major components are seasonal variations and long-term trends. Several attempts have been made to separate these various scales from the measured data, including objective curve fitting (Keeling *et al.*, 1989), digital filtering (Thoning *et al.*, 1989; Nakazawa *et al.*, 1991), or both (Conway *et al.*, 1994; Dlugokencky *et al.*, 1994).

In this report, seasonal variations derived from components of Fourier harmonics and long-term trends are extracted by low-pass filtering with a cut-off frequency of 0.48 year^{-1} for each selected site. Details are described in WDCGG *Data Summary* No. 22 (WMO, 2000).

(3) Estimation for missing periods and gaps

The number and distribution of sites used to assess trends during the analysis period should be kept as invariable as possible to avoid the effects of changes in the availability of data over time. However, only a small number of sites provided data throughout the entire analysis period; others may have covered shorter periods or had gaps in measurements due to different reasons. To use as many sites as possible, data for missing values are constructed using interpolation and extrapolation in the calculation of zonal means as described below.

Gaps in some data were filled by linear interpolation based on available data, by subtracting the seasonal variation calculated from the longest consecutive period of data with Lanczos filters (Duchon, 1979). The subtracted variation was added back to the data to obtain estimated mole fractions in a single sequence.

In the case of extrapolation, long-term trends from the existing or interpolated series of data were extrapolated based on zonal mean growth rates

calculated from other sites in the same latitudinal zone. The seasonal variation was added to the extrapolated long-term trend to obtain estimated mole fractions for the entire period of analysis.

Using these statistical procedures, the future addition of new stations should not affect the consistency in global estimates over time.

Nevertheless, while adding new sites in the analysis WDCGG performs calculations both with and without the new information to ensure the consistency of the global average calculations.

(4) Calculation of global, hemispheric and zonal means

Zonal means were calculated by determining the arithmetic average of the mole fractions in each latitudinal zone, based on consistent datasets derived as above.

Global and hemispheric means were calculated as the weighted averages of the zonal means taking account of the area of each latitudinal zone.

Deseasonalized long-term trends and growth rates for the globe, each hemisphere and each latitudinal zone were calculated from the global, hemispheric and zonal means, respectively, using the low-pass filter mentioned above and the time derivatives after filtering.

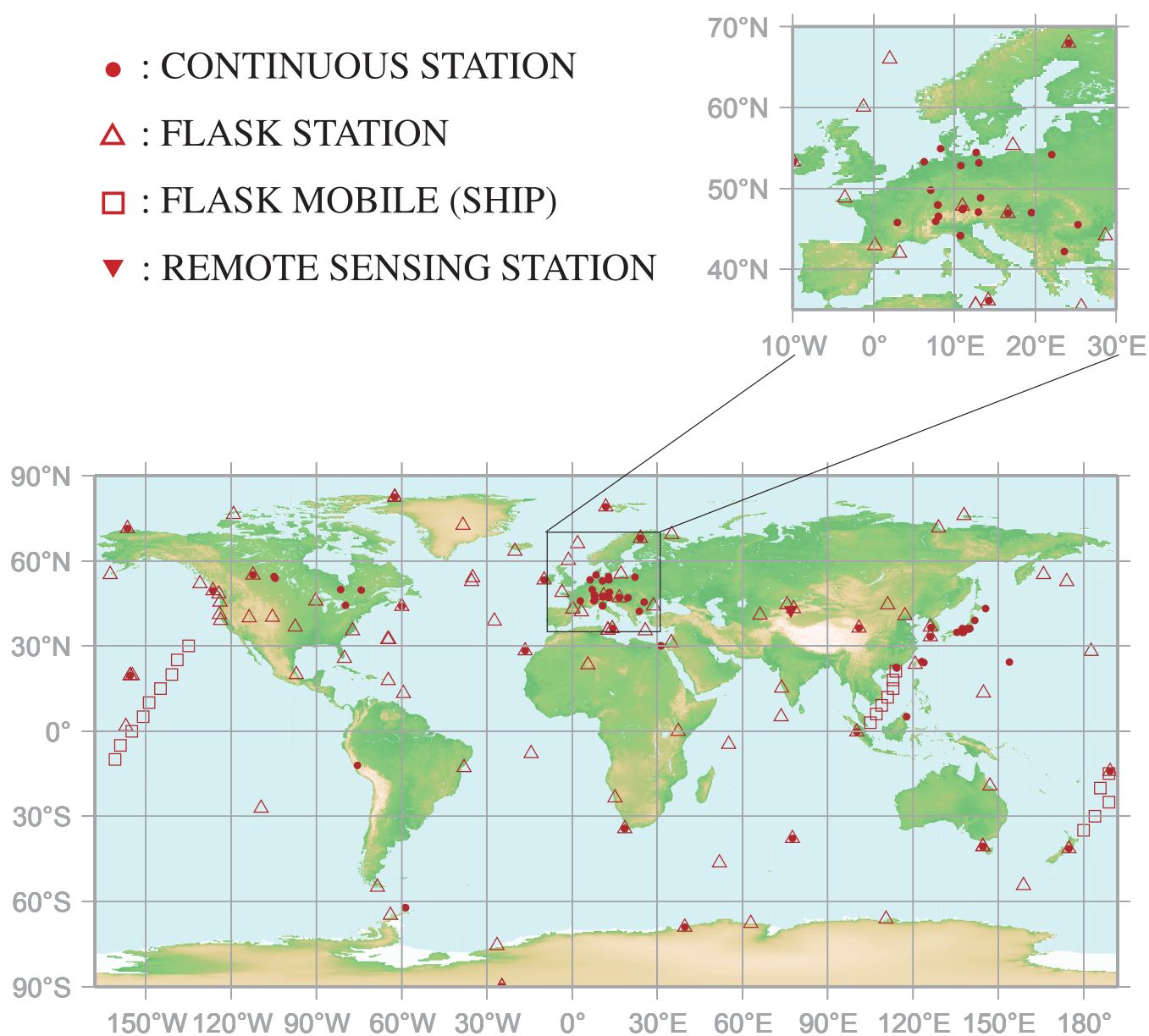
Error ranges estimated by a bootstrap method (Conway *et al.*, 1994) are included with the global means of major GHGs (CO₂, CH₄, N₂O and CO), where uncertainty is estimated as the standard deviation of many global means calculated by each bootstrap network.

3.

CARBON DIOXIDE

(CO₂)

- : CONTINUOUS STATION
- △ : FLASK STATION
- : FLASK MOBILE (SHIP)
- ▼ : REMOTE SENSING STATION



This map shows locations of the stations that have submitted data for monthly mean mole fractions.

CO₂ Monthly Data

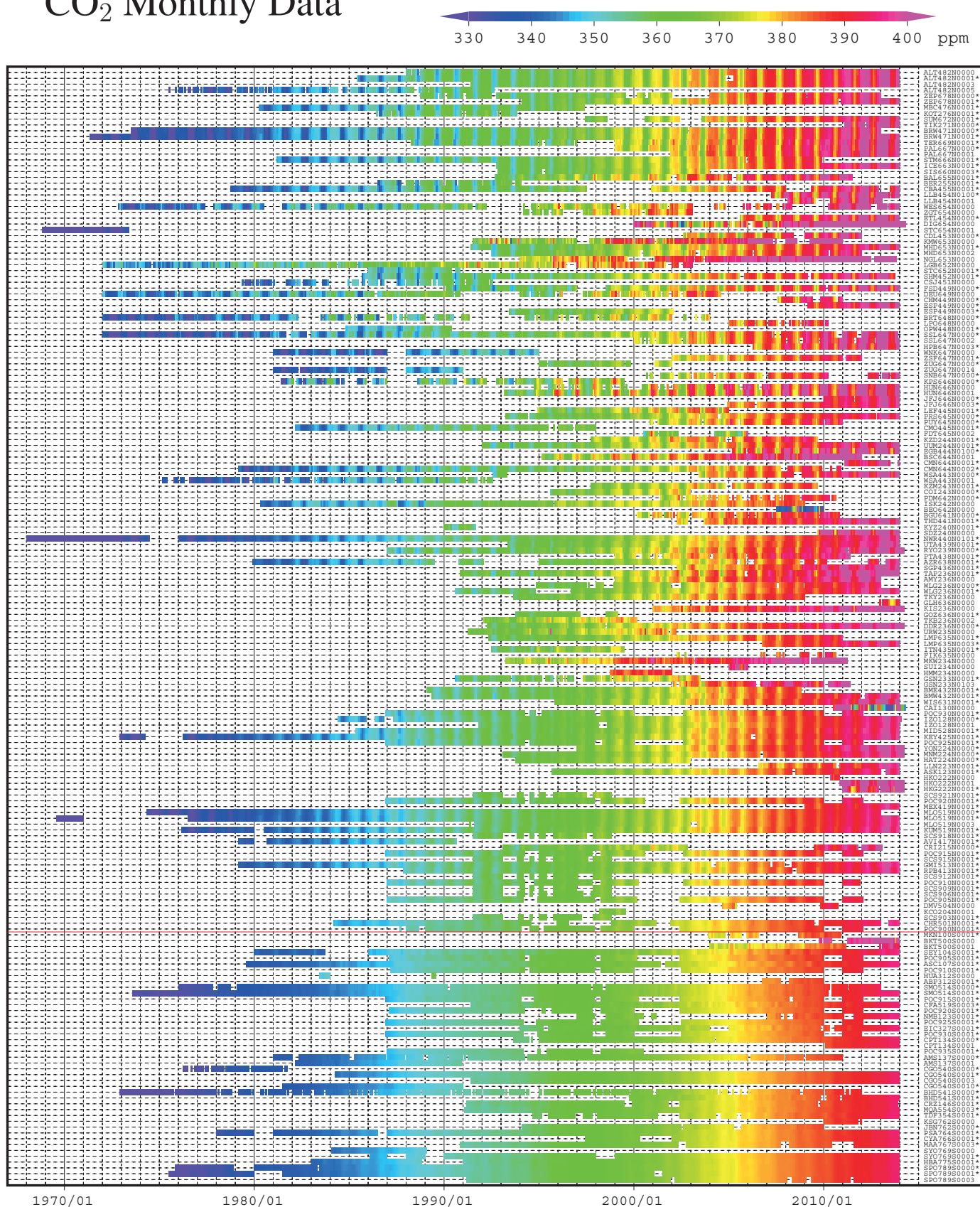
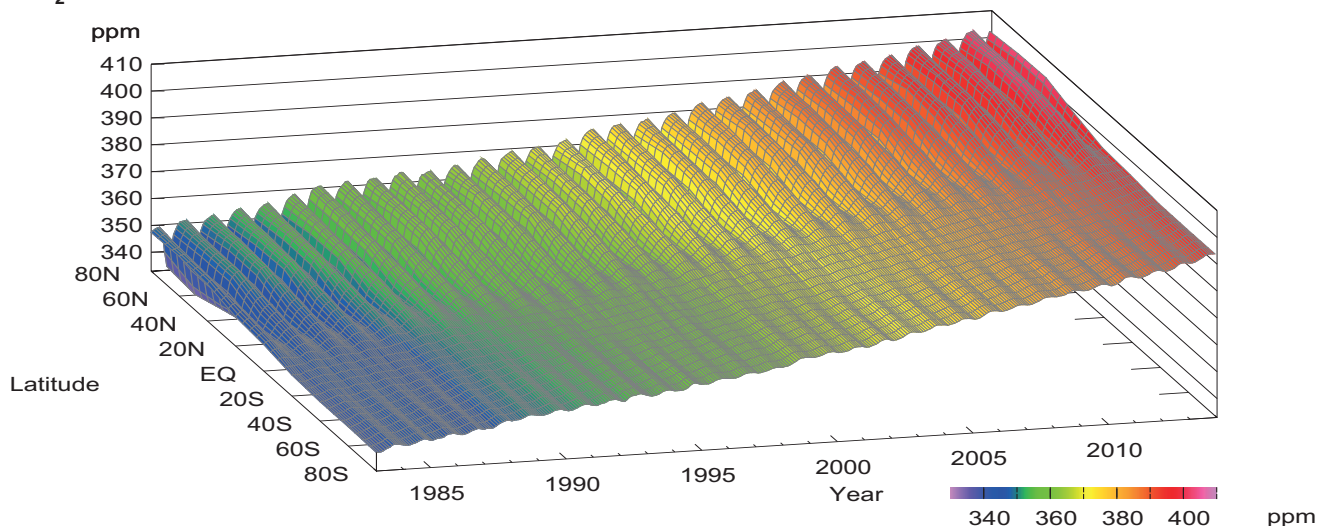
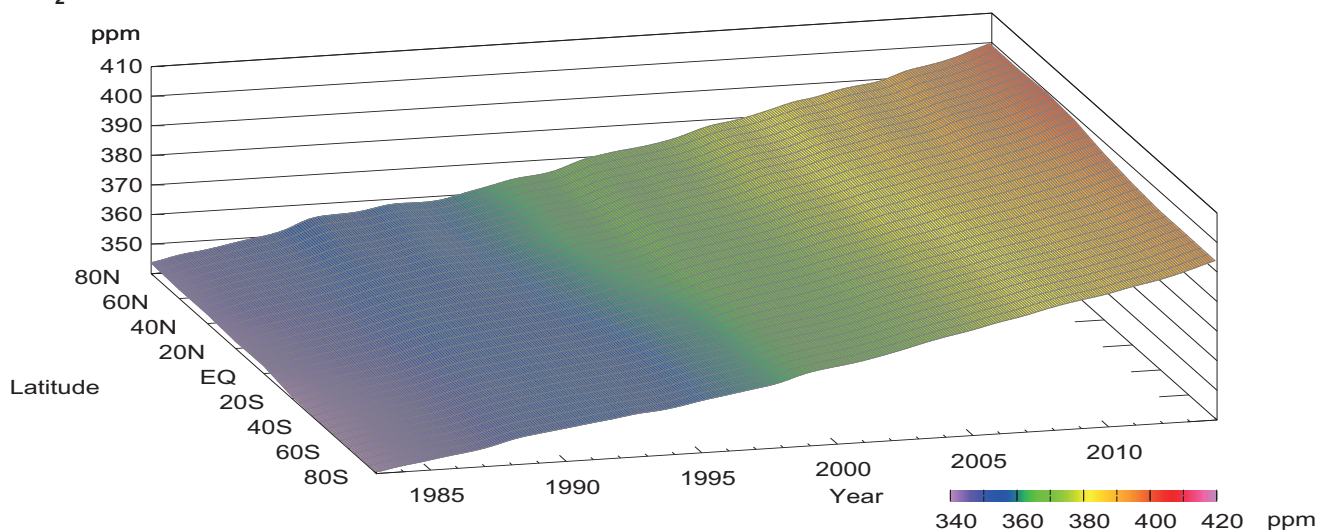


Plate 3.1 Monthly mean CO₂ mole fractions that have been reported to the WDCGG. The mole fractions are illustrated in different colors. The sites are listed in order from north to south. The red line indicates the equator. In cases where data are reported for two or three different altitudes, only the data at the highest altitudes are illustrated. In cases where monthly means are not reported, the WDCGG calculates them from hourly or other mole fractions reported to the WDCGG by simple arithmetic mean. The data from the sites with an asterisk at the end of the station index were used for the analyses shown in Plate 3.2. (see Chapter 2)

CO₂ mole fraction



CO₂ deseasonalized mole fraction



CO₂ growth rate

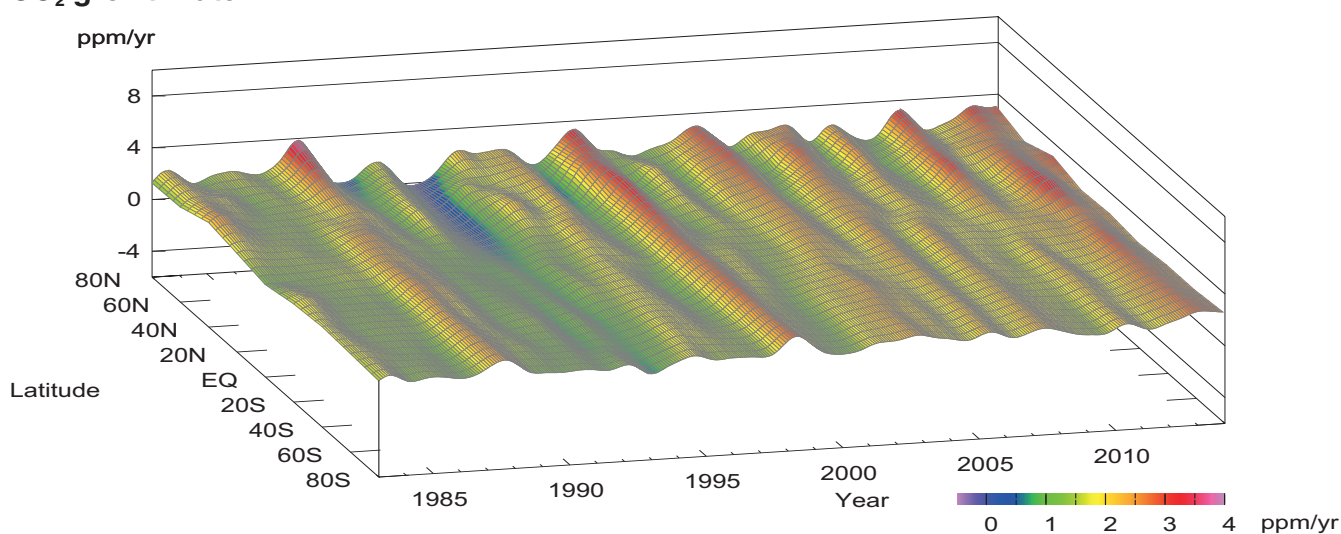


Plate 3.2 Variation of zonally averaged monthly mean CO₂ mole fractions (top), deseasonalized long-term trends (middle), and growth rates (bottom). The zonally averaged mole fractions were calculated for each 20° zone. The deseasonalized trends and growth rates were derived as described in Chapter 2.

3. CARBON DIOXIDE (CO₂)

Basic information on CO₂ with regard to environmental issues

Carbon dioxide (CO₂) has strong absorption bands in the infrared region and is the biggest anthropogenic contributor to anthropogenic greenhouse effect. CO₂ accounts for about 65% of total increase in the radiative forcing (since 1750) due to long-lived greenhouse gases in the atmosphere (WMO, 2014b). It is responsible for 84% of the increase in radiative forcing over the past decade and 83% over the past five years.

The balance of the fluxes between the atmosphere, the oceans and the biosphere determines the mole fraction of CO₂ in the atmosphere. An amount of 515 [445 to 585] PgC was emitted between 1870 and 2011 (IPCC, 2013) and annual anthropogenic emissions mainly due to fossil fuel combustion and cement production reached 9.7 ± 0.5 PgC in 2012 (<http://www.globalcarbonproject.org/>). Carbon in the atmosphere is exchanged with two other large reservoirs, the terrestrial biosphere and the oceans. CO₂ exchanges between the atmosphere and terrestrial biosphere occur mainly through absorption by photosynthesis and emission from the respiration of plants and the decomposition of organic soils. These biogenic activities vary seasonally, resulting in large seasonal variations in the level of CO₂. The direction of CO₂ exchange between the atmosphere and oceans is determined by the gradient of CO₂ mole fraction, and varies in time and space.

The current mole fractions of atmospheric CO₂ far exceed historic records, dating back at least 2.1 million years (Tans, 2009). Based on the results of ice core studies, the mole fraction of atmospheric CO₂ in pre-industrial times was about 278 ppm (IPCC, 2013). The emission of CO₂ due to human activities has increased dramatically since the beginning of the industrial era, impacting CO₂ exchange rates between different reservoirs and CO₂ levels not only in the atmosphere but in the oceans and terrestrial biosphere. The global carbon cycle, which is comprised mainly of CO₂, is not fully understood. About half of anthropogenic CO₂ emissions has remained in the atmosphere, with the remainder removed by sinks, including the terrestrial biosphere and oceans. However, the amount of CO₂ removed from the atmosphere varies significantly over time (Figure 3.1) without noticeable trend (Levin, 2012).

Carbon isotopic studies have shown the importance of the terrestrial biosphere and oceans as sources and sinks of CO₂ (Francey *et al.*, 1995; Keeling *et al.*, 1995; and Nakazawa *et al.*, 1993, 1997). In contrast, the atmospheric content of O₂ depends primarily on its removal by the burning of fossil fuels and on its release

from the terrestrial biosphere. Therefore, the uptake of carbon by the terrestrial biosphere and oceans can be estimated from the combination of measurements of O₂ (O₂/N₂) and CO₂ (Manning and Keeling, 2006; WMO, 2014b). A quasi-equilibrium amount of CO₂ is expected to be retained in the atmosphere by the end of the millennium that is surprisingly large: typically 40% of the peak concentration enhancement over pre-industrial values (278 ppm) (Solomon *et al.*, 2009).

Large amounts of CO₂ are exchanged among the reservoirs in nature, and the global carbon cycle is coupled with the climate system on seasonal, yearly and decadal time scales. Complete understanding of the global carbon cycle is essential for estimating future CO₂ mole fractions in the atmosphere.

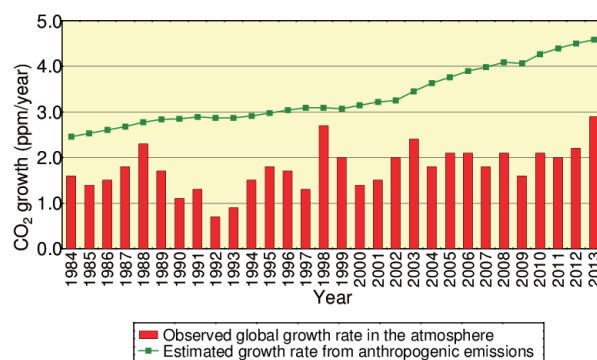


Fig. 3.1 Annual mean growth rates of CO₂ in the atmosphere, calculated from observational data (red columns) and from data for anthropogenic emissions (green curve). The estimated growth rates were calculated using CO₂ emissions as a proxy (from CDIAC, Boden *et al.*, 2013). The values from 2011 to 2013 are estimations of Carbon Dioxide Information Analysis Center (CDIAC), expressed as moles divided by the total mass of gas in the atmosphere (5.2 petatonnes) converted to moles based on the mean molar mass of dry air (about 29.0 g/mol). The observed growth rates were calculated by the WDCGG. The observed CO₂ abundance is expressed as mole fraction with respect to dry air, while the CO₂ amount calculated from anthropogenic emissions is based on the atmosphere, including water vapor, usually in a proportion less than 1%.

Mole fractions of CO₂ can be analyzed utilizing data submitted to the WDCGG from fixed stations and some ships. The observational sites from which data were used for the analysis are shown on the map at the beginning of this chapter. They include fixed stations performing continuous measurements as well as flask-sampling stations, including those in the NOAA/ESRL cooperative air sampling network. In

addition, mobile platforms such as ships and aircraft and other stations observing on an event basis report their data to the WDCGG (see Appendix: LIST OF OBSERVATIONAL STATIONS), which are not used for global analysis.

Annual variation of CO₂ mole fraction in the atmosphere

The monthly mean mole fractions of CO₂ used in the analysis are shown in Plate 3.1, with mole fraction levels illustrated in different colors. Global, hemispheric and zonal mean mole fractions were analyzed based on data from selected stations under unpolluted conditions (see the caption for Plate 3.1). Zonally averaged mole fractions of atmospheric CO₂, together with their deseasonalized components and growth rates, are shown as three-dimensional representations in Plate 3.2. These plots show that the seasonal variations in mole fraction are large in northern high and mid-latitudes, but are indistinct in the Southern Hemisphere. The increases in the Northern Hemisphere precede those in the Southern Hemisphere by one or two years, and the interannual variations in growth rate are larger in the Northern Hemisphere.

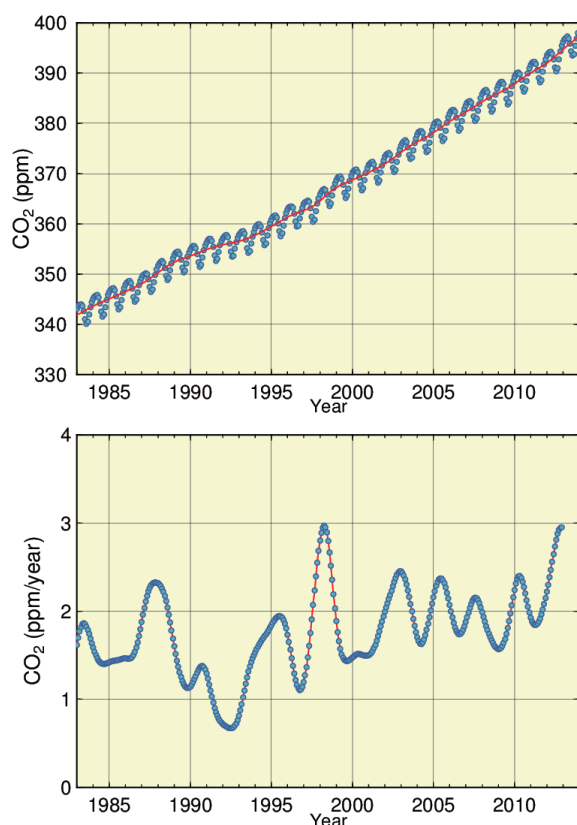


Fig. 3.2 Global monthly mean mole fraction of CO₂ from 1983 to 2013, including deseasonalized long-term trend shown as a red line (top) and annual growth rate (bottom).

Figure 3.2 shows global monthly mean CO₂ mole fractions and their growth rates from 1983 to 2013. The global average mole fraction reached a new high of 396.0 ± 0.1 ppm in 2013, which is 142% of the pre-industrial level of 278 ppm. The 2.9 ppm annual increase in 2012-2013 was the largest year to year change in the period 1984 to 2013 and much greater than the average growth rate for the 1990s (about 1.5 ppm/year) and that of the past decade (about 2.1 ppm/year).

The global growth rate shows large interannual variations, with an instantaneous maximum of about 3 ppm/year in 1998 and a minimum below 1 ppm/year in 1992. There were short periods of high rates in 1987/1988, 1997/1998, 2002/2003, 2005/2006, 2007, 2009/2010 and 2012/2013.

Figure 3.3 shows monthly mean mole fractions and long-term trends from 1983 to 2013 for each 30° latitudinal zone, indicating that there were clear long-term increases in both hemispheres and seasonal variations in the Northern Hemisphere.

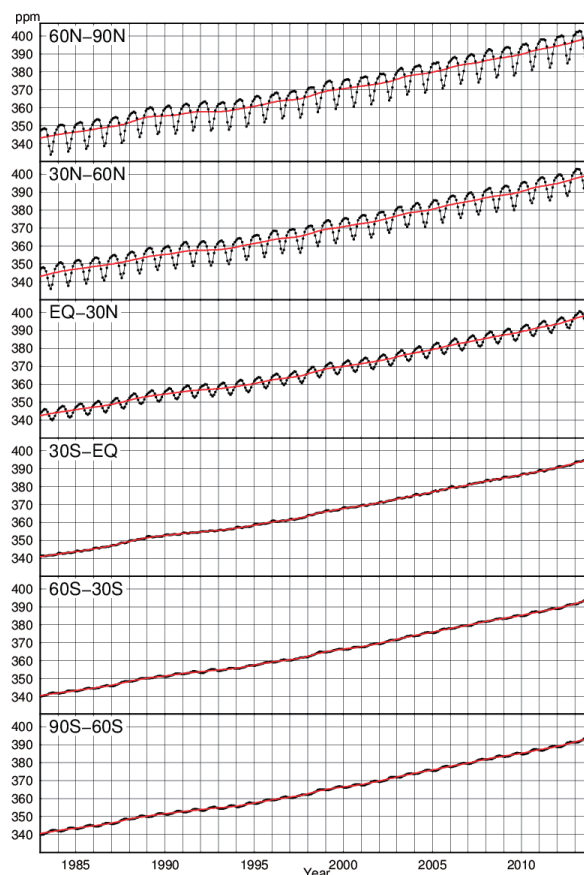


Fig. 3.3 Monthly mean mole fractions of CO₂ from 1983 to 2013 for each 30° latitudinal zone (dots) and their deseasonalized long-term trends (red lines).

As shown in Figure 3.4, the growth rates for each 30° latitudinal zone fluctuated between -0.3 and 3.6

ppm/year, with the largest interannual variability in northern high latitudes. High growth rates for all 30° latitudinal zones were observed in 1987/1988, 1997/1998, 2002/2003, 2005, 2007, 2010 and 2012/2013, with negative rates recorded in northern high latitudes in 1992.

Changes in growth rate are partly associated with ENSO. The El Niño events in 1982/1983, 1986–1988, 1991/1992, 1997/1998, 2002/2003 and 2009/2010 coincided with high growth rates of CO₂, apart from in 1992, 2005/2006 and 2012/2013. The growth rates of CO₂ observed by aircraft at high altitudes (8–13 km) over the Pacific Ocean were also associated with ENSO (Matsueda *et al.*, 2002).

During El Niño events, the up-welling of CO₂-rich ocean water in the eastern equatorial Pacific is suppressed, resulting in reduced CO₂ emissions from this area. El Niño events induce high temperature anomalies in many areas, particularly in the tropics, resulting in increased CO₂ emissions from the terrestrial biosphere due to the enhanced respiration of plants and activated decomposition of organic matter in soil (Keeling *et al.*, 1995). This effect is enhanced by the suppression of plant photosynthesis in areas of anomalously low precipitation, particularly in the tropics. These oceanic and terrestrial processes during El Niño events have opposing effects, but Heimann and Reichstein (2008) suggested that the latter was the main cause of the variation in the CO₂ growth rate.

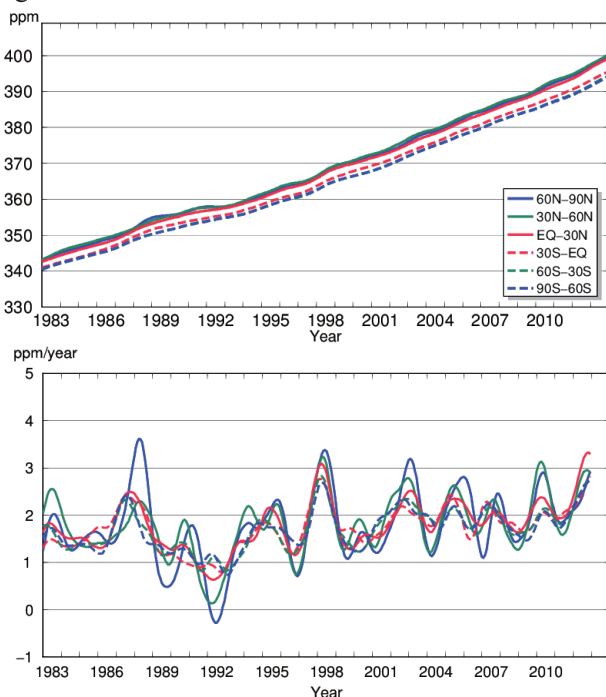


Fig. 3.4 Long-term trends in the mole fractions of CO₂ for each 30° latitudinal zone (top) and their growth rates (bottom) .

However, an exceptionally low CO₂ growth rate

occurred during the El Niño event in 1991/1992. The injection of 14 - 20 megatonnes (Mt) of SO₂ aerosols into the stratosphere by the Mount Pinatubo eruption in June 1991 affected the radiation budget and atmospheric circulation (Hansen *et al.*, 1992; Stenchikov *et al.*, 2002), resulting in a drop in global temperature. Angert *et al.* (2004) suggested that the low CO₂ growth rate observed during this El Niño event was due to reduced CO₂ emissions caused by consequent changes in the respiration of terrestrial vegetation and the decomposition of organic matter (Conway *et al.*, 1994; Lambert *et al.*, 1995; Rayner *et al.*, 1999), and by enhanced CO₂ absorption due to intensive photosynthesis caused by an increase in diffuse radiation (Gu *et al.*, 2003).

In contrast, exceptionally high CO₂ growth rates occurred in 2005/2006 and 2012/2013. That in the former period may have been related to the global high temperature. That in the latter period may be the result of small changes in fluxes between the atmosphere and terrestrial biosphere (WMO, 2014b). Typically, ~120 PgC is exchanged between the atmosphere and terrestrial biosphere annually. This accounts for the observed seasonal cycle in atmospheric CO₂ abundance in the Northern Hemisphere. Small interannual variability (1-2%) in these fluxes, either from a change in the balance between photosynthesis and respiration or the amount of biomass burned, have a large impact on the growth rate of CO₂ (~4 PgC /yr).

Seasonal cycle of CO₂ mole fraction in the atmosphere

Figure 3.5 shows average seasonal cycles in the mole fraction of CO₂ for each 30° latitudinal zone. The seasonal cycles are clearly large in amplitude in northern high and mid-latitudes and small in the Southern Hemisphere. The seasonal cycle in the Northern Hemisphere is mainly dominated by the land biosphere (Nevison *et al.*, 2008), and it is characterized by rapid decreases from June to August and large returns from September to December.

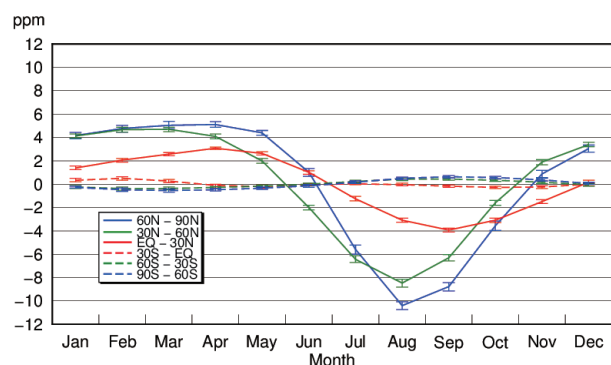


Fig. 3.5 Average seasonal cycles in the mole fractions of CO₂ for each 30° latitudinal zone obtained by subtracting long-term trends from the zonal mean time series. Vertical error bars represent the range of $\pm 1\sigma$ which is calculated for each month. (Averages from 1983 to 2013)

The mole fractions of CO₂ in northern low latitudes lagged behind that in high latitudes by one or two months. Minimum values appeared in August in northern high and mid-latitudes and in September in northern low latitudes.

In the Southern Hemisphere, seasonal variations showed small amplitudes with a half-year delay due to small amounts of net emission and absorption by the terrestrial biosphere. Seasonal variations in both northern and southern mid-latitudes were apparently superimposed in southern low latitudes (0–30°S). The direct influence of sources and sinks in the Southern Hemisphere may be partially cancelled by the propagation of an antiphase variation from the Northern Hemisphere.

Figure 3.6 shows latitudinal distributions of the mole fractions of CO₂ in January, April, July and October 2013, from sites marked with an asterisk in Plate 3.1. In latitudes north of 30°N, the mole fractions increased towards higher latitudes in January and April, and decreased towards higher latitudes in July, corresponding to the large seasonal variations in northern high and mid-latitudes, variations associated with activities of the terrestrial biosphere.

It can be seen that during periods of seasonal maximum many stations in the Northern Hemisphere observed monthly mean CO₂ mole fractions above the “symbolic” threshold of 400 ppm.

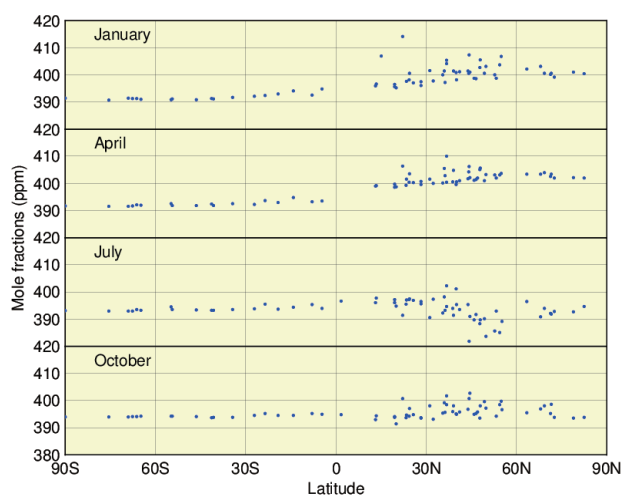


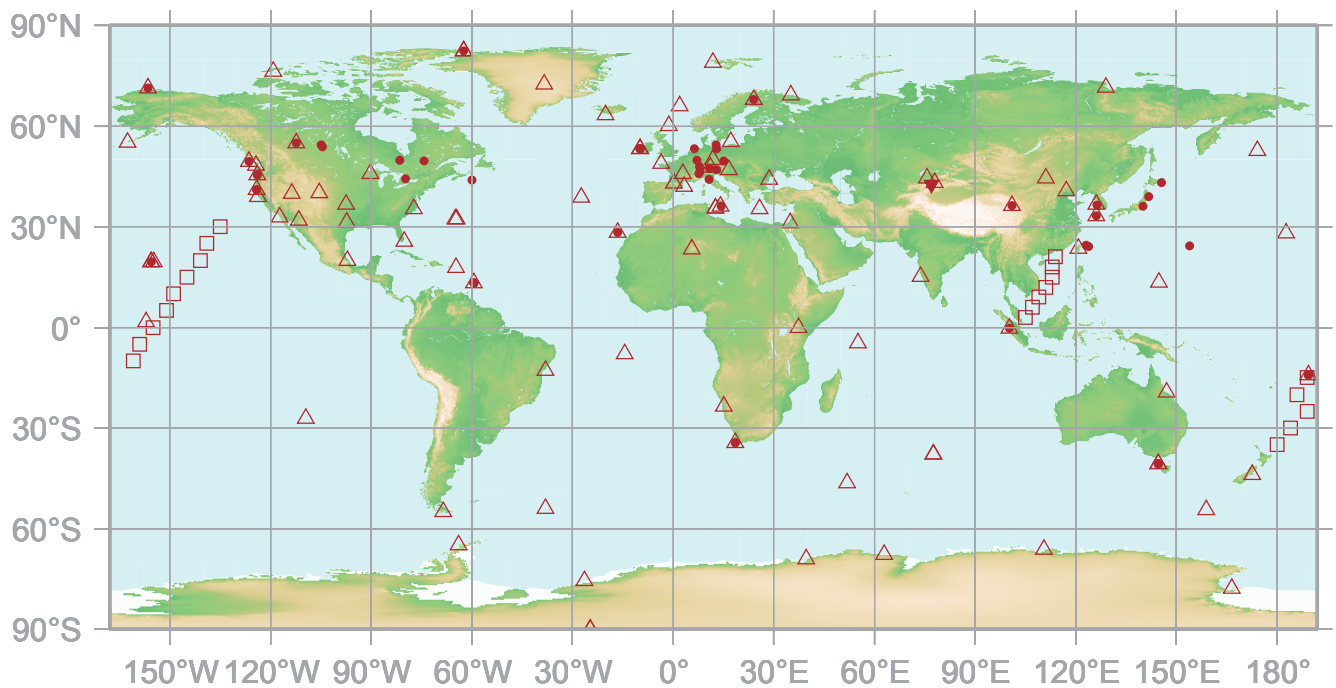
Fig. 3.6 Latitudinal distributions of the monthly mean mole fractions of CO₂ in January, April, July and October 2013.

4.

METHANE

(CH₄)

- : CONTINUOUS STATION
- △ : FLASK STATION
- : FLASK MOBILE (SHIP)
- ▼ : REMOTE SENSING STATION



This map shows locations of the stations that have submitted data for monthly mean mole fractions.

CH₄ Monthly Data

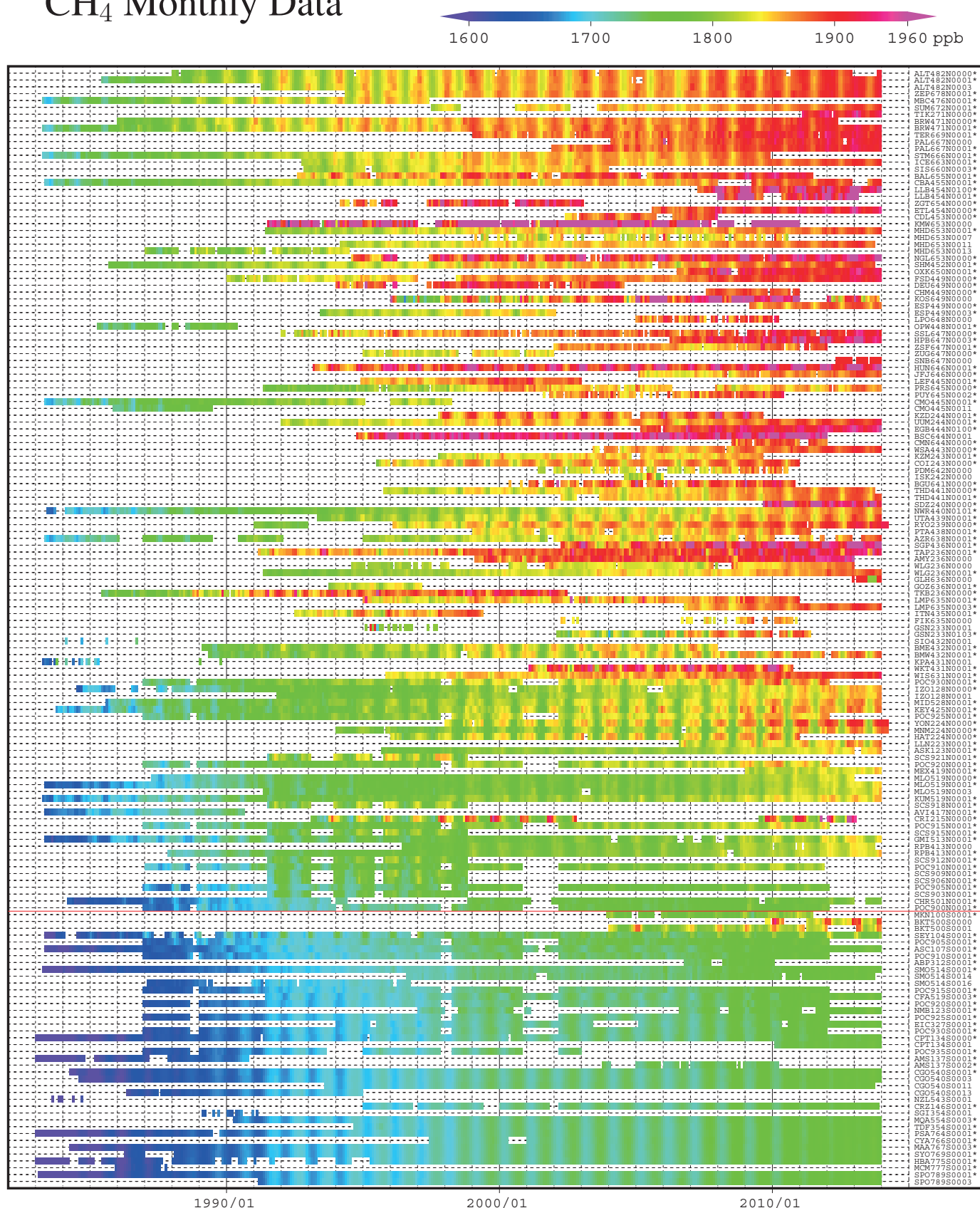
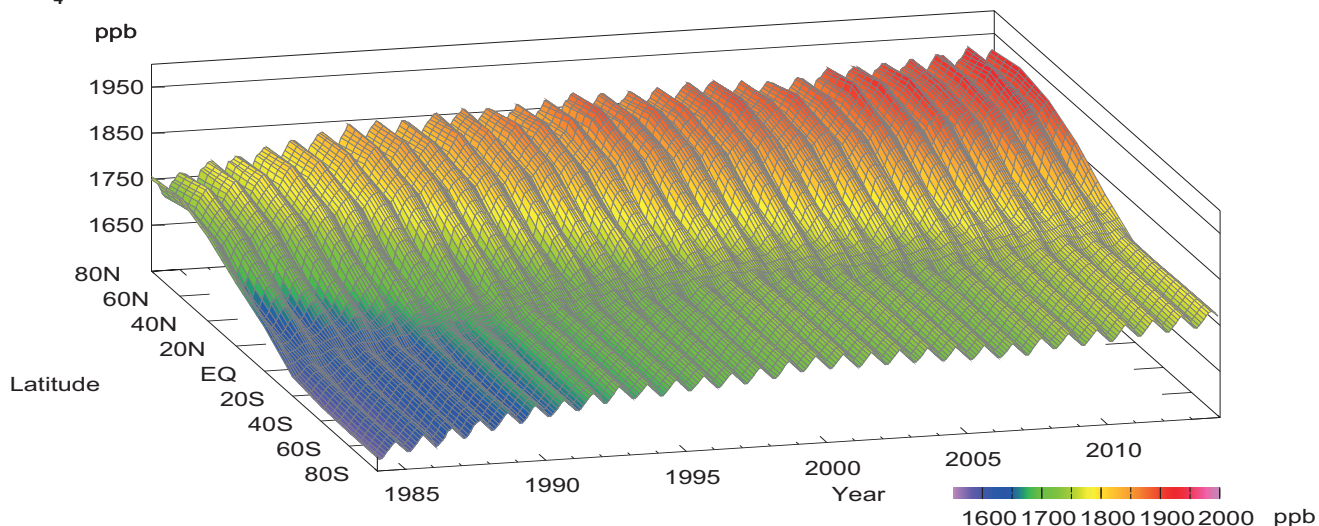
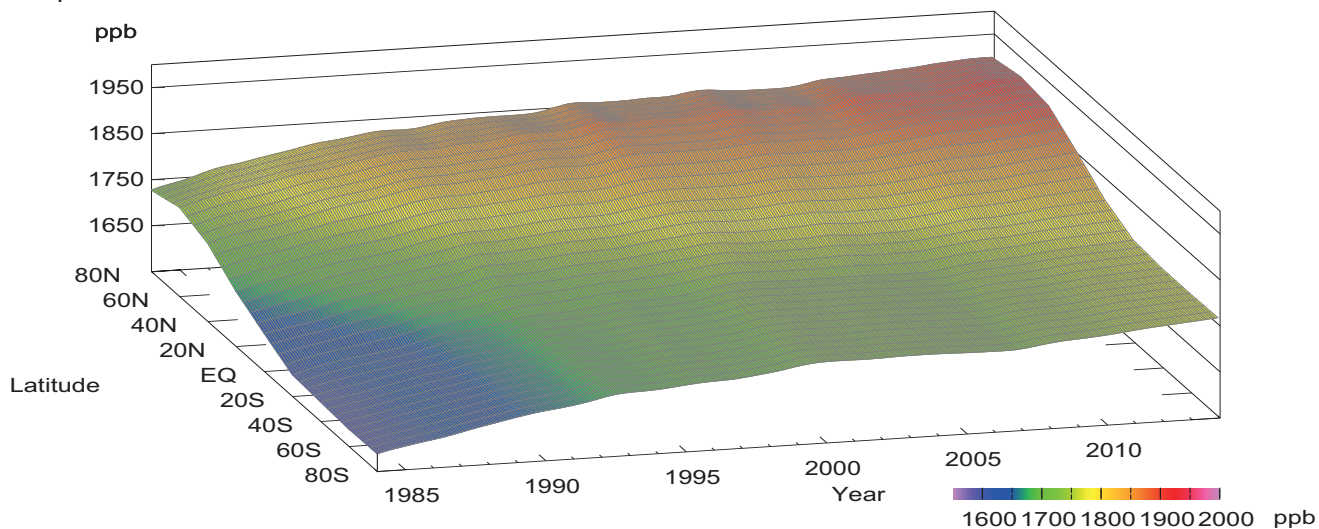


Plate 4.1 Monthly mean CH₄ mole fractions that have been reported to the WDCGG. The mole fractions are illustrated in different colors. The sites are listed in order from north to south. The red line indicates the equator. In cases where data are reported for two or three different altitudes, only the data at the highest altitudes are illustrated. In cases where monthly means are not reported, the WDCGG calculates them from hourly or other mole fractions reported to the WDCGG by simple arithmetic mean. The data from the sites with an asterisk at the end of the station index were used for the analyses shown in Plate 4.2. (see Chapter 2)

CH₄ mole fraction



CH₄ deseasonalized mole fraction



CH₄ growth rate

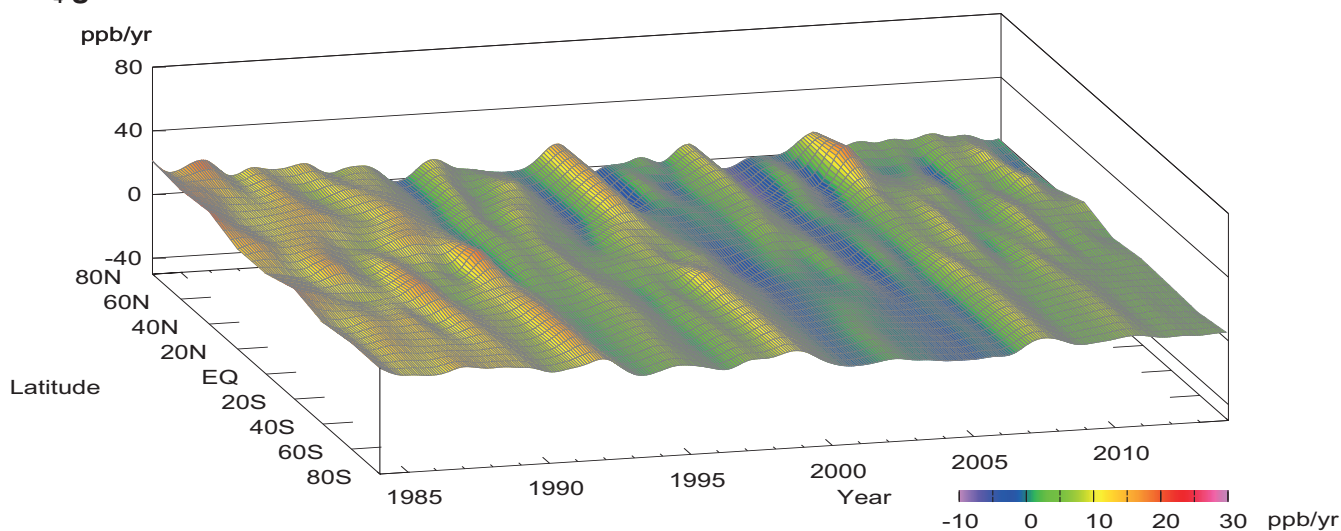


Plate 4.2 Variation of zonally averaged monthly mean CH₄ mole fractions (top), deseasonalized long-term trends (middle), and growth rates (bottom). The zonally averaged mole fractions were calculated for each 20° zone. The deseasonalized trends and growth rates were derived as described in Chapter 2.

4. METHANE (CH₄)

Basic information on CH₄ with regard to environmental issues

Methane (CH₄) is the second most important anthropogenic greenhouse gas, with an estimated global warming potential per molecule 28 times greater over a 100 year horizon and 84 times greater over a 20 years horizon than CO₂ (IPCC, 2013). Between 1750 and 2013, CH₄ accounted for about 17% of the total increase in radiative forcing due to long-lived greenhouse gases in the atmosphere (WMO, 2014).

Analyses of air trapped in ice cores from Antarctica and the Arctic revealed that the current atmospheric CH₄ mole fraction is the highest over the last 680,000 years (Nisbet *et al.*, 2014). The mole fraction of CH₄ remained at about 700 ppb from 1000 A.D. until the start of the industrial era when it started increasing. Measurements in ice cores have shown that inter-polar differences in CH₄ mole fractions between Greenland and Antarctica ranged from 24 to 58 ppb between 1000 and 1800 A.D. (Etheridge *et al.*, 1998). Atmospheric observations show that difference of the mole fractions between the high latitudinal belts of the Northern and Southern Hemisphere (see Fig 4.3) averaged over the years 1984 to 2013 reached about 140 ppb. Increase in the inter-hemispheric gradient reflects the dominant impact of the emissions from the Northern Hemisphere, where major anthropogenic and natural sources are situated. Increased emissions from the Arctic have not contributed to the continued increase in atmospheric CH₄ since 2007 (WMO, 2013), though have had an impact on annual increase in 2007.

CH₄ is emitted by both natural and anthropogenic sources, including natural wetlands, oceans, landfills, rice paddies, enteric fermentation, fossil fuel production and consumption and biomass burning. The global emission of CH₄ was 548 teragrams (Tg) CH₄ per year, with about 60% related to anthropogenic activities (<http://www.globalcarbonproject.org/methanebudget/13/hl-compact.htm>). CH₄ is removed from the atmosphere by reaction with hydroxyl radicals (OH) in both the troposphere and stratosphere, and by reaction with chlorine atoms and O(¹D), an excited state of oxygen, in the stratosphere. CH₄ is one of the most important sources of water vapor in the stratosphere and has an atmospheric lifetime of about 10 years. More information regarding sources and sinks of CH₄ must be collected to better understand the budget of atmospheric CH₄.

Mole fractions of CH₄ are analyzed using data submitted to the WDCGG from fixed stations and some ships. These observational sites are shown on the map at the beginning of this chapter.

Annual variation of CH₄ mole fraction in the atmosphere

The monthly mean dry mole fractions of CH₄ used in this analysis are shown in Plate 4.1, with the mole fraction levels illustrated in different colors. Global, hemispheric and zonal mean mole fractions have been calculated based on data from selected stations under unpolluted conditions (see the caption for Plate 4.1). Zonally averaged atmospheric CH₄ mole fractions, together with their deseasonalized components and growth rates, are shown as three-dimensional representations in Plate 4.2. These plots show that the seasonal variations in CH₄ mole fraction are larger in the Northern than in the Southern Hemisphere and that the increase in the Northern Hemisphere propagates to the Southern Hemisphere. The growth rates vary on a global scale with the patterns similar to those for CO₂ (see Chapter 3). There is a large latitudinal gradient in CH₄ mole fraction from the northern mid-latitudes to the tropics, suggesting major sinks in the tropics, where the mole fraction of OH radicals is higher.

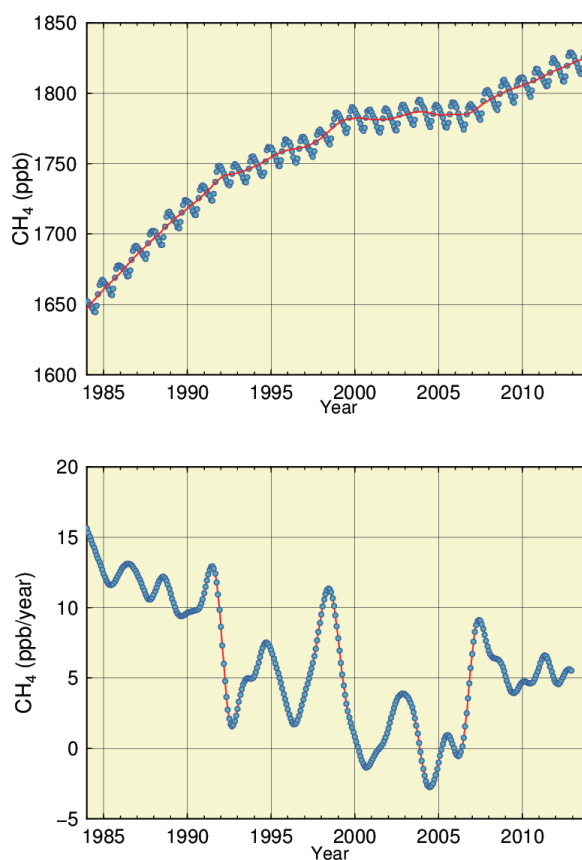


Fig. 4.1 Global monthly mean mole fraction of CH₄ from 1984 to 2013, including deseasonalized long-term trend in red line (top) and annual growth rate (bottom).

Figure 4.1 shows globally averaged monthly mean mole fractions and the growth rates for CH₄ from 1984 to 2013. The global average mole fraction was 1824±2 ppb in 2013, an increase of 6 ppb from 2012. The mole fraction changed little between 1999 and 2006. The mean annual absolute increase during the last 10 years was 3.8 ppb/year. The current mole fraction is 253% of its pre-industrial level of 722 ppb (based on IPCC (2013), the estimated pre-industrial CH₄ value was updated from previous summaries).

Figure 4.2 shows monthly mean mole fractions from 1984 to 2013 for each 30° latitudinal zone. The smallest magnitude of the seasonal variations is occurred in the latitudinal zone between the equator and 30°S.

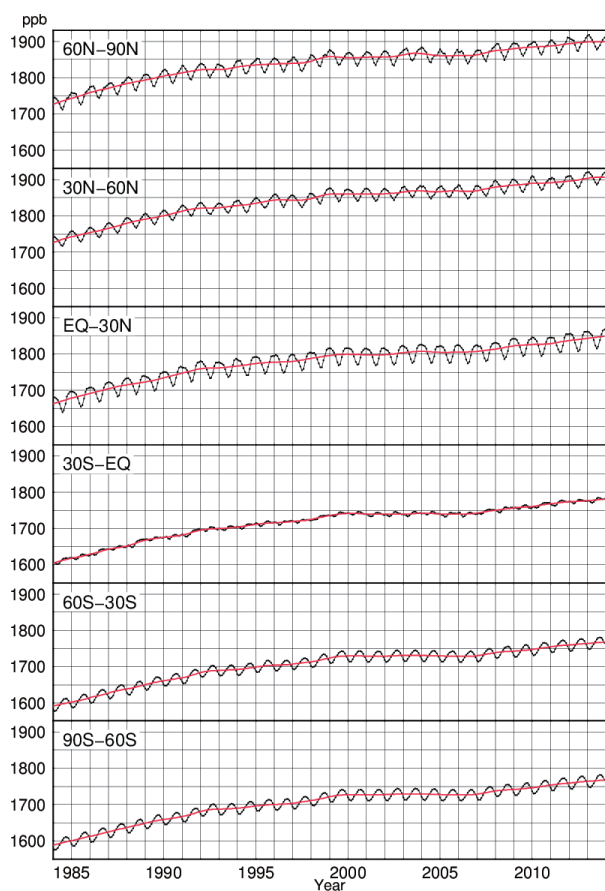


Fig. 4.2 Monthly mean mole fractions of CH₄ from 1984 to 2013 for each 30° latitudinal zone (dots) and their deseasonalized long-term trends (red lines).

Figure 4.3 summarizes deseasonalized long-term trends for each 30° latitudinal zone and their growth rates. A latitudinal gradient between the high and mid-latitudes of the Northern and Southern Hemispheres is practically missing, while the difference between high/mid-latitudes and low latitudes of the Northern Hemisphere is larger than

similar difference in the Southern Hemisphere. Fig. 4.3 also shows that mole fractions in most latitudinal belts have similar tendencies. In the 1990s, the growth rates clearly decreased in all latitudinal zones, but remained positive. The declined growth rate was especially evident during the second half of 1992, in 1996, and almost even in 1999 and in 2004/2005, when growth rates were less than 5 ppb/year in all latitudes. During the year 1998, the maximum global growth rate reached about 11 ppb/year (Fig. 4.1). Maximum increases occurred in high and mid-latitudes of the Northern Hemisphere, where the growth rates exceeded 15 ppb/year. In 2000 and 2001, the global growth rate decreased to around -1 ppb/year. Around 2002/2003, the growth rates increased in the Northern Hemisphere, especially in northern high latitudes where they exceeded 10 ppb/year. The global growth rate was as low as -3 ppb/year in 2004 and 1 ppb/year in 2005. Despite the large growth rates in 1998 and 2002/2003, during El Niño events, the global mean mole fraction was relatively stable between 1999 and 2006. However, the global mean mole fraction increased on average by 5.6 ppb/year in the last seven years through 2013.

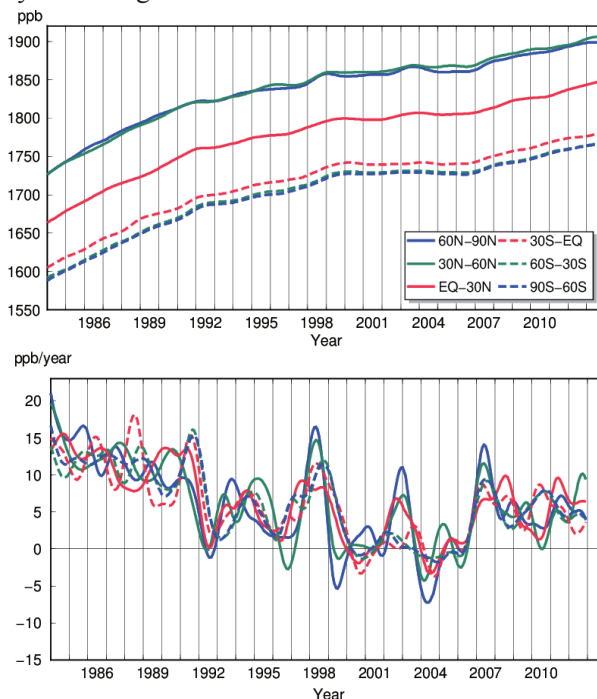


Fig. 4.3 Long-term trends in the mole fractions of CH₄ for each 30° latitudinal zone (top) and their growth rates (bottom).

The large increase in CH₄ growth rate in 1991 may have been caused by decreased levels of OH radicals in the atmosphere due to reduced UV radiation resulting from the eruption of Mt. Pinatubo in 1991 (Dlugokencky *et al.*, 1996), and the subsequent decrease in 1992 may have been due to an increase in OH radicals resulting from the depletion of

stratospheric ozone following this eruption (Bekki *et al.*, 1994).

In 1998, the growth rates were high in all latitudes, which may have been due to increased emissions in northern high latitudes and tropical wetlands caused by high temperatures and increased precipitation, as well as by biomass burning in boreal forests, mainly in Siberia (Dlugokencky *et al.*, 2001). In contrast, Morimoto *et al.* (2006) estimated from isotope observations that the contribution of biomass burning to the increase in 1998 was about half that of wetlands. The growth rates were low from 1999 to 2006, with an exception during the El Niño event of 2002/2003. The causes of these decreases and increases in CH₄ growth rates are not yet determined.

Since 2007, atmospheric CH₄ has increased significantly throughout the entire monitoring network (Rigby *et al.*, 2008; Dlugokencky *et al.*, 2009). This is due to increased emissions in the tropical and mid-latitude Northern Hemisphere (Nisbet *et al.*, 2014). The attribution of this increase to anthropogenic and natural sources is difficult because the current network is insufficient to characterize emissions by region and source process (Bergamaschi *et al.*, 2013).

The WMO/GAW observational network includes the observations of carbon stable isotopes in methane, with 20 datasets submitted to the WDCGG. Such observations can be useful for the identification of primary methane sources.

Seasonal cycle of CH₄ mole fraction in the atmosphere

Figure 4.4 shows seasonal cycles in the mole fraction of CH₄ for each 30° latitudinal zone. The seasonal cycles are driven mainly by reaction with OH radicals, a major CH₄ sink in the atmosphere. Seasonal cycles are also affected by the magnitude and timing of CH₄ emissions from sources such as wetlands and biomass burning as well as by its atmospheric transport. The seasonal cycles are large in amplitude in the Northern Hemisphere. Unlike CO₂, amplitudes were also large in high and mid-latitudes of the Southern Hemisphere. Seasonally, the Northern Hemisphere shows minima in summer and maxima in winter, while the Southern Hemisphere shows a seasonal cycle lagging two-thirds to three-quarter years behind. The seasonal variations in the mole fraction of CH₄ were almost consistent with those of the OH radical that reacts with CH₄. Southern low latitudes have a distinct antiphase annual component with that of the seasonal cycle arising from southern mid-latitudes. The maximum in the former component occurs in boreal winter due to the interhemisphere transport of CH₄ from the Northern Hemisphere.

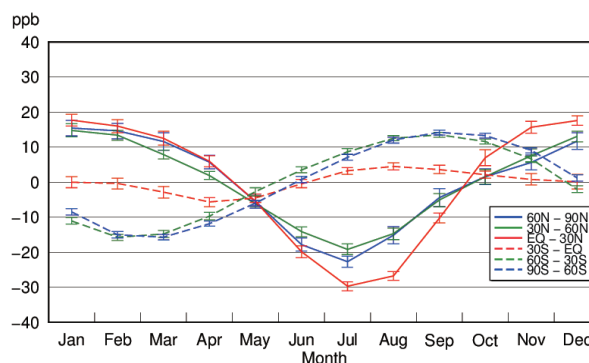


Fig. 4.4 Average seasonal cycles of CH₄ mole fractions for each 30° latitudinal zone obtained by subtracting long-term trends from the zonal mean time series. Vertical error bars represent the range of $\pm 1\sigma$ calculated for each month. (Averages from 1984 to 2013)

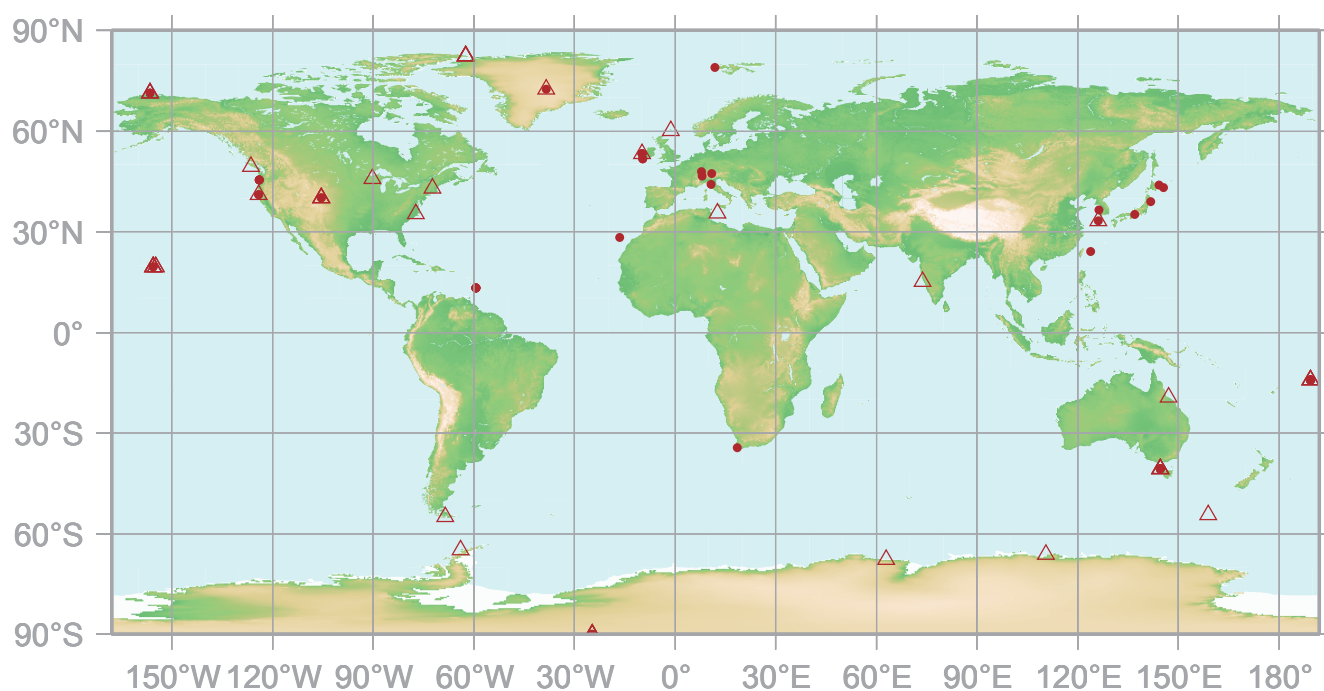
5.

NITROUS OXIDE

(N₂O)

● : CONTINUOUS STATION

△ : FLASK STATION



This map shows locations of the stations that have submitted data for monthly mean mole fractions.

N₂O Monthly Data

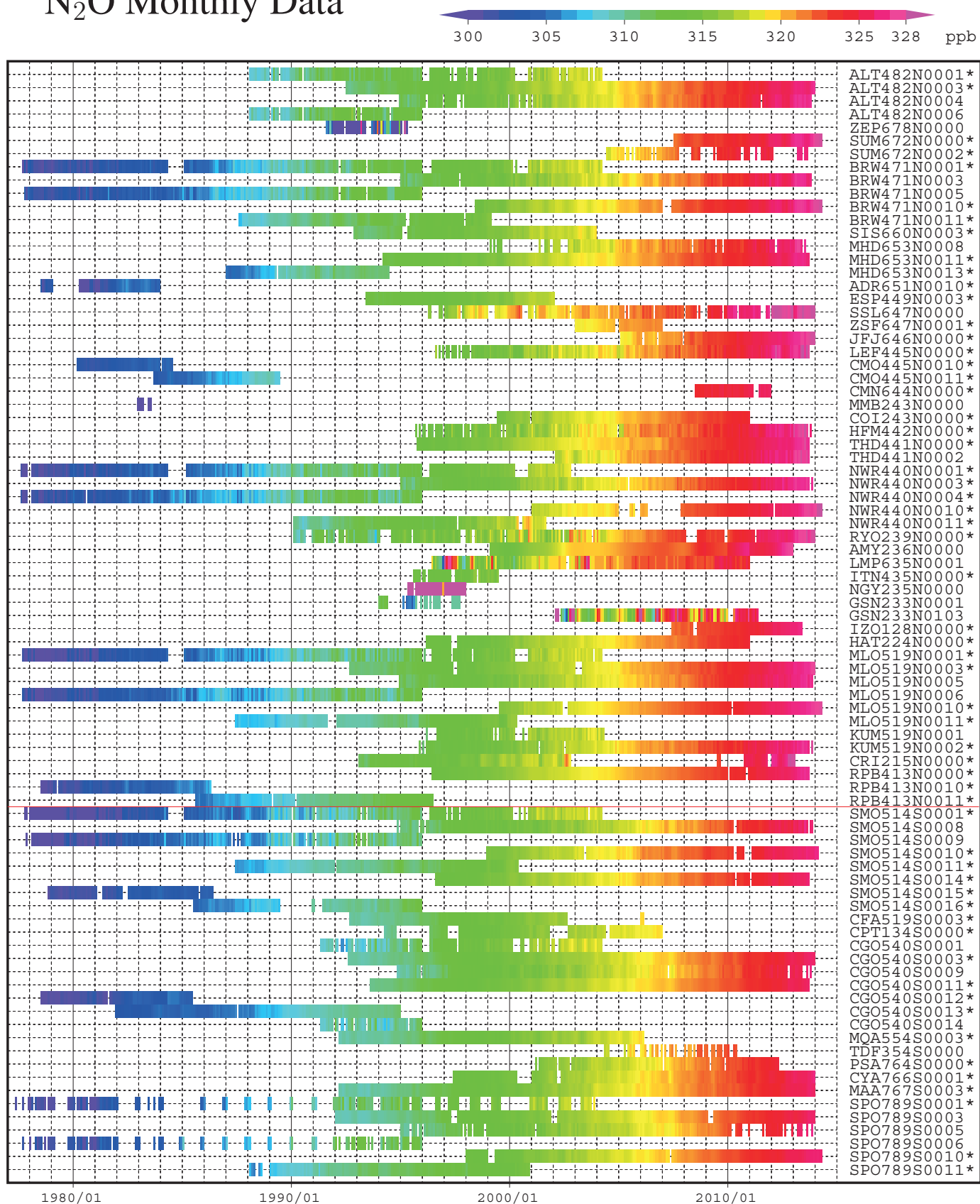
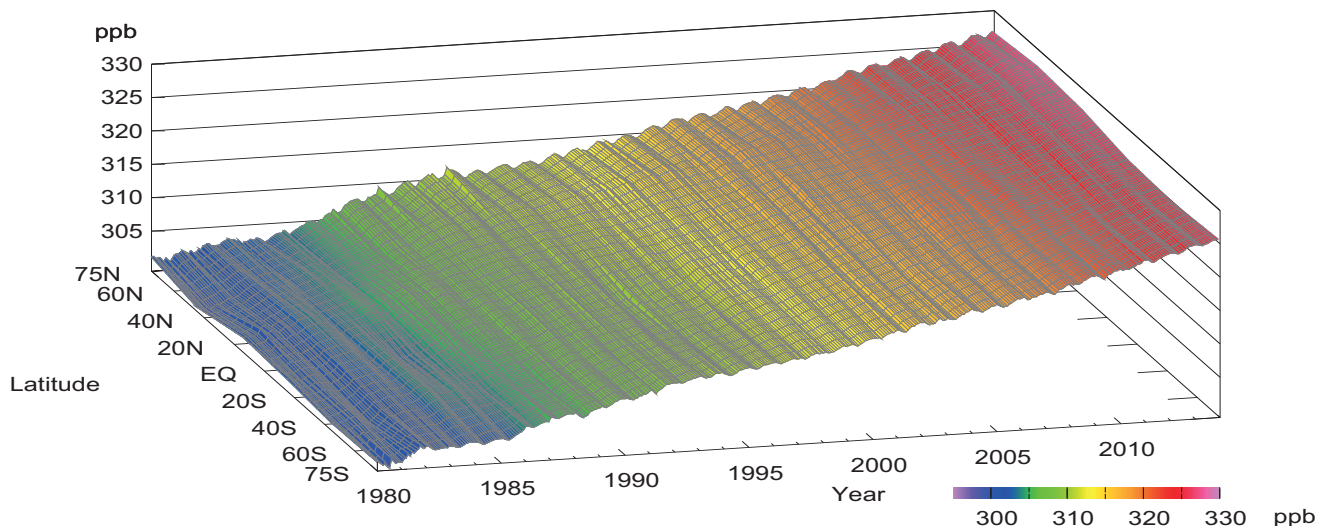
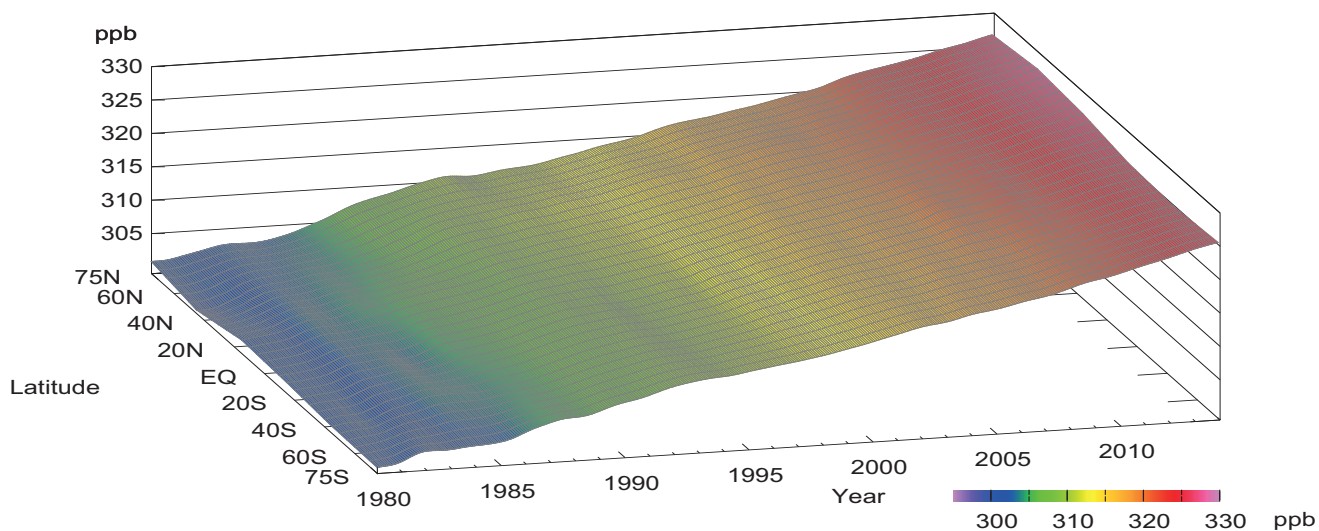


Plate 5.1 Monthly mean N₂O mole fractions that have been reported to the WDCGG. The mole fractions are illustrated in different colors. The sites are listed in order from north to south. The red line indicates the equator. The data from the sites with an asterisk at the end of the station index were used for the analyses shown in Plate 5.2. (see Chapter 2)

N₂O mole fraction



N₂O deseasonalized mole fraction



N₂O growth rate

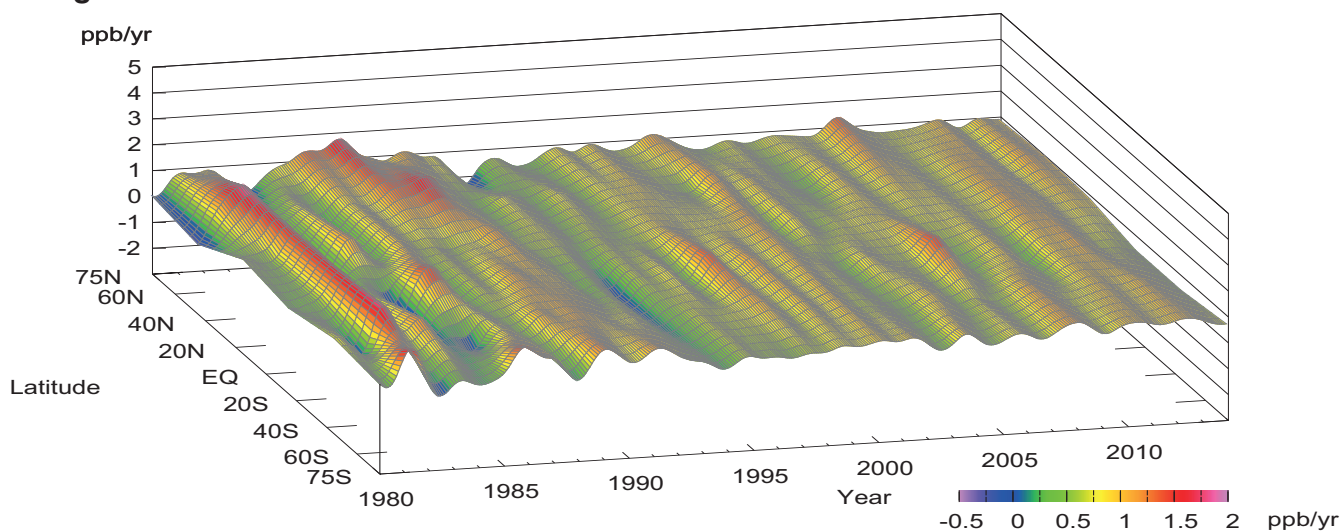


Plate 5.2 Variation of zonally averaged monthly mean N₂O mole fractions (top), deseasonalized long-term trends (middle), and growth rates (bottom). The zonally averaged mole fractions were calculated for each 30° zone. The deseasonalized trends and growth rates were derived as described in Chapter 2.

5. NITROUS OXIDE (N₂O)

Basic information on N₂O with regard to environmental issues

Nitrous oxide (N₂O) is a relatively stable greenhouse gas in the troposphere with a lifetime of 121 years (IPCC, 2013). Between 1750 and 2013, N₂O accounted for about 6% of the total increase in radiative forcing due to long-lived greenhouse gases (WMO, 2014b). N₂O is the third most important anthropogenic greenhouse gas in the atmosphere. It also plays an important role in stratospheric ozone depletion (Ravishankara *et al.*, 2009). The mole fraction of N₂O in the atmosphere has increased steadily from its pre-industrial level of 270 ppb to its current value, which is 21% higher. Prior to industrialization, the atmospheric N₂O burden reflected the balance between emissions from natural systems (soils and oceans), and chemical losses in the stratosphere. In the industrial era, additional emissions result from use of synthetic nitrogen fertilizers (direct emissions from agricultural fields and indirect emissions from waterways affected by agricultural runoff), fossil fuel combustion, biomass burning and other minor processes.

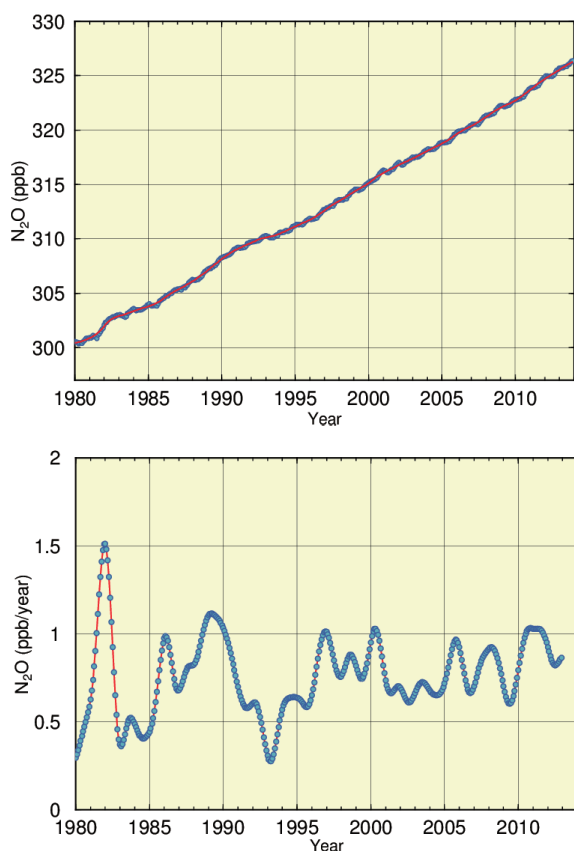


Fig. 5.1 Globally averaged monthly mean mole fraction of N₂O from 1980 to 2013, including deseasonalized long-term trend shown as a red line (top) and annual growth rate (bottom).

Currently, anthropogenic sources are responsible for ~40% of total emissions or about 16 TgN/year (WMO, 2014b). Most of the anthropogenic N₂O enters the atmosphere from the transformation of fertilizer nitrogen into N₂O and its subsequent emission from agricultural soils.

However, more research are needed to understand the role of N₂O in the global nitrogen cycle.

Long-term trend of N₂O mole fraction in the atmosphere

Dry mole fractions of N₂O are analyzed using the data submitted to the WDCGG from fixed stations and some ships. The observational sites that supplied data used for this analysis are shown on the map at the beginning of this chapter. The monthly mean mole fractions of N₂O, including the ones used in the global analysis, are shown in Plate 5.1, with the various mole fraction levels illustrated in different colors. The data submitted to the WDCGG show that N₂O mole fractions have increased at almost all stations. Zonally averaged atmospheric N₂O mole fractions, together with their deseasonalized components and growth rates, are shown as three-dimensional representations from 1980 to 2013 in Plate 5.2.

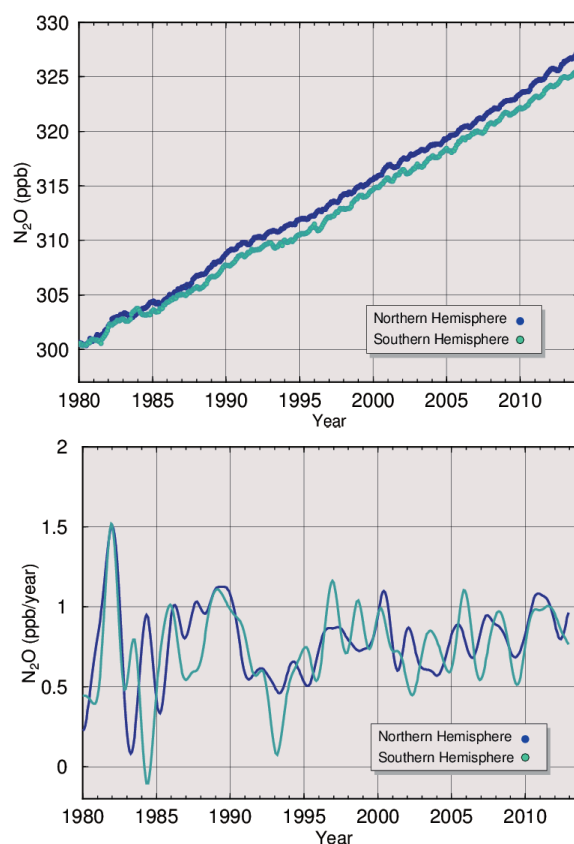


Fig. 5.2 Monthly mean mole fractions of N₂O from 1980 to 2013 (top) and annual growth rates (bottom), averaged over the Northern and Southern Hemispheres.

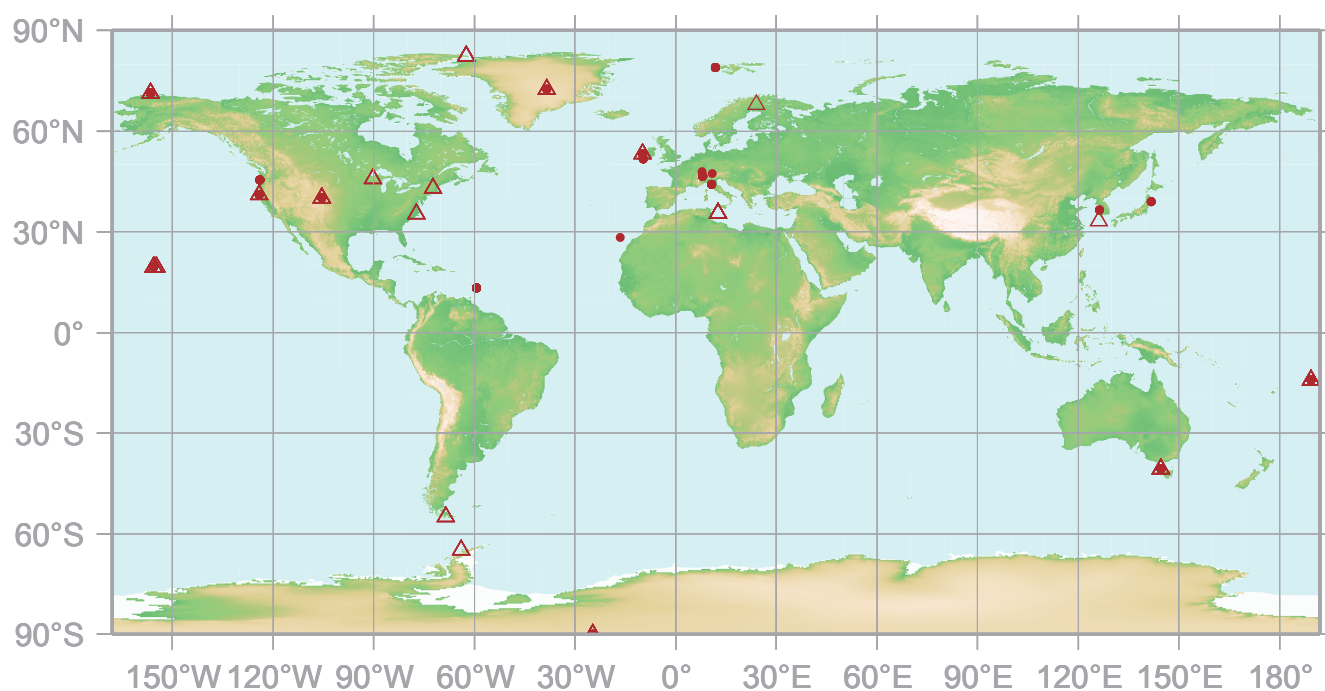
Figure 5.1 shows globally averaged monthly mean N_2O mole fractions from 1980 to 2013 and its long-term trend. The global average mole fraction reached a new high of 325.9 ± 0.1 ppb in 2013, an increase of 0.8 ppb over the previous year. The mean annual absolute increase during the last 10 years was 0.82 ppb/year. Annual averages of atmospheric growth rate showed substantial variability (from 0.4 to 1.1 ppb/year) from the beginning of observations. The interhemispheric gradient in the yearly averaged mole fraction of N_2O rose from 0.0 ppb in 1980 to 1.6 ppb in 2013 (Figure 5.2 upper panel), indicating that the majority of N_2O sources are situated in the Northern Hemisphere.

6.

HALOCARBONS AND OTHER HALOGENATED SPECIES

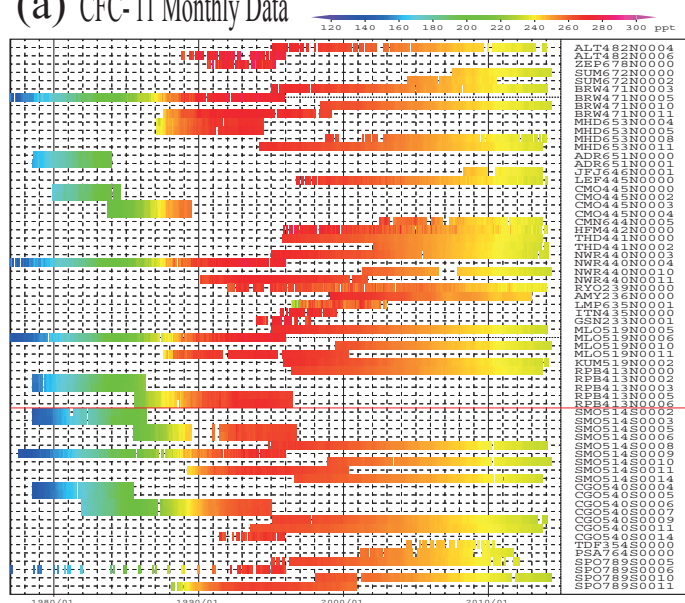
● : CONTINUOUS STATION

△ : FLASK STATION

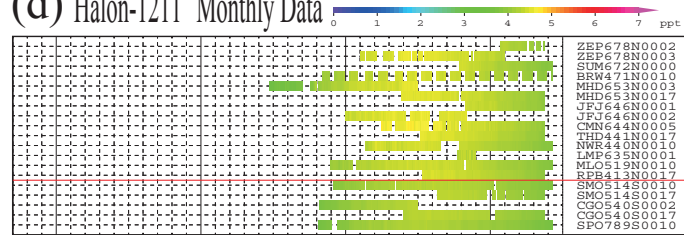


This map shows locations of the stations that have submitted data for monthly mean mole fractions.

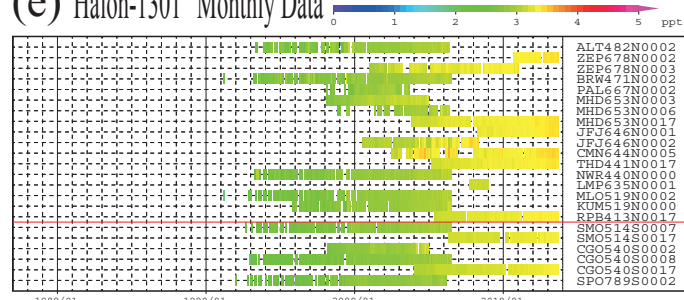
(a) CFC-11 Monthly Data



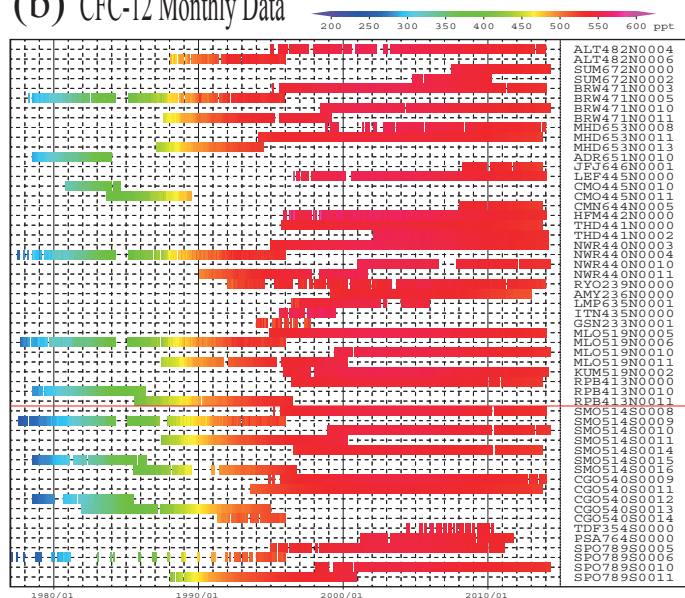
(d) Halon-1211 Monthly Data



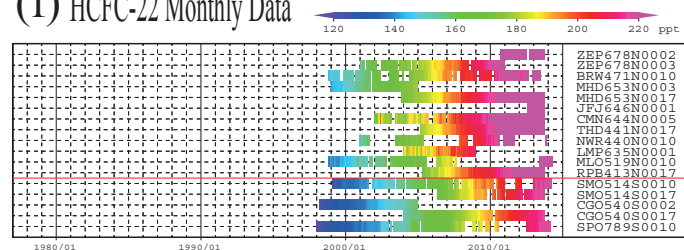
(e) Halon-1301 Monthly Data



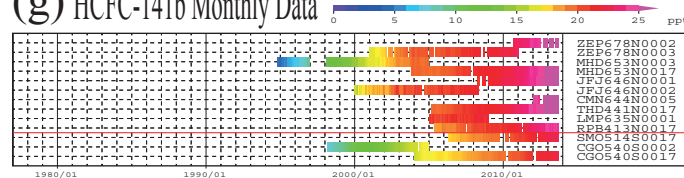
(b) CFC-12 Monthly Data



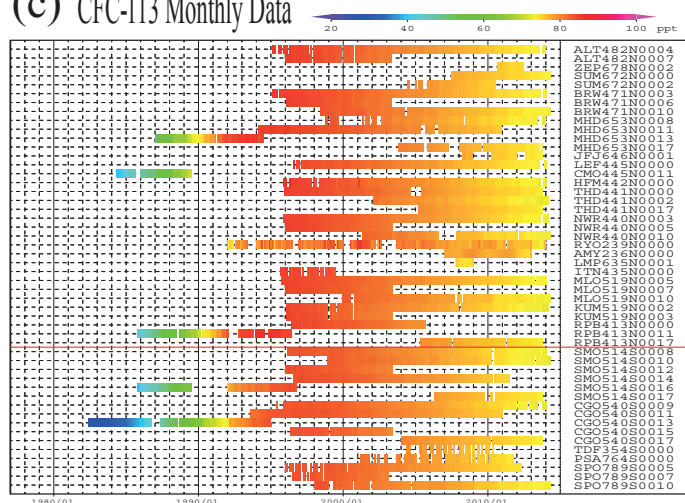
(f) HCFC-22 Monthly Data



(g) HCFC-141b Monthly Data



(c) CFC-113 Monthly Data



(h) HCFC-142b Monthly Data

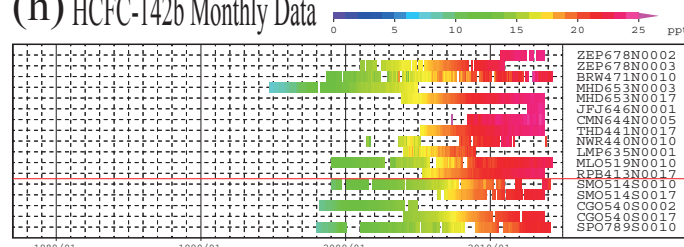
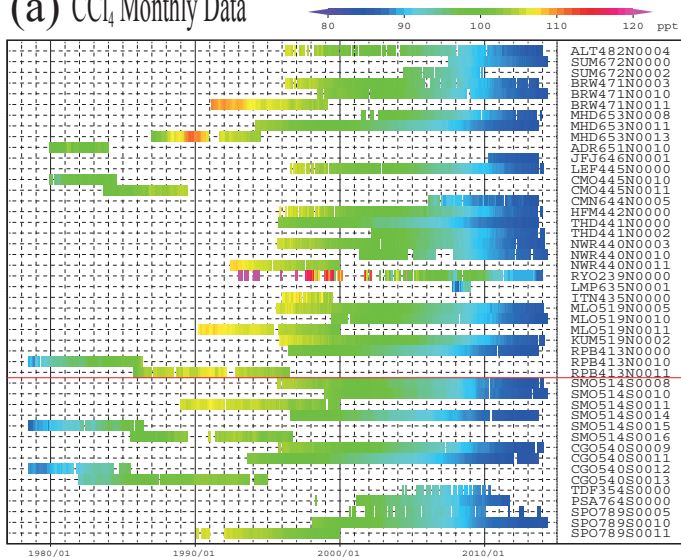
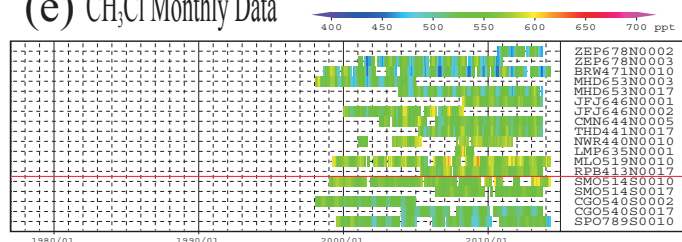


Plate 6.1 Monthly mean (a) CFC-11, (b) CFC-12, (c) CFC-113, (d) Halon-1211, (e) Halon-1301, (f) HCFC-22, (g) HCFC-141b, (h) HCFC-142b mole fractions that have been reported to the WDCGG. The mole fractions are illustrated in different colors. The sites are listed in order from north to south. The red line indicates the equator.

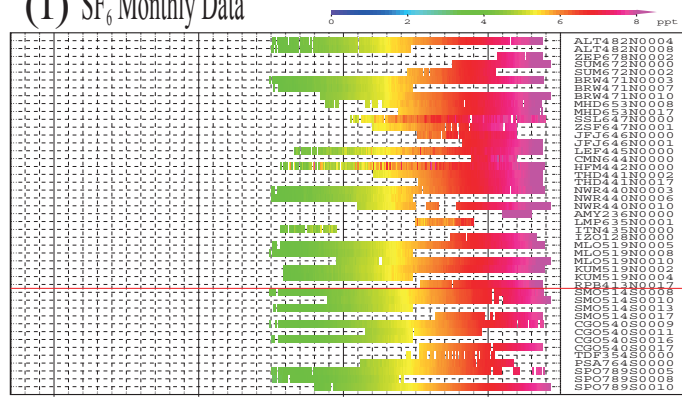
(a) CCl_4 Monthly Data



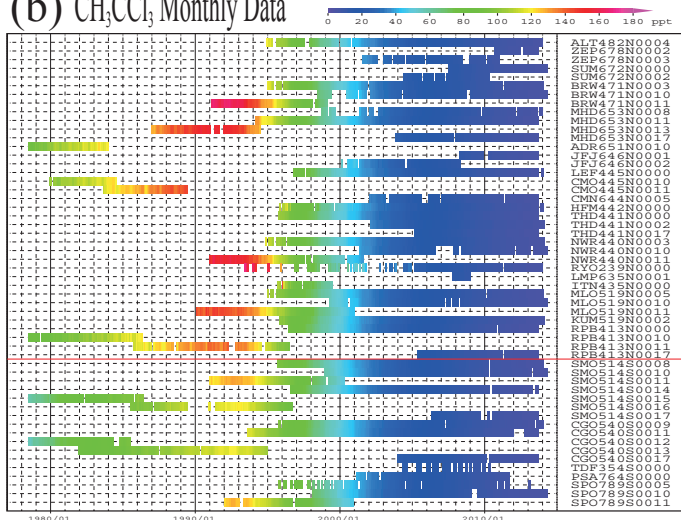
(e) CH_3Cl Monthly Data



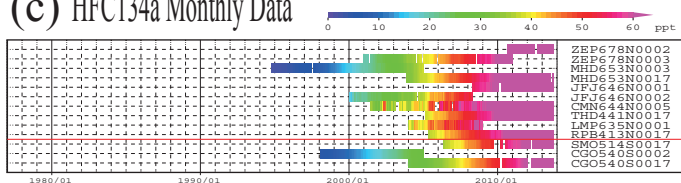
(f) SF_6 Monthly Data



(b) CH_3CCl_3 Monthly Data



(c) HFC134a Monthly Data



(d) HFC152a Monthly Data

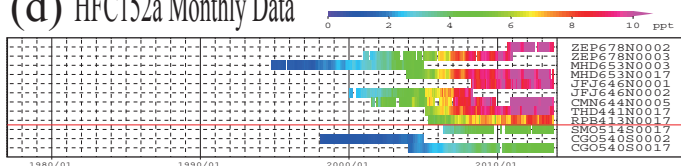


Plate 6.2 Monthly mean (a) CCl_4 , (b) CH_3CCl_3 , (c) HFC134a , (d) HFC152a , (e) CH_3Cl , (f) SF_6 mole fractions that have been reported to the WDCGG. The mole fractions are illustrated in different colors. The sites are listed in order from north to south. The red line indicates the equator.

6. HALOCARBONS AND OTHER HALOGENATED SPECIES

Basic information on halocarbons with regard to environmental issues

Halocarbons are carbon compounds containing one or more halogens, *i.e.*, fluorine, chlorine, bromine or iodine, with most being industrial products. Halocarbons are classified into chlorofluorocarbons (CFCs), which contain fluorine and chlorine; the hydrochlorofluorocarbons (HCFCs), which contain hydrogen in addition to fluorine and chlorine; and the halons, which contain bromine and other halogens. Perfluorocarbons (PFCs) are carbon compounds in which all hydrogen atoms are replaced by fluorine atoms, and hydrofluorocarbons (HFCs) are halocarbons that contain hydrogen and fluorine but no chlorine. Carbon tetrachloride (CCl_4) and methyl chloroform (CH_3CCl_3) are produced industrially, whereas methyl chloride (CH_3Cl) has natural sources. Although the mole fractions of the halocarbons are relatively low in the atmosphere, they have high global warming potentials. The halocarbons have been shown to account for about 12% of the total increase in radiative forcing due to long-lived greenhouse gases from 1750 to 2013 (WMO, 2014b).

The halocarbons are colorless, odorless and innocuous substances that can be readily gasified and liquefied and have low surface tension. Thus, they were commonly used as refrigerants, propellants and detergents for semiconductors, resulting in a rapid increase in their mole fractions in the atmosphere until the mid-1980s. Halocarbons containing chlorine and bromine led to the depletion of the ozone layer. Since the mid-1990s, the Montreal Protocol on Substances that Deplete the Ozone Layer and its subsequent Adjustments and Amendments have progressively tightened the regulations for the production, consumption and trade of ozone-depleting substances.

The CFCs are destroyed mainly by ultraviolet radiation in the stratosphere, and their lifetimes are generally long (*e.g.*, about 50 years for CFC-11). However, the HCFCs and CH_3CCl_3 , which contain hydrogen, react with hydroxyl radicals (OH) in the troposphere and have relatively short lifetimes (*e.g.*, about 5 years for CH_3CCl_3). As the reaction with OH in the troposphere is a major sink for CH_3CCl_3 , global measurements of CH_3CCl_3 provide an accurate estimate of the global mole fraction of OH (Prinn *et al.*, 2001). However, due to a substantial decrease of CH_3CCl_3 mole fraction in the atmosphere, reconstruction of OH levels using this molecule is becoming increasingly difficult and other compounds are now used as reference tracers for OH mole fraction determination.

The Kyoto Protocol to the United Nations Framework Convention on Climate Change

(UNFCCC), which came into force on 16 February 2005, specifies HFCs, PFCs and sulphur hexafluoride (SF_6) as targets for quantified emission limitation and reduction commitments.

SF_6 , although not a halocarbon, behaves similarly to halocarbons and is a potent long-lived greenhouse gas. Its emissions are almost entirely anthropogenic, and it is used mainly as an electrical insulator in power distribution equipment. SF_6 current mole fraction is about twice the level observed in the mid-1990s (WMO, 2014b). It has a very long atmospheric lifetime, 3,200 years, so emissions accumulate in the atmosphere. These emissions can be determined utilizing atmospheric observations of SF_6 and the rate of mole fraction in inverse modelling (Levin *et al.*, 2010).

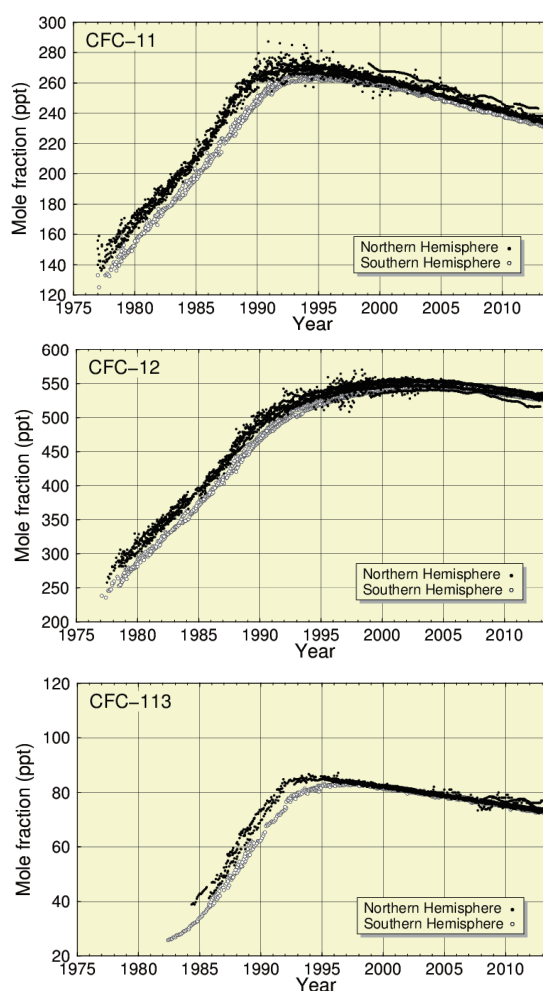


Fig. 6.1 Time series of the monthly mean mole fractions of CFC-11, CFC-12 and CFC-113 at individual stations. Solid circles show mole fractions measured in the Northern Hemisphere and open circles show mole fractions measured in the Southern Hemisphere.

Annual changes in the levels of halocarbons in the atmosphere

The cover map of this chapter shows observational sites that have submitted data on halocarbons and other halogenated species to the WDCGG. Although the number of stations measuring these species is rather limited, halocarbons are generally well mixed in the atmosphere and the data may be sufficient to reflect their global tendencies. Plates 6.1 and 6.2 show all the monthly mean mole fractions of these gases submitted to the WDCGG. The figures (6.1 – 6.7) in this chapter show the monthly mean data reported to the WDCGG without spatial averaging. Some discrepancies in the absolute mole fractions were observed between several stations, suggesting that these stations may have adopted different standard scales. Observational data expressed on the same standard scales revealed that the differences in the mole fractions between the two hemispheres were large in the 1980s for CFCs, CCl_4 and CH_3CCl_3 but have since narrowed as the emissions have been suppressed and the existing constituents have been mixed between the hemispheres.

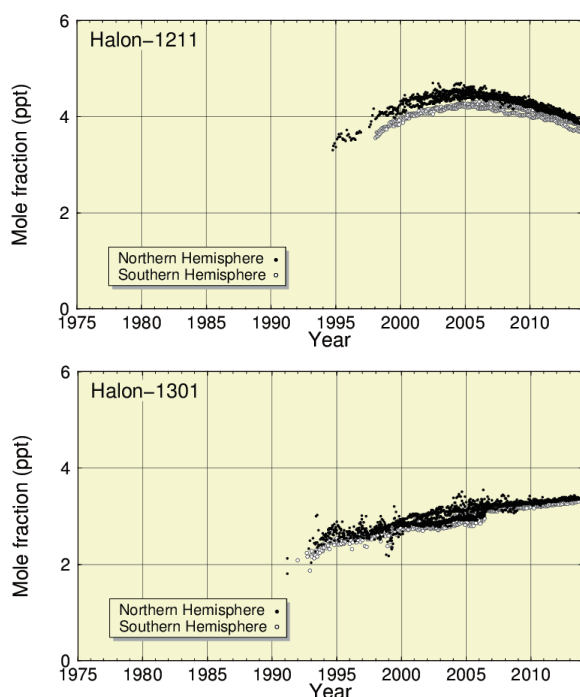


Fig. 6.2 Time series of the monthly mean mole fractions of Halon-1211 and Halon-1301 at individual stations. Solid circles show mole fractions measured in the Northern Hemisphere and open circles show those measured in the Southern Hemisphere.

Figure 6.1 shows monthly mean mole fractions of CFC-11 (CCl_3F), CFC-12 (CCl_2F_2) and CFC-113 ($\text{CCl}_2\text{FCClF}_2$) over time. The mole fractions of CFC-11 peaked around 1992 in the Northern Hemisphere, followed by a maximum about one year later in the Southern Hemisphere. The mole fractions

of CFC-113 were maximal around 1992 in the Northern Hemisphere and around 1997 in the Southern Hemisphere. The mole fractions of these gases have since been decreasing slowly in both hemispheres. The mole fraction of CFC-12 increased until around 2005 and then started decreasing gradually.

Figure 6.2 shows time series of the monthly mean mole fractions of Halon-1211 (CBrClF_2) and Halon-1301 (CBrF_3). The mole fraction of Halon-1211 has decreased since 2005, whereas the mole fraction of Halon-1301 has been increasing.

Figure 6.3 shows time series of the mole fractions of HCFC-22 (CHClF_2), HCFC-141b ($\text{CH}_3\text{CCl}_2\text{F}$) and HCFC-142b (CH_3CClF_2). The mole fractions of these gases increased significantly during the last decade as a result of their continued use as substitutes for CFCs. The growth of HCFC-141b decelerated around 2005, but has slightly accelerated again over the last few years.

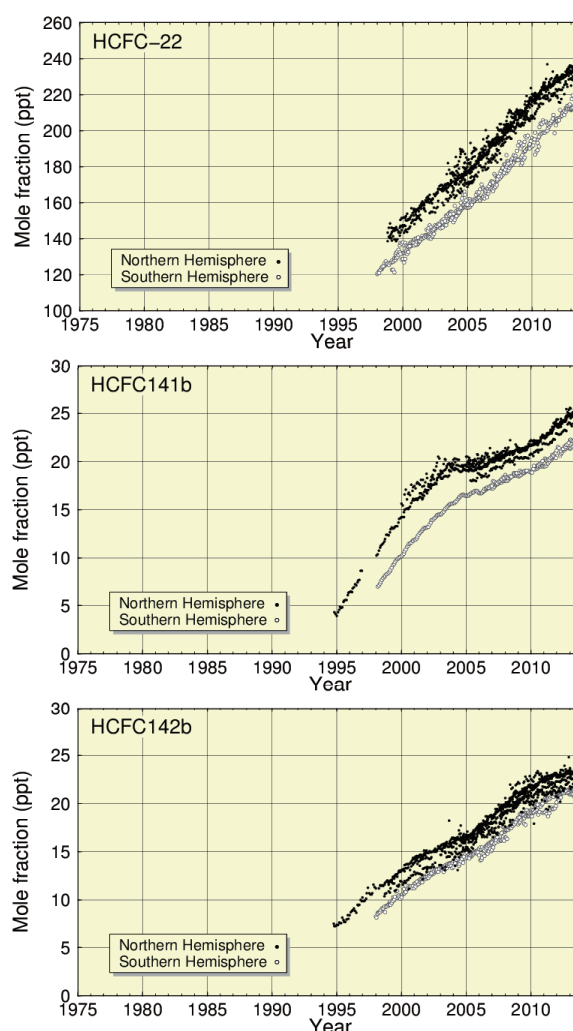


Fig. 6.3 Time series of the monthly mean mole fractions of HCFC-22, HCFC-141b and HCFC-142b at individual stations. Solid circles show mole fractions measured in the Northern Hemisphere and open circles show those measured in the Southern Hemisphere.

Figure 6.4 shows time series of the mole fractions of CCl_4 and CH_3CCl_3 . The mole fractions of CCl_4 in both hemispheres peaked around 1991. The mole fractions of CH_3CCl_3 were at a maximum around 1992 in the Northern Hemisphere and around 1993 in the Southern Hemisphere. The mole fractions of these gases have since been decreasing.

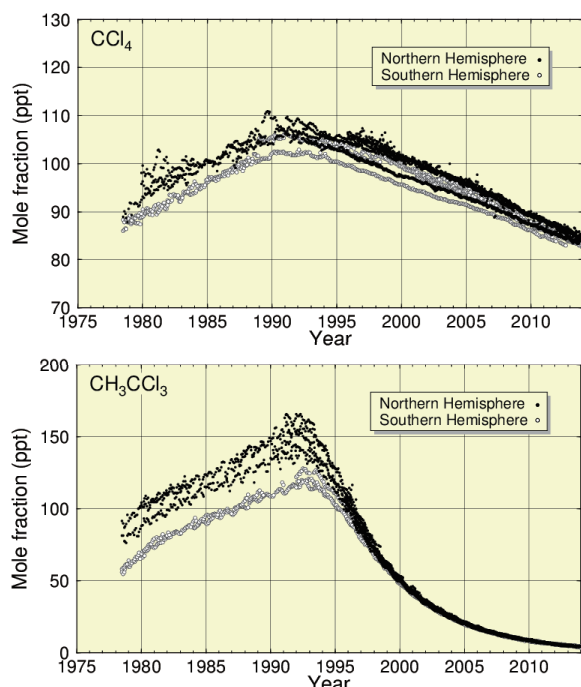


Fig. 6.4 Time series of the monthly mean mole fractions of CCl_4 and CH_3CCl_3 at individual stations. Solid circles show mole fractions measured in the Northern Hemisphere and open circles show those measured in the Southern Hemisphere.

Figure 6.5 shows time series of the monthly mean mole fractions of HFC-134a (CH_2FCF_3) and HFC-152a (CH_3CHF_2). The mole fractions of HFC-134a and HFC-152a have increased by 4 to 5-fold over the last 10 years. These increases have been larger in the Northern than in the Southern Hemisphere, suggesting that predominant sources of mentioned above compounds are located in the Northern Hemisphere.

Figure 6.6 shows time series of the monthly mean mole fractions of methyl chloride (CH_3Cl). The mole fraction of CH_3Cl does not show any particular long-term tendency although clear seasonal cycle can be seen in the dataset.

Figure 6.7 shows a time series of the monthly mean mole fractions of SF_6 . The mole fraction of SF_6 in 2013 was about twice that observed in 1995 increasing nearly linearly at a rate of 0.25 ppt/year (WMO, 2014b).

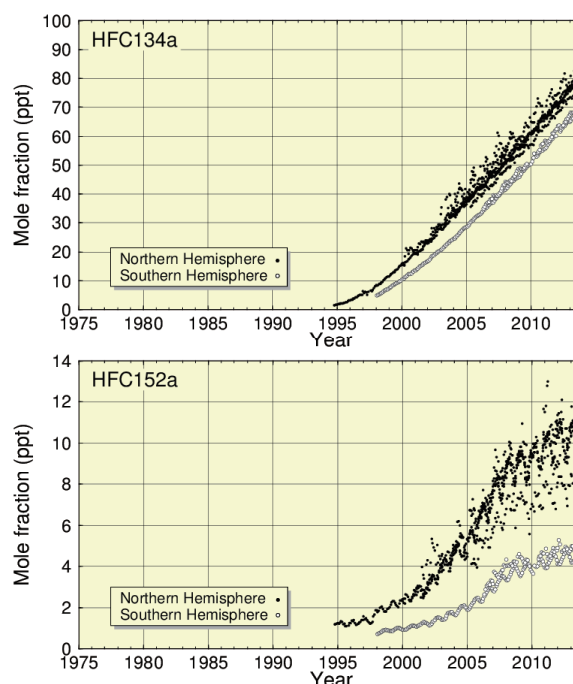


Fig. 6.5 Time series of the monthly mean mole fractions of HFC-134a and HFC-152a at individual stations. Solid circles show mole fractions measured in the Northern Hemisphere and open circles show those measured in the Southern Hemisphere.

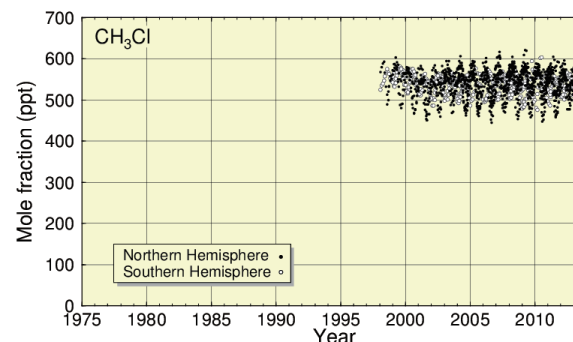


Fig. 6.6 Time series of the monthly mean mole fractions of CH_3Cl at individual stations. Solid circles show mole fractions measured in the Northern Hemisphere and open circles show those measured in the Southern Hemisphere.

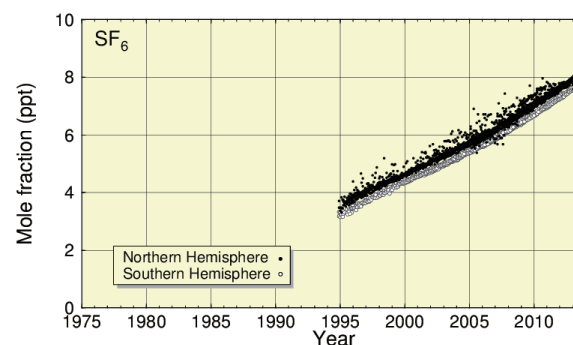
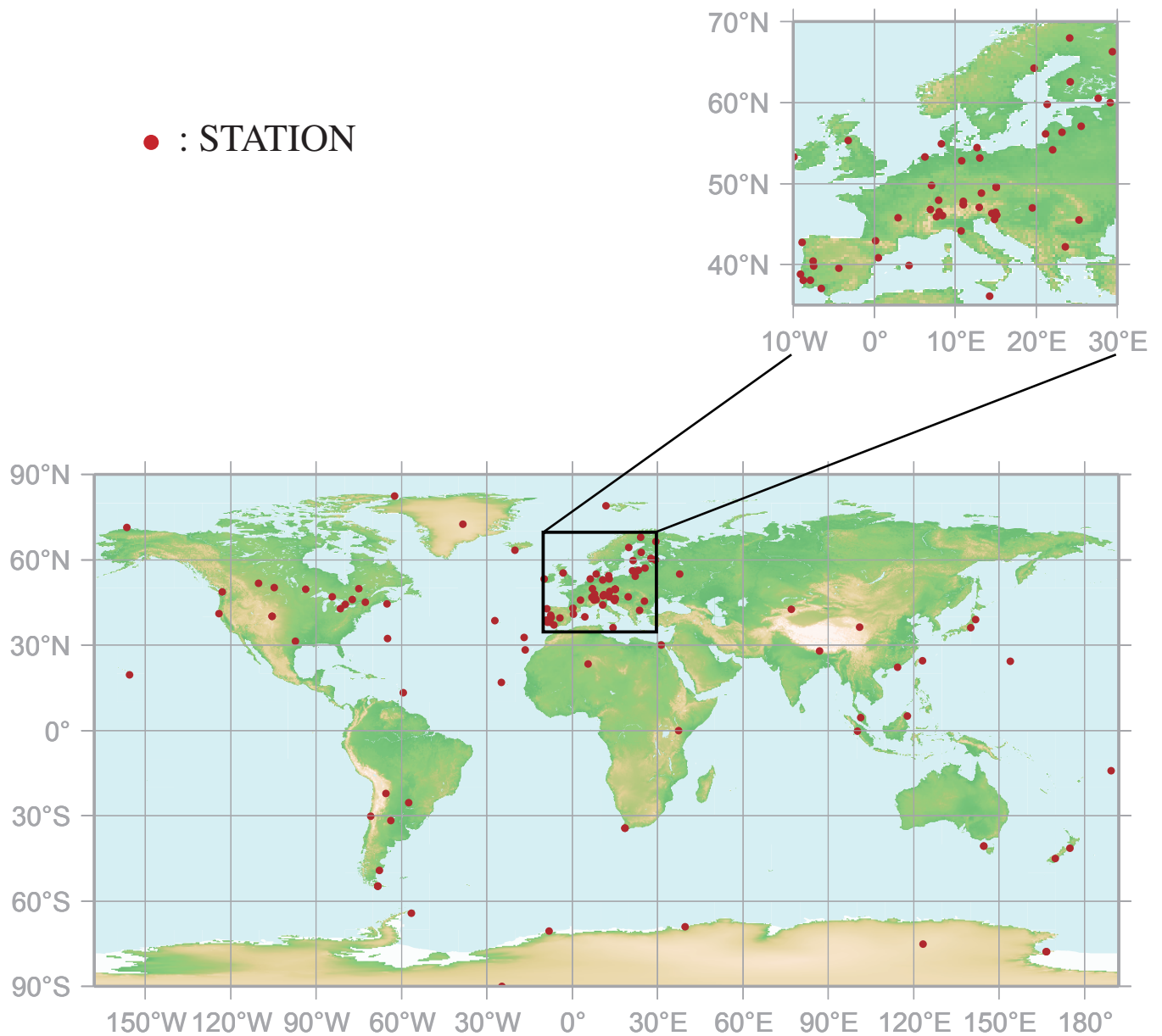


Fig. 6.7 Time series of the monthly mean mole fractions of SF_6 at individual stations. Solid circles show mole fractions measured in the Northern Hemisphere and open circles show those measured in the Southern Hemisphere.

7.

SURFACE OZONE

(O₃)



This map shows locations of the stations that have submitted data for monthly mean mole fractions.

O₃ Monthly Data

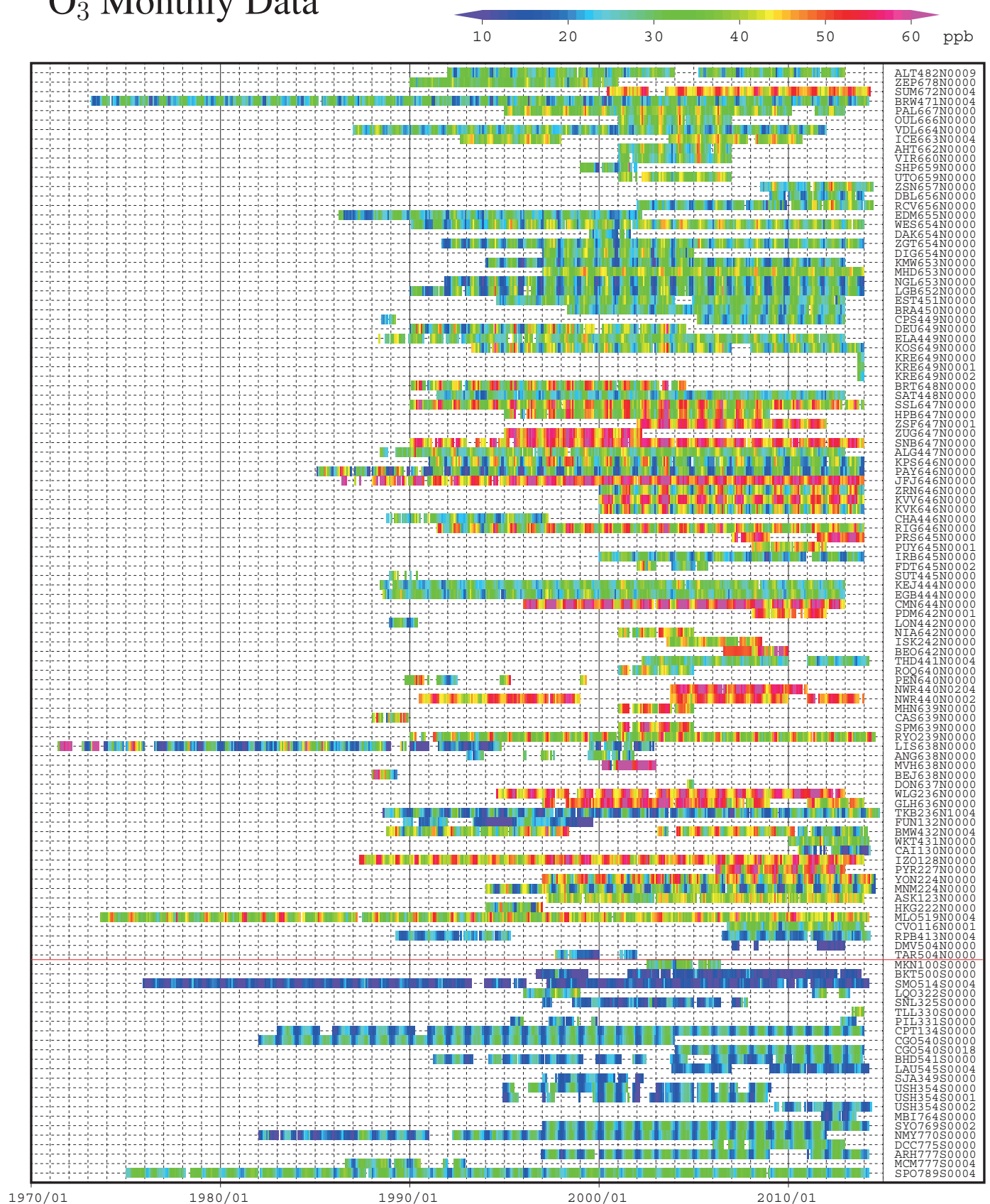


Plate 7.1 Monthly mean O₃ mole fractions that have been reported to the WDCGG. The mole fractions are illustrated in different colors. The sites are listed in order from north to south. The red line indicates the equator.

7. SURFACE OZONE (O₃)

Basic information on surface ozone (O₃) with regard to environmental issues

Ozone (O₃) in the atmosphere exists mostly in the stratosphere, with less than 10% in the troposphere. However, O₃ in the troposphere plays an important role through its impact on radiative forcing and its involvement in the chemical processes. O₃ absorbs UV radiation in the stratosphere, thus influencing vertical profile of temperature and circulation in the stratosphere. Moreover, as a greenhouse gas in the troposphere, O₃ absorbs IR radiation. The latter effect is more significant in the upper troposphere. Tropospheric O₃ in the northern extratropics was the greatest contributor to global warming during the 20th century, and increases in tropospheric O₃ resulting from industrialization in developing countries was found to contribute to accelerated warming in the tropics during the latter half of the century (Shindell *et al.*, 2006). Furthermore, by reacting with water vapor in the presence of UV radiation, O₃ produces OH radicals, which control atmospheric life time of many greenhouse gases, such as CH₄.

The observational results at high altitudes around 1990, compared with those from the end of the 19th century to the first half of the 20th century, show increases in tropospheric O₃, especially in urban areas (Staehelin *et al.*, 1994). However, ozonesonde measurements in the troposphere show stable or decreasing trends in northern mid-latitudes after 1980 (Oltmans *et al.*, 2006). Recently substantial efforts has been made to systematically review the observed trends (Cooper *et al.*, 2014). This analysis will be continued in the framework of the Tropospheric Ozone Assessment Report (TOAR) project (<http://www.igacproject.org/TOAR>). It was found that in most regions of the world — excluding East Asia — surface and free tropospheric ozone concentrations have not risen significantly since year 2000. Prior to the 1990s almost all records indicate a strong rise, while during the 1990s the picture is very diverse.

Tropospheric O₃ originates from flux/mixing from the stratosphere and in-situ photochemical production. O₃ is destroyed in various processes, including chemical reactions with NO, the hydroperoxyl radical (HO₂) and OH, and deposition at various surfaces. The lifetime of tropospheric ozone varies from one or a few days in the boundary layer to a few tens of days or even a few months in the free troposphere.

In the troposphere, the mole fractions of O₃ are high in high and mid-latitudes in both hemispheres, and low in the tropics over the Atlantic (Marengo and Said, 1989) and Pacific (Tsutsumi *et al.*, 2003) oceans. The localized sources of ozone precursors and the generally

short lifetime of surface O₃ make its distribution spatially non-uniform and time-variant.

Annual variation of surface O₃ mole fraction

The observational sites that have submitted data for surface O₃ to the WDCGG are shown on the map at the beginning of this chapter. The monthly mean wet mole fractions of O₃ that have been reported from these observational sites are shown in Plate 7.1, with different mole fraction levels illustrated in different colors. Data for the mole fractions of surface O₃ are reported in two different units, *i.e.*, mixing ratio (ppb) and concentration (μg/m³) at 25°C, though Tropospheric Ozone Measurement Guidelines (GAW Report No. 209) recommends use of mixing ratios. Concentration is converted to mixing ratio using the formula:

$$X_p [\text{ppb}] = (R \times T / M / P_0) \times 10 \times X_g [\mu\text{g}/\text{m}^3]$$

where R is the molar gas constant (8.31451 [J/K/mol]),

T is the absolute temperature reported from each station,

M is the molecular weight of O₃ (47.9982), and

P₀ is the standard pressure (1013.25 [hPa]).

If temperature is not reported by a station, T is taken to be 298K (25 °C). This approach can introduce additional uncertainty to the reported data.

The mole fraction of surface O₃ was found to vary from station to station, though many of these stations are located in Europe. Moreover, the seasonal and interannual variations were found to be relatively large at most stations, making it difficult to identify a global long-term trend in the mole fraction of surface O₃.

The seasonal cycles of monthly mean mole fraction of surface O₃ are shown in Figure 7.1. Those were the averages for each 30° latitudinal zone for all available periods subtracted the long term trends. The latitudinal mean mole fractions were found to be elevated in spring in most latitudinal zones. However, several patterns of seasonal-diurnal cycles were observed at different locations, including a pronounced spring maximum, a spring maximum at night and a summer maximum during the day, a wide spring-summer maximum, and a pronounced winter maximum (Tarasova *et al.*, 2007).

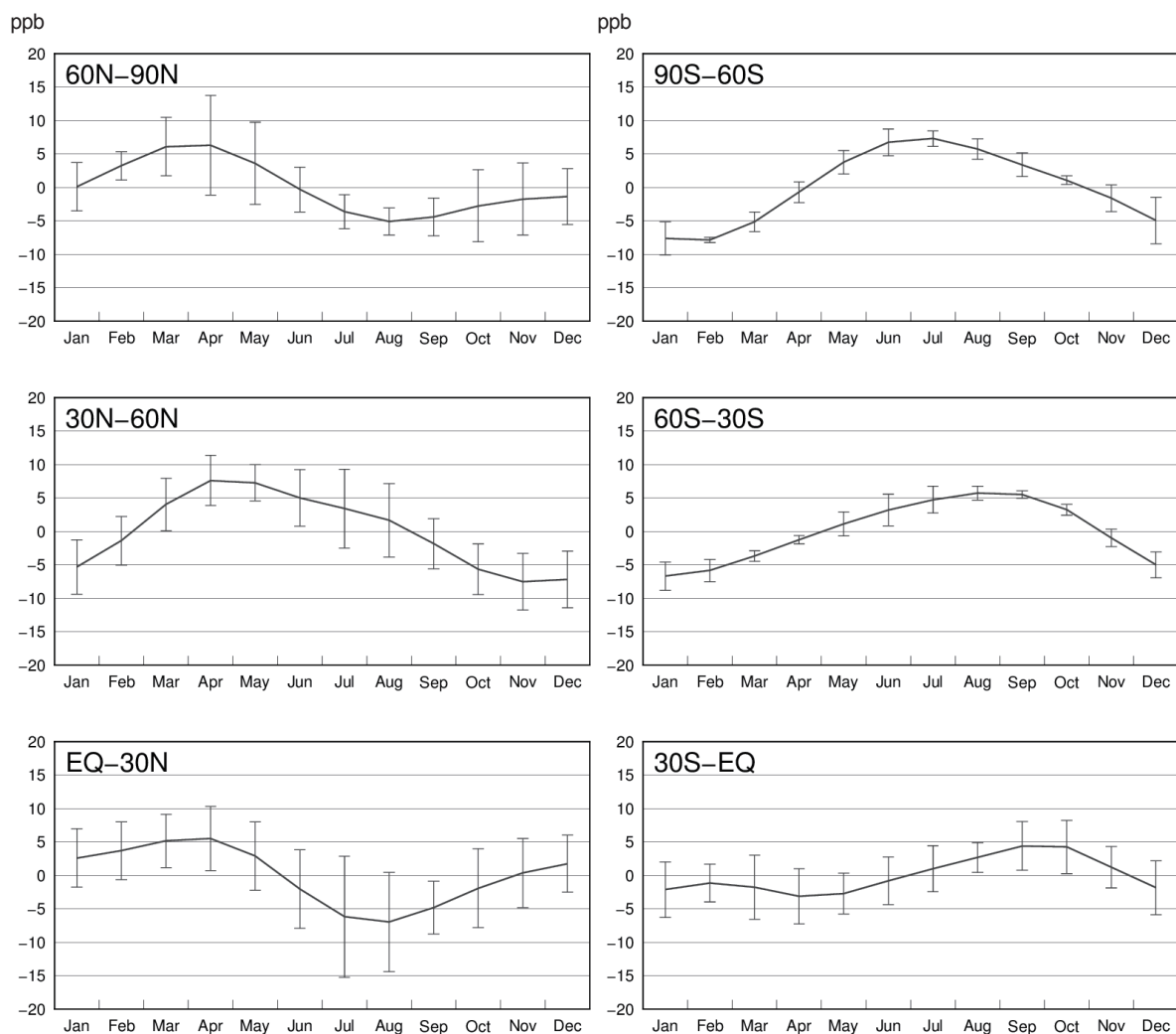
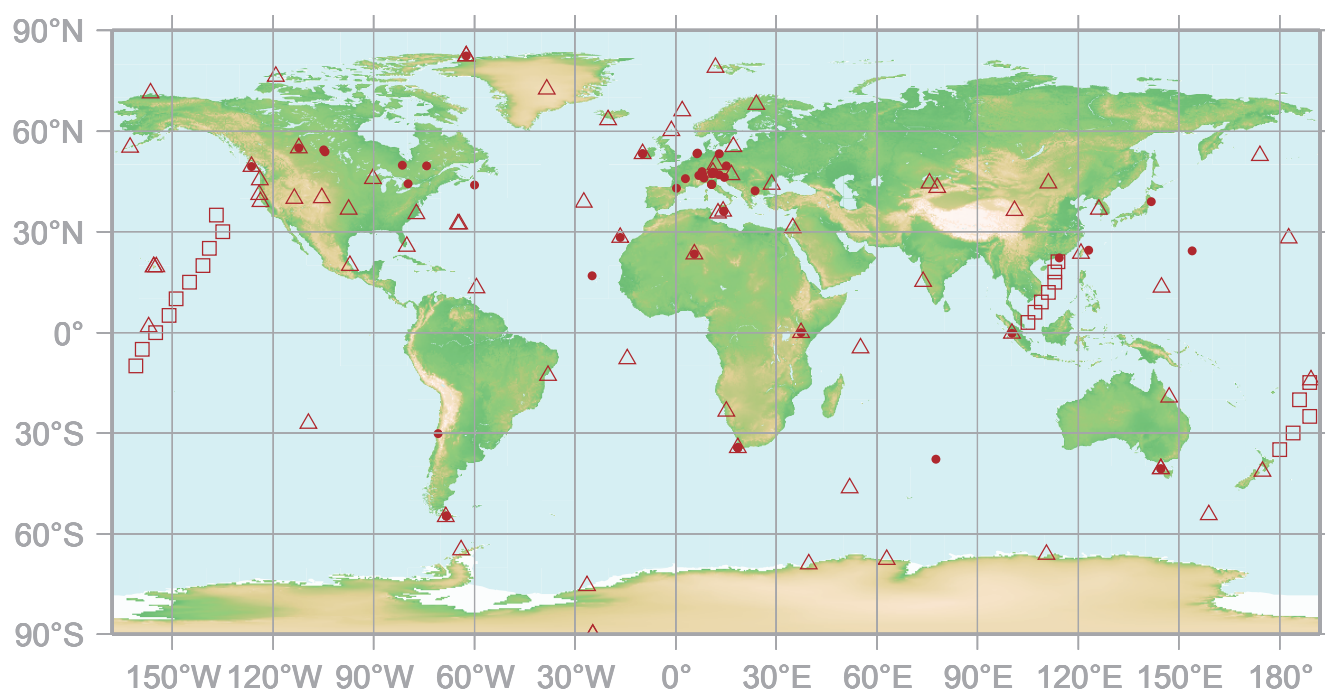


Fig. 7.1 Average seasonal cycles in the mole fractions of O₃ for each 30° latitudinal zone obtained from the seasonal cycles of each station for all available periods. Vertical error bars represent the range of $\pm 1\sigma$ calculated for each month.

8.

CARBON MONOXIDE (CO)

- : CONTINUOUS STATION
- △ : FLASK STATION
- : FLASK MOBILE (SHIP)



This map shows locations of the stations that have submitted data for monthly mean mole fractions.

CO Monthly Data

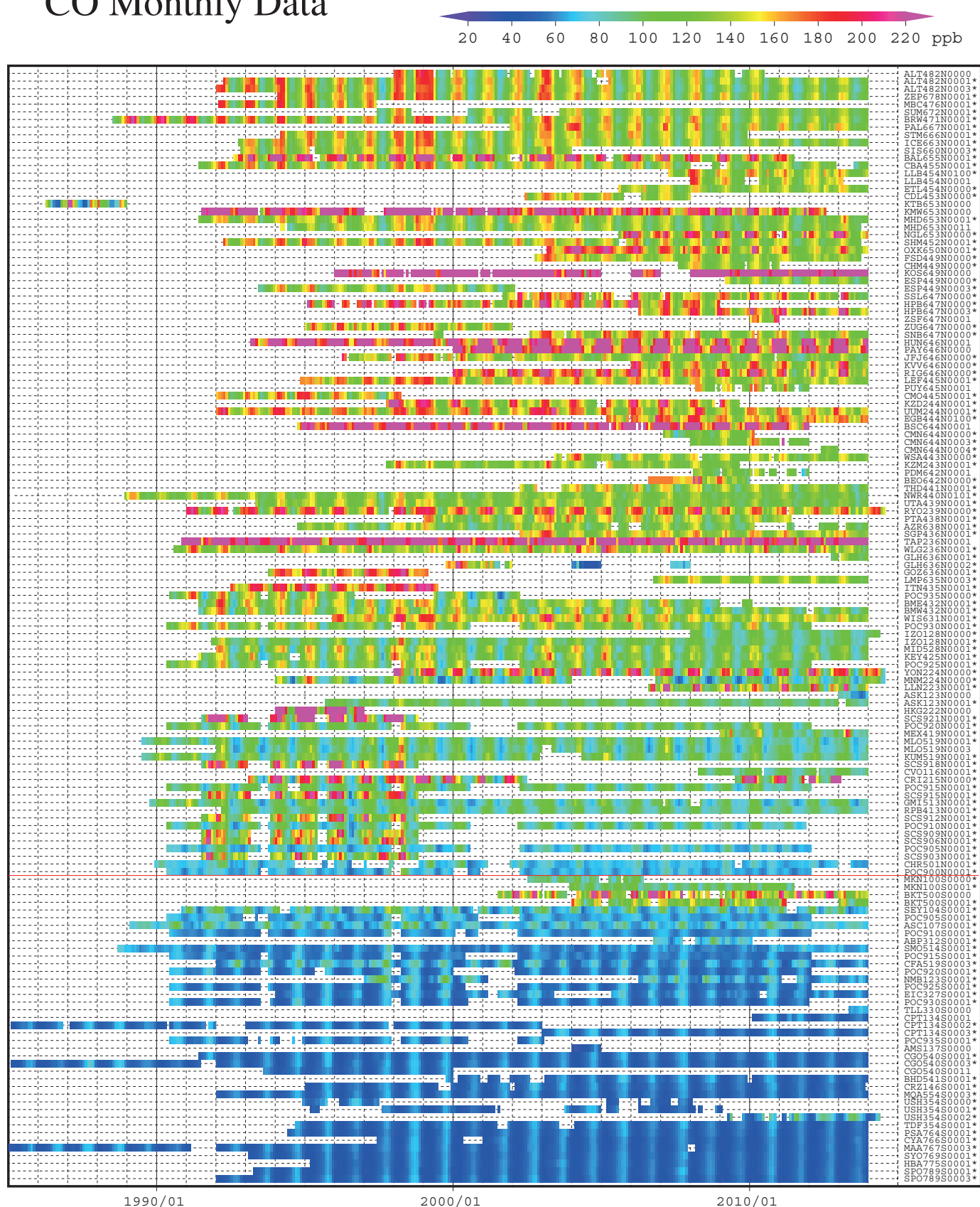
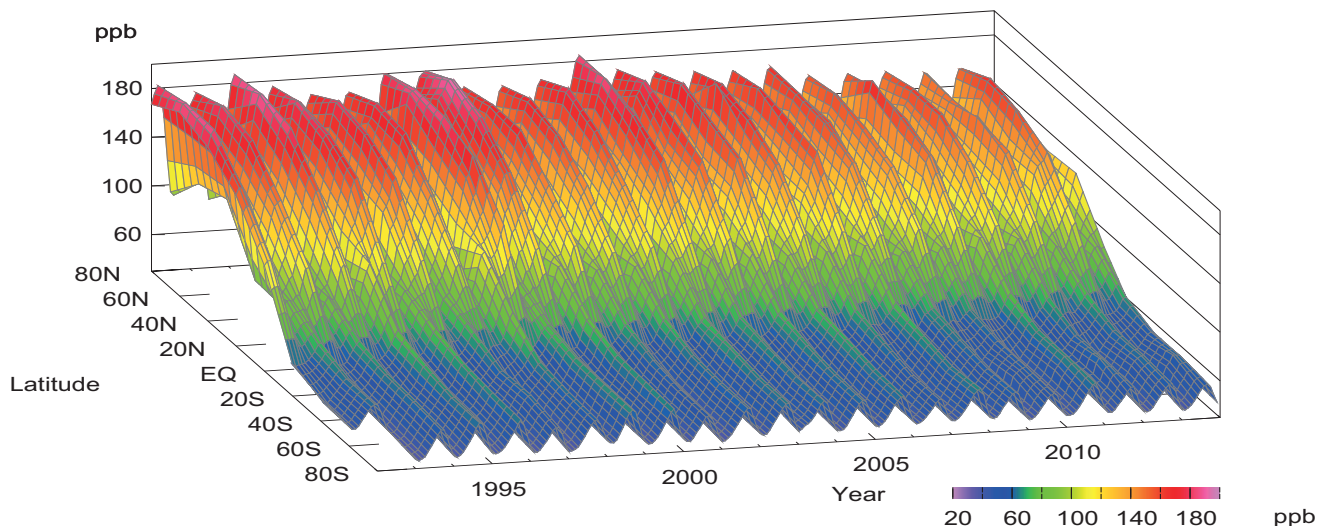
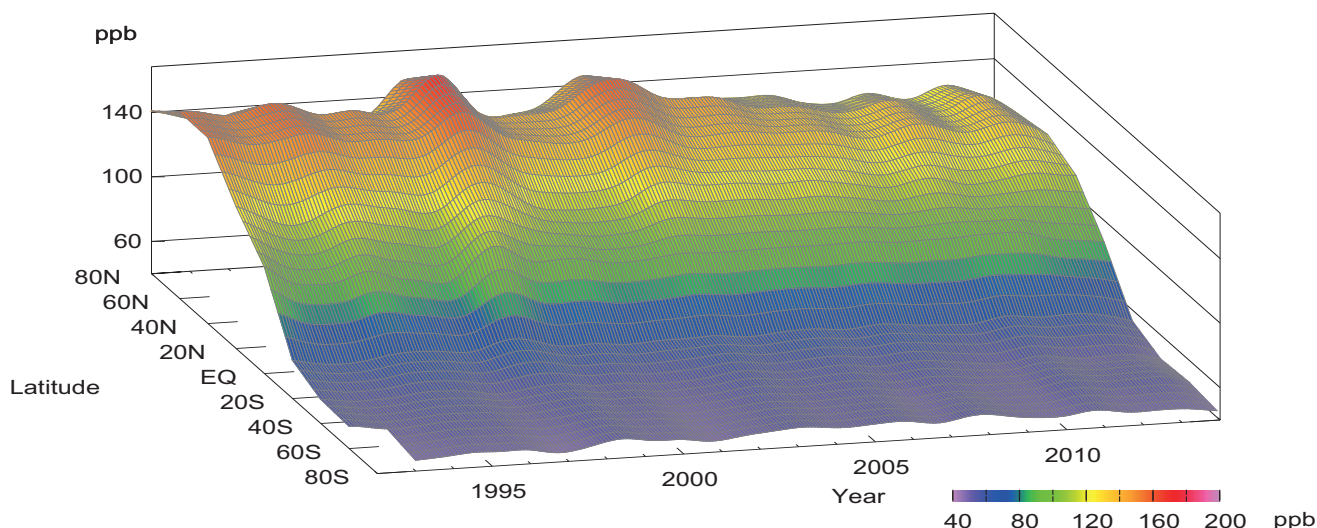


Plate 8.1 Monthly mean CO mole fractions that have been reported to the WDCGG. The mole fractions are illustrated in different colors. The sites are listed in order from north to south. The red line indicates the equator. The data from the sites with an asterisk at the end of the station index were used for the analyses shown in Plate 8.2. (see Chapter 2)

CO mole fraction



CO deseasonalized mole fraction



CO growth rate

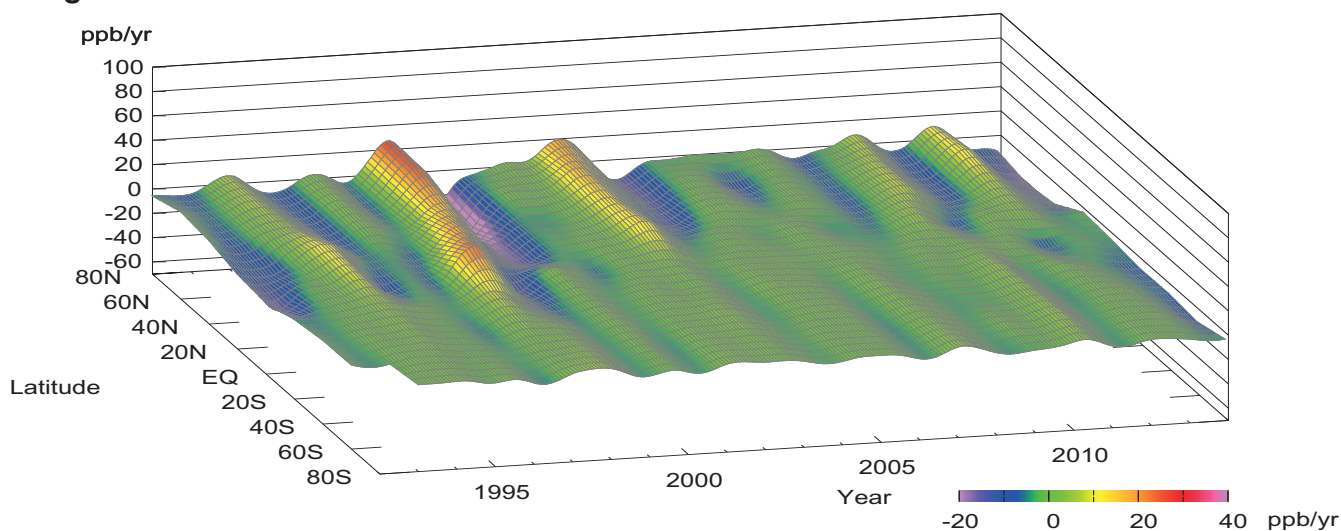


Plate 8.2 Variation of zonally averaged monthly mean CO mole fractions (top), deseasonalized long-term trends (middle), and growth rates (bottom). The zonally averaged mole fractions were calculated for each 20° zone. The deseasonalized trends and growth rates were derived as described in Chapter 2.

8. CARBON MONOXIDE (CO)

Basic information on CO with regard to environmental issues

Carbon monoxide (CO) is not a greenhouse gas; it absorbs hardly any infrared radiation from the Earth. However, CO influences the oxidation capacity of the atmosphere through its reaction with hydroxyl radicals (OH), which control the lifetimes of methane, halocarbons and tropospheric ozone. CO has been monitored due to its indirect influence on greenhouse gases through such reactions.

Sources of atmospheric CO include fossil fuel combustion and biomass burning, along with the oxidation of methane and non-methane hydrocarbons (NMHCs). Major sinks include reaction with OH and surface deposition; the reaction of CO with OH accounts for all of the chemical loss of CO in the troposphere (Seinfeld and Pandis, 1998). CO has a relatively short atmospheric lifetime, ranging from 10 days in summer in the tropics to more than a year over the polar regions in winter. Thus anthropogenic CO emissions do not lead to CO accumulation in the atmosphere. Furthermore, the uneven distribution of sources causes large spatial and temporal variations in CO mole fraction.

Measurements of trapped air in ice cores have shown that the pre-industrial CO mole fraction over central Antarctica during the last two millennia was about 50 ppb and the CO level increased to 110 ppb by 1950 in Greenland (Haan and Raynaud, 1998). Beginning in 1950, the global average CO mole fraction increased at a rate of 1% per year but started to decrease in the late 1980s (WMO, 1999). Between 1991 and 2001, the global average mole fraction of CO decreased at an annual rate of about 0.5 ppb, excluding temporal enhancements from large biomass burning events (Novelli *et al.*, 2003). In last decade, a slightly negative trend of CO mole fraction has been dominant in Northern Hemisphere with significant interannual variability, which is well reproduced by earth system models (Yoon and Pozzer, 2014).

Annual variation of CO mole fraction in the atmosphere

The monthly mean mole fractions of CO that have been reported from fixed stations and some ships to the WDCGG are shown in Plate 8.1, in which different mole fraction levels are plotted in different colors. The observational sites that provide data for global analysis are shown on the map at the beginning of this chapter.

Latitudinally averaged mole fractions of CO in the atmosphere, together with their deseasonalized mole fractions and growth rates, are shown in Plate 8.2 as three-dimensional representations.

Data for the mole fractions of CO are reported in various units, *i.e.*, ppb, $\mu\text{g}/\text{m}^3$ -25°C, $\mu\text{g}/\text{m}^3$ -20°C and mg/m^3 -25°C. Units other than ppb were converted to ppb using the formulas:

$$X_p [\text{ppb}] = (R \times T / M / P_0) \times 10 \times X_g [\mu\text{g}/\text{m}^3]$$

$$X_p [\text{ppb}] = (R \times T / M / P_0) \times 10^4 \times X_g [\text{mg}/\text{m}^3]$$

where R is the molar gas constant (8.31451 [J/K/mol]),

T is the absolute temperature reported from each station,

M is the molecular weight of CO (28.0101) and

P_0 is the standard pressure (1013.25 [hPa]).

If temperature is not reported by a station, T is taken to be 298K (25 °C).

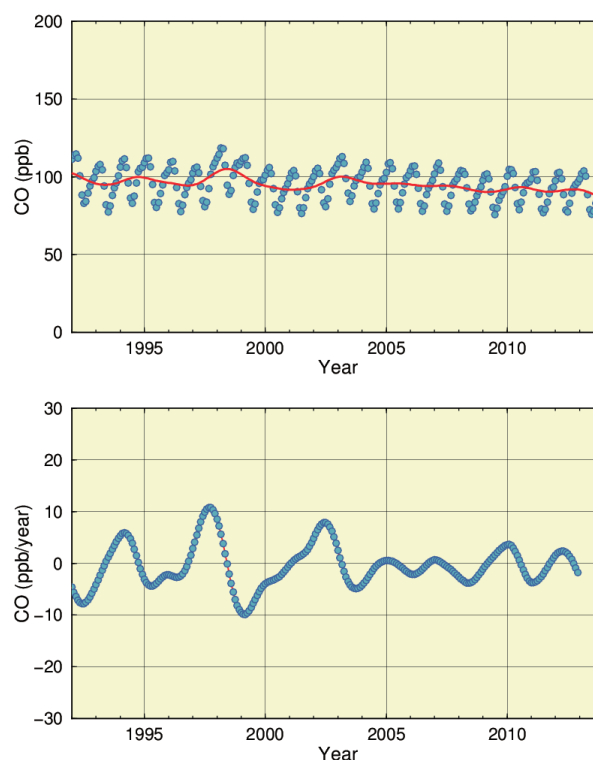


Fig. 8.1 Globally averaged monthly mean mole fraction of CO from 1992 to 2013, including deseasonalized long-term trend in red line (top) and annual growth rate (bottom).

Figure 8.1 shows globally averaged monthly mean CO mole fractions and their growth rates. Growth rates were high in 1993/1994, 1997/1998 and 2002, and low in 1992 and 1998/1999. The global annual

mean mole fraction was about 90 ± 2 ppb in 2013, which was calculated irrespective of the difference in observation scales.

Plate 8.2 shows that the seasonal variations of CO were larger in the Northern Hemisphere and smaller in the Southern Hemisphere, and that the deseasonalized mole fractions were the highest in mid-latitudes of the Northern Hemisphere and the lowest in the Southern Hemisphere, with a large latitudinal gradient from northern mid- to southern low-latitudes. This is likely due to the presence of numerous anthropogenic sources of CO in the northern mid-latitudes, combined with the destruction of CO in the tropics, where OH radicals are abundant.

Figure 8.2 shows monthly mean mole fractions of CO for each 30° latitudinal zone. Seasonal variations were observed in both hemispheres, with mole fractions being higher in winter. Amplitudes of the seasonal cycle were larger in the Northern Hemisphere than in the Southern Hemisphere.

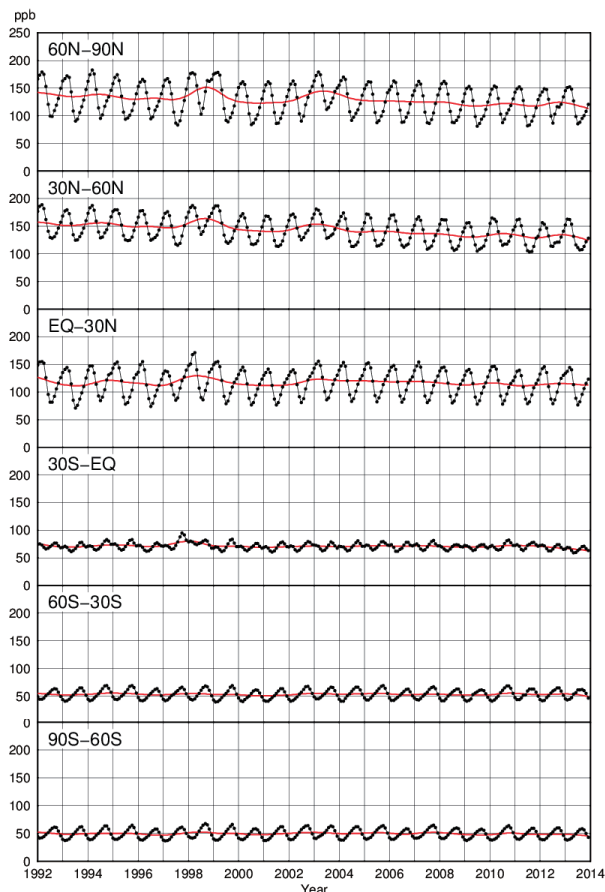


Fig. 8.2 Monthly mean mole fractions of CO from 1992 to 2013 for each 30° latitudinal zone (dots) and their deseasonalized long-term trends (red lines).

Figure 8.3 summarizes deseasonalized long-term trends for each 30° latitudinal zone and their growth rates. There was a decline in CO mole fractions around

1992, almost coinciding with the decrease in the growth rate of CH_4 mole fractions, most likely due to variations in their common sink (reaction with OH). The enhanced stratospheric ozone depletion due to increased volcanic aerosols following the eruption of Mt. Pinatubo in 1991 may have increased atmospheric OH radicals, which react with both CO and CH_4 (Dlugokencky *et al.*, 1996).

Increases in CO mole fractions were observed from 1997 to 1998 in the Northern Hemisphere and in the low latitudes of the Southern Hemisphere. These increases were attributed to large biomass burning events in Indonesia in late 1997 and in Siberia in the summer and autumn of 1998 (Novelli *et al.*, 1998).

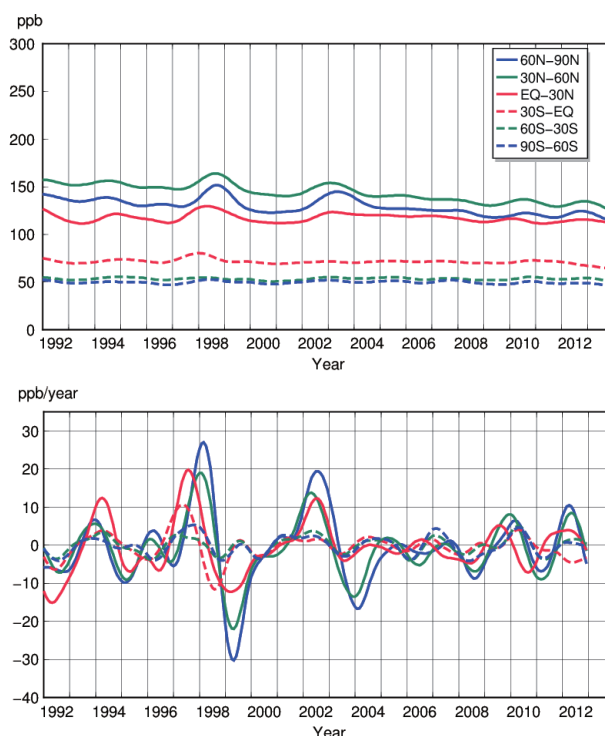


Fig. 8.3 Deseasonalized long-term trends of CO for each 30° latitudinal zone (top) and their growth rates (bottom).

The CO mole fractions returned to normal after 1999, but the growth rates in the Northern Hemisphere increased substantially again in 2002. The latter may have been due to large biomass burning events. Large-scale boreal forest fires occurred in Siberia and North America from 2002 to 2003. Large forest fires also occurred in Russia in summer 2010 which is reflected in the data in the bottom panel of Figure 8.3.

Seasonal cycle of CO mole fraction in the atmosphere

Figure 8.4 shows average seasonal cycles in the mole fraction of CO for each 30° latitudinal zone. The seasonal cycle is driven mainly by seasonal variations in OH abundance as a CO sink. This seasonality and a short lifetime of about a few months resulted in a sharp decrease in early summer followed by a relatively slow increase in autumn. The levelling-off in the beginning of the year observed in the southern low latitudes may be attributed to the transport of CO from the Northern Hemisphere.

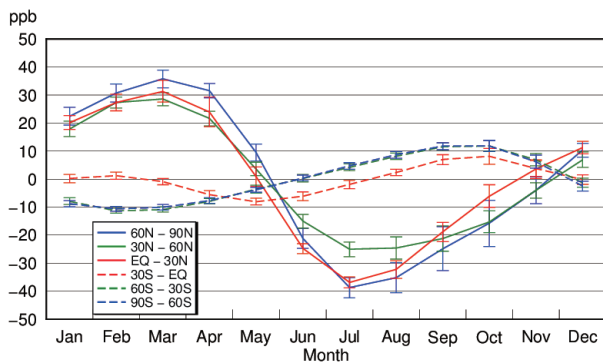


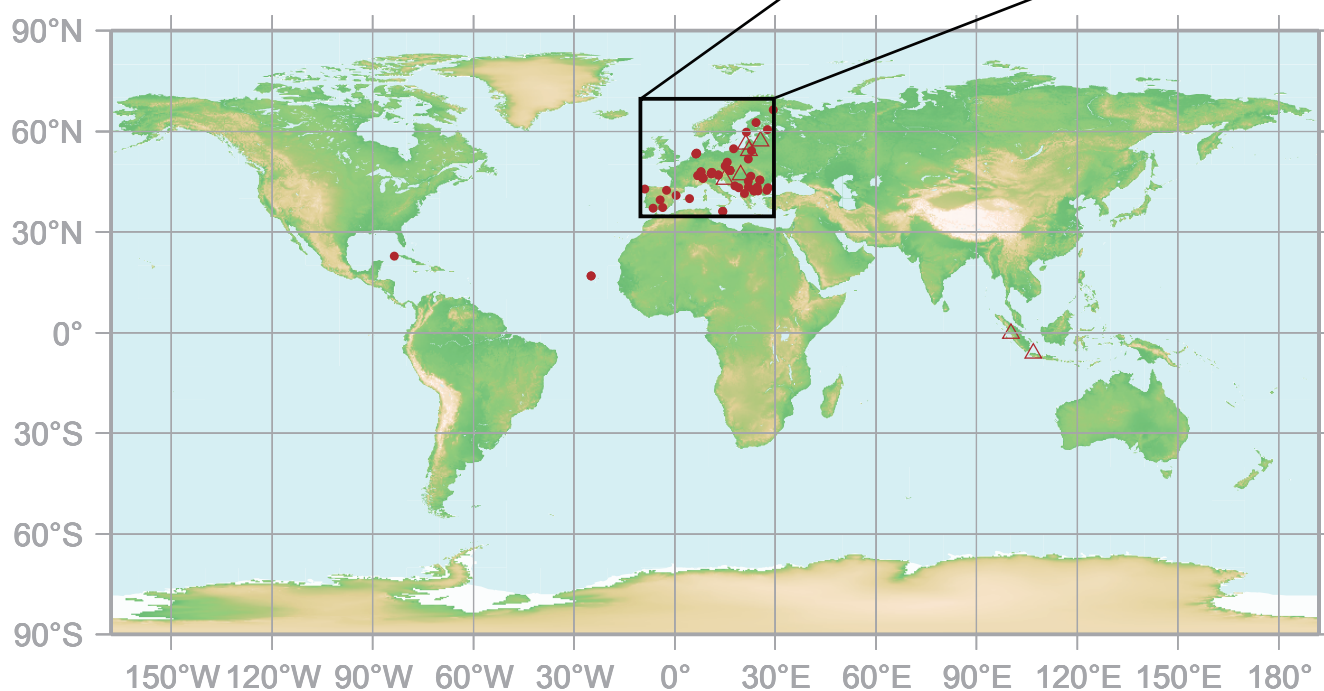
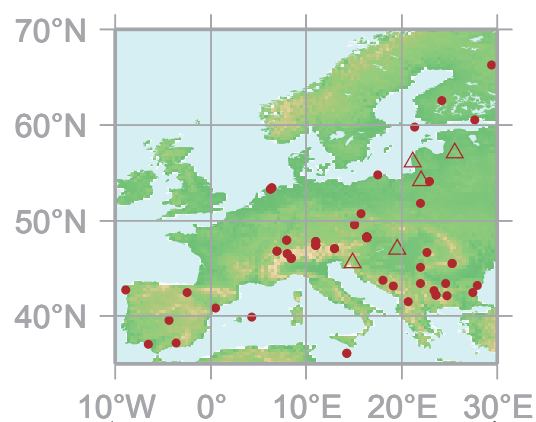
Fig. 8.4 Average seasonal cycles of CO mole fractions for each 30° latitudinal zone obtained by subtracting long-term trends from the zonal mean time series. Error bars represent the range of $\pm 1\sigma$ calculated for each month. (Average from 1992 to 2013)

9.

NITROGEN MONOXIDE (NO) AND NITROGEN DIOXIDE (NO₂)

● : CONTINUOUS STATION

△ : FILTER STATION



This map shows locations of the stations that have submitted data for monthly mean mole fractions.

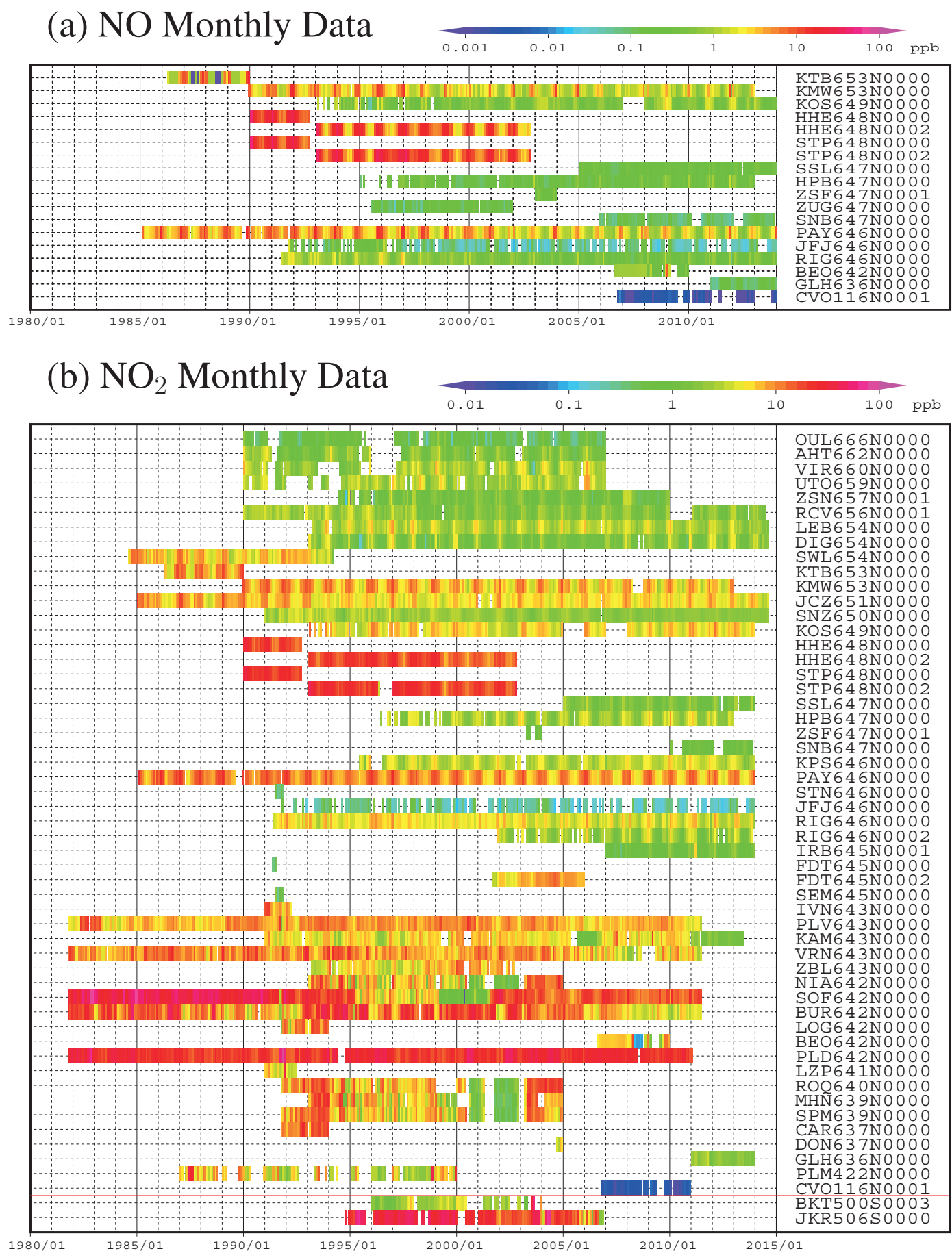


Plate 9.1 Monthly mean (a) NO and (b) NO₂ mole fractions that have been reported to the WDCGG. The mole fractions are illustrated in different colors. The sites are listed in order from north to south. The red line indicates the equator.

9. NITROGEN MONOXIDE (NO) AND NITROGEN DIOXIDE (NO₂)

Basic information on NO and NO₂ with regard to environmental issues

Nitrogen oxides (NO_x, *i.e.*, NO and NO₂) are not greenhouse gases. Nevertheless, these compounds have a central regulatory role in the free radical and oxidising chemistry of the troposphere, regulating indirectly lifetime of methane and the production of tropospheric O₃ and secondary aerosols, all of which have important roles in the natural and anthropogenic greenhouse effect.

Sources of NO_x include energy production, transport, lightning, soils and biomass burning (Reis *et al.*, 2009). They constitute major causes of acid rain and nitrogen deposition. The dominant sink of NO_x in the atmosphere is its conversion into nitric acid (HNO₃) and peroxyacetyl nitrate (PAN), which are eventually removed by dry or wet deposition. In some cases, NO_x is removed from the atmosphere directly by dry deposition. NO_x abundance varies in both space and time because of their short lifetimes and uneven source distribution. Some regional assessments are done based on satellite information to clarify such variations and trends. NO_x are one of the part of the global nitrogen cycle which recently has been addressed through a number of research initiatives.

Annual variation of NO and NO₂ mole fractions in the atmosphere

The observational stations that have submitted data for NO and NO₂ to the WDCGG are shown on the map at the beginning of this chapter. Most of these stations are located in Europe.

The monthly mean mole fractions of NO and NO₂ reported to the WDCGG are shown in Plate 9.1, in which different mole fraction levels are plotted in different colors. Data for NO_x are reported in various units, *i.e.*, ppb, µg/m³-25°C, µg/m³-20°C, µgN/m³-25°C and mg/m³-25°C. Units other than ppb were converted to ppb using the formulas:

$$\begin{aligned} X_p [\text{ppb}] &= (R \times T / M / P_0) \times 10 \times X_g [\mu\text{g}/\text{m}^3] \\ X_p [\text{ppb}] &= (R \times T / M / P_0) \times 10^4 \times X_g [\text{mg}/\text{m}^3] \\ X_p [\text{ppb}] &= (R \times T / M_N / P_0) \times 10 \times X_g [\mu\text{gN}/\text{m}^3] \end{aligned}$$

where R is the molar gas constant (8.31451 [J/K/mol]),

T is the absolute temperature reported from each station,

M is the molecular weight of NO (30.00614) or NO₂ (46.00554),

M_N is the atomic weight of N (14.00674), and

P₀ is the standard pressure (1013.25 [hPa]).

If temperature is not reported by a station, T is taken to be 298 K (25°C).

The distributions of NO and NO₂ are spatially non-uniform and variable over time. Due to the high temporal variability in the mole fraction of NO₂ at each observational site, it was difficult to identify a long-term trend. A number of stations located in southern Europe showed relatively high mole fractions, and some stations reported increased NO₂ in winter.

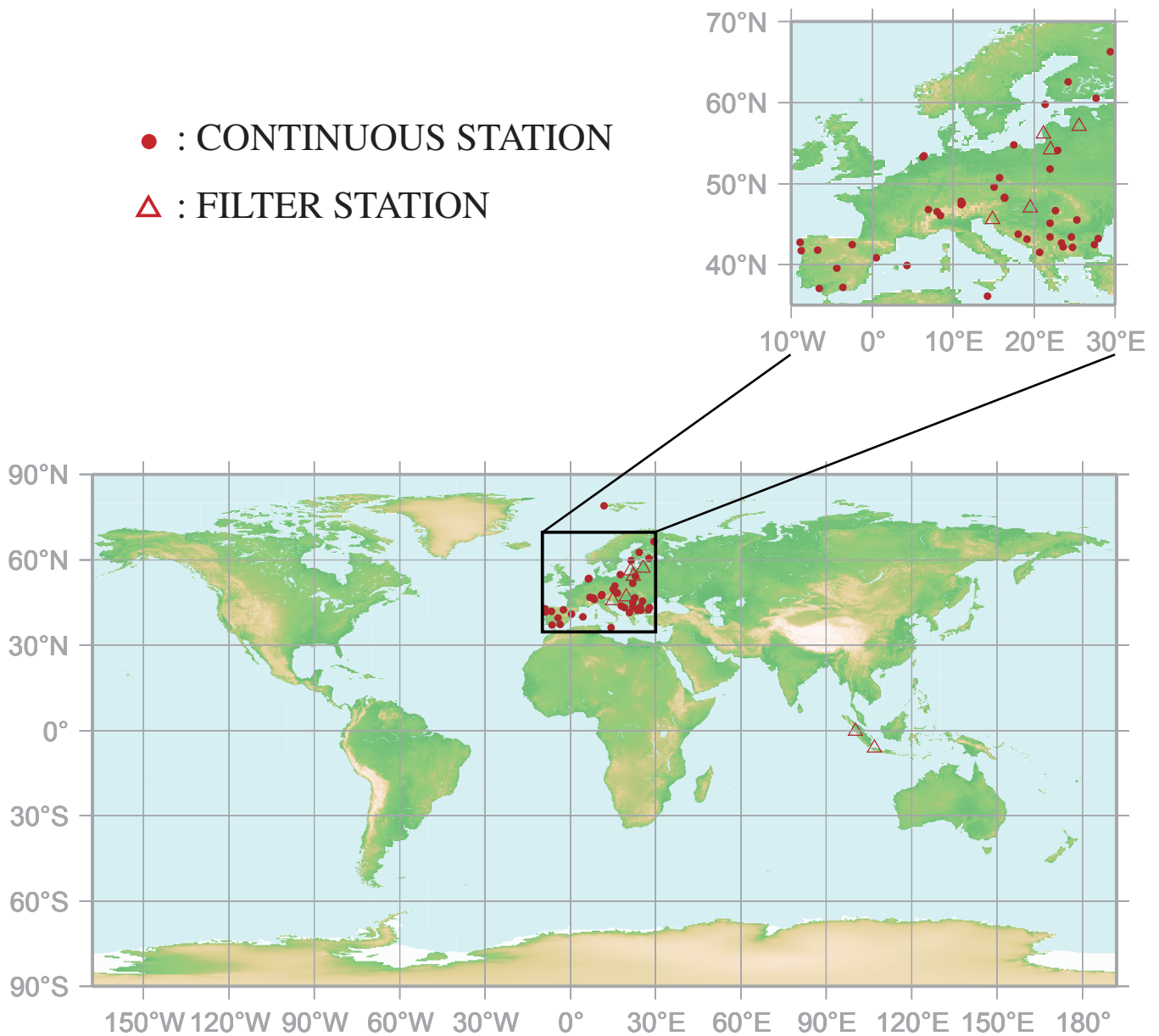
As there are few observational sites for NO, it was difficult to identify whether the global average NO mole fraction increases or decreases.

10.

SULPHUR DIOXIDE

(SO₂)

● : CONTINUOUS STATION
△ : FILTER STATION



This map shows locations of the stations that have submitted data for monthly mean mole fractions.

SO₂ Monthly Data

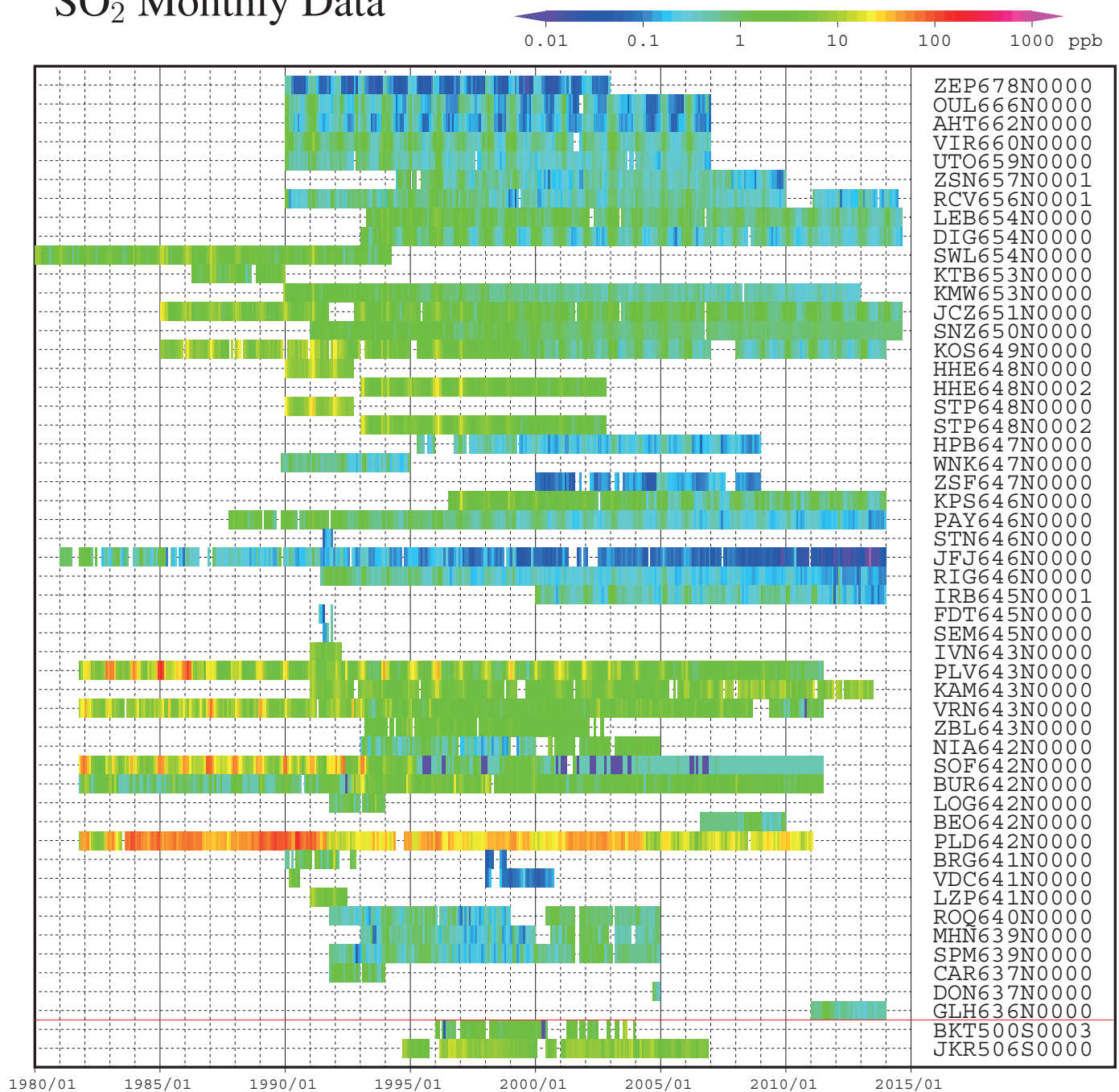


Plate 10.1 Monthly mean SO₂ mole fractions that have been reported to the WDCGG. The mole fractions are illustrated in different colors. The sites are listed in order from north to south. The red line indicates the equator.

10. SULPHUR DIOXIDE (SO₂)

Basic information on SO₂ with regard to environmental issues

Sulphur dioxide (SO₂) is not a greenhouse gas, but it is a precursor of atmospheric sulphuric acid (H₂SO₄) and sulphate aerosol. SO₂ is oxidized by hydroxyl radicals (OH) to form sulphuric acid, which then becomes aerosols through photochemical gas-to-particle conversion. While SO₂ reacts much more slowly with OH than does NO₂, SO₂ dissolves readily in suspended liquid droplets in the atmosphere. The global sulphur cycle affects atmospheric chemistry, including tropospheric ozone (Berglen *et al.*, 2004).

Sources of SO₂ include industrial fossil fuel combustion, biomass burning, volcanic release and the oxidation of dimethylsulphide (DMS) from the oceans. Major SO₂ sinks are oxidation by OH and deposition onto wet surfaces. Anthropogenic SO₂ has caused acid rain and deposition throughout the industrial era (Vet *et al.*, 2014). The mole fractions of SO₂ have shown large variations in both space and time because of the short lifetime and uneven anthropogenic source distribution of SO₂.

Annual variation of SO₂ mole fraction in the atmosphere

The observational sites that have submitted data for SO₂ to the WDCGG are shown on the map at the beginning of this chapter. Most of these stations are located in Europe.

The monthly mean mole fractions of SO₂ that have been reported to the WDCGG are shown in Plate 10.1, with different mole fraction levels illustrated in different colors. Data for SO₂ are reported in various units, *i.e.*, ppb, µg/m³, mg/m³ and µgS/m³. Units other than ppb were converted to ppb using the formulas:

$$\begin{aligned}X_p [\text{ppb}] &= (R \times T / M / P_0) \times 10 \times X_g [\mu\text{g}/\text{m}^3] \\X_p [\text{ppb}] &= (R \times T / M / P_0) \times 10^4 \times X_g [\text{mg}/\text{m}^3] \\X_p [\text{ppb}] &= (R \times T / M_s / P_0) \times 10 \times X_g [\mu\text{gS}/\text{m}^3]\end{aligned}$$

where R is the molar gas constant (8.31451 [J/K/mol]),

T is the absolute temperature reported from each station,

M is the molecular weight of SO₂ (64.0648),

M_s is the atomic weight of S (32.066), and

P₀ is the standard pressure (1013.25 [hPa]).

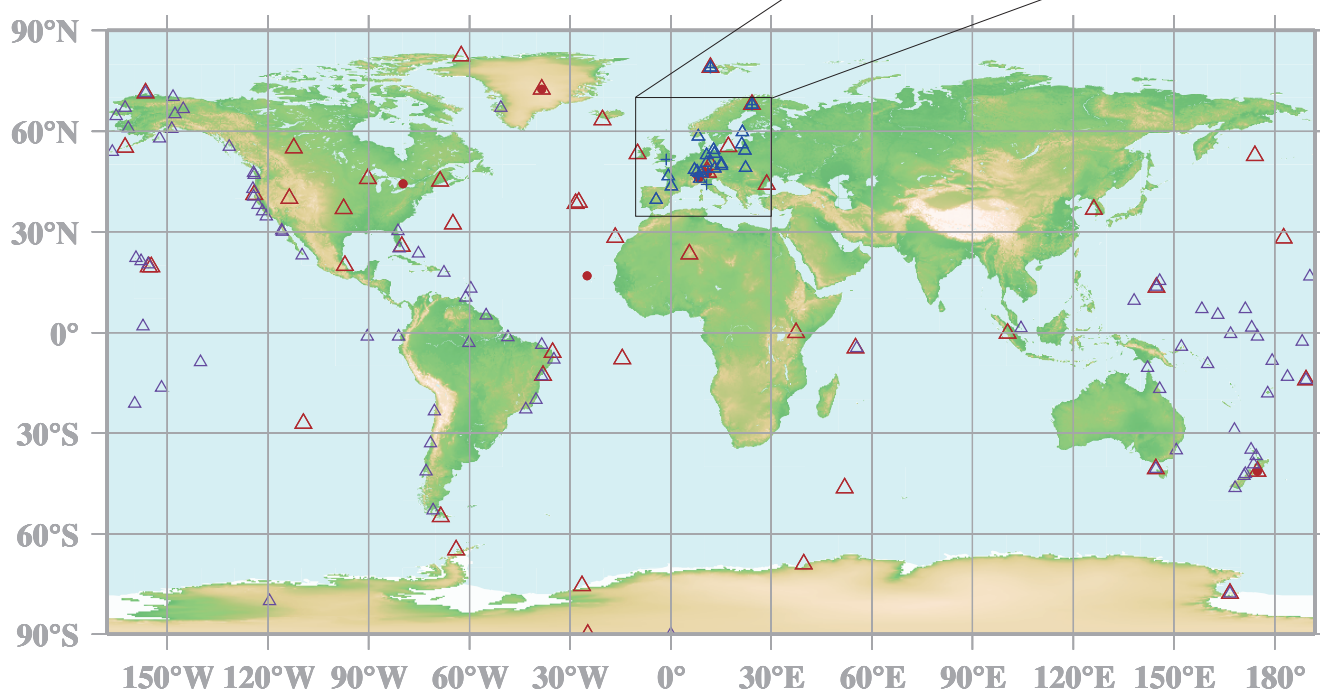
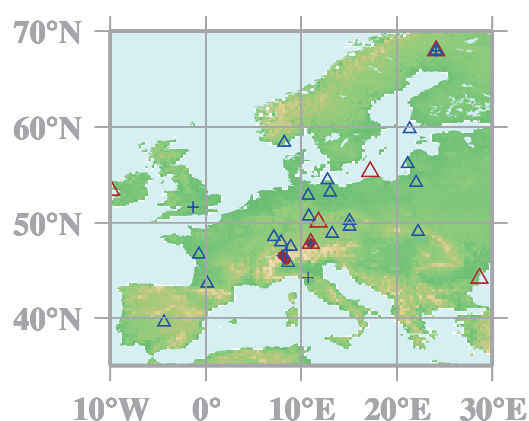
If temperature is not reported by a station, T is taken to be 298 K (25°C).

Although some stations in southern Europe have reported relatively high mole fractions, it has been difficult to identify the magnitude and direction of the trend for SO₂.

11.

VOLATILE ORGANIC COMPOUNDS (VOCs)

- : GAW CONTINUOUS
- △ : GAW FLASK
- + : EMEP CONTINUOUS
- △ : EMEP FLASK
- △ : UCI FLASK



This map shows locations of the stations that have submitted data for mole fractions of VOCs (ethane and propane) consistent with Plate.11.1 and 11.2. Most of the GAW stations are associated to the NOAA greenhouse and carbon monoxide flask sampling network, the UCI canister sampling network, and EMEP canister sampling stations, but EMEP network also includes a number of GAW stations.

Ethane Data

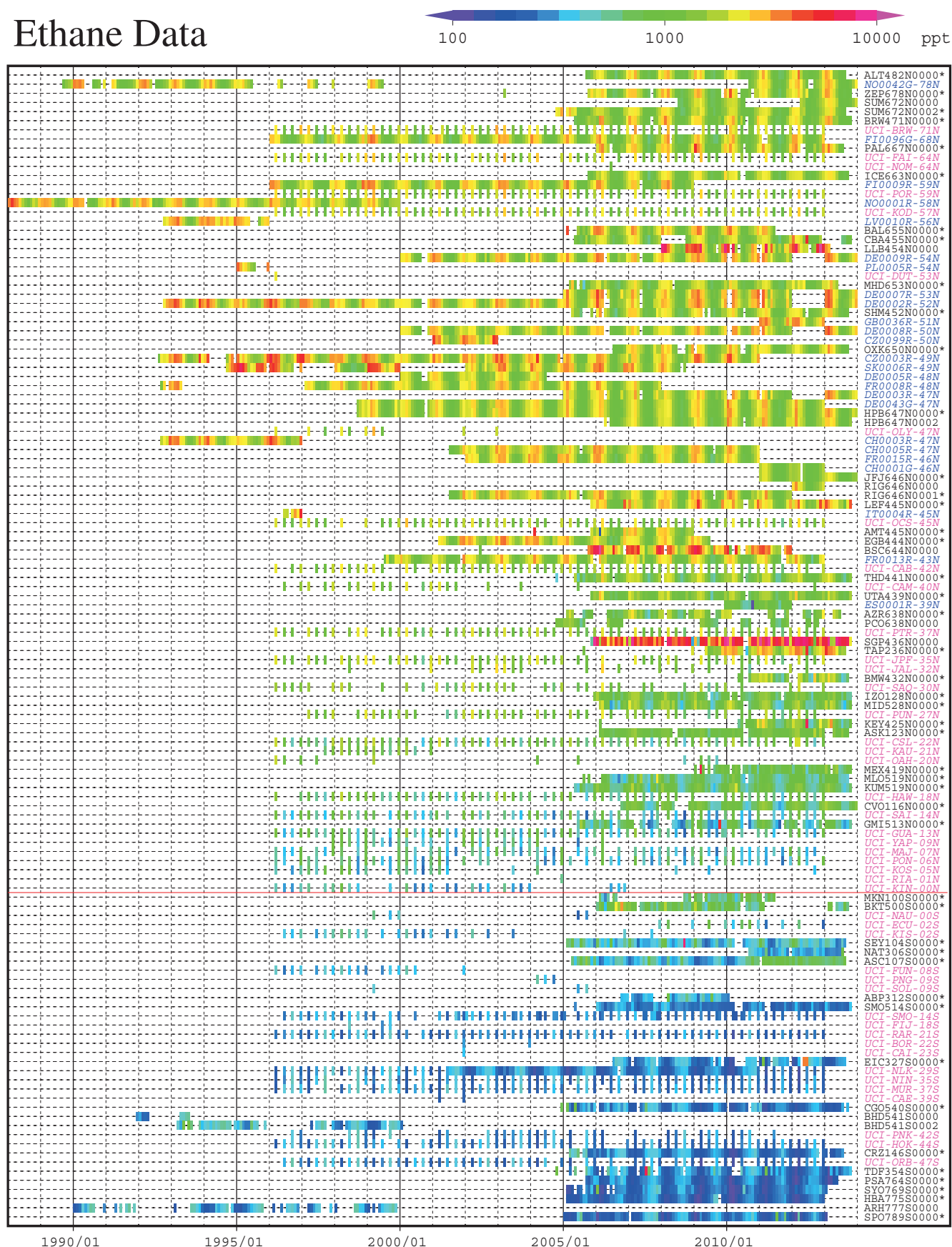


Plate 11.1 Monthly mean ethane mole fractions that have been reported to the WDCGG by GAW stations and from EMEP and UCI as regional/contributing networks. The mole fractions are illustrated in different colors. The sites are listed in order from north to south. The red line indicates the equator. Only WDCGG data from the sites with an asterisk at the end of the station index were used in Plate 11.3 after screening outliers manually. EMEP data were used with station indices (blue and italics), which consist of the EBAS code (7 characters) and the latitude. For the first time, the flask sampling network by the Department of Chemistry, University of California, Irvine (UCI) have provided data to the GAW VOC programme, which are indicated with the original site codes and latitudes in magenta and italics. See the text for details.

Propane Data

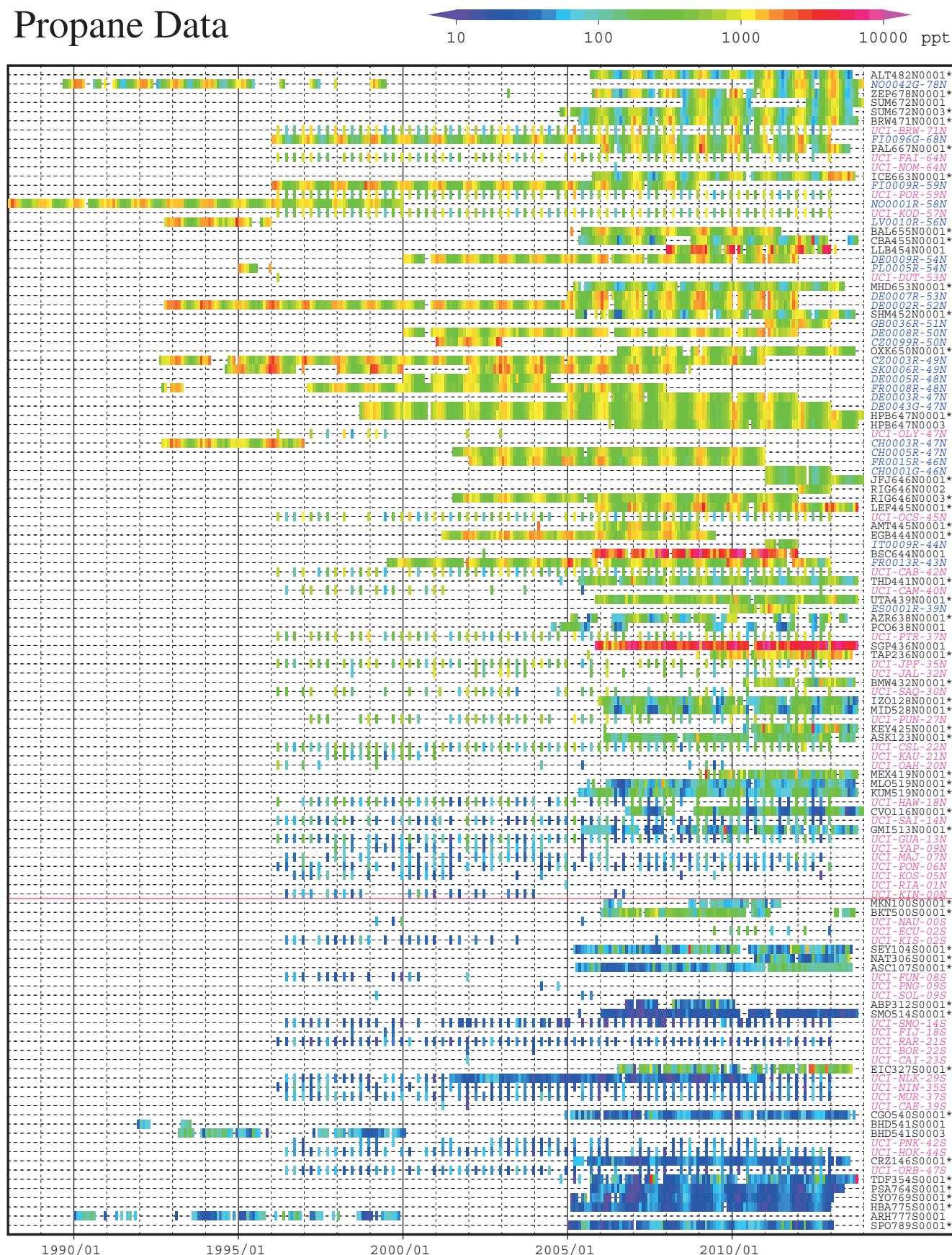
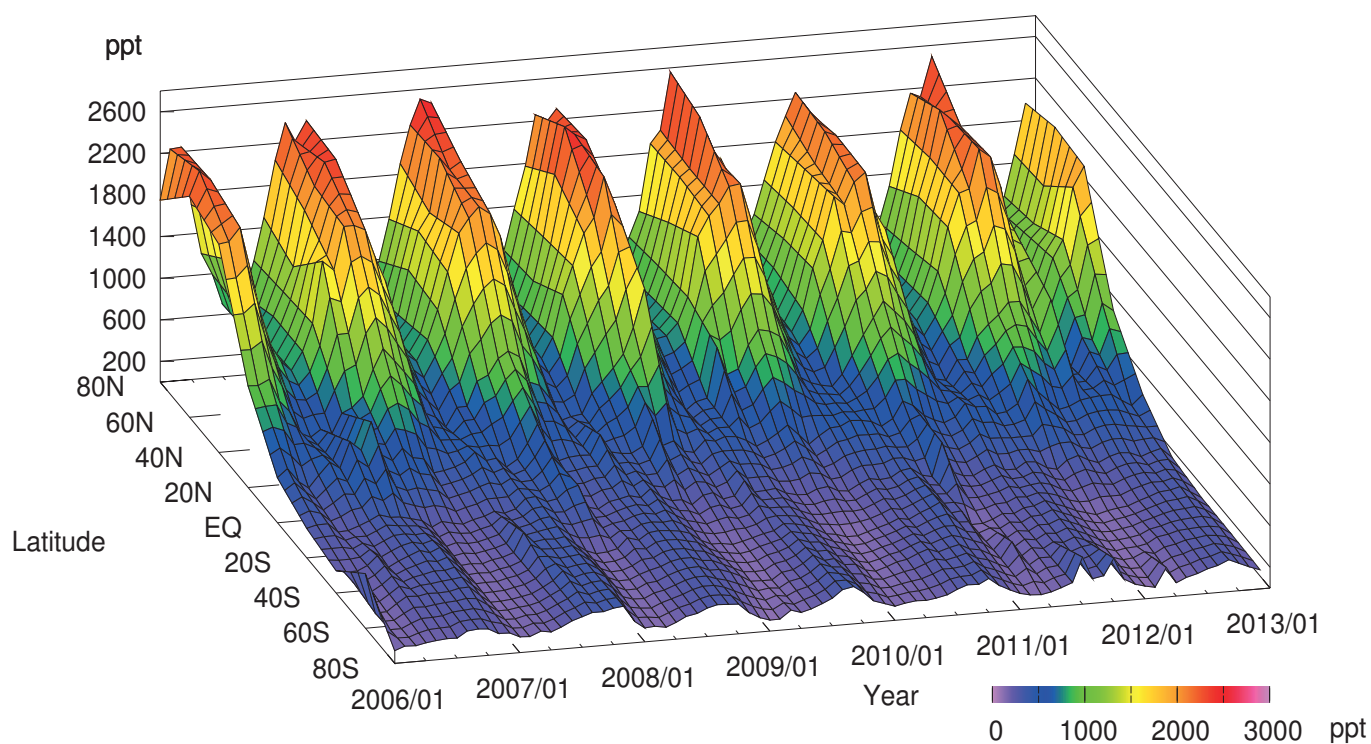


Plate 11.2 Monthly mean propane mole fractions that have been reported to the WDCGG by GAW stations and from EMEP and UCI as regional/contributing networks. The mole fractions are illustrated in different colors. The sites are listed in order from north to south. The red line indicates the equator. Only WDCGG data from the sites with an asterisk at the end of the station index were used in Plate 11.3 after screening outliers manually. EMEP data were used with station indices (blue and italics), which consist of the EBAS code (7 characters) and the latitude. UCI data are indicated with the original site codes and latitudes in magenta and italics. See the text for details.

Ethane mole fraction



Propane mole fraction

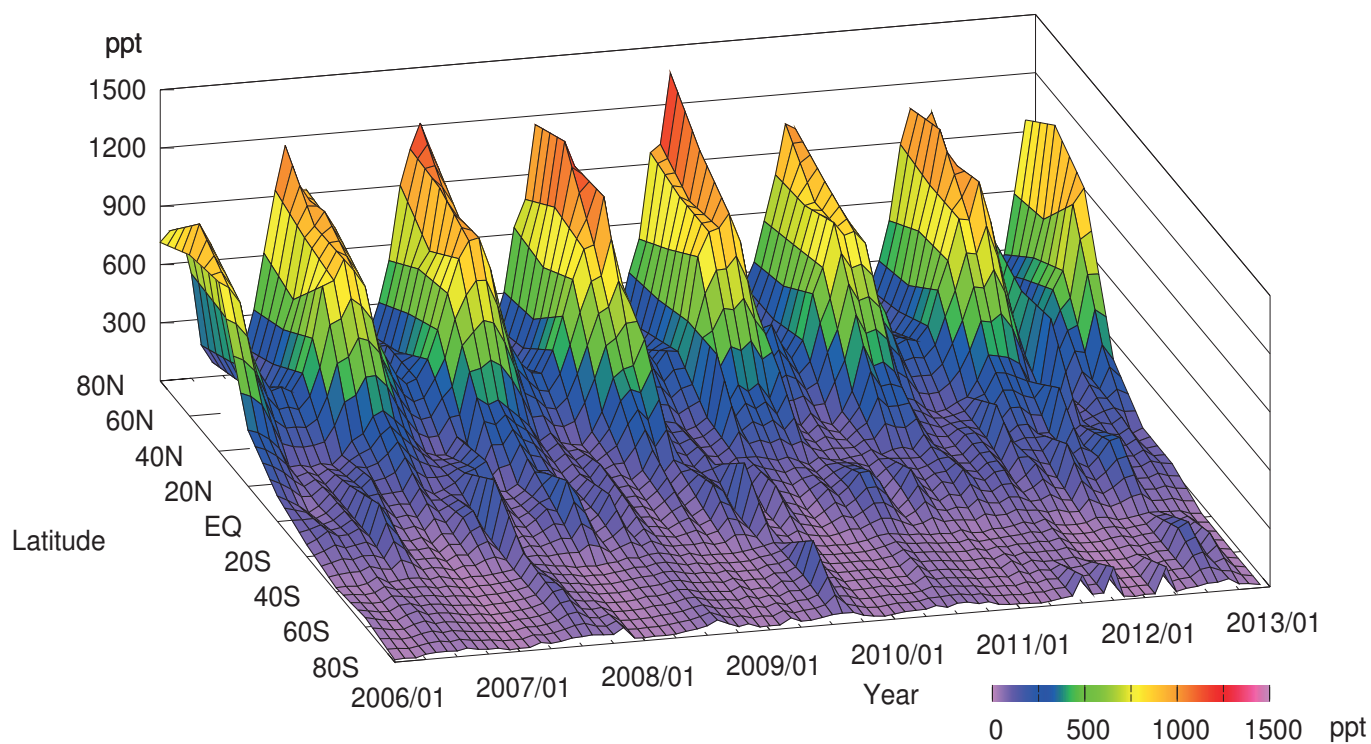


Plate 11.3 Variation of zonally averaged monthly mean ethane (upper) and propane (lower) mole fractions. The zonally averaged mole fractions were calculated for each 20° zone.

11. VOLATILE ORGANIC COMPOUNDS (VOCs)

Basic information on VOCs with regard to environmental issues

Volatile organic compounds (VOCs) have a variety of roles in atmospheric chemistry. They are major contributors to photochemical air pollution on both urban and regional scales and, together with NO_x, also impact ozone in the background troposphere. Some VOCs are injurious to human health at modest concentrations and are precursors to aerosols at quite low concentrations. VOCs also play an important indirect role for the climate change issue since they are precursors for tropospheric ozone and aerosols and since a large fraction of the VOCs eventually will be oxidized to CO₂ in the atmosphere. VOCs can serve as tracers of many atmospheric processes and emission sources. VOC molecules occur in many forms and have both natural and anthropogenic sources. The GAW Programme has sought to focus measurements on species which help to provide understanding of a wide range of atmospheric properties, and which can mostly be measured using currently approved techniques. Table 11.1 shows the molecules selected for measurements within GAW, with reasons for their selection (WMO, 2007c). The main reasons for measurements within GAW are associated with their use as tracers of the source types of greenhouse gases such as methane, to provide quantitative information on the extent of atmospheric processing by hydroxyl

radicals (OH) and other oxidants, and as precursors to ozone, organic acids and aerosols, particularly organic aerosols and sulphate aerosols. In addition, VOC measurements provide valuable information for air mass characterization at some stations to identify local sources of pollution. All of this information is of value to atmospheric modellers both in terms of input parameters and as constraints to model results.

Some GAW stations have the analytical capability to produce high quality measurements of a wide range of VOCs. Where appropriate calibration and quality assurance can be provided, these data should wherever possible be provided to WMO databases for wider scientific dissemination (WMO, 1996). The current global network of VOC measurements is shown on the front page of this chapter. Most of the stations are associated to the NOAA greenhouse and carbon monoxide flask sampling network, the UCI canister sampling network, and EMEP canister sampling stations, but it does include a number of sites where selected gases are measured at a higher frequency. These include three sites in Europe, one in Greenland (Summit) and one on the Island of Cape Verde. It is anticipated, however, that the number of sites with high frequency measurements will increase significantly in the next few years in the European region and the adjacent Arctic.

Table 11.1 Molecules selected for measurements within the GAW VOC Programme with reasons for their selection

| Molecule | Lifetime (OH=10 ⁹ cm ⁻³) | Importance to GAW | Analysis Method | Network Type |
|--------------------|--|--|------------------|---|
| Ethane | 2-4 months | •Methane sources •Natural sources •Biomass burning •Fossil fuel •Ocean production(S.hemisphere) •Trend in size of seasonal cycle | GC/FID | Global |
| Propane | 3 weeks | •Methane sources •Natural sources •Biomass burning •Fossil fuel •Ocean production(S.hemisphere) | GC/FID | Global |
| Acetylene | 3 weeks | •Motor vehicle tracer •Biomass burning tracer •Ratios to the other hydrocarbons •Trends | GC/FID | Global |
| Isoprene | 1-2 hours | •Biosphere product •Sensitive to temperature/land use/climate change •O ₃ precursor •Oxidizing capacity •Precursor to formaldehyde | GC/FID PTR-MS | Mid latitudes and tropics |
| Formaldehyde | 2 hours - 2 days | •Indicator of isoprene oxidation •Biomass burning •Comparison with satellites •Trends | DOAS | Small number of sites in Tropics for comparison with satellites |
| Terpenes | 1 hour | •Precursors to organic aerosols | GC/MS PTR-MS | Selected sites in forested areas |
| Acetonitrile | 0.4-1 year | •Biomass burning indicator •Biofuel burning indicator | GC/MS PTR-MS | Global |
| Methanol | 2 weeks | •Sources in the biosphere (methane oxidation) •Abundant oxidation product | GC/FID PTR-MS | Global |
| Ethanol | 1 week | •Tracer of alternative fuel usage | GC/FID PTR-MS | Global |
| Acetone | 1 months | •Abundant oxidation product •Free radical source in the upper troposphere | GC/FID PTR-MS | Global |
| DMS | 1 day | •Major natural sulphur source •Sulphate aerosol precursor •Tracer of marine bioproductivity | GC/FID PTR-MS | Global Marine |
| Benzene | 1 week | •Motor vehicle tracer •Biomass burning indicator | GC/FID GC-MS | Global |
| Toluene | 2 days | •Ratio to benzene used for air mass age •Precursor to particulates | GC/FID GC-MS | Global |
| Iso/normal Butane | 2-3 days | •Chemical processing indicator •Lifetime/ozone production •Indication of halogen chemistry | GC/FID GC-MS | Global |
| Iso/normal Pentane | 2-3 days | •Ratio provides impact of NO ₃ chemistry •Indication of halogen chemistry | GC/FID GC-MS | Global |

GC/FID is Gas Chromatography – Flame Ionization Detection
DOAS is Different Optical Absorption Spectrometry

GC/MS is Gas Chromatography – Mass Spectrometry
PTR-MS is Proton Transfer Reaction Mass Spectrometry

Seasonal variation and trends of VOCs

As with all other measurements within GAW that are designed to study atmospheric composition, an important use of the data is to evaluate trends over time. Sufficient data are available for many individual molecules, particularly the non-methane hydrocarbons (NMHCs). The current database also contains much information on the seasonal variation of both natural and anthropogenic hydrocarbons. The map on the front page of this chapter shows the network currently reporting VOC data, differentiating between sites where flask samples are collected for a limited set of NMHC measurements, and sites with measurements of a wider range of VOCs collected in a semi-continuous manner.

A review of the data recorded by the different sites reveals some interesting and important features, both concerning the characteristics of the measurement sites and the global and seasonal atmospheric behavior of VOCs. Focusing on ethane and propane, which have rather longer lifetimes among VOCs, Plates 11.1 and 11.2 show monthly mean mole fractions of ethane and propane, respectively, from 1988 to 2013 at each of the stations reporting to the database at WDCGG. The Department of Chemistry, University of California, Irvine (UCI) operates a flask sampling network in the Americas and Pacific region and for the first time have reported their huge VOC dataset to WDCGG as a contributing network (for details, see Simpson *et al.*, 2012). These data are now available at WDCGG. Detailed site information for UCI data are provided on pages 90-91. In addition, the figures also include data from EMEP stations (for details, see Tørseth *et al.*, 2012). The EMEP data were downloaded on 01/Dec./2014 from the EBAS database (<http://ebas.nilu.no/>) with courtesy of EMEP and its data providers. Based on recommendations from EMEP-CCC, some of these data sets were not used because of revision/update processes at EBAS.

A general feature of the data is a clear seasonal pattern with maximum concentrations in winter and minimum concentrations in summer. The sites in Plates 11.1 and 11.2 are listed by station latitude with the most northern at the top and the South Pole at the bottom. NMHCs tend to show a latitudinal concentration gradient, with concentrations decreasing from the poles to the equator, most notably during winter in the Northern Hemisphere. Some stations however, differ from these general patterns, *e.g.* higher VOC levels than other sites at similar latitudes, especially during winter. Within the GAW network, examples of the latter are the stations Lac La Biche (LLB), Constanta, Black Sea (BSC), and the Southern Great Plains (SGP), where the NMHC data indicate large local sources that elevate atmospheric NMHC mole fractions significantly above the North American

continental background. Consequently, while these data are of value for assessing the burden and long-term change of VOCs in these areas, they are unsuitable for consideration in the reconstruction of the latitudinal background of these gases.

Plates 11.3 shows globally averaged latitudinal ethane and propane mole fraction distributions, respectively, mostly from the NOAA/INSTAAR flask network between 2006 and 2013.

The ethane mole fraction shows a large seasonal variation which is mostly associated with its removal from the atmosphere by hydroxyl radical chemistry, leading to lower values in the summer months, as well as the emission seasonal cycles to contribute winter maximum and summer minimum. The greater latitudinal gradients in winter in the Northern Hemisphere compared to those in summer are also associated with corresponding larger OH gradients in winter. Absolute mole fractions are much larger in the Northern Hemisphere reflecting the preponderance of sources, mostly from oil and gas extraction in this region; Southern Hemisphere sources are dominated by emissions from biomass burning with a much smaller contribution associated with fossil fuel usage. A consideration of the budget of ethane in the atmosphere and its relevance to understanding the sources of methane was published by Simpson *et al.* (2012). This study concluded that the slow-down in the growth of atmospheric methane observed since the mid-1980s was predominantly associated with improved containment of methane emissions from processes such as flaring during oil and gas extraction. This result is a good example of how VOCs can be used as tracers to understand the behavior of important greenhouse gases.

The mole fractions of propane are generally lower than those of ethane owing to the shorter lifetime of propane by about a factor of 5 and roughly 50% lower sources for propane (mole-base). The propane distribution shows similar general features as for ethane, albeit stronger seasonality and more pronounced latitudinal gradients in the Northern Hemisphere during winter. Due to its shorter atmospheric lifetime compared to ethane, the Northern Hemisphere seasonal cycle shows a maximum close to mid-winter, whereas the ethane maximum is shifted by about two months toward spring owing to ethane reacting slower to the changes in OH. The higher rate decay of propane in summertime during transport of the air masses to remote observation sites compared to ethane contributes to the relatively lower summer minima seen in the representation of the network data.

REFERENCES

References

- Angert, A., S. Biraud, C. Bonfils, W. Buermann, and I. Fung, CO₂ seasonality indicates origins of post-Pinatubo sink, *Geophys. Res. Lett.*, **31**, L11103, doi:10.1029/2004GL019760, 2004.
- Bekki, S., K. S. Law, and J. A. Pyle, Effects of ozone depletion on atmospheric CH₄ and CO concentrations, *Nature*, **371**, 595–597, 1994.
- Bergamaschi, P., et al., Atmospheric CH₄ in the first decade of the 21st century: Inverse modeling analysis using SCIAMACHY satellite retrievals and NOAA surface measurements, *J. Geophys. Res. Atmos.*, **118**, 7350–7369, 2013.
- Berglen, T. F., T. K. Berntsen, I. S. A. Isaksen, and J. K. Sundet, A global model of the coupled sulfur/oxidant chemistry in the troposphere: The sulfur cycle, *J. Geophys. Res.*, **109**, D19310, doi:10.1029/2003JD003948, 2004.
- Boden, T. A., G. Marland, and R. J. Andres, Global, Regional, and National Fossil-Fuel CO₂ Emissions. Carbon Dioxide Information Analysis Center, Oak Ridge National Laboratory, U.S. Department of Energy, Oak Ridge, Tenn., USA, doi:10.3334/CDIAC/00001_V2013, 2013.
- Buizert C., K. M. Cuffey, J. P. Severinghaus, D. Baggenstos, T. J. Fudge, E. J. Steig, B. R. Markle, M. Winstrup, R. H. Rhodes, E. J. Brook, T. A. Sowers, G. D. Clow, H. Cheng, R. L. Edwards, M. Sigl, J. R. McConnell, and K. C. Taylor, The WAIS Divide deep ice core WD2014 chronology - Part 1: Methane synchronization (68-31 ka BP) and the gas age-ice age difference, *Clim. Past.*, **11**, 153–173, 2015.
- Cleveland, W. S., and S. J. Devlin, Locally weighted regression: an approach to regression analysis by local fitting, *J. Amer. Statist. Assn.*, **83**, 596–610, 1988.
- Conway, T. J., P. P. Tans, L. S. Waterman, K. W. Thoning, D. R. Kitzis, K. A. Masarie, and N. Zhang, Evidence for interannual variability of the carbon cycle from the National Oceanic and Atmospheric Administration/Climate Monitoring and Diagnostics Laboratory global air sampling network, *J. Geophys. Res.*, **99**, 22831–22855, 1994.
- Cooper, O. R., D. D. Parrish, J. Ziemke, N. V. Balashov, M. Cupeiro, I. E. Galbally, S. Gilge, L. Horowitz, N. R. Jensen, J.-F. Lamarque, V. Naik, S. J. Oltmans, J. Schwab, D. T. Shindell, A. M. Thompson, V. Thouret, Y. Wang and R. M. Zbinden, Global distribution and trends of tropospheric ozone: An observation-based review, *Elem. Sci. Anth.*, **2**, doi:10.12952/journal.elementa.000029., 2014.
- Dlugokencky, E. J., L. P. Steele, P. M. Lang, and K. A. Masarie, The growth rate and distribution of atmospheric methane, *J. Geophys. Res.*, **99**, 17021–17043, 1994.
- Dlugokencky, E. J., E. G. Dutton, P. C. Novelli, P. P. Tans, K. A. Masarie, K. O. Lantz, and S. Mardronich, Changes in CH₄ and CO growth rates after the eruption of Mt. Pinatubo and their link with changes in tropical tropospheric UV flux, *Geophys. Res. Lett.*, **23**, 2761–2764, 1996.
- Dlugokencky, E. J., B. P. Walter, K. A. Masarie, P. M. Lang and E. S. Kasischke, Measurements of an anomalous global methane increase during 1998, *Geophys. Res. Lett.*, **28**, 499–502, 2001.
- Dlugokencky, E. J., L. Bruhwiler, J. W. C. White, L. K. Emmons, P. C. Novelli, S. A. Montzka, K. A. Masarie, P. M. Lang, A. M. Crotwell, J. B. Miller, and L. V. Gatti, Observational constraints on recent increases in the atmospheric CH₄ burden, *Geophys. Res. Lett.*, **36**, L18803, 2009.
- Duchon, C. E., Lanczos filtering in one and two dimensions, *J. Appl. Meteor.*, **18**, 1016–1022, 1979.
- Etheridge, D. M., L. P. Steele, R. J. Francey, and R. L. Langenfelds, Atmospheric methane between 1000 A.D. and present: Evidence of anthropogenic emissions and climatic variability, *J. Geophys. Res.*, **103**, 15979–15993, 1998.
- Francey, R. J., P. P. Tans, C. E. Allison, I. G. Enting, J. W. C. White, and M. Troler, Changes in oceanic and terrestrial carbon uptake since 1982, *Nature*, **373**, 326–330, 1995.
- Gu, L., D. D. Baldocchi, S. C. Wofsy, J. W. Munger, J. J. Michalsky, S. P. Urbanski, and T. A. Bonden, Response of a deciduous forest to the Mount Pinatubo eruption enhanced photosynthesis, *Science*, **299**, 2035–2038, 2003.
- Haan, D. and D. Raynaud, Ice core record of CO variations during the last two millennia: atmospheric implications and chemical interactions within the Greenland ice, *Tellus*, **50B**, 253–262, 1998.
- Hansen, J., A. Lacis, R. Ruedy, and M. Sato, Potential Clim. Impact of Mount-Pinatubo Eruption, *Geophys. Res. Lett.*, **19(2)**, 215–218, 1992.
- Heimann, M. and M. Reichstein, Terrestrial ecosystem carbon dynamics and climate feedbacks, *Nature*, **451**, 289–292, 2008.
- IPCC, Climate Change 2013: The Physical Science Basis. Working Group I Contribution to the IPCC Fifth Assessment Report [Thomas Stocker, Qin Dahe, and Gian-Kasper Plattner]. Cambridge University Press, Cambridge, United Kingdom and New York, NY, USA, 2013.
- Keeling, C. D., R. B. Bacastow, A. F. Carter, S. C. Piper, T. P. Whorf, M. Heimann, W. G. Mook, and H. Roeloffzen, A three-dimensional model of

- atmospheric CO₂ transport based on observed winds: 1. Analysis of observational data, in aspects of climate variability in the Pacific and the Western Americas, edited by D. H. Peterson, *Geophysical Monograph* **55**, 165–236, American Geophysical Union, Washington, D.C., 1989.
- Keeling, C. D., T. P. Whorf, M. Wahlen, and J. van der Plicht, Interannual extremes in the rate of rise of atmospheric carbon dioxide since 1980, *Nature*, **375**, 666–670, 1995.
- Lambert, G., P. Monfray, B. Ardouin, G. Bonsang, A. Gaudry, V. Kazan and G. Polian, Year-to-year changes in atmospheric CO₂, *Tellus*, **47B**, 35–55, 1995.
- Levin, I., T. Naegler, R. Heinz, D. Osusko, E. Cuevas, A. Engel, J. Ilmberger, R.L. Langenfelds, B. Neiningner, C. v. Rohden, L.P. Steele, R. Weller, D.E. Worthy, and S.A. Zimov, The global SF₆ source inferred from long-term high precision atmospheric measurements and its comparison with emission inventories. *Atmos. Chem. Phys.*, **10**(6), 2655–2662, 2010.
- Levin, I., Earth science: The balance of the carbon budget, *Nature*, **488**, 35–36, 2012.
- Manning, A. C., and R. F. Keeling, Global oceanic and land biotic carbon sinks from the Scripps atmospheric oxygen flask sampling network, *Tellus*, **58B**, 95–116, 2006.
- Marenco, A., and F. Said, Meridional and vertical ozone distribution in the background troposphere from Scientific aircraft measurements during the STRATOZ III experiment, *Atmos. Env.*, **23**, 201–214, 1989.
- Matsueda, H., S. Taguchi, H. Y. Inoue, and M. Ishii, A large impact of tropical biomass burning on CO and CO₂ in the upper troposphere, *Science in China (Series C)*, **45**, 116–125, 2002.
- Morimoto, S., S. Aoki, T. Nakazawa, and T. Yamanouchi, Temporal variations of the carbon isotopic ratio of atmospheric methane observed at Ny Alesund, Svalbard from 1996 to 2004, *Geophys. Res. Lett.*, **33**, L01807, doi:10.1029/2005GL024648, 2006.
- Nakazawa, T., K. Miyashita, S. Aoki, and M. Tanaka, Temporal and spatial variations of upper tropospheric and lower stratospheric carbon dioxide, *Tellus*, **43B**, 106–117, 1991.
- Nakazawa, T., S. Morimoto, S. Aoki and M. Tanaka, Time and space variations of the carbon isotopic ratio of tropospheric carbon dioxide over Japan, *Tellus*, **45B**, 258–274, 1993.
- Nakazawa, T., S. Morimoto, S. Aoki and M. Tanaka, Temporal and spatial variations of the carbon isotopic ratio of atmospheric carbon dioxide in the western Pacific region, *J. Geophys. Res.*, **102**, 1271–1285, 1997.
- Nevison, C. D., N. M. Mahowald, S. C. Doney, I. D. Lima, G. R. van der Werf, J. T. Randerson, D. F. Baker, P. Kasibhatla, and G. A. McKinley, Contribution of ocean, fossil fuel, land biosphere, and biomass burning carbon fluxes to seasonal and interannual variability in atmospheric CO₂, *J. Geophys. Res.*, **113**, doi:10.1029/2007JG000408, 2008.
- Nisbet, E. G., E. J. Dlugokencky, and P. Bousquet, Methane on the Rise-Again, *Science*, **343**, 493–495, doi:10.1126/science.1247828, 2014.
- Novelli, P. C., K. A. Masarie, and P. M. Lang, Distributions and recent changes of carbon monoxide in the lower troposphere, *J. Geophys. Res.*, **103**, 19015–19033, 1998.
- Novelli, P. C., K. A. Masarie, P. M. Lang, B. D. Hall, R. C. Myers, and J. W. Elkins, Reanalysis of tropospheric CO trends: Effects of the 1997–1998 wildfires, *J. Geophys. Res.*, **108**(D15), 4464, doi:10.1029/2002JD003031, 2003.
- Oltmans *et al.*, Long-term changes in tropospheric ozone, *Atmos. Env.*, **40**, 3156–3173, 2006.
- Prinn, R. G., J. Huang, R. F. Weiss, D. M. Cunnold, P. J. Fraser, P. G. Simmonds, A. McCulloch, C. Harth, P. Salameh, S. O'Doherty, R. H. J. Wang, L. Porter and B. R. Miller, Evidence for substantial variations of atmospheric hydroxyl radicals in the past two decades, *Science*, **292**, 1882–1888, 2001.
- Rayner, P. J., I. G. Enting, R. J. Francey and R. Langenfelds, Reconstructing the recent carbon cycle from atmospheric CO₂, $\delta^{13}\text{C}$ and O₂/N₂ observations, *Tellus*, **51B**, 213–232, 1999.
- Ravishankara, A. R., J. S. Daniel, and R. W. Portmann, Nitrous Oxide (N₂O): the dominant ozone-depleting substance emitted in the 21st century, *Science*, **326**, 123–125, 2009.
- Reis, S., R. W. Pinder, M. Zhang, G. Lijie, and M. A. Sutton, Reactive nitrogen in atmospheric emission inventories, *Atmos. Chem. Phys.*, **9**, 7657–7677, 2009.
- Rigby, M., R. G. Prinn, P. J. Fraser, P. G. Simmonds, R. L. Langenfelds, J. Huang, D. M. Cunnold, L. P. Steele, P. B. Krummel, R. F. Weiss, S. O'Doherty, P. K. Salameh, H. J. Wang, C. M. Harth, J. Mühle, and L. W. Porter, Renewed growth of atmospheric methane, *Geophys. Res. Lett.*, **35**, L22805, 2008.
- Seinfeld, J. H., and S. N. Pandis, Atmospheric Chemistry and Physics: From Air Pollution to Climate Change, *John Wiley & Sons, Inc., New York*, 1326 pp., 1998.
- Shindell, D., G. Faluvegi, A. Lacis, J. Hansen, R. Ruedy, and E. Aguilar, Role of tropospheric ozone increases in 20th-century climate change, *J. Geophys. Res.*, **111**, D08302, doi:10.1029/2005JD006348, 2006.
- Simpson, I. J., M. P. S. Anderson, S. Meinardi, L. Bruhwiler, N. J. Blake, D. Helmig, F. S. Rowland, and D. R. Blake, Long-term decline of global

- atmospheric ethane concentrations and implications for methane, *Nature*, **488**, 490-494, 2012.
- Solomon, S., G-K. Plattner, R. Knutti and P. Friedlingstein, Irreversible climate change due to carbon dioxide emissions, *Proc. Natl. Acad. Sci. USA*, **106**, 1704-1709, 2009.
- Staehelin, J., J. Thudium, R. Buehler, A. Voltz-Thomas, and W. Graber, Trends in surface ozone concentrations at Arosa (Switzerland), *Atmos. Env.*, **28**, 75-87, 1994.
- Stenchikov, G., A. Robock, V. Ramaswamy, M. D. Schwarzkopf, K. Hamilton, and S. Ramachandran, Arctic Oscillation response to the 1991 Mount Pinatubo eruption: Effects of volcanic aerosols and ozone depletion, *J. Geophys. Res.*, **107(D24)**, 4803, doi:10.1029/2002JD002090., 2002.
- Tans, P., An accounting of the observed increase in oceanic and atmospheric CO₂ and an outlook for the future, *Oceanography*, **22(4)**, 26-35, <http://dx.doi.org/10.5670/oceanog.2009.94>, 2009.
- Tarasova, O. A., C. A. M. Brenninkmeijer, P. Jöckel, A. M. Zvyagintsev, and G.I. Kuznetsov: A climatology of surface ozone in the extra tropics: cluster analysis of observations and model results, *Atmos. Chem. Phys.*, **7**, 6099-6117, 2007.
- Thompson, R. L., F. Chevallier, A. M. Crotwell, G. Dutton, R. L. Langenfelds, R. G. Prinn, R. F. Weiss, Y. Tohjima, T. Nakazawa, P. B. Krummel, L. P. Steele, P. Fraser, S. O'Doherty, K. Ishijima and S. Aoki: Nitrous oxide emissions 1999 to 2009 from a global atmospheric inversion. *Atmos. Chem. Phys.*, **14**, 1801-1817, 2014.
- Thoning, K. W., P. P. Tans, and W. D. Komhyr, Atmospheric carbon dioxide at Mauna Loa observatory, 2. Analysis of the NOAA GMCC data, 1974-1985, *J. Geophys. Res.*, **94**, 8549-8565, 1989.
- Tørseth, K., W. Aas, K. Breivik, A. M. Fjæraa, M. Fiebig, A. G. Hjellbrekke, C. Lund Myhre, S. Solberg, and K. E. Yttri, Introduction to the European Monitoring and Evaluation Programme (EMEP) and observed atmospheric composition change during 1972-2009. *Atmos. Chem. Phys.*, **12**, 5447-5481, 2012.
- Tsutsumi, Y, Y. Makino, and J. B. Jensen, Vertical and latitudinal distributions of tropospheric ozone over the western Pacific: Case studies from the PACE aircraft missions, *J. Geophys. Res.*, **108(D8)**, 4251, doi:10.1029/2001JD001374, 2003.
- Vet, R., R. S. Artz, S. Carou, M. Shaw, C. U. Ro, W. Aas, A. Baker, V. C. Bowersox, F. Dentener, C. G. Lacaux, A. Hou, J. J. Pienaar, R. Gillett, M. C. Forti, S. Gromov, H. Hara, T. Khodzher, N. M. Mahowald, S. Nickovic, P.S.P. Rao, N. W. Reid, A global assessment of precipitation chemistry and deposition of sulfur, nitrogen, sea salt, base cations, organic acids, acidity and pH, and phosphorus, *Atmos. Env.*, **93**, 1-116, 2014.
- WMO, WMO-BMBF Workshop on VOC – Establishment of a “World Calibration/Instrument Intercomparison Facility for VOC” to Serve the WMO Global Atmosphere Watch (GAW) Programme, GAW Report No. 111, WMO TD No. 756, 1996.
- WMO, Scientific assessment of ozone depletion: 1998. WMO global ozone research and monitoring project—Report No. 44, 2-43, World Meteorological Organization, Geneva, 1999.
- WMO, World Data Centre for Greenhouse Gases (WDCGG) Data Summary, WDCGG No. 22, 84pp, 2000.
- WMO, Global Atmospheric Watch (GAW) Strategic Plan: 2008-2015, GAW Report No. 172, WMO TD No. 1384, 2007a.
- WMO, World Data Centre for Greenhouse Gases Data Submission and Dissemination Guide, GAW Report No. 174, WMO TD No. 1416, 2007b.
- WMO, A WMO/GAW Expert Workshop on Global Long-Term Measurements of Volatile Organic Compounds (VOCs), GAW Report No. 171, WMO TD No. 1373, 2007c.
- WMO, Technical Report of Global Analysis Method for Major Greenhouse Gases by the World Data Center for Greenhouse Gases, GAW Report No. 184, WMO TD No. 1473, 2009a.
- WMO, Revision of the World Data Centre for Greenhouse Gases Data Submission and Dissemination Guide, GAW Report No. 188, WMO TD No. 1507, 2009b. (http://www.wmo.int/pages/prog/arep/gaw/documents/GAW_188_web_20100128.pdf, accessed on 16 Feb. 2015)
- WMO, Addendum for the Period 2012-2015 to the WMO Global Atmosphere Watch (GAW) Strategic Plan 2008-2015, GAW Report No. 197, 2011a.
- WMO, Second Tropospheric Ozone Workshop - Tropospheric Ozone Changes: observations, state of understanding and model performances, GAW Report No.199, 2011b.
- WMO, WMO Greenhouse Gas Bulletin No.9, 2013. (<http://www.wmo.int/pages/prog/arep/gaw/ghg/GHGbuletin.html>, accessed on 16 Feb. 2015)
- WMO, 17th WMO/IAEA Meeting on Carbon Dioxide, Other Greenhouse Gases and Related Measurement Techniques (GGMT-2013), ed. Peter Tans and Christoph Zellweger, WMO/GAW Report No.213, 2014a.
- WMO, WMO Greenhouse Gas Bulletin No.10, 2014b. (<http://www.wmo.int/pages/prog/arep/gaw/ghg/GHGbuletin.html>, accessed on 16 Feb. 2015)
- Yoon, J., and A. Pozzer, Model-simulated trend of surface carbon monoxide for the 2001-2010 decade, *Atmos. Chem. Phys.*, **14**, 10465-10482, 2014.

APPENDICES

CALIBRATION AND STANDARD SCALES

1. Calibration System in the GAW Programme

Under the Global Atmosphere Watch (GAW) Programme, the Central Calibration Laboratories (CCLs) are assigned to host a Primary (Reference) Standard/scale, while the World Calibration Centres (WCCs) are responsible for the scale propagation to the stations via distribution of calibration standards for certain compounds, conducting instrument calibrations, comparison campaigns, station audits and providing

training to the station personnel. A Reference Standard/scale is designated for each variable to be used for all GAW measurements of that variable. Table 1 lists the organizations that serve as WCCs and CCLs for GAW (WMO, 2011). For CFCs and SO₂, no central facilities or quality control systems have so far been established within the GAW Programme.

Table 1. Overview of the GAW Central Calibration Laboratories (GAW-CCL, Reference Standard) and World Calibration Centres for greenhouse and other related gases. The World Calibration Centres have assumed global responsibilities, except where indicated (Am, Americas; E/A, Europe and Africa; A/O, Asia and the South-West Pacific)

| Compounds | Central Calibration Laboratory (Host of Primary Standard) | World Calibration Centre |
|---|---|--|
| Carbon Dioxide (CO ₂) | NOAA/ESRL | NOAA/ESRL (Round Robin) Empa (audits) |
| carbon isotopes | MPI-BGC | |
| Methane (CH ₄) | NOAA/ESRL | Empa (Am, E/A) JMA (A/O) |
| Nitrous Oxide (N ₂ O) | NOAA/ESRL | IMK-IFU |
| Chlorofluorocarbons (CFCs) | | |
| Sulphur Hexafluoride (SF ₆) | NOAA/ESRL | KMA |
| Molecular Hydrogen (H ₂) | MPI-BGC | |
| Surface Ozone (O ₃) | NIST | Empa |
| Carbon Monoxide (CO) | NOAA/ESRL | Empa |
| Volatile Organic Compounds (VOCs) | NPL (8 components) | KIT/IMK-IFU |
| Sulphur Dioxide (SO ₂) | | |
| Nitrogen Oxides (NO _x) | | FZ-Jurich |

2. Carbon Dioxide (CO₂)

In 1995, the National Oceanic and Atmospheric Administration's Earth System Research Laboratory (NOAA/ESRL, formerly CMDL; Climate Monitoring and Diagnostics Laboratory) in Boulder, Colorado, USA, took over the role of the Central Calibration Laboratory (CCL) from the Scripps Institution of Oceanography (SIO) in San Diego, California, USA. Since then, NOAA/ESRL has served as the CCL responsible for the maintenance of the GAW Primary Standard for CO₂. As CCL for CO₂, NOAA/ESRL maintains a high-precision manometric system for absolute calibration of CO₂ as the reference for GAW measurements throughout the world (Zhao *et al.*, 1997), as well as carrying out Round Robin in the function of

WCC. It has been recommended that the standards of the GAW measurement laboratories be calibrated at least every three years at the CCL (WMO, 2012).

Under the WMO calibration system, there have been several calibration scales for CO₂, *e.g.*, SIO-based X74, X85, X87, X93 and X2002 scales and the NOAA/ESRL-based WMO Mole Fraction Scale partially based on previous SIO scales. The CCL adopted the WMO X2005 scale, reflecting historical manometric calibrations of the CCL's set of cylinders and the possible small differences between SIO and NOAA/ESRL calibrations. The most current WMO Mole Fraction Scale is the WMO-X2007 scale.

To assess the differences in standard scales among

measuring laboratories, NOAA/ESRL organizes intercomparisons or Round Robin experiments endorsed by WMO. It is recommended that round-robins are repeated at least once every three years. Many laboratories participated in the experiments organized in 1991–1992, 1995–1997, 1999–2000, 2002–2006, and 2009–2012. Table 2 shows the results of the experiments performed in 2009–2012, in which the mole fractions measured by various laboratories are compared

with the mole fractions measured by NOAA/ESRL (http://www.esrl.noaa.gov/gmd/ccgg/wmorr/wmorr_results.php). In addition, many laboratories compare their standards bilaterally or multilaterally.

Table 3 lists laboratories and sites that contributed to the present issue of the *Data Summary* with standard scales of reported data and history of participation in WMO intercomparison experiments.

Table 2. Round Robin results for the mole fraction of carbon dioxide. Differences between the mole fractions measured by various laboratories and the mole fractions measured by NOAA (Laboratory minus NOAA, ppm).

| Laboratory | Measurement Date | Mole Fraction Difference (ppm) | | |
|--------------|------------------|--------------------------------|-----------------------|---------------------|
| | | Low 365-375 ppm | Medium 380-390 ppm | High 395-405 ppm |
| JMA | Jun-09 | –0.001 | –0.056 | –0.035 |
| MRI | Jul-09 | –0.133 | –0.045 | –0.046 |
| AIST | Sep-09 | 0.077 | 0.125 | 0.164 |
| NIES | Oct-09 | –0.033 | –0.005 | 0.034 |
| TU | Jan-10 | 0.147 | 0.205 | 0.284 |
| CMA | Apr-10 | –0.213 | –0.135 | –0.036 |
| KMA/KGAWO | Jul-10 | –0.543 | 0.005 | 0.054 |
| KRISS | Jul-10 | 0.137 | 0.195 | 0.244 |
| SNU | Nov-10 | 0.007 | 0.025 | 0.144 |
| IPEN | Jul/Aug-11 | –0.087 | –0.025 | –0.024 |
| AEMET | Sep-12 | 0.027 | –0.025 | 0.024 |
| EC | Apr-09 | –0.023 | –0.022 | –0.028 |
| SIO | May-09 | –0.197 | –0.136 | –0.112 |
| AMERIFLUX | May-09 | –0.017 | 0.034 | 0.018 |
| SAWS | Aug-09 | 0.036 | 0.064 | –0.042 |
| NIWA | Nov-09 | 0.016 | –0.023 | –0.065 |
| CSIRO | Jan-10 | 0.003 | 0.004 | –0.102 |
| PSU | Sep-10 | 0.063 | 0.084 | –0.012 |
| HU | Nov-10 | –0.037 | –0.069 | –0.093 |
| NCAR | Apr-11 | –0.015 | 0.011 | –0.021 |
| OSU | Aug-11 | 0.020 | 0.084 | 0.001 |
| ITM | May-09 | –0.861 | –0.732 | –0.197 |
| FMI | Jun-09 | 0.019 | 0.028 | 0.033 |
| UBA/SCH | Aug-09 | –0.001 | 0.014 | 0.043 |
| UHEI-IUP | Aug-09 | –0.035 | –0.043 | –0.075 |
| MRI-BGC | Sep/Oct-09 | –0.017 | 0.004 | –0.001 |
| UBA/ZUG | Dec-09 | –0.071 | –0.242 | –0.477 |
| HMS | Mar-10 | 0.069 | –0.022 | –0.027 |
| CESI/RICERCA | Apr-10 | –0.011 | 0.058 | 0.083 |
| ENEA | Jun-10 | –0.181 | –0.302 | –0.367 |
| JRC | Oct-10 | –0.041 | 0.018 | 0.003 |
| WCC-Empa | Nov-10 | 0.069 | 0.108 | 0.133 |
| Empa | Dec-10 | –0.017 | 0.044 | 0.063 |
| UEA | Dec-10 | –0.264 | –0.172 | –0.119 |
| KUP | Jan-11 | –0.154 | –0.108 | –0.041 |

| | | | | |
|------|--------|--------|--------|--------|
| ECN | Mar-11 | 0.005 | 0.030 | 0.038 |
| LSCE | Apr-11 | 0.062 | 0.010 | 0.121 |
| RHUL | Jun-11 | -0.079 | -0.066 | -0.107 |

Table 3. Status of standard scales and calibration/intercomparison for CO₂ at laboratories.

| Laboratory | WDCGG Filename Code | Calibration Scale | WMO Inter-comparison |
|--------------------|--|-------------------|-----------------------------------|
| AEMET | IZO128N0000 | WMO | 91/92, 96/97, 99/00, 09/12 |
| Aichi | MKW234N0000 | WMO | |
| AIST | TKY236N0000 | AIST | 96/97, 99/00, 02/06, 09/12 |
| BMKG & Empa | BKT500S0000 | WMO | |
| BoM & CSIRO | CGO540S0000, CGO540S0010 | WMO | |
| CMA | WLG236N0000 | WMO | 96/97, 99/00, 02/06, 09/12 |
| CNR-ICES & DNA-IAA | JBN762S0000 | WMO | |
| CSIRO | ALT482N0003, CFA519S0003, CGO540S0003, CRI215N0000, CYA766S0001, ESP449N0003, MAA767S0003, MLO519N0003, MQA554S0003, SIS660N0003, SPO789S0003 | WMO | 91/92, 96/97, 99/00, 02/06, 09/12 |
| EC | ALT482N0000, ALT482N0005, CDL453N0000, CHM449N0000, CSJ451N0000, EGB444N0100, ESP449N0000, ETL454N0000, FSD449N0000, LLB454N0100, WSA443N0000, WSA443N0001 | WMO | 91/92, 96/97, 99/00, 02/06, 09/12 |
| EMA | CAI130N0000 | | |
| Empa | JFJ646N0000 | WMO | 09/12 |
| ENEA | LMP635N0001 | WMO | 91/92, 96/97, 99/00, 02/06, 09/12 |
| FMI | PAL667N0000 | WMO | 02/06, 09/12 |
| HKO | HKG222N0001 | WMO | |
| | HKO222N0000, HKO222N0001 | NIST WMO | |
| HMS | HUN646N0000, KPS646N0000 | WMO | 91/92, 96/97, 99/00, 02/06, 09/12 |
| IAFMS | CMN644N0001, CMN644N0002 | WMO | 91/92, 96/97, 02/06 |
| IGP | HUA312S0000 | WMO | |
| IMK-IFU | WNK647N0000, ZUG647N0014 | WMO | 99/00 |
| INRNE | BEO642N0000 | WMO | |
| IOEP | DIG654N0000 | IOEP | |
| ITM | ZEP678N0000 | WMO | 96/97, 99/00, 09/12 |
| JMA | MNM224N0000, RYO239N0000, YON224N0000 | WMO | 91/92, 96/97, 99/00, 02/06, 09/12 |

| | | | |
|---------------------|---|--------------|---|
| KMA | AMY236N0000 | WMO KRISS | 02/06, 09/12 |
| | KSG762S0000 | KRISS | |
| KSNU | ISK242N0000 | | |
| KUP | JFJ646N0003 | WMO | |
| LSCE | AMS137S0000, BGU641N0000, LPO648N0000, MHD653N0002, PDM642N0000, PUY645N0000 | WMO | 91/92, 96/97, 99/00, 02/06, 09/12 |
| | FIK635N0000 | | |
| MGO | BER255N0001, KOT276N0001, KYZ240N0001, STC652N0001, TER669N0001, TIK271N0000 | WMO | |
| MMD | DMV504N0000 | WMO | |
| MRI | TKB236N0002 | | 91/92, 96/97, 99/00, 02/06, 09/12 |
| NIER | GSN233N0103 | WMO | |
| NIES | COI243N0000, HAT224N0000 | NIES 95** | 96/97, 99/00, 02/06, 09/12 |
| NIMR | GSN233N0001 | WMO | 96/97 |
| NIPR & Tohoku Univ. | SYO769S0000 | | Tohoku Univ.: 91/92, 96/97, 99/00, 02/06, 09/12 |
| NIWA | BHD541S0000 | WMO | 91/92, 96/97, 99/00, 02/06, 09/12 |
| NMA | FDT645N0002 | | |
| NOAA/ESRL | BRW471N0000, MLO519N0000, SMO514S0000, SPO789S0000, NOAA/ESRL flask network* | WMO | 91/92, 96/97, 99/00, 02/06, 09/12 |
| Osaka Univ. | SUI234N0000 | | |
| RIVM | KMW653N0000 | NIST | |
| RSE | PRS645N0000 | WMO | 99/00, 02/06 |
| Saitama | DDR236N0000, KIS236N0000, URW235N0000 | WMO | |
| SAWS | CPT134S0000 | WMO | 99/00, 02/06, 09/12 |
| Shizuoka Univ. | HMM234N0000 | | |
| UBA | BRT648N0000, DEU649N0000, LGB652N0000, NGL653N0000, SNB647N0000, SSL647N0000, SSL647N0002, WES654N0000, ZGT654N0000, ZSF647N0001, ZUG647N0000 | WMO | 91/92, 96/97, 99/00, 02/06, 09/12 |
| Univ. Malta | GLH636N0000 | | |

* NOAA/ESRL flask network:

ABP312S0001,ALT482N0001,AMS137S0001,ASC107S0001,ASK123N0001,AVI417N0001,AZR638N0001,BAL655N0001,BHD541S0001, BKT500S0001,BME432N0001,BMW432N0001,BRW471N0001,BSC644N0001,CBA455N0001,CGO540S0001,CHR501N0001,CMO445N0001, CPT134S0001,CRZ146S0001,EIC327S0001,GMI513N0001,GOZ636N0001,HBA775S0001,HPB647N0003,HUN646N0001,ICE663N0001, ITN435N0001,IZO128N0001,KCO204N0001,KEY425N0001,KUM519N0001,KZD244N0001,KZM243N0001,LEF445N0001,LLB454N0001, LLN223N0001,LMP635N0003,MBC476N0001,MEX419N0001,MHD653N0001,MID528N0001,MKN100S0001,MLO519N0001,NMB123S0001, NWR440N0101,OPW448N0001,PAL667N0001,POC900N0001,POC905N0001,POC905S0001,POC910N0001,POC910S0001,POC915N0001, POC915S0001,POC920N0001,POC920S0001,POC925N0001,POC925S0001,POC930N0001,POC930S0001,POC935S0001,PSA764S0001, PTA438N0001,RPB413N0001,SCS903N0001,SCS906N0001,SCS909N0001,SCS912N0001,SCS915N0001,SCS918N0001,SCS921N0001, SDZ240N0000,SEY104S0001,SGP436N0001,SHM452N0001,SMO514S0001,SPO789S0001,STC654N0001,STM666N0001,SUM672N0001, SYO769S0001,TAP236N0001,TDF354S0001,THD441N0001,UTA439N0001,UUM244N0001,WIS631N0001,WLG236N0001,ZEP678N0001

**NIES 95 CO₂ scale is 0.10 to 0.14 ppm lower than WMO in a range between 355 to 385 ppm.

(Machida *et al.*, WMO/GAW Report No. 186, 26-29, 2009.)

3. Methane (CH₄)

The GAW Programme has established two WCCs for CH₄, the Swiss Federal Laboratory for Materials Testing and Research (Empa), Dübendorf, Switzerland; and the Japan Meteorological Agency (JMA), Tokyo, Japan (WMO, 2007). In addition, the Central Calibration Laboratory for CH₄ has been established at NOAA/ESRL (Dlugokencky *et al.*, 2005; WMO, 2007).

The WMO X2004 (NOAA04) scale has been designated as the Primary scale of the GAW Programme. This scale results in CH₄ mole fractions that are a factor of 1.0124 higher than the previous scale (NOAA/CMDL83) used by NOAA/ESRL (Dlugokencky *et al.*, 2005).

Table 4 summarizes the CH₄ standard scales used by laboratories contributing to the WDCGG and lists tentative multiplying conversion factors applied for

analysis in this issue of the *Data Summary*. The standard is the WMO X2004 scale, and conversion factors were calculated from the results of comparisons with other laboratories performed bilaterally or multilaterally before the establishment of the GAW Standard.

The NOAA/CMDL83 scale is lower than an absolute gravimetric scale (Aoki *et al.*, 1992) by ~1.5% (Dlugokencky *et al.*, 1994) and lower than the AES (Atmospheric Environment Service, currently EC) scale by a factor of 1.0151 (Worthy *et al.*, 1998). The CMDL83 scale can be converted to the Tohoku University standard by multiplying by 1.0121 (Dlugokencky *et al.*, 2005). The conversion factors $1.0124 / 1.0151 = 0.9973$ and $1.0124 / 1.0121 = 1.0003$ have been adopted for comparisons with the NOAA04 scale.

Table 4. Status of the standard scales of CH₄ at laboratories with conversion factors.

| Laboratory | WDCGG Filename Code | Calibration Scale | Conversion Factor |
|-------------|---|-------------------|-------------------|
| AEMET | IZO128N0000 | WMO X2004 | 1 |
| AGAGE | CGO540S0011, CGO540S0013, CMO445N0011, MHD653N0011, MHD653N0013, RPB413N0000, RPB413N0011, SMO514S0014, SMO514S0016, THD441N0000 | Tohoku Univ. | 1.0003 |
| BMKG & Empa | BKT500S0000 | WMO X2004 | 1 |
| CHMI | KOS649N0000 | CHMI | |
| CMA | WLG236N0000 | WMO X2004 | 1 |
| CSIRO | ALT482N0003, CFA519S0003, CGO540S0003, CRI215N0000, CYA766S0001, ESP449N0003, MAA767S0003, MLO519N0003, MQA554S0003, SIS660N0003, SPO789S0003 | WMO X2004 | 1 |
| EC | ALT482N0000, CDL453N0000, CHM449N0000, EGB444N0100, ESP449N0000, ETL454N0000, FSD449N0000, LLB454N0100, WSA443N0000 | WMO X2004 | 1 |
| Empa | JFJ646N0000 | WMO X2004 | 1 |
| ENEA | LMP635N0001 | WMO X2004 | 1 |
| FMI | PAL667N0000 | WMO X2004 | 1 |
| ISAC | CMN644N0000 | WMO X2004 | 1 |
| JMA | MNM224N0000, RYO239N0000, YON224N0000 | WMO X2004 | 1 |
| KMA | AMY236N0000 | KRISS | |
| KSNU | ISK242N0000 | | |
| LSCE | AMS137S0002, BGU641N0000, LPO648N0000, PDM642N0000, PUY645N0002 | NOAA /CMDL83 | 1.0124 |
| | FIK635N0000, MHD653N0007 | | |
| MGO | TER669N0001, TIK271N0000 | WMO X2004 | 1 |
| MRI | TKB236N0000 | | 0.9973 |
| NIER | GSN233N0103 | WMO X2004 | 1 |
| NIES | COI243N0000, HAT224N0000 | NIES | 0.9973 |

| | | | |
|-------------|---|-----------------|--------|
| NIMR | GSN233N0001 | SIO X97 | |
| NOAA/ESRL | BRW471N0000, MLO519N0000, NOAA/ESRL flask network* | WMO X2004 | 1 |
| | KPA431N0001, LEF445N0001, MCM777S0001, NZL543S0001, POC935S0001, SGI354S0001, SIO432N0001 | NOAA /CMDL83 | 1.0124 |
| RIVM | KMW653N0000 | NIST | 0.9973 |
| RSE | PRS645N0000 | WMO X2004 | 1 |
| SAWS | CPT134S0000 | WMO X2004 | 1 |
| UBA | DEU649N0000, NGL653N0000, SSL647N0000, ZGT654N0000, ZSF647N0010, ZUG647N0000 | WMO X2004 | 1 |
| | SNB647N0000 | | |
| Univ. Malta | GLH636N0000 | | |

* NOAA/ESRL flask network:

ABP312S0001,ALT482N0001,AMS137S0001,ASC107S0001,ASK123N0001,AVI417N0001,AZR638N0001,BAL655N0001,BKT500S0001,
BME432N0001,BMW432N0001,BRW471N0001,BSC644N0001,CBA455N0001,CGO540S0001,CHR501N0001,CMO445N0001,CPT134S0001,
CRZ146S0001,EIC327S0001,GMI513N0001,GOZ636N0001,HBA775S0001,HPB647N0003,HUN646N0001,ICE663N0001,ITN435N0001,
IZO128N0001,KEY425N0001,KUM519N0001,KZD244N0001,KZM243N0001,LLB454N0001,LLN223N0001,LMP635N0003,MBK476N0001,
MEX419N0001,MHD653N0001,MID528N0001,MKN100S0001,MLO519N0001,NMB123S0001,NWR440N0101,OPW448N0001,OKK650N0001,
PAL667N0001,POC900N0001,POC905N0001,POC905S0001,POC910N0001,POC910S0001,POC915N0001,POC915S0001,POC920N0001,
POC920S0001,POC925N0001,POC925S0001,POC930N0001,POC930S0001,PSA764S0001,PTA438N0001,RPB413N0001,SCS903N0001,
SCS906N0001,SCS909N0001,SCS912N0001,SCS915N0001,SCS918N0001,SCS921N0001,SEY104S0001,SGP436N0001,SHM452N0001,
SMO514S0001,SPO789S0001,STM666N0001,SUM672N0001,SYO769S0001,TAP236N0001,TDF354S0001,THD441N0001,UTA439N0001,
UUM244N0001,WIS631N0001,WKT431N0001,WLG236N0001,ZEP678N0001

4. Nitrous Oxide (N₂O)

The Halocarbons and other Atmospheric Trace Species (HATS) Group of NOAA/ESRL maintains a set of standards for N₂O (Hall *et al.*, 2001) and serves as a CCL for N₂O. The WMO X2006 (NOAA-2006) scale (Hall *et al.*, 2007), revised and updated to WMO X2006A (NOAA-2006A) in 2011 to deal with drifting in secondary standards, has been designated as the Primary scale for the GAW Programme. CCL compares its standards with the ones of other laboratories, including those of Environment Canada (EC) and the Australian Commonwealth Scientific and Industrial Research Organisation (CSIRO). Karlsruhe Institute of Technology, Institute for

Meteorology and Climate Research, Germany, serves as the GAW WCC for N₂O.

The SIO-98 scale is essentially equivalent to the WMO X2006 scale, with an average difference of 0.01% over the range of 299–319 ppb; the WMO X2000 (NOAA-2000) scale can be converted to the X2006 scale by using the factor 0.999402 (Hall *et al.*, 2007). A constant ratio of 1.0017 between CSIRO and AGAGE data was used by Huang *et al.* (2008), and a factor of $1 / 1.0017 = 0.9983$ has been used in this report to convert CSIRO scale to the WMO X2006 scale.

Table 5. Status of the standard scales of N₂O at laboratories.

| Laboratory | WDCGG Filename Code | Calibration Scale | Conversion Factor |
|------------|---|-------------------|-------------------|
| AEMET | IZO128N0000 | WMO X2006 | 1 |
| AGAGE | ADR651N0010, CGO540S0011, CGO540S0012, CGO540S0013, CMO445N0010, CMO445N0011, MHD653N0011, MHD653N0013, RPB413N0000, RPB413N0010, RPB413N0011, SMO514S0014, SMO514S0015, SMO514S0016, THD441N0000 | SIO 1998 | 1 |
| CSIRO | ALT482N0003, CFA519S0003, CGO540S0003, CRI215N0000, CYA766S0001, ESP449N0003, MAA767S0003, MLO519N0003, MQA554S0003, SIS660N0003, SPO789S0003 | WMO X2006A | 1 |
| Empa | JFJ646N0000 | SIO 1998 | 1 |
| ENEA | LMP635N0001 | WMO X2006 | 1 |

| | | | |
|--------------|--|------------|----------|
| ISAC | CMN644N0000 | WMO X2006 | 1 |
| JMA | RYO239N0000 | WMO X2006A | 1 |
| KMA | AMY236N0000 | KRISS | |
| MRI | MMB243N0000 | | |
| Nagoya Univ. | NGY235N0000 | | |
| NIER | GSN233N0103 | WMO X2006 | 1 |
| NIES | COI243N0000, HAT224N0000 | NIES 96* | 1 |
| NILU | ZEP678N0000 | | |
| NIMR | GSN233N0001 | WMO X1997 | |
| NOAA/ESRL | ALT482N0001, BRW471N0001, CGO540S0001, KUM519N0001, MLO519N0001, NWR440N0001, SMO514S0001, SPO789S0001 | WMO X2000 | 0.999402 |
| | ALT482N0004, ALT482N0006, BRW471N0003, BRW471N0005, BRW471N0011, CGO540S0009, CGO540S0014, HFM442N0000, ITN435N0000, KUM519N0002, LEF445N0000, MHD653N0008, MLO519N0005, MLO519N0006, MLO519N0011, NWR440N0003, NWR440N0004, NWR440N0011, PSA764S0000, SMO514S0008, SMO514S0009, SMO514S0011, SPO789S0005, SPO789S0006, SPO789S0011, SUM672N0002, TDF354S0000, THD441N0002 | WMO X2006 | 1 |
| | BRW471N0010, MLO519N0010, NWR440N0010, SMO514S0010, SPO789S0010, SUM672N0000 | WMO X2006A | 1 |
| SAWS | CPT134S0000 | WMO X2000 | 0.999402 |
| UBA | SSL647N0000, ZSF647N0001 | SIO 1998 | 1 |

*NIES 96 N₂O scale is approximately 0.6 ppb lower than WMO X2006 in the range 317 to 321 ppb.
(<http://www.esrl.noaa.gov/gmd/ccgg/wmorr/results.php?rr=rr5¶m=n2o>)

5. Surface Ozone (O₃)

The National Institute of Standards and Technology (NIST) has developed and deployed Standard Reference Photometers (SRPs) in the USA and other countries. The GAW has designated SRP #2 maintained by NIST as the Primary Standard for the GAW Programme, making NIST the CCL for O₃. The Swiss Federal Laboratory for Materials Testing

and Research (Empa) maintains NIST SRP #15 as the reference and is the GAW WCC for surface ozone (Hofer *et al.*, 1998). The traceability and uncertainty of O₃ within the GAW network were reported by Klausen *et al.*, (2003). Regional Calibration Centre has been established at Observatorio Central Buenos Aires, Argentina (WMO, 2007).

Table 6. Status of surface ozone standard scales at laboratories

| Laboratory | WDCGG Filename Code | Calibration Scale | Audit Empa-WCC |
|------------|--|----------------------|------------------------|
| AEMET | IZO128N0000 | WMO (NIST & Empa) | 96, 98, 00, 04, 09, 13 |
| | DON637N0000, MHN639N0000, NIA642N0000, ROQ640N0000, SPM639N0000 | NPL (U. K.) | |
| AQRB | ALG447N0000, ALT482N0009, BRA450N0000, CHA446N0000, CPS449N0000, EGB444N0000, ELA449N0000, EST451N0000, KEJ444N0000, LON442N0000, SAT448N0000, SUT445N0000 | | Alert: 04 |
| ARSO | IRB645N0000, KVK646N0000, KVV646N0000, ZRN646N0000 | WMO (NIST & Empa) | |

| | | | |
|-------------|---|----------------------|--------------------------------------|
| AWI | NMY770S0000 | | |
| BMKG & Empa | BKT500S0000 | WMO (NIST & Empa) | 99, 01, 04, 07, 08, 11 |
| BoM & CSIRO | CGO540S0000 | | |
| | CGO540S0018 | WMO (NIST & Empa) | 02, 10 |
| CHMI | KOS649N0000 | WMO (NIST & Empa) | |
| CMA | WLG236N0000 | WMO (NIST & Empa) | |
| CVGZ | KRE649N0000, KRE649N0001, KRE6490002 | | |
| DEFRA | EDM655N0000 | | |
| DMC & Empa | TLL330S0000 | WMO (NIST & Empa) | |
| DWD | HPB647N0000 | WMO (NIST & Empa) | 97, 06, 11 |
| EMA | CAI130N0000 | | |
| Empa | JFJ646N0000, PAY646N0000, RIG646N0000 | WMO (NIST & Empa) | Jungfrauoch: 99, 06 |
| Empa & KMD | MKN100S0000 | WMO (NIST & Empa) | 00, 02, 05, 06, 08, 10 |
| FMI | AHT662N0000, OUL666N0000, PAL667N0000, UTO659N0000, VIR660N0000 | | Pallas-Sammaltunturi: 97, 03, 07, 12 |
| HMS | KPS646N0000 | WMO (NIST & Empa) | |
| IM | ANG638N0000, BEJ638N0000, CAS639N0000, FUN132N0000, LIS638N0000, MVH638N0000, PEN640N0000 | | |
| INRNE | BEO642N0000 | WMO (NIST & Empa) | |
| IOEP | DIG654N0000 | WMO (NIST & Empa) | |
| ISAC | CMN644N0000, DCC775S0000, PYR227N0000 | WMO (NIST & Empa) | Monte Cimone: 12 |
| IVL | VDL664N0000 | WMO (NIST & Empa) | |
| JMA | MNM224N0000, RYO239N0000, SYO769S0002, TKB236N1004, YON224N0000 | WMO (NIST & Empa) | JMA GAW Facilites: 05 Ryori: 05 |
| KSNU | ISK242N0000 | | |
| LA | PDM642N0001 | EMD (France) | |
| LAMP | PUY645N0001 | EMD (France) | |
| LVGMC | DBL656N0000, RCV656N0000, ZSN657N0000 | WMO (NIST & Empa) | |
| MMD | DMV504N0000, TAR504N0000 | WMO (NIST & Empa) | Danum Valley: 08, 13 |

| | | | |
|-------------|---|----------------------|--|
| NILU | ZEP678N0000 | WMO (NIST & Empa) | 97, 01, 05, 12 |
| NIWA | BHD541S0000 | WMO (NIST & Empa) | |
| NMA | FDT645N0002 | | |
| NOAA/ESRL | ARH777S0000, BMW432N0004, BRW471N0004, ICE663N0004, LAU545S0004, MLO519N0004, NWR440N0002, NWR440N0204, RPB413N0004, SMO514S0004, SPO789S0004, SUM672N0004, THD441N0004, WKT431N000 | WMO (NIST & Empa) | Mauna Loa: 03 Barrow: 08 Lauder: 10 |
| | MCM777S0004 | | |
| NUI | MHD653N0000 | WMO (NIST & Empa) | 96, 98, 02, 05, 09, 13 |
| ONM | ASK123N0000 | WMO (NIST & Empa) | 03, 07 |
| PolyU | HKG222N0000 | | |
| RIVM | KMW653N0000 | NMI | |
| Roshydromet | DAK654N0000, SHP659N0000 | | |
| RSE | PRS645N0000 | INRIM (Italy) | |
| SAWS | CPT134S0000 | WMO (NIST & Empa) | 97, 98, 02, 06, 11 |
| SMN | USH354S0000, USH354S0001 | WMO (NIST & Empa) | 98, 03, 08 |
| SMNA | LQO322S0000, MBI764S0000, PIL331S0000, SJA349S0000, USH354S0002 | WMO (NIST & Empa) | |
| UBA | BRT648N0000, DEU649N0000, LGB652N0000, NGL653N0000, SNB647N0000, SSL647N0000, WES654N0000, ZGT654N0000, ZSF647N0010, ZUG647N0000 | WMO (NIST & Empa) | Zugspitze: 96, 97, 01 Zugspitze/Schneefern erhaus: 01, 06, 11 Sonnblick: 98 |
| UNA | SNL325S0000 | | |
| Univ. Malta | GLH636N0000 | Tohoku Univ. | |
| Univ. York | CVO116N0001 | WMO (NIST & Empa) | 12 |

6. Carbon Monoxide (CO)

NOAA ESRL is the WMO/GAW CCL for carbon monoxide. The CCL has produced three CO scales during the past 24 years using a similar gravimetric method. The CCL produced two earlier scales (WMO/NOAA 1988 and WMO X2000) of which only WMO X2000 is sometimes still used for comparison purposes. WMO X2000 is based upon a larger set of the primary standards made in 1999/2000 using the

GC-HgO reduction technique.

The Swiss Federal Laboratory for Materials Testing and Research (Empa) serves as the WCC under GAW based on its secondary standards calibrated against the standard at NOAA/ESRL designated as the Primary Standard for GAW. Empa, as WCC for CO, has developed an audit system for CO measurements at GAW stations.

Table 7. Status of CO standard scales at laboratories

| Laboratory | WDCGG Filename Code | Calibration Scale | Audit Empa-WCC |
|------------|--------------------------|---------------------------------|-------------------|
| AEMET | IZO128N0000 | WMO X2004 (NOAA/ESRL & Empa) | 00, 04, 09, 13 |
| AGAGE | CGO540S0011, MHD653N0011 | CSIRO94 | |

| | | | |
|-------------|---|---------------------------------|---|
| ARSO | KVV646N0000 | CHMI | |
| BMKG & Empa | BKT500S0000 | WMO X2000 (NOAA/ESRL & Empa) | 04, 07, 08, 11 |
| CHMI | KOS649N0000 | CHMI | |
| CSIRO | ALT482N0003, CFA519S0003, CGO540S0003, CRI215N0000, CYA766S0001, ESP449N0003, MAA767S0003, MLO519N0003, MQA554S0003, SIS660N0003, SPO789S0003 | CSIRO | Cape Grim: 02, 10 |
| DMC & Empa | TTL330S0000 | WMO X2004 (NOAA/ESRL & Empa) | |
| DWD | HPB647N0000 | WMO X2004 (NOAA/ESRL & Empa) | 97, 06, 11 |
| EC | ALT482N0000, CDL453N0000, CHM449N0000, EGB444N0100, ESP449N0000, ETL454N0000, FSD449N0000, LLB454N0100, WSA443N0000 | WMO (NOAA/ESRL & Empa) | Alert: 04 |
| Empa | JFJ646N0000, PAY646N0000, RIG646N0000 | WMO (NOAA/ESRL & Empa) | Jungfrauoch: 99,06 |
| Empa & KMD | MKN100S0000 | WMO X2000 (NOAA/ESRL & Empa) | 05, 06, 08, 10 |
| INRNE | BEO642N0000 | WMO (NOAA/ESRL & Empa) | |
| ISAC | CMN644N0000, CMN644N0003, CMN644N0004 | WMO X2004 (NOAA/ESRL & Empa) | 12 |
| JMA | MNM224N0000, RYO239N0000, YON224N0000 | WMO X2000 (NOAA/ESRL) | JMA GAW Facilites: 05 Ryori: 05 |
| LA | PDM642N0001 | EMD (France) | |
| LAMP | PUY645N0001 | EMD (France) | |
| LSCE | AMS137S0000 | WMO X2004 (NOAA/ESRL & Empa) | 08 |
| NOAA/ESRL | NOAA/ESRL flask network* | WMO (NOAA/ESRL & Empa) | Mauna Loa: 03 Barrow: 08 Mt. Waliguan: 00, 04, 09 |
| ONM | ASK123N0000 | WMO X2000 (NOAA/ESRL & Empa) | 07 |
| PolyU | HKG222N0000 | | |
| RIVM | KMW653N0000, KTB653N0000 | NMI | |
| SAWS | CPT134S0002 | | 98, 02 |
| | CPT134S0003 | WMO (NOAA/CMDL) | 06, 11 |
| SMN | USH354S0000, USH354S0001 | WMO (NOAA/ESRL & Empa) | 98, 03, 08 |
| SMNA | USH354S0002 | WMO X2000 (NOAA/ESRL & Empa) | |
| UBA | NGL653N0000, SSL647N0000, ZSF647N0001, ZUG647N0000 | WMO (NOAA/CMDL) | Zugspitze: 97, 01 Zugspitze/Schne efernerhaus: |
| | SNB647N0000 | | 01, 06, 11 Sonnblick: 98 |
| Univ. Malta | GLH636N0001, GLH636N0002 | | |

| | | | |
|------------|-------------|---------------------------------|----|
| Univ. York | CVO116N0001 | WMO X2004 (NOAA/ESRL & Empa) | 12 |
|------------|-------------|---------------------------------|----|

*NOAA/ESRL flask network:

ABP312S0001,ALT482N0001,ASC107S0001,ASK123N0001,AZR638N0001,BAL655N0001,BHD541S0001,BKT500S0001,BME432N0001,BMW432N0001,BRW471N0001,BSC644N0001,CBA455N0001,CGO540S0001,CHR501N0001,CMO445N0001,CPT134S0001,CRZ146S0001,EIC327S0001,GMI513N0001,GOZ636N0001,HBA775S0001,HPB647N0003,HUN646N0001,ICE663N0001,ITN435N0001,IZO128N0001,KEY425N0001,KUM519N0001,KZD244N0001,KZM243N0001,LEF445N0001,LLB454N0001,LLN223N0001,LMP635N0003,MBC476N0001,MEX419N0001,MHD653N0001,MID528N0001,MKN100S0001,MLO519N0001,NMB123S0001,NWR440N0101,OXK650N0001,PAL667N0001,POC900N0001,POC905N0001,POC905S0001,POC910N0001,POC910S0001,POC915N0001,POC915S0001,POC920N0001,POC920S0001,POC925N0001,POC925S0001,POC930N0001,POC930S0001,POC935N0000,POC935S0001,PSA764S0001,PTA438N0001,RPB413N0001,SCS903N0001,SCS906N0001,SCS909N0001,SCS912N0001,SCS915N0001,SCS918N0001,SCS921N0001,SEY104S0001,SGP436N0001,SHM452N0001,SMO514S0001,SPO789S0001,STM666N0001,SUM672N0001,SYO769S0001,TAP236N0001,TDF354S0001,THD441N0001,UTA439N0001,UUM244N0001,WIS631N0001,WLG236N0001,ZEP678N0001

References

- Aoki, S., T. Nakazawa, S. Murayama and S. Kawaguchi, Measurements of atmospheric methane at the Japanese Antarctic station, Syowa, *Tellus, Ser. B*, **44**, 273–281, 1992.
- Dlugokencky, E. J., L. P. Steele, P. M. Lang, and K. A. Masarie, The growth rate and distribution of atmospheric methane, *J. Geophys. Res.*, **99**, 17021-17043, 1994.
- Dlugokencky, E. J., R. C. Myers, P. M. Lang, K. A. Masarie, A. M. Crotwell, K. W. Thoning, B. D. Hall, J. W. Elkins, and L. P. Steele, Conversion of NOAA atmospheric dry air CH₄ mole fractions to a gravimetrically prepared standard scale, *J. Geophys. Res.*, **110**, D18306, doi: 10.1029/2005JD006035, 2005.
- Hall, B. D. (ed.), J. W. Elkins, J. H. Butler, S. A. Montzka, T. M. Thompson, L. Del Negro, G. S. Dutton, D. F. Hurst, D. B. King, E. S. Kline, L. Lock, D. Mactaggart, D. Mondeel, F. L. Moore, J. D. Nance, E. A. Ray, and P. A. Romashkin, Halocarbons and Other Atmospheric Gases, Section 5 in Climate Monitoring and Diagnostics Laboratory, Summary Report N. 25, 1998–1999, R. S. Schnell, D. B. King, R. M. Rosson (eds.), NOAA-CMDL, Boulder, CO., USA, 2001.
- Hall, B. D., G. S. Dutton, and J. W. Elkins, The NOAA nitrous oxide standard scale for atmospheric observations, *J. Geophys. Res.*, **112**, D09305, doi:10.1029/2006JD007954, 2007.
- Hofer, P., B. Buchmann and A. Herzog, Traceability, Uncertainty and Assessment Criteria of Surface Ozone Measurements, *Empa-WCC Report 98/5*, 20 pp, 1998.
- Huang, J., A. Golombek, R. Prinn, R. Weiss, P. Fraser, P. Simmonds, E. J. Dlugokencky, B. Hall, J. Elkins, P. Steele, R. Langenfelds, P. Krummel, G. Dutton, and L. Porter, Estimation of regional emissions of nitrous oxide from 1997 to 2005 using multinet network measurements, a chemical transport model, and an inverse method, *J. Geophys. Res.*, **113**, D17313, doi:10.1029/2007JD009381, 2008.
- Klausen, J., C. Zellweger, B. Buchmann, and P. Hofer, Uncertainty and bias of surface ozone measurements at selected Global Atmosphere Watch sites, *J. Geophys. Res.*, **108(D19)**, 4622, doi:10.1029/2003JD003710, 2003.
- WMO, WMO Global Atmosphere Watch (GAW) Strategic Plan: 2008–2015, WMO/GAW Report No. 172, 108pp, 2007.
- WMO, Addendum for the Period 2012 – 2015 to the WMO Global Atmosphere Watch (GAW) Strategic Plan 2008 – 2015, WMO/GAW Report No. 197, 57pp, 2011.
- WMO, 16th WMO/IAEA Meeting on Carbon Dioxide, Other Greenhouse Gases and Related Measurement Techniques (GGMT-2011), ed. Gordon Brailsford, WMO/GAW Report No.206, 67pp, 2012.
- Worthy, D. E. J., I. Levin, N. B. A. Trivett, A. J. Kuhlmann, J. F. Hopper and M. K. Ernst, Seven years of continuous methane observations at a remote boreal site in Ontario, Canada, *J. Geophys. Res.*, **103**, 15995–16007, 1998.
- Zhao, C. L., P. P. Tans, and K. W. Thoning, A high precision manometric system for absolute calibrations of CO₂ in dry air, *J. Geophys. Res.*, **102**, 5885–5894, 1997.

LIST OF ABBREVIATIONS IN THE CALIBRATION AND STANDARD SCALES

| | |
|-----------------|---|
| AEMET | Agencia Estatal de Meteorología (Spain) |
| AGAGE | Advanced Global Atmospheric Gases Experiment |
| Aichi | Aichi Prefecture (Japan) |
| AIST | National Institute of Advanced Industrial Science and Technology (Japan) |
| AQRB | Air Quality Research Branch, Meteorological Service of Canada (Canada) |
| ARSO | Agencija Republike Slovenije za Okolje (Slovenia) |
| AWI | Alfred Wegener Institute for Polar and Marine Research (Germany) |
| BMKG | Agency for Meteorology, Climatology and Geophysics (Indonesia) |
| BoM | Commonwealth Bureau of Meteorology (Australia) |
| CHMI | Czech Hydrometeorological Institute (Czech Republic) |
| CMA | China Meteorological Administration (China) |
| CNR-ICES | International Centre for Earth Sciences, Consiglio Nazionale delle Ricerche (Italy) |
| CSIRO | Commonwealth Scientific and Industrial Research Organisation (Australia) |
| CVGZ | Centrum Vyzkumu Globalni Zmeny AV CR |
| DEFRA | Department for Environment, Food and Rural Affairs (United Kingdom) |
| DMC | Dirección Meteorológica de Chile |
| DNA-IAA | Dirección Nacional del Antártico-Instituto Antártico Argentino (Argentina) |
| DWD | Deutscher Wetterdienst (German Meteorological Service, Germany) |
| EARS | Environmental Agency of the Republic of Slovenia |
| EC | Environment Canada (Canada) |
| EMA | Egyptian Meteorological Authority (Egypt) |
| EMD | Ecole des Mines de Douai (France) |
| Empa | Swiss Federal Laboratories for Material Testing and Research (Switzerland) |
| ENEA | Italian National Agency for New Technology, Energy and the Environment (Italy) |
| FMI | Finnish Meteorological Institute |
| GAGE | Global Atmospheric Gases Experiment |
| GAW | Global Atmosphere Watch (WMO) |
| HATS | Halocarbons and other Atmospheric Trace Species Group, NOAA/ESRL |
| HKO | Hong Kong Observatory (Hong Kong, China) |
| HMS | Hungarian Meteorological Service (Hungary) |
| IAFMS | Italian Air Force Meteorological Service (Italy) |
| IEK-8 | Institute for Energy and Climate Research: Troposphere (IEK-8), Research Center Juelich GmbH (Germany) |
| IGP | Instituto Geofísico del Perú (Peru) |
| IM | Instituto de Meteorologia (Portugal) |
| IMK-IFU | Institut für Meteorologie und Klimatologie, Atmosphärische Umweltforschung, Forschungszentrum Karlsruhe (Germany) |
| INRIM | Istituto Nazionale di Ricerca Metrologica (Italy) |
| INRNE | Institute for Nuclear Research and Nuclear Energy (Bulgaria) |
| IOEP | Institute of Environmental Protection (Poland) |
| ISAC | Istituto di Scienze dell'Atmosfera e del Clima, Consiglio Nazionale delle Ricerche (Italy) |
| ITM | Department of Applied Environmental Science, Stockholm University, (Sweden) |
| IVL | Swedish Environmental Research Institute, Göteborg (Sweden) |
| JMA | Japan Meteorological Agency (Japan) |

| | |
|-----------------------|--|
| KMA | Korea Meteorological Administration (Republic of Korea) |
| KMD | Kenya Meteorological Department (Kenya) |
| KRISS | Korea Research Institute of Standards and Science (Republic of Korea) |
| KSNU | Kyrgyz State National University (Kyrgyzstan) |
| KUP | Physics Institute, Climate and Environmental Physics, University of Bern (Switzerland) |
| LA | Laboratoire d'Aérodologie (France) |
| LAMP | Laboratoire de Météorologie Physique (France) |
| LEGMA | Latvian Environment, Geology and Meteorology Agency (Latvia) |
| LSCE | Laboratoire des Sciences du Climat et de l'Environnement (France) |
| LVGMC | Latvian Environment, Geology and Meteorology Centre (Latvia) |
| MGO | Main Geophysical Observatory, Roshydromet (Russian Federation) |
| MPI-BGC | Max-Planck Institute (MPI) for Biogeochemistry in Jena (Germany) |
| MMD | Malaysian Meteorological Department |
| MRI | Meteorological Research Institute, JMA (Japan) |
| Nagoya Univ. | Nagoya University (Japan) |
| NIER | National Institute of Environmental Research (Republic of Korea) |
| NIES | National Institute for Environmental Studies (Japan) |
| NILU | Norwegian Institute for Air Research (Norway) |
| NIMR | National Institute of Meteorological Research, KMA (Republic of Korea) |
| NIPR | National Institute of Polar Research (Japan) |
| NIST | National Institute of Standards and Technology (USA) |
| NIWA | National Institute of Water & Atmospheric Research (New Zealand) |
| NMA | National Meteorological Administration (Romania) |
| NMI | Nederlands Meetinstituut |
| NOAA/ESRL | Earth System Research Laboratory, NOAA (USA) |
| NPL | National Physical Laboratory (United Kingdom) |
| NUI | National University of Ireland, Galway (Ireland) |
| ONM | Office National de la Météorologie (Algeria) |
| Osaka Univ. | Osaka University (Japan) |
| PolyU | Hong Kong Polytechnic University (Hong Kong, China) |
| RIVM | National Institute for Health and Environment (Netherlands) |
| Roshydromet | Federal Service for Hydrometeorology and Environmental Monitoring (Russian Federation) |
| RSE | Ricerca sul Sistema Elettrico (Italy) |
| Saitama | Saitama Prefecture (Japan) |
| SAWS | South African Weather Service (South Africa) |
| Shizuoka Univ. | Shizuoka University (Japan) |
| SMN(SMNA) | Servicio Meteorológico Nacional (Argentina) |
| Tohoku Univ. | Tohoku University (Japan) |
| UBA | Umweltbundesamt (Germany) |
| UNA | Universidad Nacional de Asunción (Paraguay) |
| Univ. Malta | University of Malta (Malta) |
| Univ. York | University of York (United Kingdom of Great Britain and Northern Ireland) |
| WDCGG | World Data Centre for Greenhouse Gases, operated by JMA, Japan (WMO) |
| WMO | World Meteorological Organization |

LIST OF OBSERVATIONAL STATIONS

| Station | Country/Territory | Index Number | Location | | Altitude (m) | Parameter |
|------------------------|--|--------------|-------------------|--------------------|-----------------|---|
| | | | Latitude (° ') | Longitude (° ') | | |
| REGION I (Africa) | | | | | | |
| Amsterdam Island | France | AMS137S00 | 37 48 S | 77 32 E | 55 | CH ₄ , CO ₂ |
| Amsterdam Island | France | AMS137S00 | 37 48 S | 77 32 E | 55 | CH ₄ , CO, CO ₂ , O ₃ , VOCs |
| Ascension Island | United Kingdom of Great Britain and Northern Ireland | ASC107S00 | 7 55 S | 14 25 W | 54 | ¹³ CH ₄ , ¹³ CO ₂ , C ¹⁸ O ₂ , CH ₄ , CO, CO ₂ , H ₂ , VOCs |
| Assekrem | Algeria | ASK123N00 | 23 16 N | 5 38 E | 2710 | CO, O ₃ |
| Assekrem | Algeria | ASK123N00 | 23 16 N | 5 38 E | 2710 | ¹³ CO ₂ , C ¹⁸ O ₂ , CH ₄ , CO, CO ₂ , H ₂ , VOCs |
| Cairo | Egypt | CAI130N00 | 30 05 N | 31 17 E | 35 | CO ₂ , O ₃ , SO ₂ |
| Cape Point | South Africa | CPT134S00 | 34 21 S | 18 29 E | 230 | CH ₄ , CO, CO ₂ , N ₂ O, O ₃ |
| Cape Point | South Africa | CPT134S00 | 34 21 S | 18 29 E | 230 | CH ₄ , CO, CO ₂ |
| Cape Point | South Africa | CPT134S00 | 34 21 S | 18 29 E | 230 | ²²² Rn |
| Cape Verde Observatory | Cape Verde | CVO116N00 | 16 51 N | 24 52 W | 10 | CO, NO, NO ₂ , NO _x , NO _y , O ₃ , VOCs |
| Crozet | France | CRZ146S00 | 46 27 S | 51 51 E | 120 | ¹³ CO ₂ , C ¹⁸ O ₂ , CH ₄ , CO, CO ₂ , H ₂ , VOCs |
| Funchal | Portugal | FUN132N00 | 32 39 N | 16 53 W | 58 | O ₃ |
| Gobabeb | Namibia | NMB123S00 | 23 34 S | 15 01 E | 461 | ¹³ CO ₂ , C ¹⁸ O ₂ , CH ₄ , CO, CO ₂ |
| Izaña (Tenerife) | Spain | IZO128N00 | 28 18 N | 16 30 W | 2367 | CH ₄ , CO, CO ₂ , N ₂ O, O ₃ , SF ₆ |
| Izaña (Tenerife) | Spain | IZO128N00 | 28 18 N | 16 30 W | 2367 | ¹³ CO ₂ , C ¹⁸ O ₂ , CH ₄ , CO, CO ₂ , H ₂ , VOCs |
| Mahe Island | Seychelles | SEY104S00 | 4 40 S | 55 10 E | 7 | ¹³ CO ₂ , C ¹⁸ O ₂ , CH ₄ , CO, CO ₂ , H ₂ , VOCs |
| Mt. Kenya | Kenya | MKN100S00 | 0 04 S | 37 18 E | 3678 | CO, O ₃ |
| Mt. Kenya | Kenya | MKN100S00 | 0 04 S | 37 18 E | 3678 | ¹³ CO ₂ , C ¹⁸ O ₂ , CH ₄ , CO, CO ₂ , VOCs |
| REGION II (Asia) | | | | | | |
| Anmyeon-do | Republic of Korea | AMY236N00 | 36 32 N | 126 19 E | 47 | CFCs, CH ₄ , CO ₂ , N ₂ O, SF ₆ |
| Bering Island | Russian Federation | BER255N00 | 55 12 N | 165 59 E | 13 | CO ₂ |
| Cape Ochi-ishi | Japan | COI243N00 | 43 10 N | 145 30 E | 42.5 | CFCs, CH ₄ , CO ₂ , HCFCs, HFCs, N ₂ O, SF ₆ |
| Cape Rama | India | CRI215N00 | 15 05 N | 73 50 E | 60 | ¹³ CO ₂ , CH ₄ , CO, CO ₂ , H ₂ , N ₂ O |
| Everest - Pyramid | Nepal | PYR227N00 | 27 57 N | 86 49 E | 5079 | O ₃ |
| Everest - Pyramid | Nepal | PYR227N00 | 27 57 N | 86 49 E | 5079 | C ₂ Cl ₄ , C ₂ HCl ₃ , CBrClF ₂ , CBrF ₃ , CCl ₄ , CFCs, CH ₂ Br ₂ , CH ₂ Cl ₂ , CH ₃ Br, CH ₃ CCl ₃ , CH ₃ Cl, CHBr ₃ , CHCl ₃ , HCFCs, HFCs |
| Gosan | Republic of Korea | GSN233N00 | 33 17 N | 126 10 E | 72 | CFCs, CH ₄ , CO ₂ , N ₂ O |
| Gosan | Republic of Korea | GSN233N01 | 33 10 N | 126 06 E | 72 | CFCs, CH ₄ , CO ₂ , N ₂ O |
| Hamamatsu | Japan | HMM234N00 | 34 43 N | 137 43 E | 35 | CO ₂ |
| Hateruma | Japan | HAT224N00 | 24 04 N | 123 49 E | 10.8 | CFCs, CH ₄ , CO ₂ , HCFCs, HFCs, N ₂ O, SF ₆ |
| Hok Tsui | Hong Kong, China | HKG222N00 | 22 13 N | 114 15 E | 60 | CO ₂ |
| Hok Tsui | Hong Kong, China | HKG222N00 | 22 13 N | 114 15 E | 60 | CO, O ₃ |
| Issyk-Kul | Kyrgyzstan | ISK242N00 | 42 37 N | 76 59 E | 1640 | CH ₄ , CO ₂ , O ₃ |
| Kaashidhoo | Maldives | KCO204N00 | 4 58 N | 73 28 E | 1 | ¹³ CO ₂ , CH ₄ , CO ₂ |
| King's Park | Hong Kong, China | HKO222N00 | 22 19 N | 114 10 E | 65 | CO ₂ |
| Kisai | Japan | KIS236N00 | 36 05 N | 139 33 E | 13 | CO ₂ |
| Kotelny Island | Russian Federation | KOT276N00 | 76 00 N | 137 52 E | 5 | CO ₂ |
| Kyzylcha | Uzbekistan | KYZ240N00 | 40 52 N | 66 09 E | 340 | CO ₂ |

LIST OF OBSERVATIONAL STATIONS (continued)

| Station | Country/Territory | Index Number | Location | | Altitude (m) | Parameter |
|--|--------------------|--------------|-------------------|--------------------|-----------------|---|
| | | | Latitude (° ') | Longitude (° ') | | |
| Lulin | China | LLN223N00 | 23 28 N | 120 52 E | 2867 | ¹³ CO ₂ , C ¹⁸ O ₂ , CH ₄ , CO, CO ₂ |
| Memambetsu | Japan | MMB243N00 | 43 55 N | 144 12 E | 32.9 | N ₂ O |
| Mikawa-Ichinomiya | Japan | MKW234N00 | 34 51 N | 137 26 E | 50 | CO ₂ |
| Minamitorishima | Japan | MNM224N00 | 24 17 N | 153 59 E | 8 | CH ₄ , CO, CO ₂ , O ₃ |
| Mt. Dodaira | Japan | DDR236N00 | 36 00 N | 139 11 E | 840 | CO ₂ |
| Mt. Waliguan | China | WLG236N00 | 36 17 N | 100 54 E | 3810 | CH ₄ , CO ₂ , O ₃ |
| Mt. Waliguan | China | WLG236N00 | 36 17 N | 100 54 E | 3810 | ¹³ CH ₄ , ¹³ CO ₂ , C ¹⁸ O ₂ , CH ₄ , CO, CO ₂ , H ₂ |
| Nagoya | Japan | NGY235N00 | 35 09 N | 136 58 E | 35 | N ₂ O |
| Plateau Assy | Kazakhstan | KZM243N00 | 43 15 N | 77 52 E | 2519 | ¹³ CO ₂ , C ¹⁸ O ₂ , CH ₄ , CO, CO ₂ , H ₂ |
| Ryori | Japan | RYO239N00 | 39 02 N | 141 49 E | 260 | CCl ₄ , CFCs, CH ₃ CCl ₃ , CH ₄ , CO, CO ₂ , N ₂ O, O ₃ |
| Sary Taukum | Kazakhstan | KZD244N00 | 44 27 N | 75 34 E | 412 | ¹³ CO ₂ , C ¹⁸ O ₂ , CH ₄ , CO, CO ₂ , H ₂ |
| Shangdianzi | China | SDZ240N00 | 40 39 N | 117 07 E | 287 | CH ₄ , CO ₂ |
| Ship between Ishigaki Island and Hateruma Island | Japan | SIH224N00 | 24 07 N | 123 50 E | 5 | CO ₂ |
| South China Sea (03N) | N/A | SCS903N00 | 3 00 N | 105 00 E | 15 | ¹³ CO ₂ , C ¹⁸ O ₂ , CH ₄ , CO, CO ₂ , H ₂ |
| South China Sea (06N) | N/A | SCS906N00 | 6 00 N | 107 00 E | 15 | ¹³ CO ₂ , C ¹⁸ O ₂ , CH ₄ , CO, CO ₂ , H ₂ |
| South China Sea (09N) | N/A | SCS909N00 | 9 00 N | 109 00 E | 15 | ¹³ CO ₂ , C ¹⁸ O ₂ , CH ₄ , CO, CO ₂ , H ₂ |
| South China Sea (12N) | N/A | SCS912N00 | 12 00 N | 111 00 E | 15 | ¹³ CO ₂ , C ¹⁸ O ₂ , CH ₄ , CO, CO ₂ , H ₂ |
| South China Sea (15N) | N/A | SCS915N00 | 15 00 N | 113 00 E | 15 | ¹³ CO ₂ , C ¹⁸ O ₂ , CH ₄ , CO, CO ₂ , H ₂ |
| South China Sea (18N) | N/A | SCS918N00 | 18 00 N | 113 00 E | 15 | ¹³ CO ₂ , C ¹⁸ O ₂ , CH ₄ , CO, CO ₂ , H ₂ |
| South China Sea (21N) | N/A | SCS921N00 | 21 00 N | 114 00 E | 15 | ¹³ CO ₂ , C ¹⁸ O ₂ , CH ₄ , CO, CO ₂ , H ₂ |
| Suita | Japan | SUI234N00 | 34 49 N | 135 31 E | 63 | CO ₂ |
| Tae-ahn Peninsula | Republic of Korea | TAP236N00 | 36 43 N | 126 07 E | 20 | ¹³ CH ₄ , ¹³ CO ₂ , C ¹⁸ O ₂ , CH ₄ , CO, CO ₂ , H ₂ , VOCs |
| Takayama | Japan | TKY236N00 | 36 09 N | 137 25 E | 1420 | CO ₂ |
| Tiksi | Russian Federation | TIK271N00 | 71 35 N | 128 55 E | 8 | CH ₄ , CO ₂ |
| Tsukuba | Japan | TKB236N00 | 36 03 N | 140 08 E | 26 | CH ₄ , CO ₂ |
| Tsukuba | Japan | TKB236N10 | 36 03 N | 140 08 E | 25 | O ₃ |
| Ulaan Uul | Mongolia | UUM244N00 | 44 27 N | 111 05 E | 914 | ¹³ CO ₂ , C ¹⁸ O ₂ , CH ₄ , CO, CO ₂ , H ₂ |
| Urawa | Japan | URW235N00 | 35 52 N | 139 36 E | 10 | CO ₂ |
| Yonagunijima | Japan | YON224N00 | 24 28 N | 123 01 E | 30 | CH ₄ , CO, CO ₂ , O ₃ |

REGION III (South America)

| | | | | | | |
|------------------------|--|-----------|---------|----------|------|---|
| Arembepe | Brazil | ABP312S00 | 12 46 S | 38 10 W | 0 | CH ₄ , CO, CO ₂ , N ₂ O |
| Arembepe | Brazil | ABP312S00 | 12 46 S | 38 10 W | 0 | ¹³ CO ₂ , C ¹⁸ O ₂ , CH ₄ , CO, CO ₂ , VOCs |
| Bird Island | United Kingdom of Great Britain and Northern Ireland | SGI354S00 | 54 00 S | 38 03 W | 30 | CH ₄ , CO ₂ |
| Easter Island | Chile | EIC327S00 | 27 08 S | 109 27 W | 50 | ¹³ CO ₂ , C ¹⁸ O ₂ , CH ₄ , CO, CO ₂ , H ₂ , VOCs |
| El Tololo | Chile | TLL330S00 | 30 10 S | 70 48 W | 2220 | CH ₄ , CO, CO ₂ , O ₃ |
| Huancayo | Peru | HUA312S00 | 12 04 S | 75 32 W | 3313 | CO ₂ |
| La Quiaca Observatorio | Argentina | LQO322S00 | 22 06 S | 65 36 W | 3459 | O ₃ |
| Natal | Brazil | NAT306S00 | 6 00 S | 35 12 W | 0 | VOCs |
| Pilar Observatorio | Argentina | PIL331S00 | 31 40 S | 63 53 W | 338 | O ₃ |
| San Julian Aero | Argentina | SJA349S00 | 49 18 S | 67 49 W | 58 | O ₃ |
| San Lorenzo | Paraguay | SNL325S00 | 25 22 S | 57 33 W | 133 | O ₃ |

LIST OF OBSERVATIONAL STATIONS (continued)

| Station | Country/Territory | Index Number | Location | | Altitude (m) | Parameter |
|--|--------------------------|--------------|-------------------|--------------------|-----------------|---|
| | | | Latitude (° ') | Longitude (° ') | | |
| Tierra del Fuego | Argentina | TDF354S00 | 54 52 S | 68 29 W | 20 | ¹³ CO ₂ , C ¹⁸ O ₂ , C ₂ Cl ₄ , CBrClF ₂ , CCl ₄ , CFCs, CH ₂ Cl ₂ , CH ₃ Br, CH ₃ CCl ₃ , CH ₃ Cl, CH ₄ , CO, CO ₂ , H ₂ , HCFCs, HFCs, N ₂ O, SF ₆ , VOCs |
| Ushuaia | Argentina | USH354S00 | 54 51 S | 68 19 W | 18 | CO, O ₃ |
| Ushuaia | Argentina | USH354S00 | 54 51 S | 68 19 W | 18 | CO, O ₃ |
| REGION IV (North and Central America) | | | | | | |
| Alert | Canada | ALT482N00 | 82 27 N | 62 31 W | 210 | O ₃ |
| Alert | Canada | ALT482N00 | 82 27 N | 62 31 W | 210 | ¹³ CO ₂ , CH ₄ , CO, CO ₂ , H ₂ , N ₂ O |
| Alert | Canada | ALT482N00 | 82 27 N | 62 31 W | 210 | ¹³ CO ₂ , C ¹⁸ O ₂ , CH ₄ , CO, CO ₂ , N ₂ O, SF ₆ |
| Alert | Canada | ALT482N00 | 82 27 N | 62 31 W | 210 | ¹³ CH ₄ , ¹³ CO ₂ , C ¹⁸ O ₂ , C ₂ Cl ₄ , CBrClF ₂ , CBrF ₃ , CCl ₄ , CFCs, CH ₂ Cl ₂ , CH ₃ Br, CH ₃ CCl ₃ , CH ₃ Cl, CH ₄ , CO, CO ₂ , H ₂ , HCFCs, HFCs, N ₂ O, SF ₆ , VOCs |
| Algoma | Canada | ALG447N00 | 47 02 N | 84 23 W | 411 | O ₃ |
| Argyle | United States of America | AMT445N00 | 45 02 N | 68 41 W | 50 | ¹³ CO ₂ , C ¹⁸ O ₂ , CH ₄ , VOCs |
| Barrow | United States of America | BRW471N00 | 71 19 N | 156 36 W | 11 | ¹³ CH ₄ , ¹³ CO ₂ , C ¹⁸ O ₂ , C ₂ Cl ₄ , CBrClF ₂ , CBrF ₃ , CCl ₄ , CFCs, CH ₂ Cl ₂ , CH ₃ Br, CH ₃ CCl ₃ , CH ₃ Cl, CH ₄ , CO, CO ₂ , H ₂ , HCFCs, HFCs, N ₂ O, O ₃ , SF ₆ , VOCs |
| Bratt's Lake | Canada | BRA450N00 | 50 12 N | 104 43 W | 595 | O ₃ |
| Candle Lake | Canada | CDL453N00 | 53 52 N | 104 39 W | 489 | CH ₄ , CO, CO ₂ |
| Cape Meares | United States of America | CMO445N00 | 45 28 N | 123 58 W | 30 | CCl ₄ , CFCs, CH ₃ CCl ₃ , CH ₄ , N ₂ O |
| Cape Meares | United States of America | CMO445N00 | 45 28 N | 123 58 W | 30 | ¹³ CO ₂ , C ¹⁸ O ₂ , CH ₄ , CO, CO ₂ , H ₂ |
| Cape St. James | Canada | CSJ451N00 | 51 56 N | 131 01 W | 89 | CO ₂ |
| Chalk River | Canada | CHA446N00 | 46 04 N | 77 24 W | 184 | O ₃ |
| Chapais | Canada | CPS449N00 | 49 49 N | 74 59 W | 381 | O ₃ |
| Chibougamau | Canada | CHM449N00 | 49 41 N | 74 21 W | 393 | CH ₄ , CO, CO ₂ |
| Churchill | Canada | CHL458N00 | 58 45 N | 94 04 W | 35 | ¹³ CO ₂ , C ¹⁸ O ₂ , CH ₄ , CO ₂ , N ₂ O |
| Cold Bay | United States of America | CBA455N00 | 55 12 N | 162 43 W | 25 | ¹³ CH ₄ , ¹³ CO ₂ , C ¹⁸ O ₂ , CH ₄ , CO, CO ₂ , H ₂ , VOCs |
| East Trout Lake | Canada | ETL454N00 | 54 21 N | 104 59 W | 492 | ¹³ CO ₂ , C ¹⁸ O ₂ , CH ₄ , CO, CO ₂ |
| Egbert | Canada | EGB444N00 | 44 14 N | 79 47 W | 253 | O ₃ |
| Egbert | Canada | EGB444N01 | 44 14 N | 79 47 W | 253 | CH ₄ , CO, CO ₂ , VOCs |
| Estevan Point | Canada | ESP449N00 | 49 23 N | 126 33 W | 39 | ¹³ CO ₂ , CH ₄ , CO, CO ₂ , H ₂ , N ₂ O |
| Estevan Point | Canada | ESP449N00 | 49 23 N | 126 33 W | 39 | ¹³ CO ₂ , C ¹⁸ O ₂ , CH ₄ , CO, CO ₂ , N ₂ O, SF ₆ |
| Esther | Canada | EST451N00 | 51 40 N | 110 12 W | 707 | O ₃ |
| Experimental Lakes Area | Canada | ELA449N00 | 49 40 N | 93 43 W | 369 | O ₃ |
| Fraserdale | Canada | FSD449N00 | 49 53 N | 81 34 W | 210 | ¹³ CO ₂ , C ¹⁸ O ₂ , CH ₄ , CO, CO ₂ |
| Grifton | United States of America | ITN435N00 | 35 21 N | 77 23 W | 505 | ¹³ CO ₂ , C ¹⁸ O ₂ , CCl ₄ , CFCs, CH ₃ CCl ₃ , CH ₄ , CO, CO ₂ , H ₂ , N ₂ O, SF ₆ |

LIST OF OBSERVATIONAL STATIONS (continued)

| Station | Country/Territory | Index Number | Location | | Altitude (m) | Parameter |
|--|--------------------------|--------------|-------------------|--------------------|-----------------|--|
| | | | Latitude (° ') | Longitude (° ') | | |
| Harvard Forest | United States of America | HFM442N00 | 42 54 N | 72 18 W | 340 | C ₂ Cl ₄ , CBrClF ₂ , CCl ₄ , CFCs, CH ₂ Cl ₂ , CH ₃ Br, CH ₃ CCl ₃ , CH ₃ Cl, HCFCs, HFCs, N ₂ O, SF ₆ |
| Kejimikujik | Canada | KEJ444N00 | 44 26 N | 65 12 W | 127 | O ₃ |
| Key Biscayne | United States of America | KEY425N00 | 25 40 N | 80 12 W | 3 | ¹³ CO ₂ , C ¹⁸ O ₂ , CH ₄ , CO, CO ₂ , H ₂ , VOCs |
| Kitt Peak | United States of America | KPA431N00 | 31 58 N | 111 36 W | 2083 | CH ₄ |
| La Jolla | United States of America | SIO432N00 | 32 50 N | 117 16 W | 14 | CH ₄ |
| La Palma | Cuba | PLM422N00 | 22 45 N | 83 32 W | 47 | NO ₂ |
| Lac La Biche | Canada | LLB454N00 | 54 57 N | 112 27 W | 540 | CH ₄ , CO, CO ₂ , VOCs |
| Lac La Biche (Alberta) | Canada | LLB454N01 | 54 57 N | 112 27 W | 540 | CH ₄ , CO, CO ₂ |
| Longwoods | Canada | LON442N00 | 42 53 N | 81 29 W | 239 | O ₃ |
| Mex High Altitude Global Climate Observation Center, Mexico | Mexico | MEX419N00 | 19 59 N | 97 10 W | 4560 | CH ₄ , CO, CO ₂ , VOCs |
| Moody | United States of America | WKT431N00 | 31 19 N | 97 19 W | 708 | ¹³ CO ₂ , C ¹⁸ O ₂ , CH ₄ , O ₃ |
| Mould Bay | Canada | MBC476N00 | 76 15 N | 119 20 W | 58 | ¹³ CO ₂ , C ¹⁸ O ₂ , CH ₄ , CO, CO ₂ , H ₂ |
| Niwot Ridge (C-1) | United States of America | NWR440N00 | 40 02 N | 105 32 W | 3021 | C ₂ Cl ₄ , CBrClF ₂ , CBrF ₃ , CCl ₄ , CFCs, CH ₂ Cl ₂ , CH ₃ Br, CH ₃ CCl ₃ , CH ₃ Cl, HCFCs, HFCs, N ₂ O, O ₃ , SF ₆ |
| Niwot Ridge (Saddle) | United States of America | NWR440N02 | 40 03 N | 105 35 W | 3528 | O ₃ |
| Niwot Ridge (T-van) | United States of America | NWR440N01 | 40 03 N | 105 35 W | 3523 | ¹³ CH ₄ , ¹³ CO ₂ , ¹⁴ CO ₂ , C ¹⁸ O ₂ , CH ₄ , CO, CO ₂ , H ₂ , N ₂ O |
| Olympic Peninsula | United States of America | OPW448N00 | 48 15 N | 124 25 W | 488 | CH ₄ , CO ₂ , H ₂ |
| Pacific Ocean (15N) | N/A | POC915N00 | 15 00 N | 145 00 W | 10 | ¹³ CO ₂ , C ¹⁸ O ₂ , CH ₄ , CO, CO ₂ , H ₂ |
| Pacific Ocean (20N) | N/A | POC920N00 | 20 00 N | 141 00 W | 10 | ¹³ CO ₂ , C ¹⁸ O ₂ , CH ₄ , CO, CO ₂ , H ₂ |
| Pacific Ocean (25N) | N/A | POC925N00 | 25 00 N | 139 00 W | 10 | ¹³ CO ₂ , C ¹⁸ O ₂ , CH ₄ , CO, CO ₂ , H ₂ |
| Pacific Ocean (30N) | N/A | POC930N00 | 30 00 N | 135 00 W | 10 | ¹³ CO ₂ , C ¹⁸ O ₂ , CH ₄ , CO, CO ₂ , H ₂ |
| Pacific Ocean (35N) | N/A | POC935N00 | 35 00 N | 137 00 W | 10 | ¹³ CO ₂ , C ¹⁸ O ₂ , CO, H ₂ |
| Pacific Ocean (40N) | N/A | POC940N00 | 40 00 N | 136 00 W | 10 | ¹³ CO ₂ , H ₂ |
| Pacific Ocean (45N) | N/A | POC945N00 | 45 00 N | 131 00 W | 10 | ¹³ CO ₂ , H ₂ |
| Park Falls | United States of America | LEF445N00 | 45 55 N | 90 16 W | 868 | ¹³ CO ₂ , C ¹⁸ O ₂ , C ₂ Cl ₄ , CBrClF ₂ , CCl ₄ , CFCs, CH ₂ Cl ₂ , CH ₃ Br, CH ₃ CCl ₃ , CH ₃ Cl, CH ₄ , CO, CO ₂ , H ₂ , HCFCs, HFCs, N ₂ O, SF ₆ , VOCs |
| Point Arena | United States of America | PTA438N00 | 38 57 N | 123 43 W | 17 | ¹³ CO ₂ , C ¹⁸ O ₂ , CH ₄ , CO, CO ₂ |
| Ragged Point | Barbados | RPB413N00 | 13 10 N | 59 26 W | 45 | C ₂ Cl ₄ , C ₂ HCl ₃ , CBrClF ₂ , CBrF ₃ , CCl ₄ , CFCs, CH ₂ Cl ₂ , CH ₃ Br, CH ₃ CCl ₃ , CH ₃ Cl, CH ₄ , CHCl ₃ , HCFCs, HFCs, N ₂ O, PFCs, SF ₆ , SO ₂ F ₂ |
| Ragged Point | Barbados | RPB413N00 | 13 10 N | 59 26 W | 45 | ¹³ CO ₂ , C ¹⁸ O ₂ , CH ₄ , CO, CO ₂ , H ₂ , O ₃ |
| Sable Island | Canada | WSA443N00 | 43 56 N | 60 01 W | 5 | ¹³ CO ₂ , C ¹⁸ O ₂ , CH ₄ , CO, CO ₂ , N ₂ O, SF ₆ |

LIST OF OBSERVATIONAL STATIONS (continued)

| Station | Country/Territory | Index Number | Location | | Altitude (m) | Parameter |
|-----------------------|--|--------------|-------------------|--------------------|-----------------|--|
| | | | Latitude (° ') | Longitude (° ') | | |
| Saturna | Canada | SAT448N00 | 48 47 N | 123 08 W | 178 | O ₃ |
| Shemya Island | United States of America | SHM452N00 | 52 43 N | 174 05 E | 40 | ¹³ CO ₂ , C ¹⁸ O ₂ , CH ₄ , CO, CO ₂ , H ₂ , VOCs |
| Southern Great Plains | United States of America | SGP436N00 | 36 47 N | 97 30 W | 314 | ¹³ CO ₂ , C ¹⁸ O ₂ , CH ₄ , CO, CO ₂ , H ₂ , N ₂ O, SF ₆ , VOCs |
| St. Croix | United States of America | AVI417N00 | 17 45 N | 64 45 W | 3 | CH ₄ , CO ₂ |
| St. David's Head | United Kingdom of Great Britain and Northern Ireland | BME432N00 | 32 22 N | 64 39 W | 30 | ¹³ CO ₂ , C ¹⁸ O ₂ , CH ₄ , CO, CO ₂ , H ₂ |
| Sutton | Canada | SUT445N00 | 45 05 N | 72 41 W | 243 | O ₃ |
| Trinidad Head | United States of America | THD441N00 | 41 03 N | 124 09 W | 120 | C ₂ Cl ₄ , C ₂ HCl ₃ , CBrClF ₂ , CBrF ₃ , CCl ₄ , CFCs, CH ₂ Cl ₂ , CH ₃ Br, CH ₃ CCl ₃ , CH ₃ Cl, CH ₄ , CHCl ₃ , HCFCs, HFCs, N ₂ O, PFCs, SF ₆ , SO ₂ F ₂ |
| Trinidad Head | United States of America | THD441N00 | 41 03 N | 124 09 W | 120 | ¹³ CO ₂ , C ¹⁸ O ₂ , C ₂ Cl ₄ , CBrClF ₂ , CCl ₄ , CFCs, CH ₂ Cl ₂ , CH ₃ Br, CH ₃ CCl ₃ , CH ₃ Cl, CH ₄ , CO, CO ₂ , HCFCs, HFCs, N ₂ O, O ₃ , SF ₆ , VOCs |
| Tudor Hill | United Kingdom of Great Britain and Northern Ireland | BMW432N00 | 32 16 N | 64 52 W | 30 | ¹³ CO ₂ , C ¹⁸ O ₂ , CH ₄ , CO, CO ₂ , H ₂ , O ₃ , VOCs |
| Wendover | United States of America | UTA439N00 | 39 53 N | 113 43 W | 1320 | ¹³ CO ₂ , C ¹⁸ O ₂ , CH ₄ , CO, CO ₂ , H ₂ , VOCs |
| West Branch | United States of America | WBI441N00 | 41 44 N | 91 21 W | 241.7 | ¹³ CO ₂ , C ¹⁸ O ₂ |

REGION V (South-West Pacific)

| | | | | | | |
|-------------------|-------------|-----------|---------|----------|-------|--|
| Baring Head | New Zealand | BHD541S00 | 41 25 S | 174 52 E | 85 | ¹³ CO ₂ , C ¹⁸ O ₂ , CH ₄ , CO, CO ₂ |
| Baring Head | New Zealand | BHD541S00 | 41 25 S | 174 52 E | 85 | ¹³ CH ₄ , ¹⁴ CO ₂ , CH ₄ , CO, CO ₂ , N ₂ O, O ₃ , VOCs |
| Bukit Koto Tabang | Indonesia | BKT500S00 | 0 12 S | 100 19 E | 864.5 | NO ₂ , SO ₂ |
| Bukit Koto Tabang | Indonesia | BKT500S00 | 0 12 S | 100 19 E | 864.5 | CH ₄ , CO, CO ₂ , O ₃ |
| Bukit Koto Tabang | Indonesia | BKT500S00 | 0 12 S | 100 19 E | 864.5 | ¹³ CO ₂ , C ¹⁸ O ₂ , CH ₄ , CO, CO ₂ , H ₂ , N ₂ O, SF ₆ , VOCs |
| Cape Ferguson | Australia | CFA519S00 | 19 17 S | 147 03 E | 2 | ¹³ CO ₂ , CH ₄ , CO, CO ₂ , H ₂ , N ₂ O |
| Cape Grim | Australia | CGO540S00 | 40 41 S | 144 41 E | 94 | CO ₂ , O ₃ |
| Cape Grim | Australia | CGO540S00 | 40 41 S | 144 41 E | 94 | C ₂ Cl ₄ , C ₂ HCl ₃ , CBrClF ₂ , CBrF ₃ , CCl ₄ , CFCs, CH ₂ Cl ₂ , CH ₃ Br, CH ₃ CCl ₃ , CH ₃ Cl, CH ₄ , CHCl ₃ , CO, H ₂ , HCFCs, HFCs, N ₂ O, PFCs, SF ₆ , SO ₂ F ₂ |
| Cape Grim | Australia | CGO540S00 | 40 41 S | 144 41 E | 94 | ¹³ CO ₂ , CH ₄ , CO, CO ₂ , H ₂ , N ₂ O |
| Cape Grim | Australia | CGO540S00 | 40 41 S | 144 41 E | 94 | ¹³ CH ₄ , ¹³ CO ₂ , C ¹⁸ O ₂ , C ₂ Cl ₄ , CBrClF ₂ , CBrF ₃ , CCl ₄ , CFCs, CH ₂ Cl ₂ , CH ₃ Br, CH ₃ CCl ₃ , CH ₃ Cl, CH ₄ , CO, CO ₂ , H ₂ , HCFCs, HFCs, N ₂ O, SF ₆ , VOCs |

LIST OF OBSERVATIONAL STATIONS (continued)

| Station | Country/Territory | Index Number | Location | | Altitude (m) | Parameter |
|-----------------------------------|--------------------------|--------------|-------------------|--------------------|-----------------|---|
| | | | Latitude (° ') | Longitude (° ') | | |
| Cape Kumukahi | United States of America | KUM519N00 | 19 31 N | 154 49 W | 3 | ¹³ CH ₄ , ¹³ CO ₂ , C ¹⁸ O ₂ , C ₂ Cl ₄ , CBrClF ₂ , CBrF ₃ , CCl ₄ , CFCs, CH ₂ Cl ₂ , CH ₃ Br, CH ₃ CCl ₃ , CH ₃ Cl, CH ₄ , CO, CO ₂ , H ₂ , HCFCs, HFCs, N ₂ O, SF ₆ , VOCs |
| Christmas Island | Kiribati | CHR501N00 | 1 42 N | 157 10 W | 3 | ¹³ CO ₂ , C ¹⁸ O ₂ , CH ₄ , CO, CO ₂ , H ₂ |
| Danum Valley GAW Baseline Station | Malaysia | DMV504N00 | 4 58 N | 117 50 E | 426 | CO ₂ , O ₃ |
| Guam | United States of America | GMI513N00 | 13 26 N | 144 47 E | 2 | ¹³ CO ₂ , C ¹⁸ O ₂ , CH ₄ , CO, CO ₂ , H ₂ , VOCs |
| Gunn Point | Australia | GPA512S00 | 12 15 S | 131 03 E | 25 | ¹³ CO ₂ , CH ₄ , CO, CO ₂ , H ₂ , N ₂ O |
| Jakarta | Indonesia | JKR506S00 | 6 11 S | 106 50 E | 7 | NO ₂ , SO ₂ |
| Kaitorete Spit | New Zealand | NZL543S00 | 43 50 S | 172 38 E | 3 | CH ₄ |
| Lauder | New Zealand | LAU545S00 | 45 02 S | 169 40 E | 370 | O ₃ |
| Lauder | New Zealand | LAU545S00 | 45 02 S | 169 40 E | 370 | CH ₄ |
| Macquarie Island | Australia | MQA554S00 | 54 29 S | 158 58 E | 12 | ¹³ CO ₂ , CH ₄ , CO, CO ₂ , H ₂ , N ₂ O |
| Mauna Loa | United States of America | MLO519N00 | 19 32 N | 155 35 W | 3397 | ¹³ CO ₂ , CH ₄ , CO, CO ₂ , H ₂ , N ₂ O |
| Mauna Loa | United States of America | MLO519N00 | 19 32 N | 155 35 W | 3397 | ¹³ CH ₄ , ¹³ CO ₂ , C ¹⁸ O ₂ , C ₂ Cl ₄ , CBrClF ₂ , CBrF ₃ , CCl ₄ , CFCs, CH ₂ Cl ₂ , CH ₃ Br, CH ₃ CCl ₃ , CH ₃ Cl, CH ₄ , CO, CO ₂ , H ₂ , HCFCs, HFCs, N ₂ O, O ₃ , SF ₆ , VOCs |
| Pacific Ocean (00N) | N/A | POC900N00 | 0 00 N | 155 00 W | 10 | ¹³ CO ₂ , C ¹⁸ O ₂ , CH ₄ , CO, CO ₂ , H ₂ |
| Pacific Ocean (05N) | N/A | POC905N00 | 5 00 N | 151 00 W | 10 | ¹³ CO ₂ , C ¹⁸ O ₂ , CH ₄ , CO, CO ₂ , H ₂ |
| Pacific Ocean (05S) | N/A | POC905S00 | 5 00 S | 159 00 W | 10 | ¹³ CO ₂ , C ¹⁸ O ₂ , CH ₄ , CO, CO ₂ , H ₂ |
| Pacific Ocean (10N) | N/A | POC910N00 | 10 00 N | 149 00 W | 10 | ¹³ CO ₂ , C ¹⁸ O ₂ , CH ₄ , CO, CO ₂ , H ₂ |
| Pacific Ocean (10S) | N/A | POC910S00 | 10 00 S | 161 00 W | 10 | ¹³ CO ₂ , C ¹⁸ O ₂ , CH ₄ , CO, CO ₂ , H ₂ |
| Pacific Ocean (15S) | N/A | POC915S00 | 15 00 S | 171 00 W | 10 | ¹³ CO ₂ , C ¹⁸ O ₂ , CH ₄ , CO, CO ₂ , H ₂ |
| Pacific Ocean (20S) | N/A | POC920S00 | 20 00 S | 174 00 W | 10 | ¹³ CO ₂ , C ¹⁸ O ₂ , CH ₄ , CO, CO ₂ , H ₂ |
| Pacific Ocean (25S) | N/A | POC925S00 | 25 00 S | 171 00 W | 10 | ¹³ CO ₂ , C ¹⁸ O ₂ , CH ₄ , CO, CO ₂ , H ₂ |
| Pacific Ocean (30S) | N/A | POC930S00 | 30 00 S | 176 00 W | 10 | ¹³ CO ₂ , C ¹⁸ O ₂ , CH ₄ , CO, CO ₂ , H ₂ |
| Pacific Ocean (35S) | N/A | POC935S00 | 35 00 S | 180 00 E | 10 | ¹³ CO ₂ , C ¹⁸ O ₂ , CH ₄ , CO, CO ₂ , H ₂ |
| Sand Island | United States of America | MID528N00 | 28 12 N | 177 22 W | 7.7 | ¹³ CO ₂ , C ¹⁸ O ₂ , CH ₄ , CO, CO ₂ , H ₂ , VOCs |
| Tanah Rata | Malaysia | TAR504N00 | 4 28 N | 101 23 E | 1545 | O ₃ |
| Tutuila (Cape Matatula) | United States of America | SMO514S00 | 14 14 S | 170 34 W | 42 | C ₂ Cl ₄ , C ₂ HCl ₃ , CBrClF ₂ , CBrF ₃ , CCl ₄ , CFCs, CH ₂ Cl ₂ , CH ₃ Br, CH ₃ CCl ₃ , CH ₃ Cl, CH ₄ , CHCl ₃ , HCFCs, HFCs, N ₂ O, PFCs, SF ₆ , SO ₂ F ₂ |
| Tutuila (Cape Matatula) | United States of America | SMO514S00 | 14 14 S | 170 34 W | 42 | ¹³ CH ₄ , ¹³ CO ₂ , C ¹⁸ O ₂ , C ₂ Cl ₄ , CBrClF ₂ , CBrF ₃ , CCl ₄ , CFCs, CH ₂ Cl ₂ , CH ₃ Br, CH ₃ CCl ₃ , CH ₃ Cl, CH ₄ , CO, CO ₂ , H ₂ , HCFCs, HFCs, N ₂ O, O ₃ , SF ₆ , VOCs |
| REGION VI (Europe) | | | | | | |
| Adrigole | Ireland | ADR651N00 | 51 41 N | 9 44 W | 50 | CCl ₄ , CFCs, CH ₃ CCl ₃ , N ₂ O |
| Angra do Heroismo | Portugal | ANG638N00 | 38 40 N | 27 13 W | 74 | O ₃ |

LIST OF OBSERVATIONAL STATIONS (continued)

| Station | Country/Territory | Index Number | Location | | Altitude (m) | Parameter |
|--|--|--------------|-------------------|--------------------|-----------------|---|
| | | | Latitude (° ') | Longitude (° ') | | |
| Atmospheric Station Kresin u Pacova | Czech Republic | KRE649N00 | 49 35 N | 15 05 E | 534 | O ₃ |
| BEO Moussala | Bulgaria | BEO642N00 | 42 11 N | 23 35 E | 2925 | CO, CO ₂ , NO, NO ₂ , NO _x , O ₃ , SO ₂ |
| Baltic Sea | Poland | BAL655N00 | 55 21 N | 17 13 E | 28 | ¹³ CO ₂ , C ¹⁸ O ₂ , CH ₄ , CO, CO ₂ , H ₂ , VOCs |
| Begur | Spain | BGU641N00 | 41 58 N | 3 14 E | 13 | CH ₄ , CO ₂ |
| Beja | Portugal | BEJ638N00 | 38 01 N | 7 52 W | 246 | O ₃ |
| Black Sea | Romania | BSC644N00 | 44 10 N | 28 40 E | 3 | ¹³ CO ₂ , C ¹⁸ O ₂ , CH ₄ , CO, CO ₂ , H ₂ , VOCs |
| Bragança | Portugal | BRG641N00 | 41 48 N | 6 44 W | 690 | SO ₂ |
| Brotjacklriegel | Germany | BRT648N00 | 48 49 N | 13 13 E | 1016 | CO ₂ , O ₃ |
| Burgas | Bulgaria | BUR642N00 | 42 29 N | 27 29 E | 16 | NO ₂ , SO ₂ |
| Castelo Branco | Portugal | CAS639N00 | 39 50 N | 7 28 W | 386 | O ₃ |
| Danki | Russian Federation | DAK654N00 | 54 54 N | 37 48 E | 140 | O ₃ |
| Deuselbach | Germany | DEU649N00 | 49 46 N | 7 03 E | 480 | CH ₄ , CO ₂ , O ₃ |
| Dobele | Latvia | DBL656N00 | 56 22 N | 23 11 E | 42 | O ₃ |
| Doñana | Spain | DON637N00 | 37 03 N | 6 33 W | 5 | NO ₂ , O ₃ , SO ₂ |
| Dwejra Point | Malta | GOZ636N00 | 36 03 N | 14 11 E | 30 | ¹³ CO ₂ , C ¹⁸ O ₂ , CH ₄ , CO, CO ₂ , H ₂ |
| Eskdalemuir | United Kingdom of Great Britain and Northern Ireland | EDM655N00 | 55 19 N | 3 12 W | 242 | O ₃ |
| Finokalia | Greece | FIK635N00 | 35 20 N | 25 40 E | 150 | CH ₄ , CO ₂ |
| Fundata | Romania | FDT645N00 | 45 28 N | 25 18 E | 1383.5 | NO ₂ , SO ₂ |
| Fundata | Romania | FDT645N00 | 45 28 N | 25 18 E | 1383.5 | CO ₂ , NO ₂ , O ₃ |
| Giordan Lighthouse | Malta | GLH636N00 | 36 04 N | 14 13 E | 160 | ²²² Rn, CH ₄ , CO, CO ₂ , NO, NO ₂ , NO _x , O ₃ , SO ₂ |
| Hegyhatsal | Hungary | HUN646N00 | 46 57 N | 16 39 E | 248 | CO ₂ |
| Hegyhatsal | Hungary | HUN646N00 | 46 57 N | 16 39 E | 248 | ¹³ CO ₂ , C ¹⁸ O ₂ , CH ₄ , CO, CO ₂ , H ₂ , N ₂ O, SF ₆ |
| Heimaey | Iceland | ICE663N00 | 63 24 N | 20 17 W | 100 | ¹³ CO ₂ , C ¹⁸ O ₂ , CH ₄ , CO, CO ₂ , H ₂ , O ₃ , VOCs |
| Hohe Warte | Austria | HHE648N00 | 48 15 N | 16 22 E | 202 | NO, NO ₂ , SO ₂ |
| Hohe Warte | Austria | HHE648N00 | 48 15 N | 16 22 E | 202 | NO, NO ₂ , SO ₂ |
| Hohenpeissenberg | Germany | HPB647N00 | 47 48 N | 11 01 E | 985 | ²²² Rn, CO, H ₂ O ₂ , NO, NO ₂ , NO _x , NO _y , O ₃ , PAN, ROOH, SO ₂ , VOCs |
| Hohenpeissenberg | Germany | HPB647N00 | 47 48 N | 11 01 E | 985 | ¹³ CO ₂ , C ¹⁸ O ₂ , CH ₄ , CO, CO ₂ , VOCs |
| Ile Grande | France | LPO648N00 | 48 48 N | 3 35 W | 10 | CH ₄ , CO ₂ |
| Iskrba | Slovenia | IRB645N00 | 45 34 N | 14 52 E | 520 | NO ₂ , O ₃ , SO ₂ |
| Ivan Sedlo | Bosnia and Herzegovina | IVN643N00 | 43 46 N | 18 02 E | 970 | NO ₂ , SO ₂ |
| Jarczew | Poland | JCZ651N00 | 51 49 N | 21 59 E | 180 | NO ₂ , SO ₂ |
| Jungfrauoch | Switzerland | JFJ646N00 | 46 33 N | 7 59 E | 3580 | CO ₂ |
| Jungfrauoch | Switzerland | JFJ646N00 | 46 33 N | 7 59 E | 3580 | CH ₄ , CO, CO ₂ , H ₂ , N ₂ O, NO, NO ₂ , NO _x , NO _y , O ₃ , PAN, SF ₆ , SO ₂ , VOCs |
| Jungfrauoch | Switzerland | JFJ646N00 | 46 33 N | 7 59 E | 3580 | C ₂ Cl ₄ , C ₂ HCl ₃ , CBrClF ₂ , CBrF ₃ , CCl ₄ , CFCs, CH ₂ Cl ₂ , CH ₃ Br, CH ₃ CCl ₃ , CH ₃ Cl, CHCl ₃ , HCFCs, HFCs, PFCs, SF ₆ , SO ₂ F ₂ |
| K-pusztá | Hungary | KPS646N00 | 46 58 N | 19 33 E | 125 | CO ₂ , NO ₂ , O ₃ , SO ₂ |
| Kamenicki Vis | Serbia | KAM643N00 | 43 24 N | 21 57 E | 813 | NO ₂ , SO ₂ |
| Kloosterburen | Netherlands (the) | KTB653N00 | 53 24 N | 6 25 E | 0 | CO, NO, NO ₂ , NO _x , SO ₂ |

LIST OF OBSERVATIONAL STATIONS (continued)

| Station | Country/Territory | Index Number | Location | | Altitude (m) | Parameter |
|------------------------|---|--------------|-------------------|--------------------|-----------------|--|
| | | | Latitude (° ') | Longitude (° ') | | |
| Kollumerwaard | Netherlands (the) | KMW653N00 | 53 20 N | 6 17 E | 0 | CH ₄ , CO, CO ₂ , NO, NO ₂ , NO _x , O ₃ , SO ₂ |
| Kosetice | Czech Republic | KOS649N00 | 49 35 N | 15 05 E | 534 | CH ₄ , CO, NO, NO ₂ , O ₃ , SO ₂ |
| Kovk | Slovenia | KVK646N00 | 46 07 N | 15 06 E | 600 | O ₃ |
| Krvavec | Slovenia | KVV646N00 | 46 18 N | 14 32 E | 1720 | CO, O ₃ |
| La Cartuja | Spain | CAR637N00 | 37 12 N | 3 36 W | 720 | NO ₂ , SO ₂ |
| Lampedusa | Italy | LMP635N00 | 35 31 N | 12 38 E | 45 | CBrClF ₂ , CBrF ₃ , CCl ₄ , CFCs, CH ₂ Br ₂ , CH ₂ Cl ₂ , CH ₃ Br, CH ₃ CCl ₃ , CH ₃ Cl, CH ₃ I, CH ₄ , CHCl ₃ , CO ₂ , HCFCs, HFCs, N ₂ O, SF ₆ |
| Lampedusa | Italy | LMP635N00 | 35 31 N | 12 38 E | 45 | ¹³ CO ₂ , C ¹⁸ O ₂ , CH ₄ , CO, CO ₂ |
| Lazaropole | The former Yugoslav Republic of Macedonia | LZP641N00 | 41 32 N | 20 42 E | 1320 | NO ₂ , SO ₂ |
| Leba | Poland | LEB654N00 | 54 45 N | 17 32 E | 2 | NO ₂ , SO ₂ |
| Lisboa / Gago Coutinho | Portugal | LIS638N00 | 38 46 N | 9 08 W | 105 | O ₃ |
| Logroño | Spain | LOG642N00 | 42 27 N | 2 30 W | 370 | NO ₂ , SO ₂ |
| Mace Head | Ireland | MHD653N00 | 53 20 N | 9 54 W | 8 | O ₃ |
| Mace Head | Ireland | MHD653N00 | 53 20 N | 9 54 W | 8 | CH ₄ , CO ₂ |
| Mace Head | Ireland | MHD653N00 | 53 20 N | 9 54 W | 8 | C ₂ Cl ₄ , C ₂ HCl ₃ , CBrClF ₂ , CBrF ₃ , CCl ₄ , CFCs, CH ₂ Cl ₂ , CH ₃ Br, CH ₃ CCl ₃ , CH ₃ Cl, CH ₄ , CHCl ₃ , CO, H ₂ , HCFCs, HFCs, N ₂ O, NF ₃ , PFCs, SF ₆ , SO ₂ F ₂ |
| Mace Head | Ireland | MHD653N00 | 53 20 N | 9 54 W | 8 | ¹³ CH ₄ , ¹³ CO ₂ , C ¹⁸ O ₂ , C ₂ Cl ₄ , CBrClF ₂ , CBrF ₃ , CCl ₄ , CFCs, CH ₂ Cl ₂ , CH ₃ Br, CH ₃ CCl ₃ , CH ₃ Cl, CH ₄ , CO, CO ₂ , H ₂ , HCFCs, HFCs, N ₂ O, SF ₆ , VOCs |
| Mahón | Spain | MHN639N00 | 39 52 N | 4 19 E | 78 | NO ₂ , O ₃ , SO ₂ |
| Monte Cimone | Italy | CMN644N00 | 44 11 N | 10 42 E | 2165 | CO ₂ |
| Monte Cimone | Italy | CMN644N00 | 44 11 N | 10 42 E | 2165 | CH ₄ , CO, H ₂ , N ₂ O, O ₃ , SF ₆ |
| Monte Cimone | Italy | CMN644N00 | 44 11 N | 10 42 E | 2165 | C ₂ Cl ₄ , C ₂ HCl ₃ , CBrClF ₂ , CBrF ₃ , CCl ₄ , CFCs, CH ₂ Cl ₂ , CH ₃ Br, CH ₃ CCl ₃ , CH ₃ Cl, CHCl ₃ , HCFCs, HFCs, PFCs, SO ₂ F ₂ |
| Monte Velho | Portugal | MVH638N00 | 38 05 N | 8 48 W | 43 | O ₃ |
| Neuglobsow | Germany | NGL653N00 | 53 10 N | 13 02 E | 65 | CH ₄ , CO, CO ₂ , O ₃ |
| Noia | Spain | NIA642N00 | 42 44 N | 8 55 W | 685 | NO ₂ , O ₃ , SO ₂ |
| Ocean Station "M" | Norway | STM666N00 | 66 00 N | 2 00 E | 5 | ¹³ CO ₂ , C ¹⁸ O ₂ , CH ₄ , CO, CO ₂ , H ₂ |
| Ocean Station Charlie | Russian Federation | STC652N00 | 52 45 N | 35 30 W | 5 | CO ₂ |
| Ocean Station Charlie | United States of America | STC654N00 | 54 00 N | 35 00 W | 6 | CO ₂ |
| Ochsenkopf | Germany | OXK650N00 | 50 02 N | 11 48 E | 1185 | ¹³ CO ₂ , C ¹⁸ O ₂ , CH ₄ , CO, CO ₂ , VOCs |
| Oulanka | Finland | OUL666N00 | 66 19 N | 29 24 E | 310 | NO ₂ , O ₃ , SO ₂ |
| Pallas-Sammaltunturi | Finland | PAL667N00 | 67 58 N | 24 07 E | 560 | CH ₄ , CO ₂ , O ₃ |
| Pallas-Sammaltunturi | Finland | PAL667N00 | 67 58 N | 24 07 E | 560 | ¹³ CO ₂ , C ¹⁸ O ₂ , CBrF ₃ , CH ₄ , CO, CO ₂ , VOCs |
| Payerne | Switzerland | PAY646N00 | 46 49 N | 6 57 E | 490 | CO, NO, NO ₂ , NO _x , O ₃ , SO ₂ , VOCs |
| Penhas Douradas | Portugal | PEN640N00 | 40 25 N | 7 33 W | 1380 | O ₃ |
| Pic du Midi | France | PDM642N00 | 42 56 N | 0 08 E | 2877 | CO, O ₃ |
| Pic du Midi | France | PDM642N00 | 42 56 N | 0 08 E | 2877 | CH ₄ , CO ₂ |

LIST OF OBSERVATIONAL STATIONS (continued)

| Station | Country/Territory | Index Number | Location | | Altitude (m) | Parameter |
|-----------------------------|--|--------------|-------------------|--------------------|-----------------|--|
| | | | Latitude (° ') | Longitude (° ') | | |
| Pico, Azores | Portugal | PCO638N00 | 38 28 N | 28 24 W | 2225.0 | VOCs |
| Plateau Rosa | Italy | PRS645N00 | 45 56 N | 7 42 E | 3480 | CH ₄ , CO ₂ , O ₃ |
| Pleven | Bulgaria | PLV643N00 | 43 25 N | 24 36 E | 64 | NO ₂ , SO ₂ |
| Plovdiv | Bulgaria | PLD642N00 | 42 08 N | 24 45 E | 179 | NO ₂ , SO ₂ |
| Puszcza Borecka/Diabla Gora | Poland | DIG654N00 | 54 09 N | 22 04 E | 157 | CO ₂ , NO ₂ , O ₃ , SO ₂ |
| Puy de Dome | France | PUY645N00 | 45 46 N | 2 58 E | 1465 | CO, O ₃ |
| Puy de Dome | France | PUY645N00 | 45 46 N | 2 58 E | 1465 | CH ₄ , CO ₂ |
| Ridge Hill | United Kingdom of Great Britain and Northern Ireland | RGL651N00 | 52 00 N | 2 32 W | 204 | CH ₄ , CO ₂ , N ₂ O, SF ₆ |
| Rigi | Switzerland | RIG646N00 | 46 04 N | 8 27 E | 1031 | CO, NO, NO ₂ , NO _x , O ₃ , SO ₂ , VOCs |
| Roquetes | Spain | ROQ640N00 | 40 49 N | 0 29 E | 50 | NO ₂ , O ₃ , SO ₂ |
| Rucava | Latvia | RCV656N00 | 56 10 N | 21 10 E | 18 | NO ₂ , O ₃ , SO ₂ |
| San Pablo de los Montes | Spain | SPM639N00 | 39 33 N | 4 21 W | 917 | NO ₂ , O ₃ , SO ₂ |
| Schauinsland | Germany | SSL647N00 | 47 55 N | 7 55 E | 1205 | CH ₄ , CO, CO ₂ , N ₂ O, NO, NO ₂ , O ₃ , PAN, SF ₆ |
| Sede Boker | Israel | WIS631N00 | 31 07 N | 34 52 E | 400 | ¹³ CO ₂ , C ¹⁸ O ₂ , CH ₄ , CO, CO ₂ , H ₂ |
| Semenic | Romania | SEM645N00 | 45 07 N | 21 58 E | 1432 | NO ₂ , SO ₂ |
| Shepelevo | Russian Federation | SHP659N00 | 59 58 N | 29 07 E | 4 | O ₃ |
| Shetland | United Kingdom of Great Britain and Northern Ireland | SIS660N00 | 60 05 N | 1 15 W | 30 | ¹³ CO ₂ , CH ₄ , CO, CO ₂ , H ₂ , N ₂ O |
| Site J | Denmark | GRL666N00 | 66 30 N | 46 12 W | 2030 | CH ₄ |
| Sniezka | Poland | SNZ650N00 | 50 44 N | 15 44 E | 1603 | NO ₂ , SO ₂ |
| Sofia | Bulgaria | SOF642N00 | 42 39 N | 23 23 E | 586 | NO ₂ , SO ₂ |
| Sonnblick | Austria | SNB647N00 | 47 03 N | 12 57 E | 3106 | CH ₄ , CO, CO ₂ , NO, NO ₂ , NO _y , O ₃ |
| Stephansplatz | Austria | STP648N00 | 48 13 N | 16 23 E | 171 | NO, NO ₂ , SO ₂ |
| Stephansplatz | Austria | STP648N00 | 48 13 N | 16 23 E | 171 | NO, NO ₂ , SO ₂ |
| Stîna de Vale | Romania | STN646N00 | 46 41 N | 22 37 E | 1116 | NO ₂ , SO ₂ |
| Summit | Denmark | SUM672N00 | 72 35 N | 38 29 W | 3238 | CH ₄ , VOCs |
| Summit | Denmark | SUM672N00 | 72 35 N | 38 29 W | 3238 | ¹³ CO ₂ , C ¹⁸ O ₂ , C ₂ Cl ₄ , CBrClF ₂ , CCl ₄ , CFCs, CH ₂ Cl ₂ , CH ₃ Br, CH ₃ CCl ₃ , CH ₃ Cl, CH ₄ , CO, CO ₂ , HCFCs, HFCs, N ₂ O, O ₃ , SF ₆ , VOCs |
| Suwalki | Poland | SWL654N00 | 54 08 N | 22 57 E | 184 | NO ₂ , SO ₂ |
| Tacolneston Tall Tower | United Kingdom of Great Britain and Northern Ireland | TAC652N00 | 52 31 N | 1 08 E | 56 | C ₂ Cl ₄ , C ₂ HCl ₃ , CBrClF ₂ , CBrF ₃ , CFCs, CH ₂ Cl ₂ , CH ₃ Br, CH ₃ CCl ₃ , CH ₃ Cl, CH ₄ , CHCl ₃ , CO, CO ₂ , H ₂ , HCFCs, HFCs, N ₂ O, PFCs, SF ₆ , SO ₂ F ₂ |
| Terceira Island | Portugal | AZR638N00 | 38 46 N | 27 22 W | 40 | ¹³ CH ₄ , ¹³ CO ₂ , C ¹⁸ O ₂ , CH ₄ , CO, CO ₂ , H ₂ , VOCs |
| Teriberka | Russian Federation | TER669N00 | 69 12 N | 35 06 E | 40 | CH ₄ , CO ₂ |
| Utö | Finland | UTO659N00 | 59 47 N | 21 23 E | 7 | NO ₂ , O ₃ , SO ₂ |
| Varna | Bulgaria | VRN643N00 | 43 12 N | 27 55 E | 41 | NO ₂ , SO ₂ |
| Viana do Castelo | Portugal | VDC641N00 | 41 42 N | 8 48 W | 16 | SO ₂ |
| Vindeln | Sweden | VDL664N00 | 64 15 N | 19 46 E | 271 | O ₃ |
| Virolahti | Finland | VIR660N00 | 60 32 N | 27 40 E | 4 | NO ₂ , O ₃ , SO ₂ |
| Waldhof | Germany | LGB652N00 | 52 48 N | 10 46 E | 74 | CO ₂ , O ₃ |
| Wank Peak | Germany | WNK647N00 | 47 31 N | 11 09 E | 1780 | CO ₂ , NO _x , SO ₂ |

LIST OF OBSERVATIONAL STATIONS (continued)

| Station | Country/Territory | Index Number | Location | | Altitude (m) | Parameter |
|---------------------------------|-------------------|--------------|-------------------|--------------------|-----------------|---|
| | | | Latitude (° ') | Longitude (° ') | | |
| Westerland | Germany | WES654N00 | 54 56 N | 8 19 E | 12 | CO ₂ , O ₃ |
| Zabljak | Montenegro | ZBL643N00 | 43 09 N | 19 08 E | 1450 | NO ₂ , SO ₂ |
| Zavodnje | Slovenia | ZRN646N00 | 46 26 N | 15 00 E | 770 | O ₃ |
| Zeppelinfjellet | Norway | ZEP678N00 | 78 54 N | 11 53 E | 475 | CO ₂ |
| (Ny-Alesund) | | | | | | |
| Zeppelinfjellet | Norway | ZEP678N00 | 78 54 N | 11 53 E | 475 | CCl ₄ , CFCs, CH ₃ CCl ₃ , N ₂ O, O ₃ , SO ₂ |
| (Ny-Alesund) | | | | | | |
| Zeppelinfjellet | Norway | ZEP678N00 | 78 54 N | 11 53 E | 475 | C ₂ Cl ₄ , C ₂ HCl ₃ , CBrClF ₂ , CBrF ₃ , CFCs, CH ₂ Cl ₂ , CH ₃ Br, CH ₃ CCl ₃ , CH ₃ Cl, CHCl ₃ , HCFCs, HFCs, PFCs, SF ₆ , SO ₂ F ₂ |
| (Ny-Alesund) | | | | | | |
| Zeppelinfjellet | Norway | ZEP678N00 | 78 54 N | 11 53 E | 475 | ¹³ CH ₄ , ¹³ CO ₂ , C ¹⁸ O ₂ , CH ₄ , CO, CO ₂ , H ₂ , VOCs |
| (Ny-Alesund) | | | | | | |
| Zingst | Germany | ZGT654N00 | 54 26 N | 12 44 E | 1 | CH ₄ , CO ₂ , O ₃ |
| Zoseni | Latvia | ZSN657N00 | 57 05 N | 25 32 E | 182 | NO ₂ , O ₃ , SO ₂ |
| Zugspitze | Germany | ZUG647N00 | 47 25 N | 10 59 E | 2960 | CO ₂ |
| Zugspitze | Germany | ZUG647N00 | 47 25 N | 10 59 E | 2960 | CH ₄ , CO, CO ₂ , NO, NO _x , NO _y , O ₃ |
| Zugspitze / Schneefernerhaus | Germany | ZSF647N00 | 47 25 N | 10 59 E | 2656 | SO ₂ |
| Zugspitze / Schneefernerhaus | Germany | ZSF647N00 | 47 25 N | 10 59 E | 2656 | CH ₄ , CO, CO ₂ , N ₂ O, NO, NO ₂ , NO _y , O ₃ , PAN, SF ₆ |
| Ähtäri | Finland | AHT662N00 | 62 35 N | 24 12 E | 180 | NO ₂ , O ₃ , SO ₂ |

LIST OF OBSERVATIONAL STATIONS (continued)

| Station | Country/Territory | Index Number | Location | | Altitude (m) | Parameter |
|---|--|--------------|-------------------|--------------------|-----------------|--|
| | | | Latitude (° ') | Longitude (° ') | | |
| ANTARCTICA | | | | | | |
| Arrival Heights | New Zealand | ARH777S00 | 77 48 S | 166 40 E | 184 | O ₃ |
| Arrival Heights | New Zealand | ARH777S00 | 77 48 S | 166 40 E | 184 | ¹³ CH ₄ , CH ₄ , CO, N ₂ O, VOCs |
| Casey Station | Australia | CYA766S00 | 66 17 S | 110 32 E | 60 | ¹³ CO ₂ , CH ₄ , CO, CO ₂ , H ₂ , N ₂ O |
| Concordia, Dôme C | France | DCC775S00 | 75 06 S | 123 20 E | 3233 | O ₃ |
| Halley Bay | United Kingdom of Great Britain and Northern Ireland | HBA775S00 | 75 34 S | 26 30 W | 33 | ¹³ CO ₂ , C ¹⁸ O ₂ , CH ₄ , CO, CO ₂ , H ₂ , VOCs |
| Jubany | Argentina | JBN762S00 | 62 14 S | 58 40 W | 15 | CO ₂ |
| King Sejong | Republic of Korea | KSG762S00 | 62 13 S | 58 47 W | 0 | CO ₂ |
| Marambio | Argentina | MBI764S00 | 64 14 S | 56 37 W | 198 | O ₃ |
| Mawson | Australia | MAA767S00 | 67 37 S | 62 52 E | 32 | ¹³ CO ₂ , CH ₄ , CO, CO ₂ , H ₂ , N ₂ O |
| McMurdo Station | United States of America | MCM777S00 | 77 49 S | 166 35 E | 11 | CH ₄ , O ₃ |
| Mizuho | Japan | MZH770S00 | 70 42 S | 44 18 E | 2230 | CH ₄ |
| Neumayer | Germany | NMY770S00 | 70 39 S | 8 15 W | 42 | O ₃ |
| Palmer Station | United States of America | PSA764S00 | 64 55 S | 64 00 W | 10 | ¹³ CO ₂ , C ¹⁸ O ₂ , C ₂ Cl ₄ , CBrClF ₂ , CCl ₄ , CFCs, CH ₂ Cl ₂ , CH ₃ Br, CH ₃ CCl ₃ , CH ₃ Cl, CH ₄ , CO, CO ₂ , H ₂ , HCFCs, HFCs, N ₂ O, SF ₆ , VOCs |
| South Pole | United States of America | SPO789S00 | 89 59 S | 24 48 W | 2810 | ¹³ CO ₂ , CH ₄ , CO, CO ₂ , H ₂ , N ₂ O |
| South Pole | United States of America | SPO789S00 | 89 59 S | 24 48 W | 2810 | ¹³ CH ₄ , ¹³ CO ₂ , C ¹⁸ O ₂ , C ₂ Cl ₄ , CBrClF ₂ , CBrF ₃ , CCl ₄ , CFCs, CH ₂ Cl ₂ , CH ₃ Br, CH ₃ CCl ₃ , CH ₃ Cl, CH ₄ , CO, CO ₂ , H ₂ , HCFCs, HFCs, N ₂ O, O ₃ , SF ₆ , VOCs |
| Syowa Station | Japan | SYO769S00 | 69 00 S | 39 35 E | 16 | O ₃ |
| Syowa Station | Japan | SYO769S00 | 69 00 S | 39 35 E | 16 | CO ₂ |
| Syowa Station | Japan | SYO769S00 | 69 00 S | 39 35 E | 16 | ¹³ CO ₂ , C ¹⁸ O ₂ , CH ₄ , CO, CO ₂ , H ₂ , VOCs |
| MOBILE STATION | | | | | | |
| Aircraft (over Bass Strait and Cape Grim) | Australia | AIA999900 | | | | ¹³ CO ₂ , CH ₄ , CO, CO ₂ , H ₂ , N ₂ O |
| Aircraft Observation of Atmospheric trace gases by JMA | Japan | AOA999900 | | | | CH ₄ , CO, CO ₂ , N ₂ O |
| Aircraft: Orleans | France | ORL999900 | | | 150 | CH ₄ , CO ₂ |
| Akademik Korolev, R/V | United States of America | AKD999900 | | | | CH ₄ |
| Alligator liberty, M/V | Japan | ALG999900 | | | | CO ₂ |
| Atlantic Ocean | United States of America | AOC9XXX00 | | | 10 | CH ₄ , CO ₂ |
| Comprehensive Observation Network for TRace gases by AirLiner (CONTRAIL) | Japan | EOM999900 | | | | CH ₄ , CO ₂ |

LIST OF OBSERVATIONAL STATIONS (continued)

| Station | Country/Territory | Index Number | Location | | Altitude (m) | Parameter |
|---|-----------------------------|--------------|-------------------|--------------------|-----------------|---|
| | | | Latitude (° ') | Longitude (° ') | | |
| Comprehensive Observation Network for TRace gases by AirLiner (CONTRAIL) | Japan | EOM999900 | | | | ¹³ CH ₄ , CH ₃ D |
| Discoverer 1983 & 1984, R/V | United States of America | DIS999900 | | | | CH ₄ |
| Discoverer 1985, R/V | United States of America | DSC999900 | | | | CH ₄ |
| Drake Passage | United States of America | DRP999900 | | | | ¹³ CO ₂ , C ¹⁸ O ₂ , CH ₄ , CO, CO ₂ |
| HATS Ocean Projects | United States of America | HOP999900 | | | | HFCs |
| INSTAC-I (International Strato/Tropospheric Air Chemistry Project) | Japan | INS999900 | | | | ¹³ CO ₂ , CH ₄ , CO ₂ |
| John Biscoe, R/V | United States of America | JBS999900 | | | | CH ₄ |
| Keifu Maru, R/V | Japan | KEF999900 | | | | CO ₂ , TIC |
| Kofu Maru, R/V | Japan | KOF999900 | | | | CO ₂ |
| Korolev, R/V | United States of America | KOR999900 | | | | CH ₄ |
| Long Lines Expedition, R/V | United States of America | LLE999900 | | | | CH ₄ |
| MRI Research, 1978-1986, R/V | Japan | MRI999900 | | | | CH ₄ |
| MRI Research, Hakuho Maru, R/V | Japan | HKH999900 | | | | CO ₂ |
| MRI Research, Kaiyo Maru, R/V | Japan | KIY999900 | | | | CO ₂ |
| MRI Research, Mirai, R/V | Japan | MMR999900 | | | | CO ₂ |
| MRI Research, Natushima, R/V | Japan | NTU999900 | | | | CO ₂ |
| MRI Research, Ryofu Maru, R/V | Japan | RFM999900 | | | | CO ₂ |
| MRI Research, Wellington Maru, R/V | Japan | WLT999900 | | | | CO ₂ |
| Mexico Naval H-02, R/V | United States of America | MXN999900 | | | | CH ₄ |
| NOPACCS - Hakurei Maru - | Japan | HAK999900 | | | | TIC |
| Observation of Atmospheric Chemistry Over Japan | Japan | OAJ999900 | | | | CFCs, N ₂ O |
| Oceanographer, R/V | United States of America | OCE999900 | | | | CH ₄ |
| Pacific Ocean | New Zealand | BSL999900 | | | | ¹³ CH ₄ , CH ₄ , VOCs |
| Pacific Ocean | United States of America | POC9XXX00 | | | 10 | ¹³ CO ₂ , C ¹⁸ O ₂ , CH ₄ , CO, CO ₂ , H ₂ |
| Pacific-Atlantic Ocean | United States of America | PAO999900 | | | | CH ₄ , CO ₂ |
| Polar Star, R/V | United States of America | PLS999900 | | | | CH ₄ |
| Ryofu Maru, R/V | Japan | RYF999900 | | | | CFCs, CH ₄ , CO ₂ , N ₂ O, TIC |

LIST OF OBSERVATIONAL STATIONS (continued)

| Station | Country/Territory | Index Number | Location | | Altitude (m) | Parameter |
|---|--------------------------|--------------|-------------------|--------------------|-----------------|--|
| | | | Latitude (° ') | Longitude (° ') | | |
| Santarem | Brazil | SAN999900 | | | | CH ₄ , CO, CO ₂ , N ₂ O, SF ₆ |
| South China Sea | United States of America | SCS9XXX00 | | | 15 | ¹³ CO ₂ , C ¹⁸ O ₂ , CH ₄ , CO, CO ₂ , H ₂ |
| Soyo Maru, R/V | Japan | SOY999900 | | | | CO ₂ |
| Surveyor, R/V | United States of America | SUR999900 | | | | CH ₄ |
| The Observation of Atmospheric Methane Over Japan | Japan | OAM999900 | | | | CH ₄ |
| The Observation of Atmospheric Sulfur Hexafluoride Over Japan | Japan | OAS999900 | | | | SF ₆ |
| WEST COSMIC - Hakurei Maru No.2 - | Japan | HAK999901 | | | | TIC |
| Wakataka-Mar | Japan | WAK999900 | | | | CO ₂ |
| Western Pacific | United States of America | WPC9XXX00 | | | 10 | ¹³ CH ₄ , ¹³ CO ₂ , C ¹⁸ O ₂ , CH ₄ , CO ₂ |
| northern and western Pacific | Japan | NWP999900 | | | | N ₂ O |
| over Japan between Sendai and Fukuoka | Japan | TDA999900 | | | | CH ₄ |
| over the Pacific Ocean 20-50 km off the coast of the Sendai plain | Japan | PIP999900 | | | | CH ₄ |

LIST OF UCI*¹ SAMPLING SITES

| CODE | Primary site | Region | Type* ² | Ss* ³ | Lat (°) | Long (°) | n* ⁴ |
|---------|--------------------|-----------------|--------------------|------------------|------------|-------------|-----------------|
| UCI_ANT | Antofagasta | Chile | Point | 1 | -23.50 | -70.43 | 6 |
| UCI_BAH | Bahamas | Caribbean | Islands | 2 | 23.59 | -75.26 | 7 |
| UCI_BAR | Barbados | Caribbean | Islands | 3 | 13.05 | -59.53 | 8 |
| UCI_BEL | Belem | Brazil | Point | 1 | -1.45 | -48.48 | 5 |
| UCI_BET | Bethel | Alaska | Point | 1 | 60.80 | -161.75 | 4 |
| UCI_BOR | Bora Bora | French Poly. | Islands | 3 | -16.50 | -151.75 | 42 |
| UCI_BRW | Barrow | Alaska | Point | 1 | 71.32 | -156.61 | 313 |
| UCI_BYR | Bryd Station | Antarctica | Point | 1 | -80.02 | -119.53 | 2 |
| UCI_CAB | Cape Blanco | Oregon | Range | 27 | 42.84 | -124.56 | 179 |
| UCI_CAE | Cape Egmont | New Zealand | Range | 20 | -39.27 | 173.75 | 47 |
| UCI_CAI | Cairns | Australia | Range | 7 | -16.92 | 145.77 | 25 |
| UCI_CAM | Cape Mendocino | California | Range | 19 | 40.42 | -124.40 | 66 |
| UCI_CGO | Cape Grim | Australia | Point | 1 | -40.68 | 144.69 | 1 |
| UCI_CHR | Christmas Island | Central Pacific | Island | 1 | 1.87 | -157.33 | 2 |
| UCI_CSL | Cabo San Lucas | Mexico | Range | 12 | 22.88 | -109.90 | 299 |
| UCI_DUT | Dutch Harbor | Alaska | Point | 1 | 53.88 | -166.53 | 14 |
| UCI_ECU | Isla de la Plata | Ecuador | Point | 5 | -1.27 | -81.06 | 44 |
| UCI_ENP | Everglades NP | Florida | Point | 3 | 25.13 | -80.95 | 13 |
| UCI_FAI | Fairbanks | Alaska | Point | 4 | 65.15 | -147.86 | 181 |
| UCI_FIJ | Fiji | South Pacific | Island | 1 | -18.26 | 178.00 | 20 |
| UCI_FOR | Fortaleza | Brazil | Point | 1 | -3.72 | -38.50 | 6 |
| UCI_FTY | Fort Yukon | Alaska | Point | 4 | 66.57 | -145.27 | 43 |
| UCI_FUN | Funafuti, Tuvalu | Central Pacific | Island | 1 | -8.52 | 179.20 | 44 |
| UCI_GAL | Galapagos Islands | Ecuador | Islands | 3 | -1.27 | -90.49 | 3 |
| UCI_GUA | Guam | Central Pacific | Island | 4 | 13.66 | 144.86 | 229 |
| UCI_HAW | Hawaii | Hawaii | Island | 15 | 20.27 | -155.85 | 273 |
| UCI_HOK | Hokitika | New Zealand | Range | 24 | -42.72 | 170.96 | 245 |
| UCI_JAC | Jacksonville Beach | Florida | Point | 2 | 30.28 | -81.39 | 4 |
| UCI_JAL | Jalama Beach CP | California | Range | 14 | 34.51 | -120.50 | 50 |
| UCI_JCR | Jacaraípe | Brazil | Point | 3 | -20.15 | -40.18 | 5 |
| UCI_JER | Jervis Bay | Australia | Range | 2 | -35.13 | 150.70 | 2 |
| UCI_JON | Johnston Atoll | Central Pacific | Island | 1 | 16.74 | -169.53 | 1 |
| UCI_JPF | Juia Pfeiffer SB | California | Range | 29 | 36.15 | -121.66 | 204 |
| UCI_KAN | Kanton Island | Kiritibati | Island | 1 | -2.83 | -171.68 | 2 |
| UCI_KAU | Kauai | Hawaii | Island | 3 | 22.23 | -159.40 | 66 |
| UCI_KET | Ketchikan | Alaska | Point | 2 | 55.35 | -131.65 | 17 |
| UCI_KIN | Kiritibati, North | Central Pacific | Islands | 5 | 1.42 | 173.10 | 88 |
| UCI_KIS | Kiritibati, South | Central Pacific | Islands | 9 | -1.29 | 174.83 | 116 |
| UCI_KOD | Kodiak Island | Alaska | Point | 5 | 57.84 | -152.35 | 325 |
| UCI_KOS | Kosrae | FS Micronesia | Islands | 2 | 5.32 | 163.01 | 47 |
| UCI_KOT | Kotzebue | Alaska | Point | 1 | 66.90 | -162.58 | 4 |
| UCI_MAJ | Majuro | Marshall Is. | Islands | 5 | 7.05 | 171.23 | 226 |
| UCI_MAN | Manaus | Brazil | Inland | 1 | -3.10 | -60.10 | 2 |
| UCI_MCM | McMurdo | Antarctica | Point | 4 | -77.86 | 166.70 | 10 |
| UCI_MUR | Muriwai Beach | New Zealand | Range | 16 | -36.83 | 174.43 | 222 |
| UCI_NAU | Nauru | Micronesia | Island | 2 | -0.53 | 166.91 | 45 |
| UCI_NIN | Ninety Mile Beach | New Zealand | Range | 8 | -34.90 | 173.09 | 195 |
| UCI_NLK | Norfolk Island | South Pacific | Island | 1 | -29.04 | 167.99 | 595 |
| UCI_NOM | Nome | Alaska | Point | 1 | 64.50 | -165.40 | 8 |
| UCI_NUK | Nuku Hiva | Marquesas | Island | 1 | -8.90 | -140.22 | 2 |
| UCI_OAH | Oahu/Maui | Hawaii | Islands | 14 | 21.28 | -157.83 | 55 |
| UCI_OCS | Ocean Shores | Washington | Range | 31 | 46.98 | -124.17 | 182 |
| UCI_OLY | Olympic Peninsula | Washington | Range | 8 | 47.56 | -124.36 | 26 |
| UCI_ORB | Oreti Beach | New Zealand | Range | 17 | -46.44 | 168.23 | 178 |
| UCI_PNG | Papua New Guinea | Central Pacific | Islands | 10 | -4.20 | 152.20 | 87 |
| UCI_PNK | Punakaiki | New Zealand | Range | 18 | -42.11 | 171.33 | 65 |

| CODE | Primary site | Region | Type ^{*2} | Ss ^{*3} | Lat (°) | Long (°) | n ^{*4} |
|---------|-------------------|-----------------|--------------------|------------------|------------|-------------|-----------------|
| UCI_PON | Pohnpei/Chuuk | FS Micronesia | Islands | 2 | 6.97 | 158.27 | 207 |
| UCI_POR | Portage Glacier | Alaska | Point | 9 | 60.75 | -148.78 | 202 |
| UCI_PRU | Prudhoe Bay | Alaska | Point | 1 | 70.25 | -148.37 | 7 |
| UCI_PTA | Punta Arenas | Chile | Point | 1 | -53.10 | -70.87 | 5 |
| UCI_PTR | Point Reyes | California | Range | 17 | 38.00 | -123.02 | 171 |
| UCI_PUM | Puerto Montt | Chile | Point | 1 | -41.48 | -72.95 | 5 |
| UCI_PUN | Punta Baja | Mexico | Range | 4 | 29.95 | -115.83 | 147 |
| UCI_RAR | Rarotonga | Cook Islands | Islands | 2 | -21.24 | -159.82 | 314 |
| UCI_RCF | Recife | Brazil | Point | 1 | -8.05 | -34.90 | 6 |
| UCI_RIA | Riau Island | Central Pacific | Island | 1 | 1.17 | 104.40 | 4 |
| UCI_RIO | Rio de Janeiro | Brazil | Point | 2 | -22.90 | -43.23 | 4 |
| UCI_SAI | Saipan | Central Pacific | Islands | 2 | 15.29 | 145.82 | 242 |
| UCI_SAL | Salvador | Brazil | Point | 1 | -12.98 | -38.52 | 6 |
| UCI_SAQ | San Quintin | Mexico | Range | 11 | 30.40 | -115.93 | 129 |
| UCI_SEY | Seychelles | Central Pacific | Islands | 2 | -4.59 | 55.43 | 2 |
| UCI_SMO | Tula | Samoa | Island | 1 | -14.25 | -170.56 | 257 |
| UCI_SOL | Solomon Islands | Central Pacific | Islands | 4 | -9.43 | 159.95 | 47 |
| UCI_SOS | Sondre Stromfjord | Greenland | Point | 1 | 67.00 | -50.71 | 2 |
| UCI_SPO | South Pole | Antarctica | Point | 1 | -90.00 | 0.00 | 3 |
| UCI_SUR | Affobakka | Suriname | Point | 4 | 5.08 | -55.03 | 10 |
| UCI_THU | Thursday Island | Central Pacific | Island | 1 | -10.58 | 142.22 | 2 |
| UCI_TRI | Trinidad | Caribbean | Islands | 4 | 10.43 | -61.13 | 14 |
| UCI_VIN | Vina del Mar | Chile | Point | 1 | -33.03 | -71.57 | 4 |
| UCI_VIR | Virgin Islands | Caribbean | Islands | 5 | 17.75 | -67.70 | 12 |
| UCI_WAL | Wallis Island | Central Pacific | Island | 1 | -13.30 | -176.17 | 5 |
| UCI_YAP | Yap | FS Micronesia | Island | 1 | 9.52 | 138.08 | 79 |

*1 UCI: University of California, Irvine

*2 Type: Point: Point sampling, where UCI staff fly into an airport and then sample nearby (typically within a 100 km radius); a code based on the most frequent sampling site at that location is assigned.

Range: Range sampling, where UCI staff drive down a coast and sample along; 2.5 degree latitudinal bins are adopted and the most frequent sampling site within the range is assigned.

Island: Island sampling, which is point sampling except on a small island (or islands); about 5 degree sampling bins are adopted.

*3 Ss: Number of sub sites included in the single site code

*4 n: Number of samples

LIST OF CONTRIBUTORS

| Station Country/Territory | Name | Address |
|------------------------------|-----------------------------|---|
| REGION I (Africa) | | |
| Cairo (Egypt) | AbdElhamid Gouda Elawadi | Egyptian Meteorological Authority Department of Air Pollution Study Egyptian Meteorological Authority P.O.Box:11784 - Cairo, Egypt |
| Cape Point (South Africa) | Alastair Williams | Australian Nuclear Science and Technology Organisation, Institute for Environmental Research, Atmospheric Mixing and Pollution Transport Group Locked Bag 2001, Kirrawee DC, NSW 2232, Australia |
| Izaña (Tenerife) (Spain) | Angel J. Gomez-Pelaez | Izana Atmospheric Research Center, Meteorological State Agency of Spain (AEMET) C/ La Marina, 20, Planta 6. 38001 Santa Cruz de Tenerife, Spain |
| | Carlos Marrero | Izana Atmospheric Research Center, Meteorological State Agency of Spain (AEMET) C/ La Marina, 20 - Planta 6. Apartado 880. 38071 Santa Cruz de Tenerife, Spain |
| Funchal (Portugal) | Diamantino Henriques | Instituto de Meteorologia,I.P. Observatorio Afonso Chaves, Rua Mae de Deus - Relvao, 9500-321 Ponta Delgada, S. Miguel, Portugal |
| Cape Point (South Africa) | Ernst Günther Brunke | South African Weather Service (Climate Division) SAWS, c/o CSIR (Environmentek), P.O. Box 320,Stellenbosch 7599, South Africa |
| Amsterdam Island (France) | Jean Sciare | LSCE (Laboratoire des Sciences du Climat et de l'Environnement) UMR CEA-CNRS LSCE - CEA Saclay - Orme des Merisiers - Bat.701 91191 Gif-sur-Yvette, France |
| | Michel Ramonet | LSCE (Laboratoire des Sciences du Climat et de l'Environnement) UMR CEA-CNRS LSCE - CEA Saclay - Orme des Merisiers - Bat.701 91191 Gif-sur-Yvette, France |
| Mt. Kenya (Kenya) | Josiah Kariuki Murageh | KMD, Kenyan Meteorological Department Kenya Meteorological Department Dagoretti Corner P.O. Box 30259 00100 Nairobi, Kenya |
| | Jörg Klausen | Federal Office of Meteorology and Climatology MeteoSwiss Krähbühlstrasse 58 P.O. Box 514 CH-8044 Zürich, Switzerland |

LIST OF CONTRIBUTORS (continued)

| Station Country/Territory | Name | Address |
|--|------------------|--|
| | Stephan Henne | Empa, Swiss Federal Laboratories for Materials Testing and Research Ueberlandstrasse 129 8600 Duebendorf, Switzerland |
| Cape Verde Observatory (Cape Verde) | Katie Read | Department of Chemistry, University of York Department of Chemistry, University of York, Heslington, York, Y010 5DD, United Kingdom |
| | Zoë Fleming | National Centre for Atmospheric Science (NCAS) Department of Chemistry University of Leicester National Centre for Atmospheric Science (NCAS) Department of Chemistry University of Leicester Leicester LE1 7RH, UK |
| Assekrem (Algeria) | Mimouni Mohamed | Office National de la Meteorologie POBox 31 Tamanrasset 11000, Algeria |
| REGION II (Asia) | | |
| Nagoya (Japan) | A. Matsunami | Research Center for Advanced Energy Conversion, Nagoya University Furo-cho, Chikusaku, Nagoya 464-8603, Japan |
| Anmyeon-do (Republic of Korea) | Haeyoung Lee | Korea Global Atmosphere Watch Center, Korea Meteorology Administration 1764-6, Seungen-Ri, Anmyeon-Eup, Taeon-Kun, ChungNam, 357-961, Republic of Korea |
| | Hee-Jung Yoo | Korea Global Atmosphere Watch Center, Korea Meteorology Administration 1764-6, Seungen-Ri, Anmyeon-Eup, Taeon-Kun, ChungNam, 357-961, Republic of Korea |
| Cape Ochi-ishi Hateruma (Japan) | Hitoshi MUKAI | Center for Global Environmental Research, National Institute for Environmental Studies 16-2, Onogawa, Tsukuba-shi, Ibaraki 305-8506, Japan |
| | Takuya Saito | Center for Environmental Measurement and Analysis, National Institute for Environmental Studies |
| | Yasunori TOHJIMA | Center for Global Environmental Research, National Institute for Environmental Studies 16-2, Onogawa, Tsukuba-shi, Ibaraki 305-8506, Japan |

LIST OF CONTRIBUTORS (continued)

| Station Country/Territory | Name | Address |
|--------------------------------|----------------|---|
| Gosan (Republic of Korea) | Jeong-Ah Yu | National Institute of Environmental Research Environmental Research Complex, Gyeongseo-dong, Seo-gu, Incheon, 404-708, Republic of Korea |
| | Seung-Yeon Kim | National Institute of Environmental Research Environmental Research Complex, Gyeongseo-dong, Seo-gu, Incheon, 404-708, Republic of Korea |
| Everest - Pyramid (Nepal) | Jgor Arduini | Università degli Studi di Urbino Istituto di Scienze Chimiche, piazza Rinascimento 6, 61029 Urbino - Italy |
| Hok Tsui (Hong Kong, China) | Ka Se Lam | Department of Civil and Structural Engineering, Hong Kong Polytechnic University Hung Hom, Kowloon, Hong Kong, China |
| Mikawa-Ichinomiya (Japan) | Koji Ohno | Aichi Air Environment Division 1-2 Sannomaru-3chome, Naka-ku, Nagoya, Aichi 460-8501, Japan |
| Mt. Waliguan (China) | Lingxi ZHOU | Professor, PI for Greenhouse Gases & Related Tracers Chinese Academy of Meteorological Sciences (CAMS) China Meteorological Administration (CMA) 46 Zhongguancun Nandajie Beijing 100081, China |
| | Xiaobin Xu | Key Laboratory for Atmospheric Chemistry, Institute of Atmospheric Composition, Chinese Academy of Meteorological Sciences, China Meteorological Administration Zhongguancun Nandajie 46 Beijing 100081, China |
| Memanbetsu (Japan) | Michio Hirota | Geochemical Research Department, Meteorological Research Institute 1-1, Nagamine, Tsukuba, Ibaraki 305-0052, Japan |
| Tsukuba (Japan) | Michio Hirota | Geochemical Research Department, Meteorological Research Institute 1-1, Nagamine, Tsukuba, Ibaraki 305-0052, Japan |
| | Yousuke Sawa | Geochemical Research Department, Meteorological Research Institute 1-1, Nagamine, Tsukuba, Ibaraki 305-0052, Japan |
| Hamamatsu (Japan) | Mitsuo TODA | Shizuoka University 3-5-1 Jyohoku, Hamamatsu 432-8561, Japan |

LIST OF CONTRIBUTORS (continued)

| Station Country/Territory | Name | Address |
|--|---------------------|--|
| Bering Island Kotelny Island Tiksi (Russian Federation) | Nina Paramonova | Main Geophysical Observatory (MGO) Karbyshev Street 7, St. Petersburg, 194021, Russian Federation |
| Kyzylcha (Uzbekistan) | | |
| Hok Tsui King's Park (Hong Kong, China) | Olivia S.M. Lee | Hong Kong Observatory 134A, Nathan Road, Kowloon, Hong Kong |
| | David H.Y. Lam | Hong Kong Observatory 134A, Nathan Road, Kowloon, Hong Kong |
| Everest - Pyramid (Nepal) | Paolo Cristofanelli | ISAC-CNR ISAC-CNR, Via Gobetti 101 - 40129 Bologna -Italy |
| | Paolo Bonasoni | ISAC-CNR ISAC-CNR, Via Gobetti 101 - 40129 Bologna -Italy |
| Tsukuba (Japan) | Ryodo Shigebayashi | Lower Aerological Observations Division, Aerological Observatory, Japan Meteorological Agency (JMA) Lower Aerological Observations Division, Aerological Observatory1-2 Nagamine, Tsukuba, Ibaraki, 305-0052, Japan |
| Takayama (Japan) | Shohei Murayama | Research Institute for Environmental Management Technology, National Institute of Advanced Industrial Science and Technology (AIST) AIST Tsukuba West, 16-1 Onogawa, Tsukuba, Ibaraki 305-8569, Japan |
| Gosan (Republic of Korea) | So-young Bang | Applied Meteorology Research Laboratory, Meteorological Research Institute (METRI), Korea Meteorological Administration (KMA) 460-18, Shindaebang-dong, Dongjak-gu, Seoul 156-720, Rep. of Korea |
| Ship between Ishigaki Island and Hateruma Island (Japan) | Takakiyo Nakazawa | Center for Atmospheric and Oceanic Studies, Graduate School of Science, Tohoku University Aoba, Sendai 980-8578, Japan |
| | Shuji Aoki | Center for Atmospheric and Oceanic Studies, Graduate School of Science, Tohoku University Aoba, Sendai 980-8578, Japan |

LIST OF CONTRIBUTORS (continued)

| Station Country/Territory | Name | Address |
|---|----------------|--|
| Suita (Japan) | Tomohiro Oda | Division of Sustainable Energy and Environmental Engineering, Graduate School of Engineering, Osaka University, Japan Green Engineering Lab Division of Sustainable Energy and Environmental Engineering 2-1 Yamadaoka, Suita, Osaka 565-0871 Japan |
| Issyk-Kul (Kyrgyzstan) | V. Sinyakov | Laboratory of Geophysics, Institute of Fundamental sciences at the Kyrgyz National University Manas Street 101, Bishkek, 720033, Kyrgyz Republic |
| Mt. Dodaira Kisai Urawa (Japan) | Yosuke MUTO | Center for Environmental Science in Saitama 914 Kamitanadare, Kisai-machi, Kita-Saitama-gun, Saitama 347-0115, Japan |
| Minamitorishima Ryori Yonagunijima (Japan) | Yukio Fukuyama | Atmospheric Environment Division, Global Environment and Marine Department, Japan Meteorological Agency (JMA) 1-3-4 Otemachi, Chiyoda-ku, Tokyo 100-8122, Japan |

REGION III (South America)

| | | |
|------------------------|-----------------------|--|
| Arembepe (Brazil) | Luana S. Basso | IPEN Atmospheric Chemistry Laboratory Av. Prof. Lineu Prestes, 2242, Cidade Universitaria, Sao Paulo, SP- BRAZIL CEP 05508-900 |
| | Luciana Vanni Gatti | IPEN Atmospheric Chemistry Laboratory Av. Prof. Lineu Prestes, 2242, Cidade Universitaria, Sao Paulo, SP- BRAZIL CEP 05508-900 |
| | Maria Elena Barlasina | National Weather Service Observatorio Central Villa Ortuzar División Radiación Av. de Los Constituyentes 3454 Cp 1427, Argentina |
| Ushuaia (Argentina) | Manuel Cupeiro | National Weather Service 245 Viviendas Tira 8A, Dpto 10. Ushuaia, Tierra del Fuego, Argentina |
| | Ricardo Sanchez | National Weather Service Observatorio Central Villa Ortuzar División Radiación Av. de Los Constituyentes 3454 Cp 1427, Argentina |

LIST OF CONTRIBUTORS (continued)

| Station Country/Territory | Name | Address |
|--|-----------------------|--|
| La Quiaca Observatorio Pilar Observatorio San Julian Aero (Argentina) | Maria Elena Barlasina | National Weather Service Observatorio Central Villa Ortuzar División Radiación Av. de Los Constituyentes 3454 Cp 1427, Argentina |
| | Ricardo Sanchez | National Weather Service Observatorio Central Villa Ortuzar División Radiación Av. de Los Constituyentes 3454 Cp 1427, Argentina |
| El Tololo (Chile) | Martin Steinbacher | Empa - Swiss Federal Laboratories for Materials Science and Technology Ueberlandstrasse 129 CH-8600 Duebendorf Switzerland |
| | Gaston Torres | |
| Huancayo (Peru) | Mutsumi Ishitsuka | Observatorio de Huancayo, Instituto Geofisico del Peru Apartado 46, Huancayo, Peru |
| Ushuaia (Argentina) | Sergio Luppo | Servicio Meteorológico Nacional - Gobierno de Tierra del Fuego Estación VAG Ushuaia Subsecretaria de Ciencia y Tecnología, Ministerio de Educación, Cultura, Ciencia y Tecnología Gobierno de Tierra del Fuego 9410 Ushuaia, Tierra del Fuego, Argentina |
| San Lorenzo (Paraguay) | Victor Ayala | Universidad Nacional de Asuncion, Facultad de Ciencias Exactas y Naturales, Laboratorio de Investigacion Atmosferica y Problemas Ambientales |
| | Carlos Quevedo | |

REGION IV (North and Central America)

| | | |
|--|-------------|---|
| Candle Lake Chibougamau Cape St. James Lac La Biche (Alberta) (Canada) | Doug Worthy | Environment Canada (EC) 4905 Dufferin Street, Toronto, Ontario, Canada, M3H 5T4 |
| Alert Churchill Estevan Point East Trout Lake Fraserdale Sable Island (Canada) | Doug Worthy | Environment Canada (EC) 4905 Dufferin Street, Toronto, Ontario, Canada, M3H 5T4 |

LIST OF CONTRIBUTORS (continued)

| Station Country/Territory | Name | Address |
|---|-----------------------|--|
| | Lin Huang | Environment Canada 4905 Dufferin Street, Toronto, Ontario, Canada, M3H 5T4 |
| Egbert (Canada) | Doug Worthy | Environment Canada (EC) 4905 Dufferin Street, Toronto, Ontario, Canada, M3H 5T4 |
| | Peter C. Brickell | Environment Canada (EC) 4905 Dufferin Street, Toronto, Ontario, Canada, M5T 1V7 |
| Algoma Alert Bratt's Lake Chalk River Chapais Egbert Experimental Lakes Area Esther Kejimikujik Longwoods Saturna Sutton (Canada) | Mike Shaw | Environment Canada Science and Technology Branch Air Quality Research Division 4905 Dufferin Street Toronto, Ontario CANADA M3H 5T4 |
| La Palma (Cuba) | Osvaldo Cuesta Santos | Institute of Meteorology, Atmospheric Environment Research Center Aptdo. 17032, Postal Code 11700, Havana 17, Cuba |
| REGION V (South-West Pacific) | | |
| Cape Grim (Australia) | Bruce Forgan | Commonwealth Bureau of Meteorology 700 Collins St, Docklands GPO Box 1289K, Melbourne, Victoria 3001, Australia |
| | Ian Galbally | CSIRO Marine and Atmospheric Research CSIRO Marine and Atmospheric Research Private Bag 1, Aspendale Victoria 3195 Australia |
| Lauder (New Zealand) | Dan Smale | National Institute of Water & Atmospheric Research Ltd. NIWA, Private Bag 50061, Omakau, Central Otago 9320, New Zealand |

LIST OF CONTRIBUTORS (continued)

| Station Country/Territory | Name | Address |
|--|--------------------------|---|
| | Gordon Brailsford | National Institute of Water & Atmospheric Research Ltd. 301 Evans Bay Parade, Greta Point, Private Bag 14-901, Kilbirnie, Wellington, New Zealand |
| | Sylvia Nichol | National Institute of Water & Atmospheric Research Ltd. 301 Evans Bay Parade, Greta Point, Private Bag 14-901, Kilbirnie, Wellington, New Zealand |
| Tanah Rata (Malaysia) | Lim Sze Fook | Environmental Studies Division Malaysian Meteorological Department Jalan Sultan, 46667 Petaling Jaya, Selangor, Malaysia |
| Danum Valley GAW Baseline Station (Malaysia) | Lim Sze Fook | Environmental Studies Division Malaysian Meteorological Department Jalan Sultan, 46667 Petaling Jaya, Selangor, Malaysia |
| | Maznorizan Mohamad | Environmental Studies Division Malaysian Meteorological Department |
| Bukit Koto Tabang Jakarta (Indonesia) | Mangasa Naibaho | The Indonesia Agency for Meteorology Climatology and Geophysics (BMKG) Jl. Angkasa 1, No. 2, Kemayoran Jakarta 10720, Indonesia |
| Bukit Koto Tabang (Indonesia) | Mangasa Naibaho | The Indonesia Agency for Meteorology Climatology and Geophysics (BMKG) Jl. Angkasa 1, No. 2, Kemayoran Jakarta 10720, Indonesia |
| | Nahas, Alberth Christian | The Indonesia Agency for Meteorology Climatology and Geophysics (BMKG) Jl. Raya Bukittinggi-Medan Km. 17 Palupuh, District Agam, West Sumatera, Indonesia PO BOX 11 Bukittinggi 26100 |
| | Jörg Klausen | Federal Office of Meteorology and Climatology MeteoSwiss Krähbühlstrasse 58 P.O. Box 514 CH-8044 Zürich, Switzerland |
| | Martin Steinbacher | Empa - Swiss Federal Laboratories for Materials Science and Technology Ueberlandstrasse 129 CH-8600 Dübendorf Switzerland |

LIST OF CONTRIBUTORS (continued)

| Station Country/Territory | Name | Address |
|--|-----------------------|--|
| | Sugeng Nugroho | The Indonesia Agency for Meteorology Climatology and Geophysics (BMKG) Jl.Angkasa 1,No.2,Kemayoran Jakarta 10720,Indonesia |
| Baring Head (New Zealand) | Sylvia Nichol | National Institute of Water & Atmospheric Research Ltd. 301 Evans Bay Parade, Greta Point, Private Bag 14-901, Kilbirnie, Wellington, New Zealand |
| | Gordon Brailsford | National Institute of Water & Atmospheric Research Ltd. 301 Evans Bay Parade, Greta Point,Private Bag 14-901, Kilbirnie, Wellington, New Zealand |
| | Ross Martin | National Institute of Water & Atmospheric Research Ltd. 301 Evans Bay Parade, Greta Point, Private Bag 14-901, Kilbirnie, Wellington, New Zealand |
| REGION VI (Europe) | | |
| Atmospheric Station Kresin u Pacova (Czech Republic) | Alice Dvorska | Global Change Research Centre AS CR, v.v.i. Belidla 986/4a, 603 00 Brno |
| Puszcza Borecka/Diabla Gora (Poland) | Anna Degorska | Institute of Environmental Protection Kolektorska 4 01-692 Warsaw, Poland |
| Monte Cimone (Italy) | Attilio Di Diodato | Italian Air Force Meteorological Service C.A.M.M. Mt. CIMONE,Via delle Ville 40, 41029-Sestola (MO), Italy |
| Hohe Warte Stephansplatz (Austria) | August Kaiser | Department for Environmental MeteorologyCentral Institute for Meteorology and Geodynamics Postfach 342, Hohe Warte 38, A-1191 Wien, Austria |
| Zeppelinfjellet (Ny-Alesund) (Norway) | Birgitta Noone | Department of Applied Environmental Science (ITM) Stockholm University SE-10691 Stockholm |
| | Hans-Christen Hansson | Department of Applied Environmental Science (ITM) Stockholm University SE-10691 Stockholm |
| Jungfraujoch (Switzerland) | Brigitte Buchmann | Empa - Swiss Federal Laboratories for Materials Science and Technology Überlandstrasse 129 CH-8600 Dübendorf Switzerland |

LIST OF CONTRIBUTORS (continued)

| Station Country/Territory | Name | Address |
|--|--------------------|--|
| | Hoerger Corinne | Swiss Federal Laboratories for Materials Science and Technology, EMPA, Air Pollution/Environmental Technology |
| | Stefan Reimann | Ueberlandstrasse 129,, CH-8600, Duebendorf, Switzerland |
| | Thomas Seitz | Swiss Federal Laboratories for Materials Science and Technology, EMPA, Air Pollution/Environmental Technology Ueberlandstrasse 129,, CH-8600, Duebendorf, Switzerland |
| | Martin Steinbacher | Empa - Swiss Federal Laboratories for Materials Science and Technology Überlandstrasse 129 CH-8600 Dübendorf Switzerland |
| Payerne Rigi (Switzerland) | Brigitte Buchmann | Empa - Swiss Federal Laboratories for Materials Science and Technology Überlandstrasse 129 CH-8600 Dübendorf Switzerland |
| | Thomas Seitz | Empa - Swiss Federal Laboratories for Materials Science and Technology Überlandstrasse 129 CH-8600 Dübendorf Switzerland |
| Fundata Semenic Stîna de Vale (Romania) | Daniela ZISU | National Research and Development Institute for Environmental Protection Splaiul Independentei nr. 294, sector 6, 77703 Bucuresti , Romania |
| Summit (Denmark) | Detlev Helmig | Institute of Arctic and Alpine Research (INSTAAR) INSTAAR, Univ. of Colorado 1560, 30th Street UCB 450 Boulder, CO 80309 U.S.A. |
| | Jacques Hueber | Institute of Arctic and Alpine Research (INSTAAR) INSTAAR, Univ. of Colorado 1560, 30th Street UCB 450 Boulder, CO 80309 U.S.A. |

LIST OF CONTRIBUTORS (continued)

| Station Country/Territory | Name | Address |
|---|-----------------------|--|
| Angra do Heroismo Beja Bragança Castelo Branco Lisboa / Gago Coutinho Monte Velho Penhas Douradas Viana do Castelo (Portugal) | Diamantino Henriques | Instituto de Meteorologia,I.P. Observatorio Afonso Chaves, Rua Mae de Deus - Relvao, 9500-321 Ponta Delgada, S. Miguel, Portugal |
| Kamenicki Vis (Serbia) | Dragan Djordjevic | Republic Hydrometeorological Service, Environmental Control Department Kneza Viseslava 66, 11030 Belgrade, Serbia |
| Burgas Plovdiv Pleven Sofia Varna (Bulgaria) | Ekaterina Batchvarova | National Institute of Meteorology and Hydrology 66 Tzarigradsko chaussee, 1784 Sofia, Bulgaria |
| Jarczew Leba Suwalki (Poland) | Eugeniusz Brejnak | Institute of Meteorology and Water Management;Laboratory for Research and Monitoring of Air Pollution 61 Podlesna Street, 01-673 Warszawa, Poland |
| Fundata (Romania) | Florin Nicodim | National Meteorological Administration Sos. Bucuresti-Ploiesti nr. 97, 71552 Bucharest, Romania |
| Giordan Lighthouse (Malta) | Francelle Azzopardi | |
| | Raymond Ellul | Atmospheric Research Unit / Physics Department /University of Malta Msida MSD 06, Malta |
| | Martin Saliba | |
| Plateau Rosa (Italy) | Francesco Apadula | Ricerca sul Sistema Energetico - RSE S.p.A. via Rubattino 54, 20134 Milano, Italy |
| | Daniela Heltai | Ricerca sul Sistema Energetico - RSE S.p.A. via Rubattino 54, 20134 Milano, Italy |
| | Andrea Lanza | Ricerca sul Sistema Energetico - RSE S.p.A. via Rubattino 54, 20134 Milano, Italy |
| Site J (Denmark) | Gen Hashida | National Institute of Polar Research Kaga 1-9-10, Itabashi-ku, Tokyo 173-8515, Japan |
| | Shinji Morimoto | National Institute of Polar Research Kaga 1-9-10, Itabashi-ku, Tokyo 173-8515, Japan |

LIST OF CONTRIBUTORS (continued)

| Station Country/Territory | Name | Address |
|--|---------------------|--|
| | Shuji Aoki | Center for Atmospheric and Oceanic Studies, Graduate School of Science, Tohoku University Aoba, Sendai 980-8578, Japan |
| Mace Head (Ireland) | Gerard Spain | National University of Ireland, Galway (NUI) Mace Head Research Station Carna, Co. Galway, Ireland |
| Hohe Warte Stephansplatz (Austria) | Guenther Schermann | Municipal Department 22 - Environmental Protection Air quality subdepartment, City of Vienna Ebendorferstrasse 4, A-1082 Vienna, Austria |
| Vindeln (Sweden) | Hakan Blomgren | IVL Swedish Environmental Research Institute P.O.Box 5302S-400 14 Goteborg, Sweden |
| Kloosterburen (Netherlands (the)) | Hans Berkhout | RIVM - Centre for Environmental Monitoring (MIL) PO Box 1 3720 BA Bilthoven the Netherlands |
| Kollumerwaard (Netherlands (the)) | Hans Berkhout | RIVM - Centre for Environmental Monitoring (MIL) PO Box 1 3720 BA Bilthoven the Netherlands |
| | Ronald Spoor | RIVM - Centre for Environmental Monitoring (MIL) PO Box 1 3720 BA Bilthoven the Netherlands |
| Wank Peak Zugspitze (Germany) | Hans-Eckhart Scheel | Karlsruhe Institute of Technology (KIT), IMK-IFU 82467 Garmisch-Partenkirchen, Germany |
| Danki Shepelevo (Russian Federation) | Irina Brouskina | |
| BEO Moussala (Bulgaria) | Ivo Kalapov | INRNE Institute for Nuclear Research and Nuclear Energy Tsarigradsko shose Blvd. 1784 Sofia Bulgaria |
| | Todor Arsov | |

LIST OF CONTRIBUTORS (continued)

| Station Country/Territory | Name | Address |
|---|-------------------------|--|
| La Cartuja Doñana Logroño Mahón Noia Roquetes San Pablo de los Montes (Spain) | J.M. Saenz | Servicio de Desarrollos Medioambientales, Instituto Nacional de Meteorología, Ministerio de Medio Ambiente Leonardo Prieto Castro, 8, 28071 Madrid, Spain |
| Monte Cimone (Italy) | Jgor Arduini | Università degli Studi di Urbino Istituto di Scienze Chimiche, piazza Rinascimento 6, 61029 Urbino - Italy |
| | Paolo Bonasoni | ISAC-CNR ISAC-CNR, Via Gobetti 101 - 40129 Bologna -Italy |
| | Paolo Cristofanelli | ISAC-CNR ISAC-CNR, Via Gobetti 101 - 40129 Bologna -Italy |
| | Rocco Duchi | |
| Pallas-Sammaltunturi (Finland) | Juha Hatakka | Finnish Meteorological Institute P.O.Box 503, FI-00101 Helsinki, Finland |
| | Timo Salmi | Finnish Meteorological Institute Erik Palmenin aukio 1, P.O.Box 503, FIN-00101 Helsinki, Finland |
| | Mika Vestenius | Finnish Meteorological Institute |
| Brotjacklriegel Deuselbach Waldhof Neuglobsow Schauinsland Westerland Zingst Zugspitze / Schneefernerhaus Zugspitze (Germany) | Karin Uhse | Umweltbundesamt (UBA, Federal Environmental Agency) Air Monitoring Network Paul-Ehrlich-Strasse 29 D-63225 Langen, Germany |
| Sniezka (Poland) | Krzaczkowski Piotr, MSc | Institute of Meteorology and Water Management - Wroclaw Branch, Meteorological Observatory on Sniezka Mountain |
| Hegyhatsal K-pusztá (Hungary) | Laszlo Haszpra | Hungarian Meteorological Service P.O. Box 39, H-1675 Budapest, Hungary |

LIST OF CONTRIBUTORS (continued)

| Station Country/Territory | Name | Address |
|--|-----------------------|---|
| Iskrba Kovk Krvavec Zavodnje (Slovenia) | Marijana Murovec | Slovenian Environment Agency Agencija RS za okolje / Slovenian Environment Agency Urad za meteorologijo / Meteorology Office Sektor za kakovost zraka / Air Quality Division Vojkova 1b, 1001 Ljubljana, p.p. 2608, Slovenia |
| Dobele Rucava Zoseni (Latvia) | Marina Frolova | Observation Network Department, Latvian Environment, Geology and Meteorology Centre, Ministry of Environmental 165 Maskavas str. LV-1019, Riga, Latvia |
| Sonnblick (Austria) | Marina Fröhlich | Federal Environment Agency Austria Spittelauer Lände 5, A-1090 Wien, Austria |
| | Wolfgang Spangl | Federal Environment Agency Austria Spittelauer Lände 5, A-1090 Wien, Austria |
| | Elisabeth Friedbacher | Federal Environment Agency Austria Spittelauer Lände 5, A-1090 Wien, Austria |
| Jungfraujoch (Switzerland) | Markus Leunberger | University of Bern University of Bern Physics Institute Sidlerstrasse 5 CH-3012 Bern |
| Ivan Sedlo (Bosnia and Herzegovina) | Martin Tais | Meteoroloski zavod Bosne i Hercegovine Bardakcije 12, 71000 Sarajevo, Bosnia and Herzegovina |
| Pic du Midi (France) | Meyerfeld Yves | Laboratoire d'Aérologie |
| | Gheusi Francois | |
| Ile Grande Pic du Midi Puy de Dome (France) | Michel Ramonet | LSCE (Laboratoire des Sciences du Climat et de l'Environnement) UMR CEA-CNRS LSCE - CEA Saclay - Orme des Merisiers - Bat.701 91191 Gif-sur-Yvette, France |
| Finokalia (Greece) | | |
| Mace Head (Ireland) | | |
| Begur (Spain) | | |
| Kosetice (Czech Republic) | Milan Vana | Czech Hydrometeorological Institute, Kosetice Observatory Na Sabatce 17, 143 06 Praha 4 - Komorany, Czech Republic |

LIST OF CONTRIBUTORS (continued)

| Station Country/Territory | Name | Address |
|---|----------------------|--|
| Ocean Station Charlie Teriberka (Russian Federation) | Nina Paramonova | Main Geophysical Observatory (MGO) Karbyshev Street 7, St. Petersburg, 194021, Russian Federation |
| Zeppelinfjellet (Ny-Alesund) (Norway) | Ove Hermansen | Norwegian Institute for Air Research (NILU) P. O. Box 100 Instituttveien 18, N-2027 Kjeller, Norway |
| Eskdalemuir (United Kingdom of Great Britain and Northern Ireland) | Peter Kuria | Air and Environment Quality Division, DEFRA 4/F15, Ashdown House123 Victoria StreetLondon, SW1E 3DE, United Kingdom |
| Puy de Dome (France) | Pichon Jean-Marc | Laboratoire de Météorologie Physique |
| | Meyerfeld Yves | Laboratoire d'Aérodologie |
| Lampedusa (Italy) | Salvatore Chiavarini | Italian National Agency for New Technology, Energy, and Sustainable Economic Development (ENEA) ENEA-UTPRA Via Anguillarese, 301 00123 Rome, Italy |
| | Salvatore Piacentino | Italian National Agency for New Technology, Energy, and Sustainable Economic Development (ENEA) Laboratory for Earth Observations and Analyses (UTMEA-TER) ENEA ACS-CLIMOSS, Via Catania 2, 90141 Palrmo, Italy. |
| | Damiano Sferlazzo | Italian National Agency for New Technology, Energy, and Sustainable Economic Development (ENEA) Laboratory for Earth Observations and Analyses (UTMEA-TER) Station for Climate Observations Contrada Capo Grecale 92010 Lampedusa Italy |
| | Alcide di Sarra | Italian National Agency for New Technology, Energy, and Sustainable Economic Development (ENEA) Laboratory for Earth Observations and Analyses (UTMEA-TER) Via Anguillarese, 301 00123 Rome, Italy. |

LIST OF CONTRIBUTORS (continued)

| Station Country/Territory | Name | Address |
|--|--------------------------|---|
| Ridge Hill Tacolneston Tall Tower (United Kingdom of Great Britain and Northern Ireland) | Simon O'Doherty | Atmospheric Chemistry Research Group School of Chemistry University of Bristol Atmospheric Chemistry Research Group School of Chemistry University of Bristol Cantocks Close BS8 1TS Bristol United Kingdom |
| | Aoife Grant | Atmospheric Chemistry Research Group School of Chemistry University of Bristol Atmospheric Chemistry Research Group School of Chemistry University of Bristol Cantocks Close BS8 1TS Bristol United Kingdom |
| Hohenpeissenberg Zugspitze / Schneefernerhaus (Germany) | Stefan Gilge | Deutscher Wetterdienst (DWD, German Meteorological Service) Meteorologisches Observatorium Hohenpeissenberg Albin-Schwaiger-Weg 10D-82383 Hohenpeissenberg, Germany |
| | Christian Plass-Duelmer | Deutscher Wetterdienst (DWD, German Meteorological Service) Meteorologisches Observatorium Hohenpeissenberg Albin-Schwaiger-Weg 10D-82383 Hohenpeissenberg, Germany |
| Lazaropole (The Former Yugoslav Republic of Macedonia) | Suzana Alcinova Monevska | Hydrometeorological Service Skupi bb, 1000 Skopje, The former Yugoslav Republic of Macedonia |
| Ähtäri Oulanka Utö Virolahti (Finland) | Timo Salmi | Finnish Meteorological Institute Erik Palmenin aukio 1, P.O.Box 503, FIN-00101 Helsinki, Finland |
| ANTARCTICA | | |
| Jubany (Italy) | Claudio Rafanelli | ICES (Int.l Center for Earth Sciences) c/o CNR-Istituto di Acustica- Area della Ricerca di Roma Tor Vergata, via Fosso del Cavaliere 100, 00133 Rome, Italy |
| King Sejong (Republic of Korea) | Haeyoung Lee | Korea Global Atmosphere Watch Center, Korea Meteorology Administration 1764-6, Seungen-Ri, Anmyeon-Eup, Taean-Kun, ChungNam, 357-961, Republic of Korea |

LIST OF CONTRIBUTORS (continued)

| Station Country/Territory | Name | Address |
|----------------------------------|-----------------------|--|
| | Taejin Choi | Division of Polar Climate Research, KOPRI Get-Pearl Tower, 12 Gaetbeol-ro, Yeonsu-gu, Incheon, 406-840, Republic of Korea |
| Marambio (Argentina) | Maria Elena Barlasina | National Weather Service Observatorio Central Villa Ortuzar División Radiación Av. de Los Constituyentes 3454 Cp 1427, Argentina |
| | Ricardo Sanchez | National Weather Service Observatorio Central Villa Ortuzar División Radiación Av. de Los Constituyentes 3454 Cp 1427, Argentina |
| Syowa Station (Japan) | Masato Fukuda | Office of Antarctic Observations, Japan Meteorological Agency (JMA) 1-3-4 Otemachi, Chiyoda-ku, Tokyo 100-8122, Japan |
| Concordia, Dôme C (Italy) | Paolo Cristofanelli | ISAC-CNR ISAC-CNR, Via Gobetti 101 - 40129 Bologna -Italy |
| | Paolo Bonasoni | ISAC-CNR ISAC-CNR, Via Gobetti 101 - 40129 Bologna -Italy |
| Neumayer (Germany) | Rolf Weller | Alfred Wegener Institute Am Handelshafen 12, 27570 Bremerhaven, Germany |
| Arrival Heights (New Zealand) | Sylvia Nichol | National Institute of Water & Atmospheric Research Ltd. 301 Evans Bay Parade, Greta Point, Private Bag 14-901, Kilbirnie, Wellington, New Zealand |
| | Gordon Brailsford | National Institute of Water & Atmospheric Research Ltd. 301 Evans Bay Parade, Greta Point, Private Bag 14-901, Kilbirnie, Wellington, New Zealand |
| | Ross Martin | National Institute of Water & Atmospheric Research Ltd. 301 Evans Bay Parade, Greta Point, Private Bag 14-901, Kilbirnie, Wellington, New Zealand |
| Mizuho (Japan) | Takakiyo Nakazawa | Center for Atmospheric and Oceanic Studies, Graduate School of Science, Tohoku University Aoba, Sendai 980-8578, Japan |
| Syowa Station (Japan) | Takakiyo Nakazawa | Center for Atmospheric and Oceanic Studies, Graduate School of Science, Tohoku University Aoba, Sendai 980-8578, Japan |
| | Gen Hashida | National Institute of Polar Research Kaga 1-9-10, Itabashi-ku, Tokyo 173-8515, Japan |

LIST OF CONTRIBUTORS (continued)

| Station Country/Territory | Name | Address |
|---|----------------------------------|---|
| | Shinji Morimoto | National Institute of Polar Research Kaga 1-9-10, Itabashi-ku, Tokyo 173-8515, Japan |
| MOBILE STATION | | |
| NOPACCS - Hakurei Maru - WEST COSMIC - Hakurei Maru No.2 - (Japan) | General Environmental Texhnos | The General Environmental Technos Co., Ltd. (Old:Kansai Environmental Engineering Center, Co., Ltd.) 1-3-5, Azuchi machi, Chuo-ku, Osaka 541-0052, Japan |
| INSTAC-I (International Strato/Tropospheric Air Chemistry Project) (Japan) | Hidekazu Matsueda | Geochemical Research Department, Meteorological Research Institute Nagamine 1-1, Tsukuba, Ibaraki 305-0052, Japan |
| Comprehensive Observation Network for TRace gases by AIrLiner (CONTRAIL) (Japan) | Hidekazu Matsueda | Geochemical Research Department, Meteorological Research Institute Nagamine 1-1, Tsukuba, Ibaraki 305-0052, Japan |
| | Toshinobu Machida | National Institute for Environmental Studies 16-2 Onogawa, Tsukuba 305-8506, Japan |
| MRI Research, Mirai, R/V (Japan) | Hisayuki Yoshikawa-Inoue | Laboratory of Marine and Atmospheric GeochemistryGraduate School of Environmental Earth ScienceHokkaido University N10W5, Kita-ku, Sapporo 060-0810, Japan |
| northern and western Pacific (Japan) | Kentaro Ishijima | Japan Agency for Marine-earth Science and Technology (JAMSTEC) 3173-25 Showamachi, Kanazawa-ku, Yokohama, 236-0001, Japan |
| | Shuji Aoki | Center for Atmospheric and Oceanic Studies, Graduate School of Science, Tohoku University Aoba, Sendai 980-8578, Japan |
| | Takakiyo Nakazawa | Center for Atmospheric and Oceanic Studies, Graduate School of Science, Tohoku University Aoba, Sendai 980-8578, Japan |
| Santarem (Brazil) | Luciana Vanni Gatti | IPEN Atmospheric Chemistry Laboratory Av. Prof. Lineu Prestes, 2242, Cidade Universitaria, Sao Paulo, SP- BRAZIL CEP 05508-900 |

LIST OF CONTRIBUTORS (continued)

| Station Country/Territory | Name | Address |
|---|-----------------------|---|
| | LuanaãS. Basso | IPEN Atmospheric Chemistry Laboratory Av. Prof. Lineu Prestes, 2242, Cidade Universitaria, Sao Paulo, SP- BRAZIL CEP 05508-900 |
| | Alexandre Martinewski | |
| MRI Research, Hakuho Maru, R/V MRI Research, Kaiyo Maru, R/V MRI Research, 1978-1986, R/V MRI Research, Natushima, R/V MRI Research, Ryofu Maru, R/V MRI Research, Wellington Maru, R/V (Japan) | Masao Ishii | Geochemical Research Department, Meteorological Research Institute Nagamine 1-1, Tsukuba, Ibaraki 305-0052, Japan |
| Aircraft: Orleans (France) | Michel Ramonet | LSCE (Laboratoire des Sciences du Climat et de l'Environnement) UMR CEA-CNRS LSCE - CEA Saclay - Orme des Merisiers - Bat.701 91191 Gif-sur-Yvette, France |
| Observation of Atmospheric Chemistry Over Japan The Observation of Atmospheric Methane Over Japan The Observation of Atmospheric Sulfur Hexafluoride Over Japan (Japan) | Michio Hirota | Geochemical Research Department, Meteorological Research Institute 1-1, Nagamine, Tsukuba, Ibaraki 305-0052, Japan |
| Alligator liberty, M/V Keifu Maru, R/V Kofu Maru, R/V Ryofu Maru, R/V (Japan) | Shu Saito | Marine Division, Global Environment and Marine Department, Japan Meteorological Agency (JMA) 1-3-4 Otemachi, Chiyoda-ku, Tokyo 100-8122, Japan |
| Pacific Ocean (New Zealand) | Sylvia Nichol | National Institute of Water & Atmospheric Research Ltd. 301 Evans Bay Parade, Greta Point, Private Bag 14-901, Kilbirnie, Wellington, New Zealand |
| | Gordon Brailsford | National Institute of Water & Atmospheric Research Ltd. 301 Evans Bay Parade, Greta Point, Private Bag 14-901, Kilbirnie, Wellington, New Zealand |

LIST OF CONTRIBUTORS (continued)

| Station Country/Territory | Name | Address |
|--|----------------|--|
| Comprehensive Observation Network for TRace gases by Airliner (CONTRAIL) over the Pacific Ocean 20-50 km off the coast of the Sendai plain over Japan between Sendai and Fukuoka (Japan) | Taku Umezawa | Max Planck Institute for Chemistry Atmospheric Chemistry Department |
| | Shuji Aoki | Center for Atmospheric and Oceanic Studies, Graduate School of Science, Tohoku University |
| Soyo Maru, R/V Wakataka-Marui (Japan) | Tsuneo Ono | Hokkaido National Fisheries Research Institute 116 Katsurakoi, Kushiro 085-0802, Japan |
| Aircraft Observation of Atmospheric trace gases by JMA (Japan) | Yukio Fukuyama | Atmospheric Environment Division, Global Environment and Marine Department, Japan Meteorological Agency (JMA) 1-3-4 Otemachi, Chiyoda-ku, Tokyo 100-8122, Japan |

LIST OF CONTRIBUTORS (continued)

| Station Country/Territory | Name | Address |
|---|--|--|
| NOAA/ESRL Flask Network | | |
| Assekrem (Algeria) | Bruce Vaughn** James White** ($^{13}\text{CH}_4$, $^{13}\text{CO}_2$ and C^{18}O_2) | (*)NOAA/ESRL Global Monitoring Division 325 Broadway R/GMD1 Boulder, CO 80305-3328, U.S.A. |
| Tierra del Fuego (Argentina) | Jocelyn Turnbull ($^{14}\text{CO}_2$) | (**)Institute of Arctic and Alpine Research (INSTAAR) INSTAAR, Univ. of Colorado 1560, 30th Street |
| Cape Grim (Australia) | Edward J.Dlugokencky* (CH_4) | UCB 450 Boulder, CO 80309 U.S.A. |
| Ragged Point (Barbados) | Paul C. Novelli* (CO and H_2) | |
| Arembepe Natal (Brazil) | Thomas J. Conway* (CO_2) | |
| Alert Lac La Biche Mould Bay (Canada) | Bruce Vaughn** (N_2O and SF_6) Detlev Helmig** Jacques Hueber** | |
| Easter Island (Chile) | (VOCs) | |
| Lulin Shangdianzi Mt. Waliguan (China) | | |
| Summit (Denmark) | | |
| Pallas-Sammaltunturi (Finland) | | |
| Amsterdam Island Crozet (France) | | |
| Hohenpeissenberg Ochsenkopf (Germany) | | |
| Hegyhatsal (Hungary) | | |
| Heimaey (Iceland) | | |
| Bukit Koto Tabang (Indonesia) | | |

LIST OF CONTRIBUTORS (continued)

| Station Country/Territory | Name | Address |
|---|------|---------|
| Mace Head (Ireland) | | |
| Sede Boker (Israel) | | |
| Lampedusa (Italy) | | |
| Syowa Station (Japan) | | |
| Sary Taukum Plateau Assy (Kazakhstan) | | |
| Mt. Kenya (Kenya) | | |
| Christmas Island (Kiribati) | | |
| Kaashidhoo (Maldives) | | |
| Dwejra Point (Malta) | | |
| Mex High Altitude Global Climate Observation Center, Mexico (Mexico) | | |
| Ulaan Uul (Mongolia) | | |
| Gobabeb (Namibia) | | |
| Arrival Heights Baring Head Lauder Kaitorete Spit (New Zealand) | | |
| Ocean Station "M" Zeppelinfjellet (Ny-Alesund) (Norway) | | |
| Baltic Sea (Poland) | | |

LIST OF CONTRIBUTORS (continued)

| Station Country/Territory | Name | Address |
|---|------|---------|
| Terceira Island Pico, Azores (Portugal) | | |
| Tae-ahn Peninsula (Republic of Korea) | | |
| Black Sea (Romania) | | |
| Mahe Island (Seychelles) | | |
| Cape Point (South Africa) | | |
| Izaña (Tenerife) (Spain) | | |
| Ascension Island St. David's Head Tudor Hill Halley Bay Bird Island (United Kingdom of Great Britain and Northern Ireland) | | |
| Akademik Korolev, R/V | | |
| Argyle | | |
| Atlantic Ocean | | |
| St. Croix | | |
| Barrow | | |
| Cold Bay | | |
| Cape Meares | | |
| Discoverer 1983 & 1984, R/V | | |
| Drake Passage | | |
| Discoverer 1985, R/V | | |
| Guam | | |
| Grifton | | |

LIST OF CONTRIBUTORS (continued)

| Station Country/Territory | Name | Address |
|------------------------------|-------------------------------|---------|
| | John Biscoe, R/V | |
| | Key Biscayne | |
| | Korolev, R/V | |
| | Kitt Peak | |
| | Cape Kumukahi | |
| | Park Falls | |
| | Long Lines Expedition, R/V | |
| | McMurdo Station | |
| | Sand Island | |
| | Mauna Loa | |
| | Mexico Naval H-02, R/V | |
| | Niwot Ridge (T-van) | |
| | Niwot Ridge (Saddle) | |
| | Oceanographer, R/V | |
| | Olympic Peninsula | |
| | Pacific-Atlantic Ocean | |
| | Polar Star, R/V | |
| | Pacific Ocean | |
| | Palmer Station | |
| | Point Arena | |
| | South China Sea | |
| | Southern Great Plains | |
| | Shemya Island | |
| | La Jolla | |
| | Tutuila (Cape Matatula) | |
| | South Pole | |

LIST OF CONTRIBUTORS (continued)

| Station Country/Territory | Name | Address |
|---------------------------------|---|--|
| Ocean Station Charlie | | |
| Surveyor, R/V | | |
| Trinidad Head | | |
| Wendover | | |
| West Branch | | |
| Moody | | |
| Western Pacific | | |
| (United States of America) | | |
| NOAA/ESRL/HATS Network | | |
| Tierra del Fuego (Argentina) | James W. Elkins Stephen A. Montzka Geoffrey S. Dutton | Halocarbons and Other Atmosphere Trace Species Group (HATS)/NOAA/ESRL Global Monitoring Division 325 Broadway R/GMD1 Boulder, CO 80305-3328, U.S.A |
| Cape Grim (Australia) | | |
| Alert (Canada) | | |
| Summit (Denmark) | | |
| Mace Head (Ireland) | | |
| BACPAC 99 | | |
| BLAST1 | | |
| BLAST2 | | |
| BLAST3 | | |
| Barrow | | |
| CLIVAR 01 | | |
| Gas Change Experiment | | |
| Harvard Forest | | |
| HATS Ocean Projects | | |

LIST OF CONTRIBUTORS (continued)

| Station Country/Territory | Name | Address |
|------------------------------|------|---------|
| Grifton | | |
| Cape Kumukahi | | |
| Park Falls | | |
| Mauna Loa | | |
| Niwot Ridge (C-1) | | |
| PHASE I-04 | | |
| Palmer Station | | |
| Tutuila (Cape Matatula) | | |
| South Pole | | |
| Trinidad Head | | |
| (United States of America) | | |

NOAA/ESRL Surface Ozone Network

| | | |
|--|--|--|
| Ragged Point (Barbados) | Audra McClure-Begley Irina Petropavlovskikh | NOAA/ESRL Global Monitoring Division 325 Broadway, R/GMD1, Boulder, CO 80305, U.S.A |
| Summit (Denmark) | | |
| Heimaey (Iceland) | | |
| Arrival Heights Lauder (New Zealand) | | |
| Tudor Hill (United Kingdom of Great Britain and Northern Ireland) | | |
| Barrow | | |
| McMurdo Station | | |
| Mauna Loa | | |
| Niwot Ridge (C-1) | | |
| Niwot Ridge (Saddle) | | |

LIST OF CONTRIBUTORS (continued)

| Station Country/Territory | Name | Address |
|------------------------------|------|---------|
| Tutuila (Cape Matatula) | | |
| South Pole | | |
| Trinidad Head | | |
| Moody | | |
| (United States of America) | | |

LIST OF CONTRIBUTORS (continued)

| Station Country/Territory | Name | Address |
|--|-----------------------|---|
| CSIRO Flask Network | | |
| Aircraft (over Bass Strait and Cape Grim) | Paul Krummel | Commonwealth Scientific and Industrial Research Organisation (CSIRO) |
| Cape Ferguson | Paul Steele | CSIRO Marine and Atmospheric Research |
| Cape Grim | Ray Langenfelds | Private Bag 1 |
| Casey Station | Marcel van der Schoot | Aspendale, Vic, Australia 3195 |
| Gunn Point | Colin Allison | |
| Mawson | | |
| Macquarie Island (Australia) | | |
| Alert | | |
| Estevan Point (Canada) | | |
| Cape Rama (India) | | |
| Shetland (United Kingdom of Great Britain and Northern Ireland) | | |
| Mauna Loa | | |
| South Pole (United States of America) | | |
| ALE/GAGE/AGAGE Network | | |
| Cape Grim (Australia) | Stefan Reimann | School of Earth and Atmospheric Sciences, Georgia Institute of Technology |
| | Paul Krummel | 311 Ferst Drive School of Earth and Atmospheric Sciences Georgia Institute of Technology Atlanta, GA |
| | Paul Steele | 30332-0340, U.S.A |
| Ragged Point (Barbados) | Prof. Michela Maione | |
| | Simon O'Doherty | |
| | Jgor Arduini | |
| Adrigole | Ray Wang | |
| Mace Head (Ireland) | Ray F. Weiss | |
| Monte Cimone (Italy) | | |
| Zeppelinfjellet (Ny-Alesund) (Norway) | | |
| Jungfraujoch (Switzerland) | | |

LIST OF CONTRIBUTORS (continued)

| Station | Name | Address |
|----------------------------|------|---------|
| Country/Territory | | |
| Cape Meares | | |
| Tutuila (Cape Matatula) | | |
| Trinidad Head | | |
| (United States of America) | | |

GLOSSARY

ATMOSPHERIC SPECIES:

| | |
|--------------------------------------|--|
| CCl₄ | tetrachloromethane (carbon tetrachloride) |
| C₂Cl₄ | tetrachloroethylene |
| CFC-11 | chlorofluorocarbon-11 (trichlorofluoromethane, CCl ₃ F) |
| CFC-12 | chlorofluorocarbon-12 (dichlorodifluoromethane, CCl ₂ F ₂) |
| CFC-113 | chlorofluorocarbon-113 (1,1,2-trichlorotrifluoroethane, CCl ₂ FCFClF ₂) |
| CFCs | chlorofluorocarbons |
| CH₄ | methane |
| CHBr₃ | tribromomethane (bromoform) |
| CH₂Br₂ | dibromomethane |
| CH₃Br | bromomethane |
| CH₃CCl₃ | 1,1,1-trichloroethane (methyl chloroform) |
| CHCl₃ | trichloromethane (chloroform) |
| CH₂Cl₂ | dichloromethane (methylene chloride) |
| CH₃Cl | chloromethane (methyl chloride) |
| C₂HCl₃ | trichloroethylene |
| CO | carbon monoxide |
| CO₂ | carbon dioxide |
| H₂ | hydrogen |
| Halon-1211 | chlorodifluorobromomethane (CBrClF ₂) |
| Halon-1301 | bromotrifluoromethane (CBrF ₃) |
| HCFC-141b | hydrochlorofluorocarbon-141b (1,1-dichloro-1-fluoroethane, CH ₃ CCl ₂ F) |
| HCFC-142b | hydrochlorofluorocarbon-142b (1,1-difluoro-1-chloroethane, CH ₃ CClF ₂) |
| HCFC-22 | hydrochlorofluorocarbon-22 (chlorodifluoromethane, CHClF ₂) |
| HCFCs | hydrochlorofluorocarbons |
| HFC-134a | hydrofluorocarbon-134a (1,1,1,2-tetrafluoroethane, CH ₂ FCF ₃) |
| HFC-152a | hydrofluorocarbon-152a (1,1-difluoroethane, CHF ₂ CH ₃) |
| HFCs | hydrofluorocarbons |
| N₂O | nitrous oxide |
| NO | nitrogen monoxide |
| NO₂ | nitrogen dioxide |
| NO_x | nitrogen oxides |
| O₃ | ozone |
| PAN | peroxyacyl nitrate |
| PFCs | perfluorocarbons |
| Rn | radon |
| SF₆ | sulphur hexafluoride |
| SO₂ | sulphur dioxide |
| TIC | total inorganic carbon |
| VOCs | volatile organic compounds |

UNITS:

| | |
|------------|--------------------|
| ppm | parts per million |
| ppb | parts per billion |
| ppt | parts per trillion |

Others:

| | |
|-------------|------------------------------|
| ENSO | El Niño-Southern Oscillation |
| M/V | merchant vessel |
| R/V | research vessel |

LIST OF WMO/WDCGG PUBLICATIONS

DATA REPORTING MANUAL:

WDCGG No. 1 January 1991

WMO WDCGG DATA REPORT:

(period of data accepted)

| | | | | | | | |
|--------------------|-----------|------|-----------|------|---|-----------|------|
| WDCGG No. 2 Part A | October | 1992 | October | 1990 | ~ | August | 1992 |
| WDCGG No. 2 Part B | October | 1992 | October | 1990 | ~ | August | 1992 |
| WDCGG No. 3 | October | 1993 | September | 1992 | ~ | March | 1993 |
| WDCGG No. 5 | March | 1994 | April | 1993 | ~ | September | 1993 |
| WDCGG No. 6 | September | 1994 | September | 1993 | ~ | March | 1994 |
| WDCGG No. 7 | March | 1995 | April | 1994 | ~ | December | 1994 |
| WDCGG No. 9 | September | 1995 | January | 1995 | ~ | June | 1995 |
| WDCGG No.10 | March | 1996 | July | 1995 | ~ | December | 1995 |
| WDCGG No.11 | September | 1996 | January | 1996 | ~ | June | 1996 |
| WDCGG No.12 | March | 1997 | July | 1996 | ~ | November | 1996 |
| WDCGG No.14 | September | 1997 | December | 1996 | ~ | June | 1997 |
| WDCGG No.16 | March | 1998 | July | 1997 | ~ | December | 1997 |
| WDCGG No.17 | September | 1998 | January | 1998 | ~ | June | 1998 |
| WDCGG No.18 | March | 1999 | July | 1998 | ~ | December | 1998 |
| WDCGG No.20 | September | 1999 | January | 1999 | ~ | June | 1999 |
| WDCGG No.21 | March | 2000 | July | 1999 | ~ | December | 1999 |
| WDCGG No.23 | September | 2000 | January | 2000 | ~ | June | 2000 |
| WDCGG No.25 | March | 2001 | July | 2000 | ~ | December | 2000 |

WMO WDCGG DATA CATALOGUE:

| | | |
|-------------|----------|------|
| WDCGG No. 4 | December | 1993 |
| WDCGG No.13 | March | 1997 |
| WDCGG No.19 | March | 1999 |
| WDCGG No.24 | March | 2001 |

WMO WDCGG DATA SUMMARY:

| | | |
|-------------|---------|------|
| WDCGG No. 8 | October | 1995 |
| WDCGG No.15 | March | 1998 |
| WDCGG No.22 | March | 2000 |
| WDCGG No.26 | March | 2002 |
| WDCGG No.27 | March | 2003 |
| WDCGG No.28 | March | 2004 |
| WDCGG No.29 | March | 2005 |
| WDCGG No.30 | March | 2006 |
| WDCGG No.31 | March | 2007 |
| WDCGG No.32 | March | 2008 |
| WDCGG No.33 | March | 2009 |
| WDCGG No.34 | March | 2010 |
| WDCGG No.35 | March | 2011 |
| WDCGG No.36 | March | 2012 |
| WDCGG No.37 | March | 2013 |
| WDCGG No.38 | March | 2014 |
| WDCGG No.39 | March | 2015 |

WMO WDCGG CD-ROM:

(period of data accepted)

| | | | | | | | |
|--------------|-------|------|---------|------|---|----------|------|
| CD-ROM No. 1 | March | 1995 | October | 1990 | ~ | December | 1994 |
| CD-ROM No. 2 | March | 1996 | October | 1990 | ~ | June | 1995 |
| CD-ROM No. 3 | March | 1997 | October | 1990 | ~ | June | 1996 |

| | | | | | | | |
|--------------|-------|------|---------|------|---|----------|------|
| CD-ROM No. 4 | March | 1998 | October | 1990 | ~ | December | 1997 |
| CD-ROM No. 5 | March | 1999 | October | 1990 | ~ | December | 1998 |
| CD-ROM No. 6 | March | 2000 | October | 1990 | ~ | December | 1999 |
| CD-ROM No. 7 | March | 2001 | October | 1990 | ~ | December | 2000 |
| CD-ROM No. 8 | March | 2002 | October | 1990 | ~ | January | 2002 |
| CD-ROM No. 9 | March | 2003 | October | 1990 | ~ | December | 2002 |
| CD-ROM No.10 | March | 2004 | October | 1990 | ~ | December | 2003 |
| CD-ROM No.11 | March | 2005 | October | 1990 | ~ | December | 2004 |
| CD-ROM No.12 | March | 2006 | October | 1990 | ~ | December | 2005 |
| CD-ROM No.13 | March | 2007 | October | 1990 | ~ | November | 2006 |
| CD-ROM No.14 | March | 2008 | October | 1990 | ~ | November | 2007 |

WMO WDCGG DVD:

(period of data accepted)

| | | | | | | | |
|-----------|-------|------|---------|------|---|----------|------|
| DVD No. 1 | March | 2009 | October | 1990 | ~ | November | 2008 |
| DVD No. 2 | March | 2010 | October | 1990 | ~ | November | 2009 |
| DVD No. 3 | March | 2011 | October | 1990 | ~ | November | 2010 |
| DVD No. 4 | March | 2012 | October | 1990 | ~ | November | 2011 |
| DVD No. 5 | March | 2013 | October | 1990 | ~ | November | 2012 |
| DVD No. 6 | March | 2014 | October | 1990 | ~ | November | 2013 |
| DVD No. 7 | March | 2015 | October | 1990 | ~ | November | 2014 |